**Evaluating an Alternative Endothelial Cell Source to Vascularize Engineered Tissue Constructs**

by

Jonathan Robert Bezenah

A dissertation submitted in partial fulfillment
of the requirements for the degree of
Doctor of Philosophy
(Chemical Engineering)
in the University of Michigan
2018

Doctoral Committee:

Professor Andrew J. Putnam, Chair
Professor Lola Eniola-Adefeso
Professor Lonnie D. Shea
Professor Steven J. Weiss

Jonathan R. Bezenah

bezenahj@umich.edu

ORCD iD: 0000-0002-3271-2809

# ACKNOWLEDGEMENTS

First, I would like to thank my thesis advisor, Dr. Andrew J. Putnam. Thank you for all your support and guidance over these past few years. You welcomed me into your research group at a point when I didn't think I had what it takes to pursue a doctorate degree. Not only did you believe in me, but you showed me that I was capable of the ingenuity required to complete my graduate education as well as anything else I set my mind on. You taught me to approach scientific questions practically, to push through the failures, and to be confident in my research. Thank you for all the discussions and conversations beyond science and research. You are a stimulating mentor, a patient teacher, and a cherished friend. For this, I am forever grateful, as I truly believe I would not be here without you.

Next, I would like to thank my thesis committee members, Dr. Lola Eniola-Adefeso, Dr. Lonnie D. Shea, and Steven J. Weiss for asking the hard questions and for the continuing collaboration and feedback which strengthened my dissertation.

I also gratefully acknowledge several funding sources. A predoctoral fellowship support from the NIH Cellular Biotechnology Training Grant (T32-GM008353) at the University of Michigan facilitated my research project and educational activities. This work was also partially supported by a grant from the National Institutes of Health (R01-HL085339).

I would like to thank all my current and former lab members of the Cell Signaling in Engineered Tissues (CEST) group. Your advice and input for my research project was much

appreciated. Also, thank you Nicole Friend and Benjamin Juliar for helping me quantify data. To Dr. Ana Y. Rioja – your help, guidance, and hard work was instrumental in the timely compelition of my animal studies and I am forever grateful. To Dr. Yen P. Kong – Thank you for all your advice and assistance throughout my dissertation. Not only did you aid in countless research projects, but our conversations made the time more enjoyable.

To all my friends, thank you for all the great times over the past years. Whether having dinner, playing games, or just hanging out, these moments provided the perfect relief during stressful times, and I will always cherish them.

Next, I would also like to thank my family for your support. Most importantly, I deeply thank my parents, Robert and Renee Bezenah, for all your love, guidance, and encouragement through not only my graduate education, but my entire educational journey. You both were my first teachers, mentors, and role models as I grew and continued to learn. You guys pushed me ever since I was young to be the best I could because you both always knew I was capable of extraordinary things. Although I probably don't say it enough, I gratefully appreciate everything you do for me and all the support you have given me – for this, thank you, a million times over.

Finally, I would like to thank my partner, Kristina, for all your love, patience, encouragement, and motivation. Whether working late, midnight trips to change media, or putting things on hold when I needed, you endlessly supported me in countless ways. You have always challenged me, encouraged new ways of thinking, and pushed me to better myself, providing the drive for my education. Most importantly, you always believed in me and I couldn't have done any of this without you.

# TABLE OF CONTENT

# LIST OF FIGURES

# LIST OF VIDEOS

# LIST OF APPENDICIES

# LIST OF ABBREVIATIONS

(Symbols, Numerical Order, Alphabetical Order)

| | |
|---|---|
| °C | Celsius |
| 2D | Two-dimensional |
| 3D | Three-dimensional |
| α-SMA | Alpha-smooth muscle actin |
| AdSC | Adipose derived stem cells |
| ANGPT | Angiopotein |
| ANOVA | Analysis of variance |
| ASC | Adult stem cells |
| BCEC | Bovine capillary endothelial cells |
| bFGF | Basic fibroblast growth factor |
| BSA | Bovine serum albumin |
| CD31 | Cluster of differentiation – 31 |
| CD34 | Cluster of differentiation – 34 |
| CLI | Critical limb ischemia |
| COL | Collagen |
| CVD | Cardiovascular disease |
| DAPI | 4′,6- diamidino-2-phenylindole |
| DNA | Deoxyribonucleic acid |
| DMEM | Dulbecco's modified eagle medium |
| DMSO | Dimethyl sulfoxide |
| EC | Endothelial cells |
| ECM | Extracellular matrix |
| EDTA | Ethylenediaminetetraacetic acid |
| EGM-2 | Endothelial growth medium |

| | |
|---|---|
| EGM-2MV | Endothelial growth medium microvascular |
| ESC | Embryonic stem cell |
| FGF | Fibroblast growth factor |
| EPCs | Endothelial progenitor cells |
| ESC | Embryonic stem cells |
| FACS | Fluorescent activated cell sorting |
| FBS | Fetal bovine serum |
| FDA | Food and Drug Administration |
| FU | Fibrin degradation units |
| G’ | Shear modulus |
| H&E | Hematoxylin and eosin |
| HAEC | Human aortic endothelial cells |
| HCAEC | Human coronary endothelial cells |
| HPEC | Human pulmonary endothelial cells |
| HUVECs | Human umbilical vein endothelial cells |
| IACUC | Institutional Animal Care and Use Committee |
| IF | Immunofluorescent |
| IL-6 | Interleukin-6 |
| iPSC | Induced pluripotent stem cells |
| iPSC-ECs | Induced pluripotent stem cells derived endothelial cells |
| KLF4 | Kruppel like factor – 4 |
| LAM | Laminin |
| LDL | Low-density lipoprotein |
| LDPI | Laser Doppler perfusion imaging |
| M199 | Medium 199 |
| MMP | Matrix metalloprotease |
| MSCs | Mesenchymal stem cells |
| MVECs | Microvascular endothelial cells |
| NAOH | Sodium hydroxide |
| NHLFs | Normal human lung fibroblasts |
| NIH | National Institutes of Health |

| | |
|---|---|
| OCT-4 | Octamer binding transcription factor - 4 |
| PAD | Peripheral arterial disease |
| PBS | Phosphate buffered saline |
| PCR | Polymerase chain reaction |
| PLGA | Poly(lactic-co-glycolic acid) |
| PVDF | Polyvinylidene fluoride |
| RNA | Ribonucleic acid |
| RPM | Revolutions per minute |
| SCID | Severe combined immunodeficiency |
| SEM | Standard error of the mean |
| SFEGM-2 | Serum free endothelial growth medium |
| SMC | Smooth muscle cells |
| SOX -2 | Sex determining region T-box-2 |
| TBS-T | Tris buffered saline – tween 20 |
| TCP | Tissue culture plastic |
| TGF-β | Transforming growth factor beta |
| TIMP-3 | Tissue inhibitor of metalloproteinases - 3 |
| UEA-I | Ulex europaeus agglutinin I |
| PPM | Parts per million |
| VE- Cadherin | Vascular endothelial cadherin |
| VEGF | Vascular endothelial growth factor |
| VEGF-A | Vascular endothelial growth factor A |
| VEGFR2 | Vascular endothelial growth factor receptor 2 |
| vWF | von Willebrand factor |
| Z-fix | Zinc-buffered formalin solution |

# ABSTRACT

A major translational challenge in the fields of therapeutic angiogenesis and regenerative medicine is the need to create functional microvasculature. Cell-based strategies to promote neovascularization have been widely explored, but cell sourcing remains a significant limitation. Induced pluripotent stem cell-derived endothelial cells (iPSC-ECs) are a promising, autologous, alternative cell source. The purpose of this study was to assess whether a potentially autologous endothelial cell (EC) source derived from iPSC-ECs can form the same robust, stable microvasculature as previously documented for other sources of ECs.

The endothelial lineage of iPSC-ECs was first characterized as through endothelial marker expression and compared to human umbilical vein endothelial cells (HUVECs). Similarities in endothelial markers were demonstrated and genetic expression profile analysis revealed significant genotypic similarities between the iPSC-ECs and HUVECs.

A well-established *in vitro* assay was utilized, in which endothelial cell-coated (iPSC-ECs or HUVECs) beads were co-embedded with fibroblasts in a 3D fibrin matrix, to assess the iPSC-ECs' ability to form stable microvessels. iPSC-ECs exhibited a five-fold reduction in capillary network formation compared to HUVECs in this assay. Variation of cell sourcing, lot, cell density, and media formulation demonstrated no differences in iPSC-EC sprouting, eliminating these variables as the underlying cause. Despite quantitative differences, iPSC-ECs demonstrated some characteristics of mature vasculature including hollow lumen formation, pericyte recruitment and association, and deposition of basement membrane components.

To determine a cause of the *in vitro* sprouting attenuation, iPSC-ECs' capillary morphogenetic mechanisms were identified through chemical inhibition of sprouting and analysis of the expression levels of key proteases. Increasing matrix density reduced sprouting, although this effect was attenuated by distributing the normal human lung fibroblasts (NHLFs) within the 3D matrix. Inhibition of both MMP- and plasmin-mediated fibrinolysis was required to completely block sprouting of both HUVECs and iPSC-ECs. Further analysis revealed MMP-9 expression and activity were significantly lower in iPSC-EC/NHLF co-cultures than in HUVEC/NHLF co-cultures, which may account for the observed deficiencies in angiogenic sprouting of the iPSC-ECs.

To investigate if the *in vitro* attenuation was also an *in vivo* phenomenon, iPSC-ECs were evaluated for their ability to form functional microvasculature in a well-established *in vivo* model, in which endothelial cells (iPSC-ECs or HUVECs) were co-injected with fibroblasts and a fibrin matrix into the dorsal flank of severe combined immunodeficiency (SCID) mice. Qualitatively, iPSC-ECs were capable of forming perfused vessels that inosculated with mouse vessels and demonstrated similar vessel morphologies to HUVECs. However, quantitatively, iPSC-ECs exhibited a two-fold reduction in vessel density and a three-fold reduction in the number of perfused vessels compared to HUVECs. Further analysis revealed that the presence of the basement membrane component, type IV collagen, and the mural cell marker, alpha-smooth muscle actin, were significantly lower, roughly 25% and 33% respectively, around iPSC-EC/NHLF vasculature relative to that observed in HUVEC/NHLF implants, suggesting reduced vessel maturity. Collectively, these findings demonstrate that a potentially autologous EC with an unlimited source, specifically iPSC-ECs, has the ability to revascularize tissue and argues for a

deeper understanding of iPSC-ECs and their differences to enable the promise and potential of iPSC-ECs for clinical translation.

# CHAPTER 1
# Introduction

## 1.1 Motivation

Cardiovascular disease is the leading cause of death worldwide, accounting for nearly 30% of all global deaths and claiming more lives than all forms of cancer combined. In 2011, one out of every three deaths in America was attributed to cardiovascular disease. The number of deaths associated with cardiovascular disease continues to rise, with an expected 23.6 million deaths per year by 2030. Including health expenditures and lost productivity, it is estimated that the direct and indirect cost of cardiovascular disease and stroke total more than $320.1 billion [1].

Atherosclerosis, the obstruction of blood flow due to the deposition of cholesterol and fibrous tissue in the arterial walls, is the major cause of many cardiovascular diseases [2]. Atherosclerosis begins when the endothelium, the lining of blood vessels, becomes damaged, typically caused by high blood pressure, high cholesterol, smoking, or inflammation from other diseases [3]. Cholesterol, or low-density lipoprotein (LDL), then enters the damaged endothelium, initiating an inflammatory response and signaling macrophages to digest the excess fat. These cells leave behind debris and lipids, causing additional cell recruitment, such as smooth muscle cells (SMCs), and the deposition of fibrous matrices [4]. Over time, the plaque calcifies, resulting in ischemia, the reduction/obstruction of oxygenated blood supply to tissues [5]. Ischemia causes cells and tissues to die and lose function, which leads to additional health complications, including

heart attacks and peripheral arterial disease (PAD) [6]. In the U.S., 10 to 12 million people suffer from some form of PAD, approximately 20% of whom are more than 60 years of age [7], [8]. While PAD causes a variety of symptoms, intermittent claudication, pain or cramping in the legs upon exertion, is the most common [9]. This pain is intermittent and can quickly subside after exertion, resulting in many patients avoiding medical attention and compounding their health problems [10].

In severe cases, PAD can lead to critical limb ischemia (CLI), where oxygenated blood no longer reaches the lower extremities of the body. Approximately 1% of patients with PAD are diagnosed with CLI [11]. However, with the increasing prevalence of diabetes, the number of patients with CLI is expected to rise, as the progression of CLI is accelerated in diabetics [12]. Patients with CLI can experience resting pain and eventually tissue loss [13]. One year after diagnosis, 25% of patients suffering from CLI will die and 30% will have some form of amputation [14]. After 5 years, over 60% of patients will die. Due to the increasing number of deaths and costs attributed to these ischemic diseases, it is critical to create new therapies focused on rebuilding vasculature to provide cells with sufficient oxygen and nutrients to prevent necrosis and amputations.

## 1.2 Current Cardiovascular Disease Treatments

The current treatment methods for patients afflicted with PAD include lifestyle modifications, pharmaceutical therapies, and surgical treatment. In the early stages of PAD, patients experience mild symptoms, which can be managed through exercise and pharmaceuticals. Patients with more severe symptoms may undergo surgical intervention to first determine the extent of the disease and then to restore blood flow.

As mentioned, exercise is one effective non-invasive method to treat PAD. Patients who underwent supervised exercise programs demonstrated improved walking ability and reduced intermittent claudication [15]. However, exercise is not always an option due to age of the patient or functional limitations caused by the disease [16]. Other lifestyle changes include diet modification. As many patients with PAD have high cholesterol levels [6], a diet low in saturated and trans-fat may help lower cholesterol levels [17]. Since some patients with PAD are also likely to suffer from diabetes, management of diabetic symptoms may help reduce limb-related complications as diabetes causes endothelial dysfunction through increased adhesion molecule expression [18]. Smoking is also a major cause of many CVDs, including heart attacks, stroke, and PAD [19]. Smoking cessation is also effective in reduction of PAD symptoms [20].

While lifestyle changes can aid in the treatment of PAD, medication is prescribed when lifestyle modifications are not effective. Typically, pharmaceutical therapies involve medications to reduce blood pressure and/or cholesterol [9]. Atorvastatin has been shown to improve claudication symptoms by lowering lipid levels [21]. To reduce the risk of stroke or vascular death, patients may also be given aspirin first and then clopidogrel, if patients experience additional complications with aspirin, as an antiplatelet therapy [22], [23]. Various vasodilators are also prescribed, including cilostazol, minoxidil, and hydralazine, to augment blood flow. Research has shown cilostazol reduced patients intermittent claudication and increased pain-free walking [24]. While all these medications improve symptoms, these various pharmaceuticals are limited to patients with mild to moderate PAD [23].

In severe cases when CLI is a factor, or when the above treatments are not effective, surgery may be required. Depending on the location and severity, an angiography is performed to determine the surgical treatment [25]. Less severe cases can be treated with endovascular

interventions, such as stenting and angioplasty. These procedures involve insertion of a surgical device into the patient's artery. The device is moved through the patient's vessels to the site of plaque deposition. Either a stent is inserted, to keep the vessel dilated, or a balloon is inflated, to break apart the plaque, resulting in improved blood flow [26]. More complicated surgeries require revascularization intervention. The most common is bypass surgery, a technique in which the obstructed blood vessel is bypassed through the creation of a new blood vessel [27]. Most bypass surgeries involve the removal of a blood vessel from healthy tissue to replace the diseased vessel [28]. Typically, 50-90% of CLI patients will require one or more of these surgical interventions [10]. Despite the success of surgery at preventing amputation and death, complications can arise from surgery and additional surgery may be needed for the continued treatment of PAD [29]. Unfortunately, due to the progression of their disease, surgery may not be suitable for some patients, leading to the critical need for new solutions/therapies in PAD treatment.

## 1.3 Vascular Development and Physiology

To develop alternative revascularization therapies, intimate understanding of the cardiovascular system is necessary. The function of the cardiovascular system is to maintain homeostasis throughout the body, through delivering oxygen and nutrients to cells, and in return, removing waste from cellular production [30]. The cardiovascular system consists of the heart and blood vessels that run throughout the entire body. Blood vessels are broken down into multiple subsets: arteries, veins, arterioles, venules, and capillaries [31]. The heart pumps blood through the arteries, carrying oxygenated blood away from the heart. Arteries consist of multiple layers of cells, including smooth muscle cells which maintain vascular tone [32]. The arteries branch into arterioles and ultimately, capillaries, the smallest blood vessels. Capillaries are typically one cell

layer, ranging in size from 10 to 15 μm in diameter, and directly involved in nutrient delivery to cells [33]. Ultimately, the venous system returns the deoxygenated blood back to the heart through venules and then veins [34].

The structure of blood vessels varies depending on their type. Veins and arteries are the largest, consisting of three layers [35]. The outer layer, called the tunica adventitia, is composed collagen, which anchor the blood vessel to the surrounding tissues [36]. The middle layer, called the tunica media, is made up of smooth muscle cells and elastic fibers, which are larger in arteries than veins. Not only does this layer provide support for blood vessels, but also changes the shape of blood vessels to regulate blood flow and blood pressure [37]. The inner layer, called the tunica intima, is the thinnest layer consisting of a simple squamous endothelium and connective tissue [38].

The endothelium is present in all blood vessels, including capillaries, and is made up of endothelial cells (ECs), the building blocks of blood vessels, and mural cells [39]. Endothelial cells make up the inner lining of blood vessels and are in direct contact with the blood. In general, the main function of these cells is to regulate hemostasis, but other functions include leukocyte trafficking, regulation of vascular tone, and coagulation [40]. Endothelial cells can signal mural cells to aid in vessel stabilization [41]. Mural cells also have a role in angiogenesis and the maturation of blood vessels. In capillaries, mural cells are typically pericytes, while in arteries and veins, these are typically smooth muscles cells [42].

Blood vessels can form via three distinct, yet complementary mechanisms, vasculogenesis, angiogenesis, and arteriogenesis. Vasculogenesis is the de novo formation of vessels from the differentiation of endothelial and hematopoietic progenitor cells into a primitive vascular plexus [43], [44]. Typically, this process occurs primarily in embryonic development, but recent research

has shown the ability of vasculogenesis in adults [45]. Angiogenesis is the sprouting of new vessels from pre-existing vessels and is the major process for blood vessel development in adults [46]–[48]. In brief, angiogenesis is a complex process regulated by endothelial cells in response to various signals present in the extracellular matrix (ECM) [49]–[51]. Angiogenesis will be discussed in more detail in Chapter 4. Arteriogenesis is a distinct process and the second major form of blood vessel growth after birth [52]. During arteriogenesis, pre-existing arterioles are remodeled into larger diameter arteries. In contrast to angiogenesis, arteriogenesis is driven in response to increased blood pressure instead of hypoxia [53]. Arteriogenesis is critical for the ischemic limb survival as increased vessel diameters can handle increased blood volumes, resulting in decrease blood pressure [54].

## 1.4 Tissue Engineering Approaches

As previously mentioned, the current strategies for PAD treatment are not suitable or effective for every patient, especially those with more severe conditions, such as CLI. Several tissue engineering approaches have, for this reason, emerged to promote angiogenesis and vasculogenesis as the formation of new blood vessels will provide an alternative route to deliver oxygen and nutrients to cells and tissues. Approaches such as angiogenic growth factor delivery and cell-based tissue engineering constructs have shown potential to facilitate revascularization. These approaches generally implement two different strategies, implantation of vasculature formed *ex vivo* or vascularization formation *in vivo*. Both approaches aim to treat ischemic conditions and prevent tissue death and organ failure.

During angiogenesis, growth factors are key in signaling ECs to sprout and proliferate, creating new vasculature [55], [56]. In theory, delivering growth factors to patients could stimulate

revascularization of ischemic regions. As a result, many growth factor therapies involve the delivery of angiogenic factors, such as vascular endothelial growth factor (VEGF), transforming growth factor (TGF-β), or basic fibroblast growth factor (bFGF), to stimulate endothelial cells recruitment, and, eventually, increase vessel formation [57]–[59]. VEGF is the most common growth factor used to promote capillary morphogenesis. VEGF has been shown to recruit ECs while signaling them to proliferate and to facilitate pericyte recruitment for vessel stabilization [58], [60]. bFGF stimulates VEGF expression in endothelial cells and stromal cells, furthering invasion, migration, proliferation, and vessel formation [61]–[63]. TGF-β induces angiogenesis indirectly through stimulating the expression of VEGF or other angiogenic factors in epithelial or other cell types [64]. TGF-β also aids in pericyte adhesion and differentiation [65].

In many cases, the growth factors are administered systematically i.e. via the blood stream. In some cases, engineered nanoparticles or scaffolds can be used to control the release of the growth factors. For nanoparticles, PLGA can be used to encapsulate the growth factors, creating 1 – 100 nm diameter particles [66]. These nanoparticles can also be designed to target specific tissues, aiding in delivery [67]. Nanoparticles can either be directly injected into the tissue or intravenously [68]. Similarly, scaffolds can be designed to conjugate growth factors to natural or synthetic biomaterials [69]–[71]. These scaffolds mimic the ECM, allowing growth factors to be readily active or activated through cleavage from cells [68]. However, preformed scaffolds, as opposed to hydrogels that gel *in situ*, are the more invasive of the previously mentioned techniques, as they involve surgical implantation [72].

Unfortunately, growth factor delivery approaches are limited by rapid diffusion, short half-lives, and poor biostability, leading to the formation of immature and often unstable vasculature [73]. In addition, growth factors must also be delivered in a specific order to mimic their natural

expression patterns observed in vessel development [73], [74]. Due to these complexities, human clinical trials have not been successful using growth factor delivery [75], [76].

While growth factor delivery focuses on stimulating the existing cells and vasculature, cell-based therapies focus on providing new cells for vessel formation. Many cell-based approaches involve the delivery of cells to directly differentiate into capillary structures or provide angiogenic cues to accelerate revascularization. Various cell types have been shown to create new capillary networks *in vivo*, such as human umbilical vein endothelial cells (HUVECs), human aortic endothelial cells (HAECs), and human microvascular endothelial cells (HMVECs) [77]–[81]. However, the delivery of endothelial cells alone typically results in the formation of immature vessels. These vessels are unstable, unable to regulate permeability, and do not demonstrate characteristics associated with mature vessels [82]. Recent studies have demonstrated the co-delivery of endothelial cells and some type of stromal cells promotes the formation of stable, mature vasculature [83], [84].

Similar to growth factor therapies, cell-based approaches involve directly injecting cells into the patient or incorporating the cells into some type of engineered construct using either a top-down or bottom-up approach. Top-down approaches involve encapsulating cells in larger structures, such as scaffolds, to create an engineered tissue [85]. Scaffolds are created with natural or synthetic biomaterials and embedded with various growth factors and proteins to mimic the chemical, mechanical, and biological properties of the extracellular matrix (ECM) [72]. Bottom-up approaches, or modular tissue engineering, involve the creation of smaller building blocks which are assembled into larger tissues structures for enhanced biomimicry [86]. These building blocks, comprised of cells and a supporting matrix, can be created in a number of ways, such as self-assembled aggregation, hydrogel microfabrication, or direct printing [87]–[90].

Despite these advances, there are still critical challenges that plague the application of engineered tissues for revascularization. Immunological response is one of these concerns. Since most of the proposed therapies involve transplanting cells and other supporting material, the host body may elicit an immunological response to the cells (if they are not autologous), materials, or both, resulting in rejection of the implant [91]. There are other issues related to ethics and misinformation, especially when stem cells are involved. The term stem cell carries a stigma because many believe all stem cells are embryonic stem cells. While stem cells can come from a variety of sources, translational applications may be limited, whether or not embryonic cells are involved, due to this misunderstood stigma [92], [93]. Teratoma formation is another risk, which can lead to additional health complications [94], [95].

The biggest hurdle for the clinical translation of cell-based approaches is the limited supply of cells [96]. While cell sourcing may be abundant for *in vitro* or even small mammal *in vivo* studies, the number of cells required significantly increases when shifting to human applications. One study using endothelial progenitor cells (EPCs) for therapeutic neovascularization in mice required 0.5-2.0 x $10^4$ human EPCs/ g of host body weight [97]. Typical expansion of EPCs from peripheral blood mononuclear cells (MNCs) from human volunteers yields 5 million cells per 100 mL of blood, which would equate to over 12 L of blood needed to harvest enough EPCs for one clinical human trial [97]. Another therapeutic angiogenesis pilot study required over 1.6 billion cells per treatment per individual [98]. While one clinical study found the effects of cell number directly correlated with the success of the therapy, the results are inconclusive due to a limited sampling size [99]. Additional experiments/clinical trials are needed to ultimately determine if cell numbers correlate with therapeutic success.

## 1.5 Induced Pluripotent Stem Cells (iPSCs)

To address the limitations of these cell-based therapies, various alternative cell sources have been considered, including a new type of stem cell. Self-renewing, living cells were first discovered in 1961 [100]. These cells, since coined stem cells, have the potential for differentiation into different cell types and self-renewal without senescence [101]–[104]. Stem cells are typically classified as embryonic (ESC) or adult (ASC) and can have varying degrees of multi lineage potential, i.e. how many cell type differentiations are possible [105], [106]. Unfortunately, as these cells differentiate, they lose their self-renewal potential, limiting their lifespan [107]. While research has demonstrated the promising potential of stem cells for the treatment of various diseases [108]–[111], as previously mentioned, the ethical issues and stigma surrounding ESC isolation from embryos creates a barrier for use of other stem cells [112]–[114].

However, in 2006, the excitement for stem cell applications was reignited with the generation of a new type of stem cell, induced pluripotent stem cells (iPSCs). Unlike ESCs, or ASCs, this cell type is derived from reprogramming adult somatic cells to an embryonic stem cell-like state with properties similar to ESCs. iPSCs were first generated by using a combination of 4 reprogramming factors, including Oct4 (Octamer binding transcription factor-4), Sox2 (Sex determining region Y-box 2), Klf4 (Kruppel Like Factor-4), and c -Myc [115]. These genes are highly expressed in ESCs and implicated in pluripotency and the self-renewal abilities of cells [116]. Additional research since the discovery of iPSCs has found other reprograming factors to replace one or more of the original factors or enhance the reprogramming efficiency [117]–[120]. Most importantly, the ability of iPSCs to self-renew and differentiate like ESCs has been demonstrated in research [121]–[123]. Due to these similarities, iPSCs could be used as an alternative for ESCs in various clinical applications.

iPSCs may solve many of the challenges current cell-based approaches face. First, iPSCs can be autologous, i.e. derived from the same individual, possibly eliminating any immunological concerns as the patient's body should recognize these cells as being native. Second, since these cells theoretically can be derived from numerous adult cell types, there is reduced ethical concern over as some claim that iPSCs should be considered equally to ESC because, in theory, iPSCs could be used to create human embryos [124]. Third, these cells are pluripotent meaning they can theoretically differentiate into any cell, allowing for their application not only in revascularization but various other therapies [115]. Ultimately, iPSCs can be created from a plentiful source, such as skin, and theoretically have the potential to proliferate indefinitely, resulting in a potentially larger reservoir of cells. While iPSCs offer great potential for regenerative medicine, there are limited research and clinical studies on how these cells behave *in vitro* and *in vivo* [125]–[127].

iPSCs have been successfully differentiated into an endothelial cell lineage. These induced pluripotent stem cell derived endothelial cells (iPSC-ECs) express markers, morphologies, and phenotypes characteristic of other endothelial cells [128]–[131]. iPSC-ECs also have the ability to differentiate and form vessel-like networks when seeded on top of Matrigel [132]–[134]. Additionally, iPSC-ECs are capable of forming vasculature in Matrigel plugs *in vivo*, demonstrating some therapeutic revascularization potential [133], [135], [136]. However, comparison of the iPSC-ECs' vasculogenic potential to other endothelial cells, specifically in terms of quantity, quality, and mechanisms of vasculature formation is mostly unknown. While similar capillary networks between iPSC-ECs and human umbilical vein endothelial cells (HUVECs) was demonstrated in recent research, these studies investigated 2D vessel formation, which has little physiological relevance to the proposed therapeutic applications [137].

## 1.6 Hypothesis

This project will characterize the vascularization potential of ECs derived from induced pluripotent stem cells (iPSCs), a potentially autologous source of ECs, that may overcome many of the limitations of current cell sources. *The overall goal of this research is to assess whether iPSC-ECs form the same robust, stable microvasculature as previously documented for other sources of ECs.* Preliminary experiments from a 3D fibrin-based sprouting angiogenesis assay consisting of ECs co-cultured with normal human lung fibroblasts (NHLF) have shown that these iPSC-ECs create vessel-like networks *in vitro* at a slower rate than human umbilical vein endothelial cells (HUVECs). Based on these preliminary data, ***we hypothesize the following:***

1) ***iPSC-ECs exhibit sprouting deficiencies, in both quantity and quality, compared to HUVECs.***
2) ***iPSC-ECs exhibit differential ECM remodeling capabilities during capillary morphogenesis compared to HUVECs.***

## 1.7 Specific Aims

We propose the following specific aims to address the hypotheses and outline how the overall project will be accomplished:

**Aim 1. Quantify the ability of iPSC- ECs to form new vasculature in 3D fibrin culture models of angiogenic sprouting and compare their potential to that of more established EC sources.** This aim will focus on assessing the functionality of iPSC-EC vasculature and how these cells affect the characteristics of the microenvironment using the an established microcarrier bead assay. Fluorescent microscopy will be used to quantify the total network lengths of neovasculature

in 3D fibrin cultures sprouting from EC-coated microcarrier beads. Several hallmarks of functional vessels will also be assessed to qualify iPSC-EC vasculature.

**Aim 2. Identify the expression and/or activity of critical matrix metalloproteinases in the development of microvasculature networks formed via iPSC-ECs.** In order to understand how iPSC-ECs remodel the fibrin matrix during capillary morphogenesis, this aim will focus on inhibiting critical proteases implicated in capillary morphogenesis and determining quantitatively if the rate of capillary sprouting in 3D tissue assays change. Experiments will be performed in elevated matrix densities or with the addition of chemical inhibitors to affect the sprouting formation of the ECs. The quantity and quality of capillary networks formed will be assessed in 3D tissue cultures using an established microcarrier bead assay. Furthermore, the expression of these key proteases at the RNA, protein, and activity level will be quantified.

**Aim 3. Determine the ability of iPSC-ECs to stimulate vascularization *in vivo* using a subcutaneous injection model in a SCID-mouse.** This aim will assess the capability of iPSC-ECs to form functional microvascualture. ECs, fibroblasts, and fibrin will be injected in a subcutaneous dorsal flank of SCID mice and monitored over time. Immunohistochemical and immunofluorescent staining and imaging of the removed implants will be used to determine the efficiency and potential of using iPSC-ECs in a clinical setting.

The insights gained from these aims will guide the choice of using autologous sources of ECs, specifically iPSC-ECs, to build functional vasculature, and most importantly provide fundamental knowledge about the mechanisms by which iPSC-ECs form vasculature. In the long term, this project will move cell-based revascularization therapy closer to clinical applications through a fundamental understanding of cell sourcing potential.

## 1.8 Translational Potential

As previously mentioned, cardiovascular disease is the leading cause of death worldwide and the number of patients affected is rising. While various pharmaceutical or surgical treatments are currently available to reestablish proper blood flow in ischemic tissue, these methods can be highly invasive. As a result, development of regenerative medicine therapies offers one potential solution to restore blood flow to damaged tissue.

For patient translation, all therapeutic products need to be approved by the US Food and Drug Administration (FDA). Therapies, such as the growth factor delivery, utilizing defined biomaterials and compounds are more commercially successful in regenerative medicine [138], [139]. Despite promising pre-clinical and early clinical results, many of the approaches to deliver growth factors to signal angiogenesis in ischemic tissue did not result in functional restoration [140]. While cell-based approaches may offer more control over vascular formation, FDA approval of these methods is more complex. Aside from approval over the supporting material administered, cells activity and function can be highly variable, raising the question about safety and efficacy [141]. For this reason, there is no FDA approved cell-based therapy currently employed for cardiovascular disease treatment [138], [139]. We employed fibrin as the supporting matrix, as it is FDA cleared for use in human patients [142].

iPSCs and their derivatives offer additional complications to clinical translation. One of the major obstacles for iPSCs is their tendency to form tumors *in vivo.* Once differentiated, cells lose their pluripotent potential. However, the viruses, used originally to alter the cells, encode for oncogenic transcription factors [143]. Furthermore, as cells can be differentiated into multiple lineages, iPSC therapies could potentially delivery an incorrect population of cells [144]. While iPSC-ECs potential autologous nature would ease translation due to reduced or no immunological

concerns, additional research is necessary to ensure the patients do not elicit an immunological response to the cells [145].

## 1.9 Overview of Thesis

Chapter 1 discussed the motivation for the dissertation, current treatment methods for CVD, an overview of the cardiovascular system, possible new tissue engineering therapies, the overall hypothesis, the aims addressing the hypothesis, and the translational potential of this work. Chapter 2 defines the nature of endothelial cells and their importance in the angiogenic/vasculogenic process. This chapter also establishes whether the iPSC-ECs display an endothelial cell lineage through characterization of key markers expressed by other mature endothelial cells.

Parts of Chapter 3 were first published in 2018 in Scientific Reports following peer review, and address aim 1 by performing an *in vitro* assessment of iPSC-EC microvascular formation in comparison to HUVECs. Endothelial cells were coated on microcarrier beads and embedded with fibroblasts in a fibrin matrix to quantify the capillary morphogenic process. Microvascular formation, by both HUVECs and iPSC-ECs, was characterized with variations of cell lots, media formulation, and cell density. Vessel maturity was also qualitatively assessed by visually examining microvessels for the presence of hollow lumens, basement membrane deposition, and pericyte association.

Parts of Chapter 4 were also first published in 2018 in Scientific Reports following peer review and address aim 2 by identifying a candidate mechanism by which iPSC-ECs remodel the ECM during capillary morphogenesis. Various inhibition studies were conducted, either through elevated matrix densities or the addition of chemical protease inhibitors, and the expression of key

proteases implicated in capillary morphogenesis were evaluated. The goal of this study was to better understand iPSC-ECs' invasive mechanisms and determine a possible cause for iPSC-EC vessel network differences *in vitro*.

In Chapter 5, the *in vivo* potential of iPSC-ECs is evaluated in a physiologically relevant mouse model. This chapter addresses aim 3 by evaluating iPSC-ECs' ability to form vessels and inosculate with the host vasculature in comparison to HUVECs. These cells were co-injected with NHLFs and fibrin subcutaneously on the dorsal surface of SCID mice. This study also investigated vessel maturation and determined whether there are differences between *in vivo* and *in vitro* iPSC-EC vessel formation.

Finally, the key findings and results are summarized in Chapter 6, with additional discussion of future directions and translational implications. The appendices contain detailed experimental procedures, to facilitate future reproducibility, and smaller studies, involving the reprograming and differentiation of iPSC-ECs and characterization of media composition effects on HUVECs.

## 1.10 References


[1] D. Mozaffarian *et al.*, "Heart disease and stroke statistics--2015 update: a report from the American Heart Association," *Circulation*, vol. 131, no. 4, pp. e29-322, Jan. 2015.

[2] "Atherosclerosis | National Heart, Lung, and Blood Institute (NHLBI)." [Online]. Available: https://www.nhlbi.nih.gov/health-topics/atherosclerosis. [Accessed: 13-Jun-2018].

[3] "Atherosclerosis." [Online]. Available: http://www.heart.org/HEARTORG/Conditions/Cholesterol/AboutCholesterol/Atherosclerosis_UCM_305564_Article.jsp#.WyGC-y2ZNE4. [Accessed: 13-Jun-2018].

[4] J. F. Bentzon, F. Otsuka, R. Virmani, and E. Falk, "Mechanisms of Plaque Formation and Rupture," *Circ. Res.*, vol. 114, no. 12, pp. 1852–1866, Jun. 2014.

[5] A. Shioi and Y. Ikari, “Plaque Calcification During Atherosclerosis Progression and Regression,” *J. Atheroscler. Thromb.*, vol. 25, no. 4, pp. 294–303, Apr. 2018.

[6] K. Ouriel, “Peripheral arterial disease,” *The Lancet*, vol. 358, no. 9289, pp. 1257–1264, Oct. 2001.

[7] V. L. Roger *et al.*, “Heart Disease and Stroke Statistics—2011 Update,” *Circulation*, vol. 123, no. 4, pp. e18–e209, Feb. 2011.

[8] “Peripheral Artery Disease | National Heart, Lung, and Blood Institute (NHLBI).” [Online]. Available: https://www.nhlbi.nih.gov/health-topics/peripheral-artery-disease. [Accessed: 13-Jun-2018].

[9] R. J. Valentine, D. C. MacGillivray, J. W. DeNobile, D. A. Snyder, and N. M. Rich, “Intermittent claudication caused by atherosclerosis in patients aged forty years and younger,” *Surgery*, vol. 107, no. 5, pp. 560–565, May 1990.

[10] L. Norgren *et al.*, “Inter-Society Consensus for the Management of Peripheral Arterial Disease (TASC II),” *J. Vasc. Surg.*, vol. 45 Suppl S, pp. S5-67, Jan. 2007.

[11] “Prevalence, Incidence, and Outcomes of Critical Limb Ischemia in the US Medicare Population,” *Vascular Disease Management*. [Online]. Available: http://www.vasculardiseasemanagement.com/content/prevalence-incidence-and-outcomes-critical-limb-ischemia-us-medicare-population. [Accessed: 13-Jun-2018].

[12] M. Engelhardt *et al.*, “Critical Limb Ischaemia: Initial Treatment and Predictors of Amputation-free Survival,” *Eur. J. Vasc. Endovasc. Surg.*, vol. 43, no. 1, pp. 55–61, Jan. 2012.

[13] H. Lawall, P. Bramlage, and B. Amann, “Treatment of peripheral arterial disease using stem and progenitor cell therapy,” *J. Vasc. Surg.*, vol. 53, no. 2, pp. 445–453, Feb. 2011.

[14] M. G. Davies, “Criticial Limb Ischemia: Epidemiology,” *Methodist DeBakey Cardiovasc. J.*, vol. 8, no. 4, pp. 10–14, 2012.

[15] G. G. Schiattarella *et al.*, “Physical activity in the prevention of peripheral artery disease in the elderly,” *Front. Physiol.*, vol. 5, Mar. 2014.

[16] N. M. Hamburg and G. J. Balady, “Exercise Rehabilitation in Peripheral Artery Disease: Functional Impact and Mechanisms of Benefits,” *Circulation*, vol. 123, no. 1, pp. 87–97, Jan. 2011.

[17] “The Skinny on Fats.” [Online]. Available: http://www.heart.org/HEARTORG/Conditions/Cholesterol/PreventionTreatmentofHighCholesterol/The-Skinny-on-Fats_UCM_305628_Article.jsp#.WyGjIC2ZNE4. [Accessed: 13-Jun-2018].

[18] A. D. Association, “Peripheral Arterial Disease in People With Diabetes,” *Diabetes Care*, vol. 26, no. 12, pp. 3333–3341, Dec. 2003.

[19] C. for D. C. and Prevention (US), N. C. for C. D. P. and H. Promotion (US), and O. on S. and Health (US), *Cardiovascular Diseases*. Centers for Disease Control and Prevention (US), 2010.

[20] D. Hennrikus *et al.*, “Effectiveness of a Smoking Cessation Program for Peripheral Artery Disease Patients: A Randomized Controlled Trial,” *J. Am. Coll. Cardiol.*, vol. 56, no. 25, pp. 2105–2112, Dec. 2010.

[21] E. R. Mohler, W. R. Hiatt, and M. A. Creager, “Cholesterol Reduction With Atorvastatin Improves Walking Distance in Patients With Peripheral Arterial Disease,” *Circulation*, vol. 108, no. 12, pp. 1481–1486, Sep. 2003.

[22] T. W. Rooke *et al.*, “2011 ACCF/AHA Focused Update of the Guideline for the Management of Patients With Peripheral Artery Disease (Updating the 2005 Guideline): A Report of the American College of Cardiology Foundation/American Heart Association Task Force on Practice Guidelines,” *Circulation*, vol. 124, no. 18, pp. 2020–2045, Nov. 2011.

[23] D. R. Hennion and K. A. Siano, “Diagnosis and Treatment of Peripheral Arterial Disease,” *Am. Fam. Physician*, vol. 88, no. 5, pp. 306–310, Sep. 2013.

[24] R. L. Pande, W. R. Hiatt, P. Zhang, N. Hittel, and M. A. Creager, “A pooled analysis of the durability and predictors of treatment response of cilostazol in patients with intermittent claudication,” *Vasc. Med. Lond. Engl.*, vol. 15, no. 3, pp. 181–188, Jun. 2010.

[25] J. P. Eiberg, J. B. Grønvall Rasmussen, M. A. Hansen, and T. V. Schroeder, “Duplex Ultrasound Scanning of Peripheral Arterial Disease of the Lower Limb,” *Eur. J. Vasc. Endovasc. Surg.*, vol. 40, no. 4, pp. 507–512, Oct. 2010.

[26] A. K. Thukkani and S. Kinlay, “Endovascular Intervention for Peripheral Artery Disease,” *Circ. Res.*, vol. 116, no. 9, pp. 1599–1613, Apr. 2015.

[27] S. M. Vartanian and M. S. Conte, “Surgical Intervention for Peripheral Arterial Disease,” *Circ. Res.*, vol. 116, no. 9, pp. 1614–1628, Apr. 2015.

[28] “Cardiac Procedures and Surgeries.” [Online]. Available: http://www.heart.org/HEARTORG/Conditions/HeartAttack/TreatmentofaHeartAttack/Cardiac-Procedures-and-Surgeries_UCM_303939_Article.jsp#.WyGs8S2ZNE4. [Accessed: 13-Jun-2018].

[29] D. J. Adam *et al.*, “Bypass versus angioplasty in severe ischaemia of the leg (BASIL): multicentre, randomised controlled trial,” *Lancet Lond. Engl.*, vol. 366, no. 9501, pp. 1925–1934, Dec. 2005.

[30] M. K. Pugsley and R. Tabrizchi, “The vascular system: An overview of structure and function,” *J. Pharmacol. Toxicol. Methods*, vol. 44, no. 2, pp. 333–340, Sep. 2000.

[31] pmhdev, “How does the blood circulatory system work?,” *PubMed Health*, Aug. 2016.

[32] R. E. Shadwick, “Mechanical design in arteries,” *J. Exp. Biol.*, vol. 202, no. 23, pp. 3305–3313, Dec. 1999.

[33] J. M. Felner, “An Overview of the Cardiovascular System,” in *Clinical Methods: The History, Physical, and Laboratory Examinations*, 3rd ed., H. K. Walker, W. D. Hall, and J. W. Hurst, Eds. Boston: Butterworths, 1990.

[34] S. Hochauf, R. Sternitzky, and S. M. Schellong, “[Structure and function of the peripheral venous system],” *Herz*, vol. 32, no. 1, pp. 3–9, Feb. 2007.

[35] W. D. Tucker and S. S. Bhimji, “Anatomy, Blood Vessels,” in *StatPearls*, Treasure Island (FL): StatPearls Publishing, 2018.

[36] M. Corselli, C.-W. Chen, B. Sun, S. Yap, J. P. Rubin, and B. Péault, “The Tunica Adventitia of Human Arteries and Veins As a Source of Mesenchymal Stem Cells,” *Stem Cells Dev.*, vol. 21, no. 8, pp. 1299–1308, May 2012.

[37] pmhdev, “Tunica Media - National Library of Medicine,” *PubMed Health*. [Online]. Available: https://www.ncbi.nlm.nih.gov/pubmedhealth/PMHT0030285/. [Accessed: 14-Jun-2018].

[38] pmhdev, “Tunica Intima - National Library of Medicine,” *PubMed Health*. [Online]. Available: https://www.ncbi.nlm.nih.gov/pubmedhealth/PMHT0030284/. [Accessed: 14-Jun-2018].

[39] B. Alberts, A. Johnson, J. Lewis, M. Raff, K. Roberts, and P. Walter, “Blood Vessels and Endothelial Cells,” *Mol. Biol. Cell 4th Ed.*, 2002.

[40] M. Félétou, *Multiple Functions of the Endothelial Cells*. Morgan & Claypool Life Sciences, 2011.

[41] K. Gaengel, G. Genové, A. Armulik, and C. Betsholtz, “Endothelial-Mural Cell Signaling in Vascular Development and Angiogenesis,” *Arterioscler. Thromb. Vasc. Biol.*, vol. 29, no. 5, pp. 630–638, May 2009.

[42] “Specification and Diversification of Pericytes and Smooth Muscle Cells from Mesenchymoangioblasts: Cell Reports.” [Online]. Available: https://www.cell.com/cell-reports/abstract/S2211-1247(17)30644-7. [Accessed: 14-Jun-2018].

[43] G. L. Semenza, “Vasculogenesis, angiogenesis, and arteriogenesis: Mechanisms of blood vessel formation and remodeling,” *J. Cell. Biochem.*, vol. 102, no. 4, pp. 840–847, Sep. 2007.

[44] S. Murasawa and T. Asahara, “Endothelial progenitor cells for vasculogenesis,” *Physiol. Bethesda Md*, vol. 20, pp. 36–42, Feb. 2005.

[45] T. Asahara and A. Kawamoto, “Endothelial progenitor cells for postnatal vasculogenesis,” *Am. J. Physiol. Cell Physiol.*, vol. 287, no. 3, pp. C572-579, Sep. 2004.

[46] T. H. Adair and J.-P. Montani, *Overview of Angiogenesis*. Morgan & Claypool Life Sciences, 2010.

[47] D. H. Ausprunk and J. Folkman, “Migration and proliferation of endothelial cells in preformed and newly formed blood vessels during tumor angiogenesis,” *Microvasc. Res.*, vol. 14, no. 1, pp. 53–65, Jul. 1977.

[48] “Endothelial Cells, Angiogenesis, and Vasculogenesis.” [Online]. Available: https://www.stemcell.com/endothelial-cells-angiogenesis-and-vasculogenesis-lp.html. [Accessed: 11-Jun-2018].

[49] T. H. Barker, “The role of ECM proteins and protein fragments in guiding cell behavior in regenerative medicine,” *Biomaterials*, vol. 32, no. 18, pp. 4211–4214, Jun. 2011.

[50] T. T. Chen, A. Luque, S. Lee, S. M. Anderson, T. Segura, and M. L. Iruela-Arispe, “Anchorage of VEGF to the extracellular matrix conveys differential signaling responses to endothelial cells,” *J. Cell Biol.*, vol. 188, no. 4, pp. 595–609, Feb. 2010.

[51] A. A. Ucuzian, D. V. Bufalino, Y. Pang, and H. P. Greisler, “Angiogenic endothelail cell invasion into fibrin is stimulated by proliferating smooth muscle cells,” *Microvasc. Res.*, vol. 90, Nov. 2013.

[52] N. van Royen, J. J. Piek, I. Buschmann, I. Hoefer, M. Voskuil, and W. Schaper, “Stimulation of arteriogenesis; a new concept for the treatment of arterial occlusive disease,” *Cardiovasc. Res.*, vol. 49, no. 3, pp. 543–553, Feb. 2001.

[53] D. Della-Morte and T. Rundek, “The role of shear stress and arteriogenesis in maintaining vascular homeostasis and preventing cerebral atherosclerosis,” *Brain Circ.*, vol. 1, no. 1, p. 53, Jan. 2015.

[54] I. Buschmann and W. Schaper, “Arteriogenesis Versus Angiogenesis: Two Mechanisms of Vessel Growth,” *News Physiol. Sci. Int. J. Physiol. Prod. Jointly Int. Union Physiol. Sci. Am. Physiol. Soc.*, vol. 14, pp. 121–125, Jun. 1999.

[55] S. S. Said, J. G. Pickering, and K. Mequanint, “Advances in Growth Factor Delivery for Therapeutic Angiogenesis,” *J. Vasc. Res.*, vol. 50, no. 1, pp. 35–51, 2013.

[56] J. E. Markkanen, T. T. Rissanen, A. Kivelä, and S. Ylä-Herttuala, “Growth factor-induced therapeutic angiogenesis and arteriogenesis in the heart–gene therapy,” *Cardiovasc. Res.*, vol. 65, no. 3, pp. 656–664, Feb. 2005.

[57] J. E. Nör, J. Christensen, D. J. Mooney, and P. J. Polverini, “Vascular Endothelial Growth Factor (VEGF)-Mediated Angiogenesis Is Associated with Enhanced Endothelial Cell Survival and Induction of Bcl-2 Expression,” *Am. J. Pathol.*, vol. 154, no. 2, pp. 375–384, Feb. 1999.

[58] G. D. Yancopoulos, S. Davis, N. W. Gale, J. S. Rudge, S. J. Wiegand, and J. Holash, “Vascular-specific growth factors and blood vessel formation,” *Nature*, vol. 407, no. 6801, pp. 242–248, Sep. 2000.

[59] R. Y. Kannan, H. J. Salacinski, K. Sales, P. Butler, and A. M. Seifalian, “The roles of tissue engineering and vascularisation in the development of micro-vascular networks: a review,” *Biomaterials*, vol. 26, no. 14, pp. 1857–1875, May 2005.

[60] L. E. Benjamin, I. Hemo, and E. Keshet, “A plasticity window for blood vessel remodelling is defined by pericyte coverage of the preformed endothelial network and is regulated by PDGF-B and VEGF,” *Dev. Camb. Engl.*, vol. 125, no. 9, pp. 1591–1598, May 1998.

[61] R. Montesano, J. D. Vassalli, A. Baird, R. Guillemin, and L. Orci, “Basic fibroblast growth factor induces angiogenesis in vitro.,” *Proc. Natl. Acad. Sci. U. S. A.*, vol. 83, no. 19, pp. 7297–7301, Oct. 1986.

[62] S. Villaschi and R. F. Nicosia, “Angiogenic role of endogenous basic fibroblast growth factor released by rat aorta after injury.,” *Am. J. Pathol.*, vol. 143, no. 1, pp. 181–190, Jul. 1993.

[63] M. Murakami and M. Simons, “Fibroblast growth factor regulation of neovascularization,” *Curr. Opin. Hematol.*, vol. 15, no. 3, pp. 215–220, May 2008.

[64] G. Ferrari, B. D. Cook, V. Terushkin, G. Pintucci, and P. Mignatti, “Transforming growth factor-beta 1 (TGF-B1) induces angiogenesis through vascular endothelial growth factor (VEGF)-mediated apoptosis,” *J. Cell. Physiol.*, vol. 219, no. 2, pp. 449–458, May 2009.

[65] M. D. Sweeney, S. Ayyadurai, and B. V. Zlokovic, “Pericytes of the neurovascular unit: Key functions and signaling pathways,” *Nat. Neurosci.*, vol. 19, no. 6, pp. 771–783, May 2016.

[66] R. S. Roy *et al.*, “Coupling growth-factor engineering with nanotechnology for therapeutic angiogenesis,” *Proc. Natl. Acad. Sci.*, vol. 107, no. 31, pp. 13608–13613, Aug. 2010.

[67] D. Banerjee, R. Harfouche, and S. Sengupta, “Nanotechnology-mediated targeting of tumor angiogenesis,” *Vasc. Cell*, vol. 3, p. 3, Jan. 2011.

[68] K. Lee, E. A. Silva, and D. J. Mooney, “Growth factor delivery-based tissue engineering: general approaches and a review of recent developments,” *J. R. Soc. Interface*, vol. 8, no. 55, pp. 153–170, Feb. 2011.

[69] B. Li *et al.*, “VEGF-loaded biomimetic scaffolds: a promising approach to improve angiogenesis and osteogenesis in an ischemic environment,” *RSC Adv.*, vol. 7, no. 8, pp. 4253–4259, 2017.

[70] Z. Wang, Z. Wang, W. W. Lu, W. Zhen, D. Yang, and S. Peng, “Novel biomaterial strategies for controlled growth factor delivery for biomedical applications,” *NPG Asia Mater.*, vol. 9, no. 10, p. e435, Oct. 2017.

[71] D. Suárez-González *et al.*, “Controlled Multiple Growth Factor Delivery from Bone Tissue Engineering Scaffolds via Designed Affinity,” *Tissue Eng. Part A*, vol. 20, no. 15–16, pp. 2077–2087, Aug. 2014.

[72] J. V. Serbo and S. Gerecht, “Vascular tissue engineering: biodegradable scaffold platforms to promote angiogenesis,” *Stem Cell Res. Ther.*, vol. 4, no. 1, p. 8, Jan. 2013.

[73] Q. Sun *et al.*, “Sustained release of multiple growth factors from injectable polymeric system as a novel therapeutic approach towards angiogenesis,” *Pharm. Res.*, vol. 27, no. 2, pp. 264–271, Feb. 2010.

[74] A. G. Mikos *et al.*, “Engineering complex tissues,” *Tissue Eng.*, vol. 12, no. 12, pp. 3307–3339, Dec. 2006.

[75] T. D. Henry *et al.*, “Intracoronary administration of recombinant human vascular endothelial growth factor to patients with coronary artery disease,” *Am. Heart J.*, vol. 142, no. 5, pp. 872–880, Nov. 2001.

[76] R. J. Powell, P. Goodney, F. O. Mendelsohn, E. K. Moen, and B. H. Annex, “Safety and efficacy of patient specific intramuscular injection of HGF plasmid gene therapy on limb perfusion and wound healing in patients with ischemic lower extremity ulceration: Results of the HGF-0205 trial,” *J. Vasc. Surg.*, vol. 52, no. 6, pp. 1525–1530, Dec. 2010.

[77] J. Nanobashvili *et al.*, “Comparison of Angiogenic Potential of Human Microvascular Endothelial Cells and Human Umbilical Vein Endothelial Cells,” *Eur. Surg.*, vol. 35, no. 4, pp. 214–219, Aug. 2003.

[78] C. J. Jackson and M. Nguyen, “Human microvascular endothelial cells differ from macrovascular endothelial cells in their expression of matrix metalloproteinases,” *Int. J. Biochem. Cell Biol.*, vol. 29, no. 10, pp. 1167–1177, Oct. 1997.

[79] Z. Chen *et al.*, “In vitro angiogenesis by human umbilical vein endothelial cells (HUVEC) induced by three-dimensional co-culture with glioblastoma cells,” *J. Neurooncol.*, vol. 92, no. 2, pp. 121–128, Apr. 2009.

[80] E. M. Conway and P. Carmeliet, “The diversity of endothelial cells: a challenge for therapeutic angiogenesis,” *Genome Biol.*, vol. 5, no. 2, p. 207, 2004.

[81] H.-R. Seo *et al.*, “Intrinsic FGF2 and FGF5 promotes angiogenesis of human aortic endothelial cells in 3D microfluidic angiogenesis system,” *Sci. Rep.*, vol. 6, p. 28832, Jun. 2016.

[82] W. J. Zhang, W. Liu, L. Cui, and Y. Cao, “Tissue engineering of blood vessel,” *J. Cell. Mol. Med.*, vol. 11, no. 5, pp. 945–957, Oct. 2007.

[83] P. Au, J. Tam, D. Fukumura, and R. K. Jain, “Bone marrow-derived mesenchymal stem cells facilitate engineering of long-lasting functional vasculature,” *Blood*, vol. 111, no. 9, pp. 4551–4558, May 2008.

[84] S. J. Grainger and A. J. Putnam, “Assessing the permeability of engineered capillary networks in a 3D culture,” *PloS One*, vol. 6, no. 7, p. e22086, 2011.

[85] C. J. Connon, “Approaches to Corneal Tissue Engineering: Top-down or Bottom-up?,” *Procedia Eng.*, vol. 110, pp. 15–20, Jan. 2015.

[86] A. W. Peterson, D. J. Caldwell, A. Y. Rioja, R. R. Rao, A. J. Putnam, and J. P. Stegemann, “Vasculogenesis and Angiogenesis in Modular Collagen-Fibrin Microtissues,” *Biomater. Sci.*, vol. 2, no. 10, pp. 1497–1508, Oct. 2014.

[87] D. M. Dean, A. P. Napolitano, J. Youssef, and J. R. Morgan, “Rods, tori, and honeycombs: the directed self-assembly of microtissues with prescribed microscale geometries,” *FASEB J. Off. Publ. Fed. Am. Soc. Exp. Biol.*, vol. 21, no. 14, pp. 4005–4012, Dec. 2007.

[88] J. Yeh *et al.*, “Micromolding of shape-controlled, harvestable cell-laden hydrogels,” *Biomaterials*, vol. 27, no. 31, pp. 5391–5398, Nov. 2006.

[89] V. Mironov, T. Boland, T. Trusk, G. Forgacs, and R. R. Markwald, “Organ printing: computer-aided jet-based 3D tissue engineering,” *Trends Biotechnol.*, vol. 21, no. 4, pp. 157–161, Apr. 2003.

[90] J. W. Nichol and A. Khademhosseini, “Modular Tissue Engineering: Engineering Biological Tissues from the Bottom Up,” *Soft Matter*, vol. 5, no. 7, pp. 1312–1319, 2009.

[91] Y. Ikada, “Challenges in tissue engineering,” *J. R. Soc. Interface*, vol. 3, no. 10, pp. 589–601, Oct. 2006.

[92] R. B. M. de Vries, A. Oerlemans, L. Trommelmans, K. Dierickx, and B. Gordijn, "Ethical aspects of tissue engineering: a review," *Tissue Eng. Part B Rev.*, vol. 14, no. 4, pp. 367–375, Dec. 2008.

[93] B. Lo and L. Parham, "Ethical Issues in Stem Cell Research," *Endocr. Rev.*, vol. 30, no. 3, pp. 204–213, May 2009.

[94] S. Y. Lim *et al.*, "In vivo tissue engineering chamber supports human induced pluripotent stem cell survival and rapid differentiation," *Biochem. Biophys. Res. Commun.*, vol. 422, no. 1, pp. 75–79, May 2012.

[95] H. Stachelscheid *et al.*, "Teratoma formation of human embryonic stem cells in three-dimensional perfusion culture bioreactors," *J. Tissue Eng. Regen. Med.*, vol. 7, no. 9, pp. 729–741, Sep. 2013.

[96] C. J. Koh and A. Atala, "Tissue engineering, stem cells, and cloning: opportunities for regenerative medicine," *J. Am. Soc. Nephrol. JASN*, vol. 15, no. 5, pp. 1113–1125, May 2004.

[97] C. Kalka *et al.*, "Transplantation of ex vivo expanded endothelial progenitor cells for therapeutic neovascularization," *Proc. Natl. Acad. Sci.*, vol. 97, no. 7, pp. 3422–3427, Mar. 2000.

[98] E. Tateishi-Yuyama *et al.*, "Therapeutic angiogenesis for patients with limb ischaemia by autologous transplantation of bone-marrow cells: a pilot study and a randomised controlled trial," *Lancet Lond. Engl.*, vol. 360, no. 9331, pp. 427–435, Aug. 2002.

[99] T. Saigawa *et al.*, "Clinical application of bone marrow implantation in patients with arteriosclerosis obliterans, and the association between efficacy and the number of implanted bone marrow cells," *Circ. J. Off. J. Jpn. Circ. Soc.*, vol. 68, no. 12, pp. 1189–1193, Dec. 2004.

[100] J. E. Till and E. A. McCULLOCH, "A direct measurement of the radiation sensitivity of normal mouse bone marrow cells," *Radiat. Res.*, vol. 14, pp. 213–222, Feb. 1961.

[101] G. Keller, "Embryonic stem cell differentiation: emergence of a new era in biology and medicine," *Genes Dev.*, vol. 19, no. 10, pp. 1129–1155, May 2005.

[102] N. Shyh-Chang and G. Q. Daley, "Metabolic Switches Linked to Pluripotency and Embryonic Stem Cell Differentiation," *Cell Metab.*, vol. 21, no. 3, pp. 349–350, Mar. 2015.

[103] A. S. I. Ahmed, M. H. Sheng, S. Wasnik, D. J. Baylink, and K.-H. W. Lau, "Effect of aging on stem cells," *World J. Exp. Med.*, vol. 7, no. 1, pp. 1–10, Feb. 2017.

[104] F. M. Watt and R. R. Driskell, "The therapeutic potential of stem cells," *Philos. Trans. R. Soc. B Biol. Sci.*, vol. 365, no. 1537, pp. 155–163, Jan. 2010.

[105] U. Bissels, D. Eckardt, and A. Bosio, “Characterization and Classification of Stem Cells,” in *Regenerative Medicine*, Springer, Dordrecht, 2013, pp. 155–176.

[106] V. K. Singh, A. Saini, M. Kalsan, N. Kumar, and R. Chandra, “Describing the Stem Cell Potency: The Various Methods of Functional Assessment and In silico Diagnostics,” *Front. Cell Dev. Biol.*, vol. 4, Nov. 2016.

[107] E. Fuchs and T. Chen, “A matter of life and death: self-renewal in stem cells,” *EMBO Rep.*, vol. 14, no. 1, pp. 39–48, Jan. 2013.

[108] P. H. Lerou and G. Q. Daley, “Therapeutic potential of embryonic stem cells,” *Blood Rev.*, vol. 19, no. 6, pp. 321–331, Nov. 2005.

[109] I. Kuehnle and M. A. Goodell, “The therapeutic potential of stem cells from adults,” *BMJ*, vol. 325, no. 7360, pp. 372–376, Aug. 2002.

[110] C. V. Alvarez *et al.*, “Defining stem cell types: understanding the therapeutic potential of ESCs, ASCs, and iPS cells,” *J. Mol. Endocrinol.*, vol. 49, no. 2, pp. R89–R111, Oct. 2012.

[111] C. Y. Lee *et al.*, “Therapeutic Potential of Stem Cells Strategy for Cardiovascular Diseases,” *Stem Cells International*, 2016. [Online]. Available: https://www.hindawi.com/journals/sci/2016/4285938/. [Accessed: 15-Jun-2018].

[112] P. Lachmann, “Stem cell research—why is it regarded as a threat?,” *EMBO Rep.*, vol. 2, no. 3, pp. 165–168, Mar. 2001.

[113] G. D. Fischbach and R. L. Fischbach, “Stem cells: science, policy, and ethics,” *J. Clin. Invest.*, vol. 114, no. 10, pp. 1364–1370, Nov. 2004.

[114] A. McLaren, “Ethical and social considerations of stem cell research,” *Nature*, vol. 414, no. 6859, pp. 129–131, Nov. 2001.

[115] K. Takahashi and S. Yamanaka, “Induction of pluripotent stem cells from mouse embryonic and adult fibroblast cultures by defined factors,” *Cell*, vol. 126, no. 4, pp. 663–676, Aug. 2006.

[116] X. Liu *et al.*, “Yamanaka factors critically regulate the developmental signaling network in mouse embryonic stem cells,” *Cell Res.*, vol. 18, no. 12, pp. 1177–1189, Dec. 2008.

[117] J. Yu *et al.*, “Induced pluripotent stem cell lines derived from human somatic cells,” *Science*, vol. 318, no. 5858, pp. 1917–1920, Dec. 2007.

[118] P. Mali *et al.*, “Improved efficiency and pace of generating induced pluripotent stem cells from human adult and fetal fibroblasts,” *Stem Cells Dayt. Ohio*, vol. 26, no. 8, pp. 1998–2005, Aug. 2008.

[119] W. Li *et al.*, "Generation of rat and human induced pluripotent stem cells by combining genetic reprogramming and chemical inhibitors," *Cell Stem Cell*, vol. 4, no. 1, pp. 16–19, Jan. 2009.

[120] Y. Zhao *et al.*, "Two supporting factors greatly improve the efficiency of human iPSC generation," *Cell Stem Cell*, vol. 3, no. 5, pp. 475–479, Nov. 2008.

[121] E. Kingham and R. O. C. Oreffo, "Embryonic and Induced Pluripotent Stem Cells: Understanding, Creating, and Exploiting the Nano-Niche for Regenerative Medicine," *ACS Nano*, vol. 7, no. 3, pp. 1867–1881, Mar. 2013.

[122] A. Romito and G. Cobellis, "Pluripotent Stem Cells: Current Understanding and Future Directions," *Stem Cells Int.*, vol. 2016, 2016.

[123] Y. Zhou *et al.*, "Trend of telomerase activity change during human iPSC self-renewal and differentiation revealed by a quartz crystal microbalance based assay," *Sci. Rep.*, vol. 4, p. 6978, Nov. 2014.

[124] "Undifferentiated Ethics: Why Stem Cells from Adult Skin Are as Morally Fraught as Embryonic Stem Cells - Scientific American." [Online]. Available: https://www.scientificamerican.com/article/undifferentiatied-ethics/. [Accessed: 15-Jun-2018].

[125] "Pluripotent Stem Cells, iPs cells | Learn Science at Scitable." [Online]. Available: https://www.nature.com/scitable/topicpage/turning-somatic-cells-into-pluripotent-stem-cells-14431451. [Accessed: 15-Jun-2018].

[126] K. Saha and R. Jaenisch, "Technical challenges in using human induced pluripotent stem cells to model disease," *Cell Stem Cell*, vol. 5, no. 6, pp. 584–595, Dec. 2009.

[127] Y. Yu, X. Wang, and S. L. Nyberg, "Potential and Challenges of Induced Pluripotent Stem Cells in Liver Diseases Treatment," *J. Clin. Med.*, vol. 3, no. 3, pp. 997–1017, Sep. 2014.

[128] T. Ikuno *et al.*, "Efficient and robust differentiation of endothelial cells from human induced pluripotent stem cells via lineage control with VEGF and cyclic AMP," *PLOS ONE*, vol. 12, no. 3, p. e0173271, Mar. 2017.

[129] A. Harding *et al.*, "Highly Efficient Differentiation of Endothelial Cells from Pluripotent Stem Cells Requires the MAPK and the PI3K Pathways," *Stem Cells Dayt. Ohio*, vol. 35, no. 4, pp. 909–919, 2017.

[130] X. Lian *et al.*, "Efficient Differentiation of Human Pluripotent Stem Cells to Endothelial Progenitors via Small-Molecule Activation of WNT Signaling," *Stem Cell Rep.*, vol. 3, no. 5, pp. 804–816, Nov. 2014.

[131] E. D. Bernardini *et al.*, "Endothelial Lineage Differentiation from Induced Pluripotent Stem Cells Is Regulated by MicroRNA-21 and Transforming Growth Factor β2 (TGF-β2) Pathways," *J. Biol. Chem.*, vol. 289, no. 6, pp. 3383–3393, Feb. 2014.

[132] W. J. Adams *et al.*, "Functional Vascular Endothelium Derived from Human Induced Pluripotent Stem Cells," *Stem Cell Rep.*, vol. 1, no. 2, pp. 105–113, Jul. 2013.

[133] A. Margariti *et al.*, "Direct reprogramming of fibroblasts into endothelial cells capable of angiogenesis and reendothelialization in tissue-engineered vessels," *Proc. Natl. Acad. Sci. U. S. A.*, vol. 109, no. 34, pp. 13793–13798, Aug. 2012.

[134] A. J. Rufaihah *et al.*, "Human induced pluripotent stem cell-derived endothelial cells exhibit functional heterogeneity," *Am. J. Transl. Res.*, vol. 5, no. 1, pp. 21–35, Jan. 2013.

[135] R. P. Tan *et al.*, "Integration of induced pluripotent stem cell-derived endothelial cells with polycaprolactone/gelatin-based electrospun scaffolds for enhanced therapeutic angiogenesis," *Stem Cell Res. Ther.*, vol. 9, Mar. 2018.

[136] W.-H. Lai *et al.*, "Attenuation of Hind-Limb Ischemia in Mice with Endothelial-Like Cells Derived from Different Sources of Human Stem Cells," *PLOS ONE*, vol. 8, no. 3, p. e57876, Mar. 2013.

[137] O. V. Halaidych *et al.*, "Inflammatory Responses and Barrier Function of Endothelial Cells Derived from Human Induced Pluripotent Stem Cells," *Stem Cell Rep.*, vol. 10, no. 5, pp. 1642–1656, May 2018.

[138] E. T. Pashuck and M. M. Stevens, "Designing regenerative biomaterial therapies for the clinic," *Sci. Transl. Med.*, vol. 4, no. 160, p. 160sr4, Nov. 2012.

[139] G. D. Prestwich *et al.*, "What is the greatest regulatory challenge in the translation of biomaterials to the clinic?," *Sci. Transl. Med.*, vol. 4, no. 160, p. 160cm14, Nov. 2012.

[140] M. Simons and J. A. Ware, "Therapeutic angiogenesis in cardiovascular disease," *Nat. Rev. Drug Discov.*, vol. 2, no. 11, pp. 863–871, Nov. 2003.

[141] D. G. Halme and D. A. Kessler, "FDA Regulation of Stem-Cell–Based Therapies," *N. Engl. J. Med.*, vol. 355, no. 16, pp. 1730–1735, Oct. 2006.

[142] C. for B. E. and Research, "Fractionated Plasma Products - Fibrinogen." [Online]. Available: https://www.fda.gov/BiologicsBloodVaccines/BloodBloodProducts/ApprovedProducts/LicensedProductsBLAs/FractionatedPlasmaProducts/ucm127588.htm. [Accessed: 15-Jun-2018].

[143] A. S. Lee, C. Tang, M. S. Rao, I. L. Weissman, and J. C. Wu, “Tumorigenicity as a clinical hurdle for pluripotent stem cell therapies,” *Nat. Med.*, vol. 19, no. 8, pp. 998–1004, Aug. 2013.

[144] E. Neofytou, C. G. O’Brien, L. A. Couture, and J. C. Wu, “Hurdles to clinical translation of human induced pluripotent stem cells,” *J. Clin. Invest.*, vol. 125, no. 7, pp. 2551–2557, Jul. 2015.

[145] M. Reisman and K. T. Adams, “Stem Cell Therapy: a Look at Current Research, Regulations, and Remaining Hurdles,” *Pharm. Ther.*, vol. 39, no. 12, pp. 846–857, Dec. 2014.

# CHAPTER 2

# Evaluation of iPSC-ECs' Phenotype and Relevancy as an Endothelial Cell

## 2.1 Introduction

Almost all tissue in the human body requires some form of blood supply to deliver nutrients and remove waste products [1]. While blood vessels transport the blood supply, their development and function depend on endothelial cells (ECs), the main cellular component of blood vessels [2]. These cells proliferate, migrate, and remodel the extracellular matrix (ECM) to form the luminal structure that characterize blood vessels [3]. In addition, endothelial cells act as the main interface between the blood and surrounding tissue, responding to any tissue changes and regulating vascular hemostasis [4]. Because these cells are the main component of blood vessels, understanding endothelial cells is key to the development of therapeutic revascularization.

As mentioned iPSCs, which are derived from somatic cells, can be used to create endothelial cells. However, this is different from traditional endothelial cell generation [5]. Originally, endothelial cells were thought to originate exclusively from the proliferation of existing endothelial cells postnatally [6]. However, recent studies have demonstrated EC proliferation is not the only mechanism contributing to adult EC production. Similar to vasculogenesis in

embryonic development, endothelial progenitor cells (EPCs) were found to contribute to adult vascular formation [7]. EPCs are bone marrow-derived cells expressing high levels of endothelial cell surface markers and low levels of hematopoietic markers [8]. Various studies have demonstrated the vasculogenic potential of EPCs and their ability to form endothelial colonies for the regeneration of endothelial cells [9]–[13]. The true role of EPCs in angiogenesis remains controversial as a majority of the cells characterized as EPCs were derived from a myeloid-monocytic lineage and demonstrated minimal proliferative ability [14]–[16].

While a full characterization and classification of EPCs is yet to be determined, endothelial cell characterization has been extensively studied [17]–[21]. Key endothelial cell markers include von Willebrand Factor (vWF), Angiopotein (ANGPT), and vascular endothelial cadherin (VE-Cadherin). vWF is a blood glycoprotein which binds biological compounds for platelet adhesion in hemostasis [22]. ANGPT is a family of vascular growth factors involved in the signaling pathway for angiogenesis [23]. VE-Cadherin is a cell adhesion molecule found in the intercellular junctions of endothelial cells and maintains the restrictive endothelial cell barrier [24]. Along with VE-Cadherin, various other cluster of differentiation (CD) proteins are also used to identify endothelial cells. Cluster of differentiation-31 (CD31), also known as platelet endothelial cell adhesion molecule (PECAM-1), is found in intercellular junctions between endothelial cells. CD31 functions to maintain junctional integrity and to aid in restoration of the vascular permeability barrier following inflammation [25], [26]. Similarly, cluster of differentiation-34 (CD34) is another glycoprotein found in endothelial cells which may aid in adhesion [27], [28]. However, the true function of CD34 is yet to be determined [29]. Unlike the previous markers, both CD31 and CD34 can also be found in other cell lineages, specifically platelets, monocytes, and

neutrophils and progenitor cells respectively [27], [30]. Ultimately, despite the large expression of the aforementioned markers, endothelial cell markers can vary depending on their origin [31].

Since the circulatory system spans the whole body, various endothelial cell phenotypes exist. These phenotypes not only vary between different organs but can also vary within the same organ depending on its venous or arterial origin [32]. While some characteristics are similar, the structure and function of each type varies significantly [18], [33]–[36]. For example, ECs in arteries and veins have a continuous, uninterrupted pattern of cells [37], [38]. On the other hand, ECs in capillaries may have a continuous, fenestrated, or discontinuous pattern of cells [32]. These structural differences result from the functional needs of the underlying tissue, as capillaries need to readily transport material and arteries need to supply the blood with losing any during delivery [37]. Permeability of the ECs can vary as well, with ECs in the brain have tightly regulated permeabilities to prevent loss or entry of various blood components [39]. On the contrary, ECs in organs such as the liver, kidney, and lymphatics are highly permeable to allow for an easier exchange of blood compounds [38].

Selection of an EC phenotype for revascularization is dependent on the type of treatment needed. For revascularization of the microvasculature, several sources, including HUVECs and human microvascular endothelial cells (HMVECs), have been extensively tested [40]–[46]. iPSC-ECs offer another potential cell source. However, unlike other endothelial cells, iPSC-ECs can originate from any type of somatic cell [47]–[49]. While the selection of most iPSC-ECs is based on the aforementioned endothelial cell markers, such as CD31 and CD34, variations in reprograming and differentiation could result in vastly different expression levels [50]–[53]. There is limited research on how iPSC-ECs' phenotype compares to other endothelial cells [54]–[57].

Prior to understanding the vasculogenic potential of iPSC-ECs, the authenticity of iPSC-ECs as endothelial cells must first be determined.

The present study explores whether our source of iPSC-ECs represents an endothelial cell lineage based on the presence of key EC characteristics prominent for a well-established EC source. Endothelial cells were cultured in 2D on tissue culture plates/flasks until confluency. Key endothelial cell markers were then identified and quantified by immunofluorescent microscopy and fluorescent activated cell sorting respectively. The proliferation rates of each EC source on varying matrix stiffnesses were also explored. Total RNA was harvested to investigate key differences in the genetic expression profile of iPSC-ECs in comparison to HUVECs via an Affymetrix microarray.

## 2.2 Materials and Methods

### 2.2.1 HUVEC Isolation and Cell Culture

Human umbilical vein endothelial cells were harvested from fresh umbilical cords obtained from the University of Michigan Mott Children's Hospital via an IRB-exempt protocol and isolated using methods previously described [40]. Briefly, umbilical cords were rinsed in phosphate buffer saline (PBS) and then digested with 0.1% collagenase type I (195 U/ml, Worthington Biochemical, Lakewood, NJ) for 20 min at 37°C. The digested product was subsequently washed in PBS, collected, and centrifuged (200×G for 5 min). The pellet was resuspended in endothelial growth media (EGM-2, Lonza), and the cells were plated in tissue culture flasks/plates and cultured at 37°C and 5% $CO_2$. After 24 hours, HUVECs were rinsed with PBS to remove any non-adherent cells. Media were exchanged every 48 hours. Cells from passage

3 were utilized for all experiments. iPSC-ECs of human fibroblastic origin were commercially purchased, iCell endothelial cells (Cellular Dynamics International, Madison, WI), and cultured at 37°C and 5% $CO_2$ in Vasculife VEGF endothelial media (Lifeline Cell Technology, Fredrick, MD) supplemented with iCell Endothelial Cell Medium Supplement (Cellular Dynamics International) per the manufacturer's instructions. iPSC-ECs tissue culture flasks/plates were coated with 35 µg/mL fibronectin (Invitrogen, Carlsbad, CA) for 1 hr at room temp prior to plating the cells. Culture media was replaced every 48 hours and cells from passage 3 were used in experiments.

### 2.2.2 Immunofluorescent Staining on Tissue Culture Plates

Once cells reached confluency (~4 days), cells were briefly rinsed 2x with PBS solution for 10 seconds at room temperature. Cells were then fixed with 4% paraformaldehyde (Sigma) for 10 min at room temperature. Cells were then permeabilized with 0.1% Triton-X100 in TBS for 10 min at room temperature. Samples were blocked overnight at 4 °C with a 2% Abdil solution (bovine serum albumin (Sigma) dissolved in TBS-T). The primary antibody/staining agent was dissolved in 2% Abdil at the appropriate concentration (anti-CD31, 1:200 (Dako, Santa Clara, CA); VE-Cadherin, 1:200 (Invitrogen, Waltham, MA); vWF, 1:200 (Invitrogen)) and this solution was added to the cells for a 1 hr incubation at room temperature. Cells were then rinsed 3x for 5 min with TBS-T. The appropriate secondary antibody (1:400, Alexa Fluor 488 Goat anti-mouse IgG, Invitrogen) dissolved in 2% Abdil was added for a 45 min incubation at room temperature. Following a 3x rinse for 5 min at room temperature with TBS-T, cells were incubated with TBS-T at 4 °C until microscopy imaging.

### 2.2.3 Fluorescent Imaging and Microscopy

Fluorescent images were captured utilizing an Olympus IX81 equipped with a 100 W high-pressure mercury burner (Olympus America, Center Valley, PA), a Hamamatsu Orca II CCD camera (Hamamatsu Photonics, K.K., Hamamatsu City, Japan), and Metamorph Premier software (Molecular Devices, Sunnyvale, CA).

### 2.2.4 Immunofluorescent Staining in Suspension and FACS Analysis

Endothelial cells were cultured in T-75 flasks to 80% confluency and rinsed with PBS before being harvested via 0.25% trypsin incubation for 5 min at 37 °C and 5% $CO_2$. Trypsin was neutralized using DMEM supplemented with 10% FBS. The cellular suspension was centrifuged (200×G for 5 min) and supernatant was aspirated immediately. Cells were resuspended and counted using a hematocytometer. The cell solution was then filtered through a 40 μm filter and the pellet recovered following centrifugation at 200×G for 5 min. Cells were re-suspended in an ice cold solution of 0.1% BSA, dissolved in PBS, and placed in microcentrifuge tubes. Cells were then rinsed 3X with the ice cold 0.1% BSA – PBS solution, with centrifugation (200×G for 5 min) between each rinse. The primary antibody/staining agent was dissolved in a 0.1% BSA – PBS solution at the appropriate concentration (anti-CD31, 1:50 (Dako, Santa Clara, CA); VE-Cadherin, 1:50 (Invitrogen, Waltham, MA). Cells were re-suspended in 1 mL of this solution and placed on tube rotator for a 1 hr incubation at 4 °C. Cells were then rinsed 3X with the ice cold 0.1% BSA – PBS solution, with centrifugation (200×G for 5 min) between each rinse. Cells were resuspended in 1 mL of the appropriate secondary antibody (1:400, Alexa Fluor 488 Goat anti-mouse IgG, Invitrogen) dissolved in a 0.1% BSA – PBS solution and placed on a tube rotator for a 45 min incubation at 4 °C. Following a 3X rinse with the ice cold 0.1% BSA – PBS solution and

centrifugation (200×G for 5 min) between each rinse, cells were fixed for 10 min at 4 °C on a tube rotator with 1% paraformaldehyde in PBS. Lastly, cells were rinsed 2X with the ice cold 0.1% BSA – PBS solution. Cells were then analyzed using a MoFlo Astrios cell sorter (Beckman Coulter, Pasadena, CA).

### 2.2.5 Fibrin Gel Assembly

A fibrinogen (Sigma-Aldrich) solution of the desired concentration (2.5 mg/mL) was dissolved in an appropriate amount of serum-free EGM-2 and placed at 37 °C in a water bath. The solution was sterile filtered through a 0.22 μm syringe filter (Millipore, Billerica, MA). 500 μL of fibrinogen solution was added to a single well of a 24-well tissue culture plate and polymerized with 10 μL of thrombin (50 U/mL, Sigma-Aldrich). Fibrin gels were left undisturbed for 5 min at room temperature before incubation for 30 min at 37 °C and 5% $CO_2$. ECs, cultured and prepared as described above, were added on top of the gels along with media following fibrin polymerization. Media were changed the following day and every other day thereafter.

### 2.2.6 Proliferation Assay

Endothelial cells were cultured either on TCP or 2.5 mg/mL fibrin gels in a 24 well plate at a starting seeding density of 20K per well. At various time points, cells were removed from the wells depending on their culture condition. For cells cultured on TCP, cells were rinsed with PBS before being harvested via 0.25% trypsin incubation for 5 min at 37 °C and 5% $CO_2$. Trypsin was neutralized using DMEM supplemented with 10% FBS. The cellular suspension was centrifuged (200×G for 5 min) and supernatant was aspirated immediately. Cells were resuspended and counted using a hematocytometer. For cells on fibrin gels, the fibrin gel was first digested using

Natto Kinase (NSK-SD, Japan BioSceince Laboratoy Co. Ltd) dissolved in a 1 mM EDTA PBS solution. 1 mL of the aforementioned solution was added to each well and incubated for 45 min at 37 °C. The degraded fibrin cell solution was centrifuged (200×G for 5 min) and supernatant was aspirated immediately. The cells pellet was then suspended in 0.25% trypsin incubation for 5 min at 37 °C and 5% $CO_2$ to break apart the cell sheet. Trypsin was neutralized, the cellular suspension was centrifuged (200×G for 5 min), and the supernatant was aspirated immediately. Cells were re-suspended and counted using a hematocytometer.

### 2.2.7 RNA Isolation and Affymetrix Analysis

iPSC-ECs and HUVECs were cultured in 24 well plates using the previously described methods for 3-4 days or until confluency. Total RNA was purified using the RNeasy kit (Qiagen, Valencia, CA) per manufacturer's protocol and quantified using a Nanodrop ND-1000 (Thermo Fisher Scientific, Rochester, NY). At least 200 ng of the harvest RNA was then processed by the University of Michigan's DNA Core using an Affymetrix Human Gene 2.1 ST Array. Expression profiles were analyzed by a biostatistician and reported using the iPathwayGuide Software (Adviata Bioinformatics, Plymouth, MI). Any fold changes above 1.0 (2-fold change) were noted as significantly different between the two populations of ECs.

## 2.3 Results

### 2.3.1 iPSC-ECs exhibit morphological similarities to HUVECs in 2D culture.

In this study, iPSC-derived ECs were cultured in 2D and characterized for their phenotypic similarities to HUVECs, a mature and well-established EC population. Brightfield images from these cultures demonstrated morphological similarities between the HUVECs and iPSC-derived-ECs (Fig. 2-1), with the iPSC-derived-ECs displaying a cobblestone-like morphology and a spindle-like shape for each individual cell, which are characteristic of cultured endothelial cells [58].

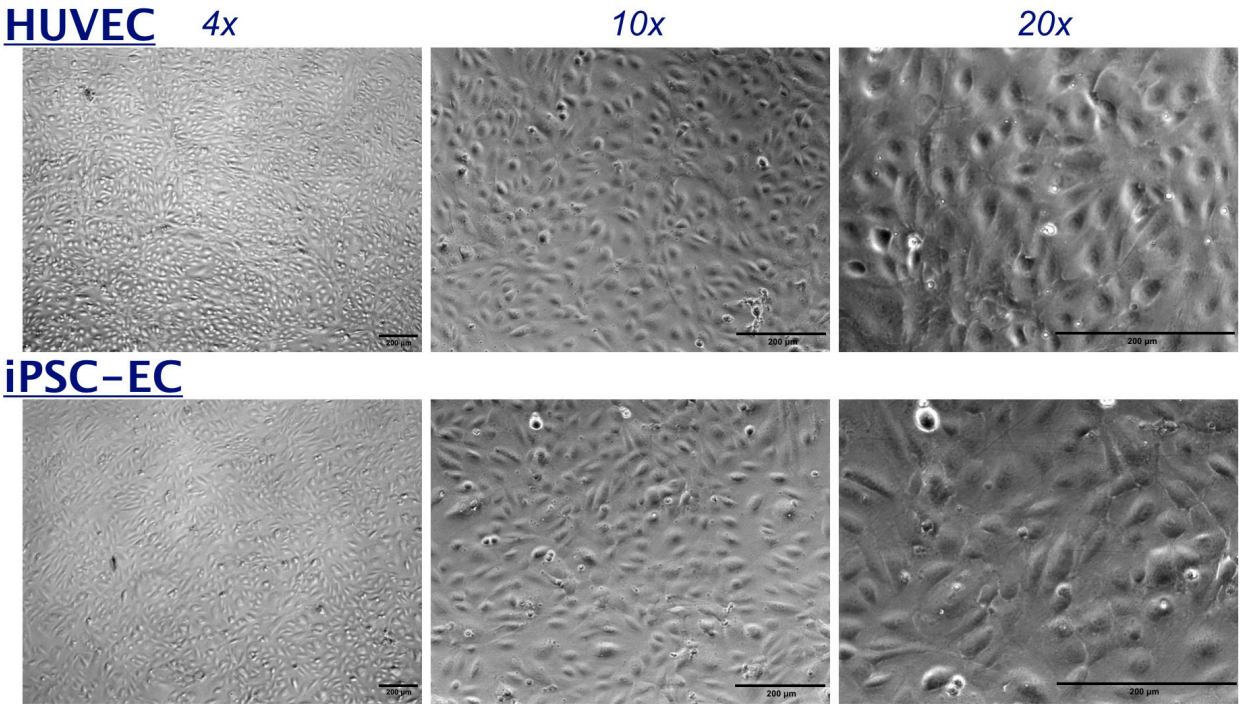


**Figure 2-1: iPSC-ECs exhibit morphological similarities to HUVECs in 2D culture.**
Representative brightfield images of confluent ECs cultures on TCP at varying magnification intensities. Scale bar = 200 µm.

### 2.3.2 iPSC-ECs demonstrate comparable expression levels of a panel of EC markers compared to HUVECs

To validate the observations from the brightfield images and confirm an endothelial cell phenotype, ECs were immunofluorescently (IF) stained for various endothelial cell markers (Fig. 2-2). Cluster of differentiation 31 (CD31) is a molecule expressed in the intercellular junctions of endothelial cells within blood vessels [30]. IF staining revealed both HUVECs (Fig. 2-2A) and iPSC-ECs (Fig. 2-2.1A') expressed CD31 around their peripheries. Vascular endothelial cadherin (VE-Cadherin) is a cadherin required for maintaining a restrictive endothelial barrier and a major component in the integrity of endothelium intercellular junctions [24]. Both HUVECs and iPSC-ECs expressed VE-Cadherin at their junctions (Fig. 2-2.1B-B') as gauged by IF staining. Lastly, both cell types demonstrated the production of von Williebrand factor (vWF) (Fig. 2-2.1C-C'), a glycoprotein involved in hemostasis and produced by the endothelium during blood clotting [22].

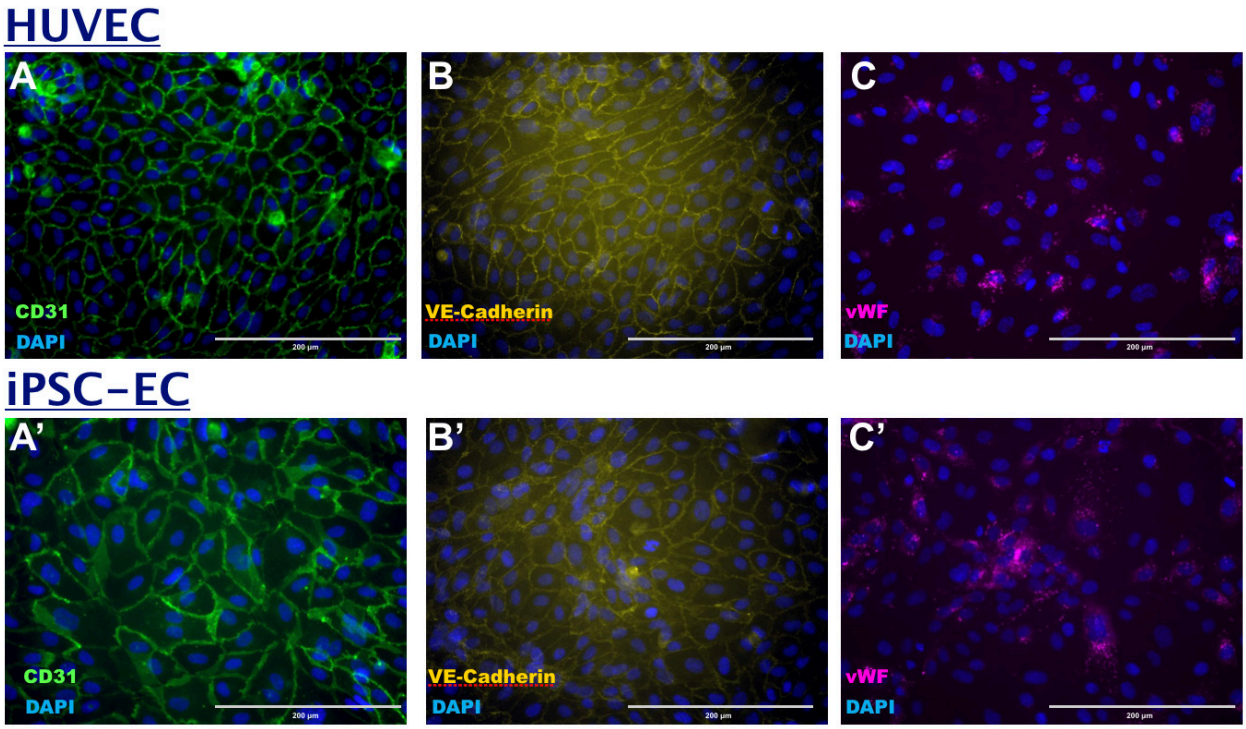


**Figure 2-2.1: iPSC-ECs demonstrate comparable EC marker expression compared to HUVECs.**
HUVECs (A-C) or iPSC-ECs (A'-C') were cultured in 24-well plates. Cultures were monitored for confluency over a 4 day period. Cultures were fixed and IF stained for (A,A') CD31 (green), (B,B') VE-Cadherin (yellow), (C,C') vWF (magenta), and DAPI (blue). Scale bar = 200 µm.

In addition to qualitative expression, iPSC-ECs expressing endothelial cell markers were quantified via fluorescent activated cell sorting (FACS) to further characterize their endothelial lineage. Cells were cultured, immunofluorescently stained in suspension, and analyzed to determine the number of cells expressing both CD31 (Fig. 2-2.2) and VE-Cadherin (Fig. 2-2.3). Both populations of cells demonstrated high levels of cells expressing CD31 (99.88% for HUVECs and 98.46% for iPSC-derived-ECs). Similarly, high levels of iPSC-ECs and HUVECs expressing VE-Cadherin was observed (82.03% for HUVECs and 95.26% for iPSC-derived-ECs). Collectively, these results, and the previous qualitative EC marker and EC morphology experiments, demonstrate the iPSC-derived-ECs share many phenotypic similarities to an endothelial lineage.

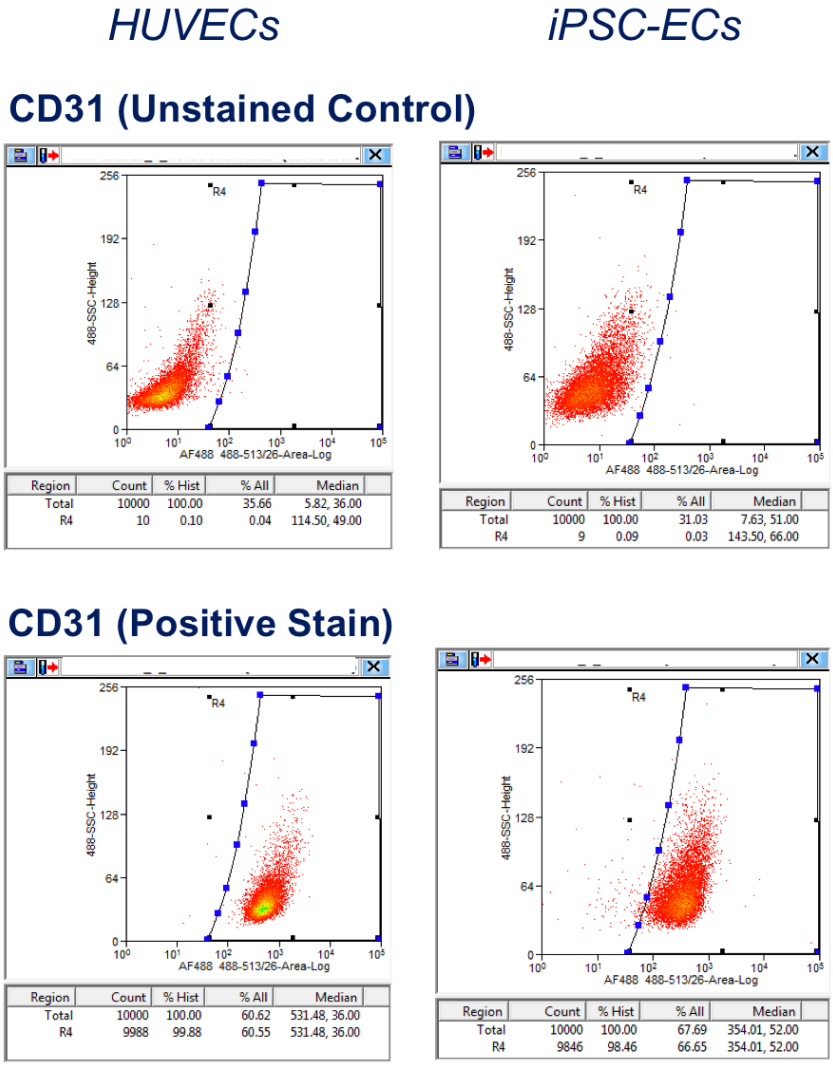


**Figure 2-2.2: iPSC-ECs express similar levels of key markers characteristic of endothelial cell lineage *[Absorbance Plots]*** HUVECs or iPSC-ECs were IF stained for CD31. IF stained cells were analyzed using FACS and the number of cells expressing the indicated marker were quantified.

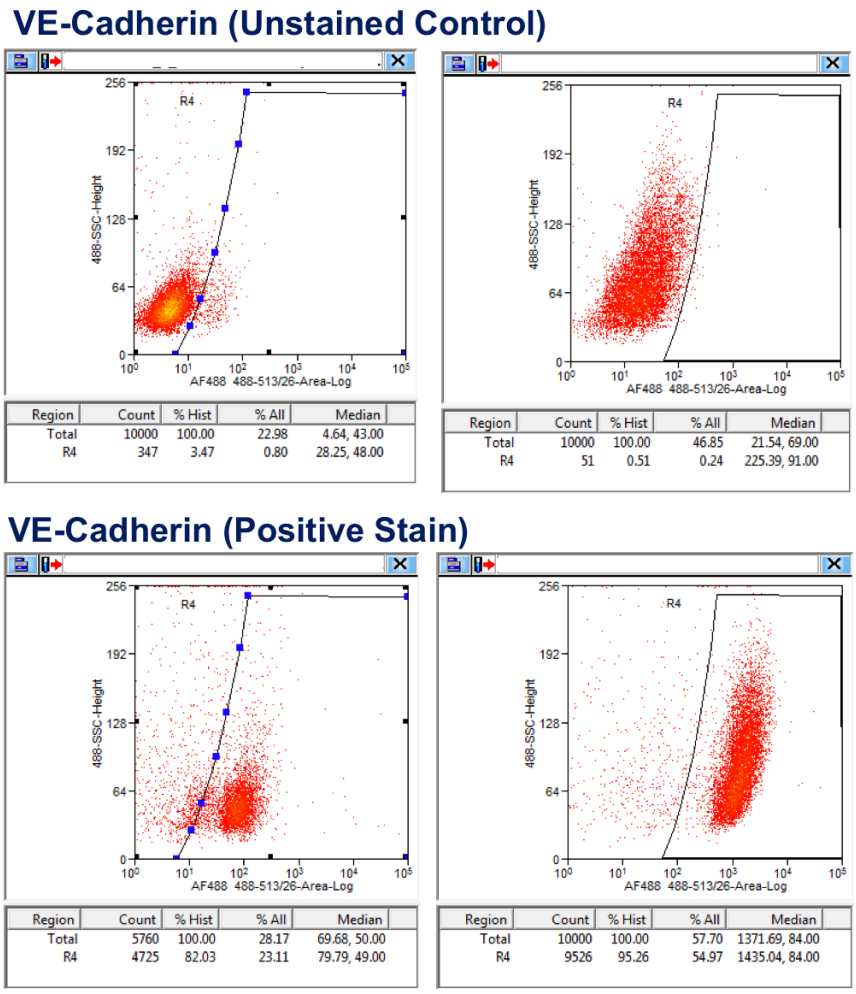


**Figure 2-2.3: iPSC-ECs express similar levels of key markers characteristic of endothelial cell lineage *[Absorbance Plots]*** HUVECs or iPSC-ECs were IF stained for VE-Cadherin. IF stained cells were analyzed using FACS and the number of cells expressing the indicated marker were quantified.

## 2.3.3 iPSC-ECs proliferate at a similar rate compared to HUVECs in 2D

Although the iPSC-ECs displayed some characteristics of an endothelial cell phenotype, there could potentially be other phenotypic differences between the iPSC-ECs and HUVECs. The ultimate goal of this research is to determine the vasculogenic potential of the iPSC-ECs through the creation of vasculature both *in vitro* and *in vivo*. Since proliferation is a key aspect of vessel formation [3], [59], [60], we sought to characterize the proliferation rate of iPSC-ECs. Endothelial cells were plated at a constant seeding density (20K) on either tissue culture plastic (TCP) or 2.5

mg/mL fibrin gels. At various time points, cells were harvested, and the total number of cells counted. While total cell numbers were lower for iPSC-ECs in comparison to HUVECs on TCP across all timepoints, there was no significant difference between the two populations (Fig. 2-3A). Similarly, both endothelial cell populations proliferated at a similar rate on fibrin gels with no significant difference in total cell number for any of the time points examined (Fig. 2-3B).

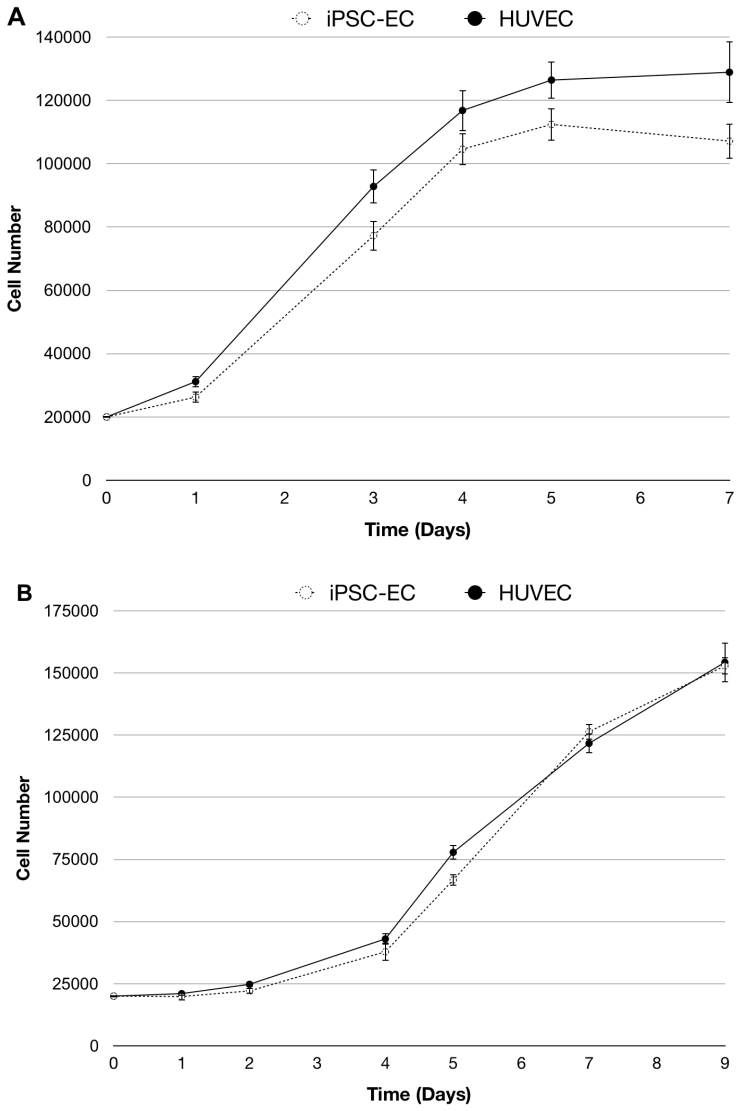


**Figure 2-3: iPSC-ECs proliferate at a similar rate compared to HUVECs in 2D.**
HUVECs or iPSC-ECs were cultured in 24 well plates either on top of **(A)** TCP or **(B)** 2.5 mg/mL fibrin gels. Cells were removed from their wells at various time points and the number of cells were counted. * $p < 0.05$ denotes statistical significance. Error bars indicate ±SEM

### 2.3.4 Genetic expression profiles of iPSC-ECs are comparable to HUVECs

Despite the phenotypic similarities observed between the iPSC-ECs and HUVECs, these cells may still have genotypic differences. The iPSC-ECs were synthetically reprogramed into a pluripotent state from a fibroblastic lineage and then differentiated into an endothelial cell lineage using techniques proprietary to the vendor [56], [61]. Due to the iPSC-ECs' origin, the gene expression profiles could largely differ from HUVECs. Furthermore, while the iPSC-ECs phenotypically have characteristics of an endothelial lineage, the expression of endothelial genes could vary [55]. To determine genotypic differences between the iPSC-ECs and HUVECs, total RNA was harvested from cells and analyzed via an AffyMetrix gene chip microarray. The expression profiles were quantified and the fold change between the iPSC-ECs and HUVECs was calculated. Of all the genes analyzed, the genetic expressions profiles of the two ECs differ by only 5.92% with respect to a greater than 2-fold change. Of the 14,352 genes analyzed, 13,502 genes were within a 2-fold difference between the two populations, suggesting their expression levels were not significantly different. However, there was a 2-fold higher expression of 422 genes in the iPSC-ECs with respect to HUVECs. In comparison, there was a 2-fold lower expression of 428 genes in the iPSC-ECs with respect to HUVECs (Fig. 2-4.1A).

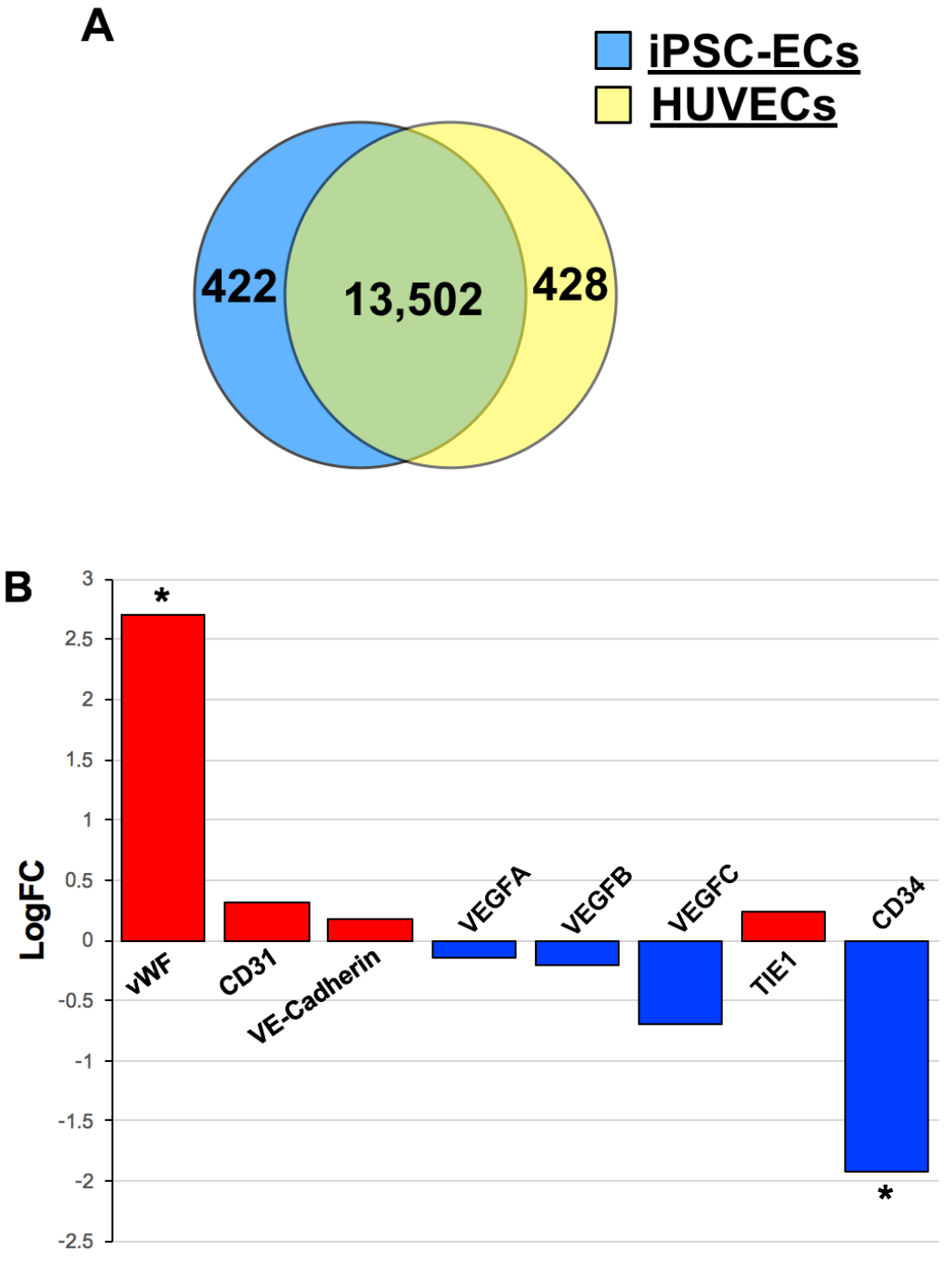


**Figure 2-4.1: Genetic expression profiles of iPSC-ECs are comparable to HUVECs**
HUVECs' or iPSC-ECs' RNA was harvested from the cells after 4 days culture. RNA was analyzed via an AffyMetrix assay to determine gene expression profiles. (A) The Venn diagram show the total number of genes with similar expression profiles between the two populations and the number of genes with expression profiles 2-fold higher in the respective cell type. (B) Quantification of iPSC-ECs' expression fold change for specific genes associated with an endothelial lineage in respect HUVECs.

To further characterize the endothelial cell nature of iPSC-ECs, the fold change of key endothelial cell marker genes was investigated. Fold changes greater than a 2-fold difference (LogFC = 1.0) were considered significantly different. CD31, VE-Cadherin, VEGFA, VEGFB, VEGFC, and TIE1 showed no significant fold changes. However, vWF was expressed 6.5-fold greater in iPSC-ECs. A 4-fold lower difference was also seen for CD34 (Fig. 2-4.1B). Furthermore, pluripotency genes were investigated to determine whether the iPSC-ECs were still expressing genes inserted during reprogramming (Fig. 2-4.2). Once again, any fold changes greater than a 2-fold difference (LogFC = 1.0) were considered significantly different. While c-Myc, Klf4, and Sox2 showed no significant expression difference, Oct3/4 was expressed significantly higher in the iPSC-ECs.

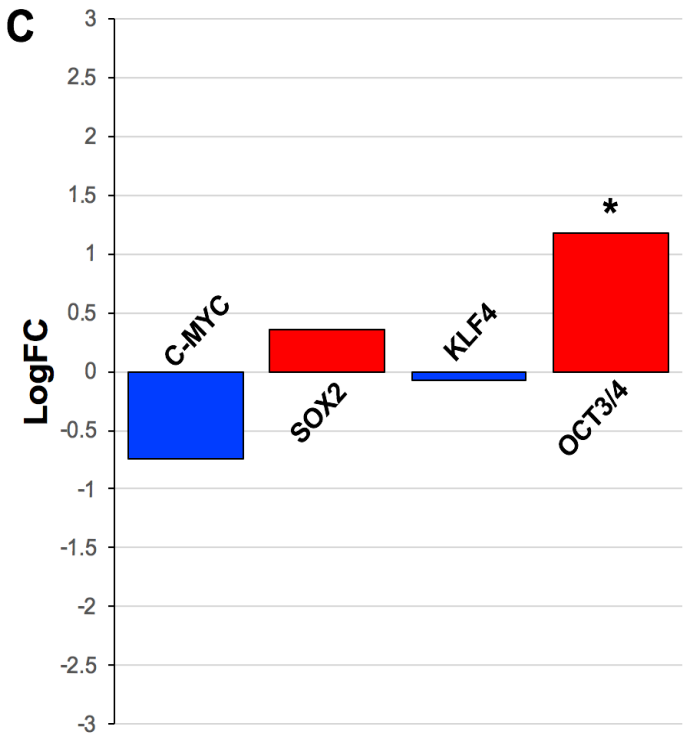


**Figure 2-4.2: Genetic expression profiles of iPSC-ECs are comparable to HUVECs.**
(C) Quantification of iPSC-ECs' expression fold change for genes associated with reprogramming cells into pluripotency.

## 2.4 Discussion

While prior studies have extensively investigated the ability of iPSC-ECs to express EC-like characteristics, the reprograming and differentiation process for iPSC-EC creation can vary significantly, resulting in potential phenotypic differences [50], [51], [56], [62]. Therefore, this study characterized the phenotype of iPSC-ECs in comparison to the endothelial phenotype of a well-established EC line with demonstrated capabilities of stable, robust microvascular formation, HUVECs. iPSC-ECs were cultured in 2D on flasks, alongside HUVECs, and then analyzed for various characteristic of endothelial cells. Despite small genotypic differences, the data in this chapter demonstrate that iPSC-ECs are phenotypically similar to HUVECs.

Although iPSC-ECs exhibited slight morphological differences, key endothelial cell markers were expressed by the cells. CD31, VE-Cadherin, and vWF are typically associated with endothelial cells [22], [24], [30], and thus the presence of these components is indicative of the iPSC-ECs' endothelial cell nature. Both CD31 and VE-Cadherin were localized to the cortex of the cells; however, VE-Cadherin demonstrated less intense signaling. The signal intensity may be an artifact of imaging or background interference; nevertheless, the presence of both CD31 and VE-Cadherin suggests the iPSC-ECs are ECs. The expression of these markers is expected as iPSC-EC selection after differentiation is typically based on CD31 and VE-Cadherin. Both HUVECs and iPSC-ECs showed limited expression of vWF. Furthermore, the vWF strands were relatively short and close to the cell surface which is expected in non-inflammatory conditions. vWF is released from cells upon stimulation of inflammatory cytokines [65]. Since these cells were left undisturbed during culture, the production of vWF should be limited.

To quantify the number of cells expressing the endothelial cell markers, iPSC-ECs were analyzed via FACS. Both CD31 and VE-Cadherin were highly expressed in both HUVECs and

iPSC-ECs. While CD31 expression was slightly higher, by roughly 1%, VE-Cadherin was expressed at lower levels in HUVECs. While most HUVECs should express VE-Cadherin [68], [69], one possible explanation for the lower number of HUVECs expressing VE-Cadherin is the increased presence of dead cells, noted by the smaller registered events for the HUVECs, which can affect the accuracy of flow cytometry analysis [70]. Collectively, the similarities between cell morphology and endothelial cell marker expression, both via IF staining and FACS analysis, suggest iPSC-ECs are phenotypically an endothelial cell lineage.

In addition, iPSC-ECs demonstrated the same proliferative ability in comparison to HUVECs. While no statistical differences were observed between the two populations, difference were observed depending on the substrate in which cells were cultured. In comparison to TCP in which increased cell counts were noticeable on day 1, fibrin cultures showed relatively similar cell counts for the first few time points suggesting a slower proliferative ability on fibrin. The effect of matrix stiffness on cellular activity is well documented [41], [71]–[74], with "softer" matrices reducing cell proliferation in 2D [75]. However, both iPSC-ECs and HUVECs demonstrated higher cell numbers when seeded on fibrin gels. Although cells were cultured longer on fibrin than TCP, cell growth started to level off, and in the case of iPSC-ECs, decrease by day 7 on TCP. This difference could be attributed to the cell's density dependence, a well-known limitation in the cell cycle [76], [77]. On TCP, the cells reached a finite density and stop proliferating. However, for fibrin, a dimensionality is added to the culture, allowing for ECs to potentially invaded the matrix and continue their growth and proliferation.

Although similarities exist between iPSC-ECs and HUVECs, considerable differences could exist between them, especially in regard to their origin. To further investigate any differences, we performed a comparative analysis of the gene expression profile of iPSC-ECs

versus HUVECs. This study revealed iPSC-ECs have similar gene expression profiles to HUVECs. In addition, no significant differences were seen for many endothelial cell-specific genes. However, vWF was expressed higher in iPSC-ECs than HUVECs suggesting iPSC-ECs may be more suitable for wound healing. As previously mentioned, vWF is a glycoprotein secreted by endothelial cells and involved in platelet adhesion in wound healing [65]. While studies indicate vWF is involved in many vascular processes, elevated vWF levels may inhibit tube formation, proliferation, and migration of ECs in vitro through pathways that involve VEGFR-2 signaling [78]. Furthermore, CD34 was expressed lower in iPSC-ECs than HUVECs. CD34 is a glycoprotein involved in cell-cell adhesions and found in hematopoietic cells or endothelial progenitor cells [27]. HUVECs have been implicated in the support of hematopoiesis [79], possibly explaining the increased expression of CD34. Interestingly, pluripotent genes such as Oct3/4 can still be detected in the iPSC-ECs. Oct-3/4 expression is typically associated with an undifferentiated phenotype [80]. Oct3/4, along with other pluripotency genes, are introduced during the reprograming phase of iPSC-EC generation to induce a stem-cell like state [56]. Once differentiated to a specific cell lineage, the expression of these genes should be down-regulated. The higher Oct3/4 expression in iPSC-ECs is consistent with previous research and may indicate partial differentiation into the endothelial cell lineage [56], [81]. While additional differences may exist between the iPSC-ECs and HUVECs, this study demonstrates the large genotypic similarities between the two populations.

One caveat to interpreting the observed similarities and differences is the fact that iPSC-ECs were only compared to one source of endothelial cells. While HUVECs are an established and robust EC source [42], [43], [71], other ECs, such as microvascular endothelial cells (MVECs), may exhibit different phenotypes and gene expression profiles, which could be used to further

characterize the endothelial cell nature of iPSC-ECs [36], [82], [83]. Additionally, we only investigated a small number of endothelial cell markers via IF staining and FACS. While the selected markers are typically used to characterize ECs, a variety of other EC markers exist, such as CD34 [33], [34], [36], [63]. Fibrin was selected due to FDA clearance for clinical use and is found naturally in the human body during wound healing [84]. Other matrices could have been used in addition to fibrin, such as collagen or synthetic hydrogels, to better understand the effect of matrix identity on proliferation [74], [85]–[87]. Most importantly, these experiments were all conducted in 2D. Various studies have investigated the effect of 2D versus 3D on cells [88], [89]. While our study noted similarities to the HUVECs on 2D, iPSC-ECs may have different phenotypes when cultured in 3D, which will be investigated in Chapter 3.

## 2.5 Conclusions

In summary, this work characterized whether iPSC-ECs expressed an endothelial-like phenotype and a genetic profile similar to an established EC line. Both HUVECs and iPSC-ECs formed EC-like morphologies, expressed high levels of endothelial cell markers, and demonstrated similar proliferation rates on varying matrix stiffnesses. Despite small differences in the gene expression profiles, iPSC-ECs were approximately 94% similar to HUVECs in their genotypes. Future *in vitro* studies are necessary to assess phenotypic difference in 3D cultures, discussed in chapter 3, and if the various differences in the expression profile affect the iPSC-ECs' vasculogenic potential. Ultimately, these findings suggest additional characterization of fundamental phenotypic differences is necessary to implement a successful clinical translation of iPSC-ECs for therapeutic revascularization.

## 2.6 References


[1] R. N. Pittman, *The Circulatory System and Oxygen Transport*. Morgan & Claypool Life Sciences, 2011.

[2] B. Alberts, A. Johnson, J. Lewis, M. Raff, K. Roberts, and P. Walter, "Blood Vessels and Endothelial Cells," *Mol. Biol. Cell 4th Ed.*, 2002.

[3] D. R. Senger and G. E. Davis, "Angiogenesis," *Cold Spring Harb. Perspect. Biol.*, vol. 3, no. 8, Aug. 2011.

[4] C. Michiels, "Endothelial cell functions," *J. Cell. Physiol.*, vol. 196, no. 3, pp. 430–443.

[5] Y. Lin, D. J. Weisdorf, A. Solovey, and R. P. Hebbel, "Origins of circulating endothelial cells and endothelial outgrowth from blood," *J. Clin. Invest.*, vol. 105, no. 1, pp. 71–77, Jan. 2000.

[6] J. Folkman and Y. Shing, "Angiogenesis," *J. Biol. Chem.*, vol. 267, no. 16, pp. 10931–10934, Jun. 1992.

[7] T. Asahara *et al.*, "Isolation of putative progenitor endothelial cells for angiogenesis," *Science*, vol. 275, no. 5302, pp. 964–967, Feb. 1997.

[8] M. C. Yoder, "Endothelial stem and progenitor cells (stem cells): (2017 Grover Conference Series)," *Pulm. Circ.*, vol. 8, no. 1, Nov. 2017.

[9] G. Finkenzeller, S. Graner, C. J. Kirkpatrick, S. Fuchs, and G. B. Stark, "Impaired in vivo vasculogenic potential of endothelial progenitor cells in comparison to human umbilical vein endothelial cells in a spheroid-based implantation model," *Cell Prolif.*, vol. 42, no. 4, pp. 498–505, Aug. 2009.

[10] S. TAKIZAWA, E. NAGATA, T. NAKAYAMA, H. MASUDA, and T. ASAHARA, "Recent Progress in Endothelial Progenitor Cell Culture Systems: Potential for Stroke Therapy," *Neurol. Med. Chir. (Tokyo)*, vol. 56, no. 6, pp. 302–309, Jun. 2016.

[11] S.-J. Park *et al.*, "Enhancement of angiogenic and vasculogenic potential of endothelial progenitor cells by haptoglobin," *FEBS Lett.*, vol. 583, no. 19, pp. 3235–3240, Oct. 2009.

[12] T. Asahara and A. Kawamoto, "Endothelial progenitor cells for postnatal vasculogenesis," *Am. J. Physiol. Cell Physiol.*, vol. 287, no. 3, pp. C572-579, Sep. 2004.

[13] S. Murasawa and T. Asahara, "Endothelial progenitor cells for vasculogenesis," *Physiol. Bethesda Md*, vol. 20, pp. 36–42, Feb. 2005.

[14] E. Pasquier and S. Dias, “Endothelial progenitor cells: hope beyond controversy,” *Curr. Cancer Drug Targets*, vol. 10, no. 8, pp. 914–921, Dec. 2010.

[15] M. Zhang, J. Rehman, and A. B. Malik, “Endothelial Progenitor Cells and Vascular Repair,” *Curr. Opin. Hematol.*, vol. 21, no. 3, pp. 224–228, May 2014.

[16] C. R. Balistreri, S. Buffa, C. Pisano, D. Lio, G. Ruvolo, and G. Mazzesi, “Are Endothelial Progenitor Cells the Real Solution for Cardiovascular Diseases? Focus on Controversies and Perspectives,” *BioMed Res. Int.*, vol. 2015, 2015.

[17] K. J. G. Kenswil *et al.*, “Characterization of Endothelial Cells Associated with Hematopoietic Niche Formation in Humans Identifies IL-33 As an Anabolic Factor,” *Cell Rep.*, vol. 22, no. 3, pp. 666–678, Jan. 2018.

[18] D. Talavera-Adame, T. T. Ng, A. Gupta, S. Kurtovic, G. D. Wu, and D. C. Dafoe, “Characterization of microvascular endothelial cells isolated from the dermis of adult mouse tails,” *Microvasc. Res.*, vol. 82, no. 2, pp. 97–104, Sep. 2011.

[19] M. Bhasin, L. Yuan, D. B. Keskin, H. H. Otu, T. A. Libermann, and P. Oettgen, “Bioinformatic identification and characterization of human endothelial cell-restricted genes,” *BMC Genomics*, vol. 11, p. 342, May 2010.

[20] B. Pratumvinit, K. Reesukumal, K. Janebodin, N. Ieronimakis, and M. Reyes, “Isolation, Characterization, and Transplantation of Cardiac Endothelial Cells,” *BioMed Research International*, 2013. [Online]. Available: https://www.hindawi.com/journals/bmri/2013/359412/. [Accessed: 12-Jun-2018].

[21] F. Schatz, C. Soderland, K. D. Hendricks-Muñoz, R. P. Gerrets, and C. J. Lockwood, “Human Endometrial Endothelial Cells: Isolation, Characterization, and Inflammatory-Mediated Expression of Tissue Factor and Type 1 Plasminogen Activator Inhibitor,” *Biol. Reprod.*, vol. 62, no. 3, pp. 691–697, Mar. 2000.

[22] A. M. Randi, M. A. Laffan, and R. D. Starke, “Von Willebrand Factor, Angiodysplasia and Angiogenesis,” *Mediterr. J. Hematol. Infect. Dis.*, vol. 5, no. 1, Sep. 2013.

[23] G. Thurston and C. Daly, “The Complex Role of Angiopoietin-2 in the Angiopoietin–Tie Signaling Pathway,” *Cold Spring Harb. Perspect. Med.*, vol. 2, no. 9, Sep. 2012.

[24] D. Vestweber, “VE-cadherin: the major endothelial adhesion molecule controlling cellular junctions and blood vessel formation,” *Arterioscler. Thromb. Vasc. Biol.*, vol. 28, no. 2, pp. 223–232, Feb. 2008.

[25] A. Woodfin, M.-B. Voisin, and S. Nourshargh, “PECAM-1: A Multi-Functional Molecule in Inflammation and Vascular Biology,” *Arterioscler. Thromb. Vasc. Biol.*, vol. 27, no. 12, pp. 2514–2523, Dec. 2007.

[26] P. Lertkiatmongkol, D. Liao, H. Mei, Y. Hu, and P. J. Newman, “Endothelial functions of PECAM-1 (CD31),” *Curr. Opin. Hematol.*, vol. 23, no. 3, pp. 253–259, May 2016.

[27] J. S. Nielsen and K. M. McNagny, “Novel functions of the CD34 family,” *J. Cell Sci.*, vol. 121, no. 22, pp. 3683–3692, Nov. 2008.

[28] L. E. Sidney, M. J. Branch, S. E. Dunphy, H. S. Dua, and A. Hopkinson, “Concise Review: Evidence for CD34 as a Common Marker for Diverse Progenitors,” *Stem Cells Dayt. Ohio*, vol. 32, no. 6, pp. 1380–1389, Jun. 2014.

[29] S. G. B. Furness and K. McNagny, “Beyond mere markers: functions for CD34 family of sialomucins in hematopoiesis,” *Immunol. Res.*, vol. 34, no. 1, pp. 13–32, 2006.

[30] L. Liu and G.-P. Shi, “CD31: beyond a marker for endothelial cells,” *Cardiovasc. Res.*, vol. 94, no. 1, pp. 3–5, Apr. 2012.

[31] M. P. Pusztaszeri, W. Seelentag, and F. T. Bosman, “Immunohistochemical Expression of Endothelial Markers CD31, CD34, von Willebrand Factor, and Fli-1 in Normal Human Tissues,” *J. Histochem. Cytochem.*, vol. 54, no. 4, pp. 385–395, Apr. 2006.

[32] W. C. Aird, “Endothelial Cell Heterogeneity,” *Cold Spring Harb. Perspect. Med.*, vol. 2, no. 1, Jan. 2012.

[33] M. I. Townsley, “Structure and composition of pulmonary arteries, capillaries and veins,” *Compr. Physiol.*, vol. 2, pp. 675–709, Jan. 2012.

[34] D. Donnini, G. Perrella, G. Stel, F. S. Ambesi-Impiombato, and F. Curcio, “A new model of human aortic endothelial cells in vitro,” *Biochimie*, vol. 82, no. 12, pp. 1107–1114, Dec. 2000.

[35] S. Rounds, Q. Lu, E. O. Harrington, J. Newton, and B. Casserly, “Pulmonary Endothelial Cell Signaling and Function,” *Trans. Am. Clin. Climatol. Assoc.*, vol. 119, pp. 155–169, 2008.

[36] A. Miura *et al.*, “Differential responses of normal human coronary artery endothelial cells against multiple cytokines comparatively assessed by gene expression profiles,” *FEBS Lett.*, vol. 580, no. 30, pp. 6871–6879, Dec. 2006.

[37] W. C. Aird, “Phenotypic Heterogeneity of the Endothelium: II. Representative Vascular Beds,” *Circ. Res.*, vol. 100, no. 2, pp. 174–190, Feb. 2007.

[38] S. Sukriti, M. Tauseef, P. Yazbeck, and D. Mehta, “Mechanisms regulating endothelial permeability,” *Pulm. Circ.*, vol. 4, no. 4, pp. 535–551, Dec. 2014.

[39] W. C. Aird, “Phenotypic Heterogeneity of the Endothelium: I. Structure, Function, and Mechanisms,” *Circ. Res.*, vol. 100, no. 2, pp. 158–173, Feb. 2007.

[40] C. M. Ghajar, K. S. Blevins, C. C. W. Hughes, S. C. George, and A. J. Putnam, "Mesenchymal stem cells enhance angiogenesis in mechanically viable prevascularized tissues via early matrix metalloproteinase upregulation," *Tissue Eng.*, vol. 12, no. 10, pp. 2875–2888, Oct. 2006.

[41] C. M. Ghajar *et al.*, "The Effect of Matrix Density on the Regulation of 3-D Capillary Morphogenesis," *Biophys. J.*, vol. 94, no. 5, pp. 1930–1941, Mar. 2008.

[42] S. Kachgal, B. Carrion, I. A. Janson, and A. J. Putnam, "Bone marrow stromal cells stimulate an angiogenic program that requires endothelial MT1-MMP," *J. Cell. Physiol.*, vol. 227, no. 11, pp. 3546–3555, Nov. 2012.

[43] Z. Chen *et al.*, "In vitro angiogenesis by human umbilical vein endothelial cells (HUVEC) induced by three-dimensional co-culture with glioblastoma cells," *J. Neurooncol.*, vol. 92, no. 2, pp. 121–128, Apr. 2009.

[44] R. Tiruvannamalai Annamalai, A. Y. Rioja, A. J. Putnam, and J. P. Stegemann, "Vascular Network Formation by Human Microvascular Endothelial Cells in Modular Fibrin Microtissues," *ACS Biomater. Sci. Eng.*, vol. 2, no. 11, pp. 1914–1925, Nov. 2016.

[45] C. J. Jackson and M. Nguyen, "Human microvascular endothelial cells differ from macrovascular endothelial cells in their expression of matrix metalloproteinases," *Int. J. Biochem. Cell Biol.*, vol. 29, no. 10, pp. 1167–1177, Oct. 1997.

[46] D. M. SUPP, K. WILSON-LANDY, and S. T. BOYCE, "Human dermal microvascular endothelial cells form vascular analogs in cultured skin substitutes after grafting to athymic mice," *FASEB J. Off. Publ. Fed. Am. Soc. Exp. Biol.*, vol. 16, no. 8, pp. 797–804, Jun. 2002.

[47] S. Hu *et al.*, "Effects of cellular origin on differentiation of human induced pluripotent stem cell–derived endothelial cells," *JCI Insight*, vol. 1, no. 8.

[48] R. P. Tan *et al.*, "Integration of induced pluripotent stem cell-derived endothelial cells with polycaprolactone/gelatin-based electrospun scaffolds for enhanced therapeutic angiogenesis," *Stem Cell Res. Ther.*, vol. 9, Mar. 2018.

[49] A. A. Youssef, E. G. Ross, R. Bolli, C. J. Pepine, N. J. Leeper, and P. C. Yang, "The Promise and Challenge of Induced Pluripotent Stem Cells for Cardiovascular Applications," *JACC Basic Transl. Sci.*, vol. 1, no. 6, pp. 510–523, Oct. 2016.

[50] Z. E. Clayton *et al.*, "A comparison of the pro-angiogenic potential of human induced pluripotent stem cell derived endothelial cells and induced endothelial cells in a murine model of peripheral arterial disease," *Int. J. Cardiol.*, vol. 234, pp. 81–89, May 2017.

[51] T. Ikuno *et al.*, “Efficient and robust differentiation of endothelial cells from human induced pluripotent stem cells via lineage control with VEGF and cyclic AMP,” *PLOS ONE*, vol. 12, no. 3, p. e0173271, Mar. 2017.

[52] X. Lian *et al.*, “Efficient Differentiation of Human Pluripotent Stem Cells to Endothelial Progenitors via Small-Molecule Activation of WNT Signaling,” *Stem Cell Rep.*, vol. 3, no. 5, pp. 804–816, Nov. 2014.

[53] Y. Lin, C.-H. Gil, and M. C. Yoder, “Differentiation, Evaluation, and Application of Human Induced Pluripotent Stem Cell–Derived Endothelial Cells,” *Arterioscler. Thromb. Vasc. Biol.*, vol. 37, no. 11, pp. 2014–2025, Nov. 2017.

[54] J. R. Bezenah, Y. P. Kong, and A. J. Putnam, “Evaluating the potential of endothelial cells derived from human induced pluripotent stem cells to form microvascular networks in 3D cultures,” *Sci. Rep.*, vol. 8, no. 1, p. 2671, Feb. 2018.

[55] J. Zhang *et al.*, “A Genome-wide Analysis of Human Pluripotent Stem Cell-Derived Endothelial Cells in 2D or 3D Culture,” *Stem Cell Rep.*, vol. 8, no. 4, pp. 907–918, Mar. 2017.

[56] Z. Li, S. Hu, Z. Ghosh, Z. Han, and J. C. Wu, “Functional Characterization and Expression Profiling of Human Induced Pluripotent Stem Cell- and Embryonic Stem Cell-Derived Endothelial Cells,” *Stem Cells Dev.*, vol. 20, no. 10, pp. 1701–1710, Oct. 2011.

[57] O. V. Halaidych *et al.*, “Inflammatory Responses and Barrier Function of Endothelial Cells Derived from Human Induced Pluripotent Stem Cells,” *Stem Cell Rep.*, vol. 10, no. 5, pp. 1642–1656, May 2018.

[58] C. C. Haudenschild, “Morphology of vascular endothelial cells in culture,” in *Biology of Endothelial Cells*, Springer, Boston, MA, 1984, pp. 129–140.

[59] “Endothelial Cells, Angiogenesis, and Vasculogenesis.” [Online]. Available: https://www.stemcell.com/endothelial-cells-angiogenesis-and-vasculogenesis-lp.html. [Accessed: 11-Jun-2018].

[60] T. H. Adair and J.-P. Montani, *Overview of Angiogenesis*. Morgan & Claypool Life Sciences, 2010.

[61] W. J. Adams *et al.*, “Functional Vascular Endothelium Derived from Human Induced Pluripotent Stem Cells,” *Stem Cell Rep.*, vol. 1, no. 2, pp. 105–113, Jul. 2013.

[62] V. V. Orlova *et al.*, “Functionality of Endothelial Cells and Pericytes From Human Pluripotent Stem Cells Demonstrated in Cultured Vascular Plexus and Zebrafish Xenografts,” *Arterioscler. Thromb. Vasc. Biol.*, p. ATVBAHA.113.302598, Jan. 2013.

[63] L. K. Christenson and R. L. Stouffer, “Isolation and culture of microvascular endothelial cells from the primate corpus luteum,” *Biol. Reprod.*, vol. 55, no. 6, pp. 1397–1404, Dec. 1996.

[64] R. H. Adamson, “Microvascular endothelial cell shape and size in situ,” *Microvasc. Res.*, vol. 46, no. 1, pp. 77–88, Jul. 1993.

[65] J. E. Sadler, “Biochemistry and Genetics of von Willebrand Factor,” *Annu. Rev. Biochem.*, vol. 67, no. 1, pp. 395–424, Jun. 1998.

[66] S.-Y. Jin, C. G. Skipwith, D. Shang, and X. L. Zheng, “von Willebrand factor cleaved from endothelial cells by ADAMTS13 remains ultra large in size,” *J. Thromb. Haemost. JTH*, vol. 7, no. 10, pp. 1749–1752, Oct. 2009.

[67] K. K. Hamilton, L. J. Fretto, D. S. Grierson, and P. A. McKee, “Effects of plasmin on von Willebrand factor multimers. Degradation in vitro and stimulation of release in vivo,” *J. Clin. Invest.*, vol. 76, no. 1, pp. 261–270, Jul. 1985.

[68] M. S. Kluger, P. R. Clark, G. Tellides, V. Gerke, and J. S. Pober, “Claudin-5 Controls Intercellular Barriers of Human Dermal Microvascular but Not Human Umbilical Vein Endothelial Cells,” *Arterioscler. Thromb. Vasc. Biol.*, vol. 33, no. 3, pp. 489–500, Mar. 2013.

[69] O. M. Benavides, J. J. Petsche, K. J. Moise, A. Johnson, and J. G. Jacot, “Evaluation of endothelial cells differentiated from amniotic fluid-derived stem cells,” *Tissue Eng. Part A*, vol. 18, no. 11–12, pp. 1123–1131, Jun. 2012.

[70] “Dead Cell Identification in Flow Cytometry: Eliminate Dead Cells for Increased Accuracy - US.” [Online]. Available: https://www.thermofisher.com/us/en/home/references/newsletters-and-journals/bioprobes-journal-of-cell-biology-applications/bioprobes-issues-2011/bioprobes-64-april-2011/eliminate-dead-cells-for-increased-accuracy-april-2011.html. [Accessed: 09-Jun-2018].

[71] E. Kniazeva, S. Kachgal, and A. J. Putnam, “Effects of extracellular matrix density and mesenchymal stem cells on neovascularization in vivo,” *Tissue Eng. Part A*, vol. 17, no. 7–8, pp. 905–914, Apr. 2011.

[72] E. Kniazeva and A. J. Putnam, “Endothelial cell traction and ECM density influence both capillary morphogenesis and maintenance in 3-D,” *Am. J. Physiol. Cell Physiol.*, vol. 297, no. 1, pp. C179-187, Jul. 2009.

[73] M. Mongiat, E. Andreuzzi, G. Tarticchio, and A. Paulitti, “Extracellular Matrix, a Hard Player in Angiogenesis,” *Int. J. Mol. Sci.*, vol. 17, no. 11, Nov. 2016.

[74] R. R. Rao, A. W. Peterson, J. Ceccarelli, A. J. Putnam, and J. P. Stegemann, “Matrix Composition Regulates Three-Dimensional Network Formation by Endothelial Cells and

Mesenchymal Stem Cells in Collagen/Fibrin Materials," *Angiogenesis*, vol. 15, no. 2, pp. 253–264, Jun. 2012.

[75] J. Liu *et al.*, "Soft fibrin gels promote selection and growth of tumourigenic cells," *Nat. Mater.*, vol. 11, no. 8, pp. 734–741, Jul. 2012.

[76] M. A. Lieberman and L. Glaser, "Density-dependent regulation of cell growth: an example of a cell-cell recognition phenomenon," *J. Membr. Biol.*, vol. 63, no. 1–2, pp. 1–11, 1981.

[77] D. A. Gilbert, "Density-dependent limitation of growth and the regulation of cell replication by changes in the triggering level of the cell cycle switch," *Biosystems*, vol. 9, no. 4, pp. 215–228, Dec. 1977.

[78] R. D. Starke *et al.*, "Endothelial von Willebrand factor regulates angiogenesis," *Blood*, vol. 117, no. 3, pp. 1071–1080, Jan. 2011.

[79] H. Yamaguchp, E. Ishii, K. Tashiro, and S. Miyazaki, "Role of Umbilical Vein Endothelial Cells in Hematopoiesis," *Leuk. Lymphoma*, vol. 31, no. 1–2, pp. 61–69, Jan. 1998.

[80] G. Wu and H. R. Schöler, "Role of Oct4 in the early embryo development," *Cell Regen.*, vol. 3, no. 1, Apr. 2014.

[81] J. Jozefczuk, A. Prigione, L. Chavez, and J. Adjaye, "Comparative Analysis of Human Embryonic Stem Cell and Induced Pluripotent Stem Cell-Derived Hepatocyte-Like Cells Reveals Current Drawbacks and Possible Strategies for Improved Differentiation," *Stem Cells Dev.*, vol. 20, no. 7, pp. 1259–1275, Dec. 2010.

[82] M. Ho *et al.*, "Identification of endothelial cell genes by combined database mining and microarray analysis," *Physiol. Genomics*, vol. 13, no. 3, pp. 249–262, May 2003.

[83] A. C. Browning *et al.*, "Comparative gene expression profiling of human umbilical vein endothelial cells and ocular vascular endothelial cells," *Br. J. Ophthalmol.*, vol. 96, no. 1, pp. 128–132, Jan. 2012.

[84] "The Molecular and Cellular Biology of Wound Repair | Richard Clark | Springer." [Online]. Available: https://www.springer.com/us/book/9780306451591. [Accessed: 12-Jun-2018].

[85] A. W. Peterson, D. J. Caldwell, A. Y. Rioja, R. R. Rao, A. J. Putnam, and J. P. Stegemann, "Vasculogenesis and Angiogenesis in Modular Collagen-Fibrin Microtissues," *Biomater. Sci.*, vol. 2, no. 10, pp. 1497–1508, Oct. 2014.

[86] R. K. Singh, D. Seliktar, and A. J. Putnam, "Capillary morphogenesis in PEG-collagen hydrogels," *Biomaterials*, vol. 34, no. 37, pp. 9331–9340, Dec. 2013.

[87] M. Vigen, J. Ceccarelli, and A. J. Putnam, “Protease-sensitive PEG hydrogels regulate vascularization in vitro and in vivo,” *Macromol. Biosci.*, vol. 14, no. 10, pp. 1368–1379, Oct. 2014.

[88] K. Duval *et al.*, “Modeling Physiological Events in 2D vs. 3D Cell Culture,” *Physiology*, vol. 32, no. 4, pp. 266–277, Jul. 2017.

[89] R. Edmondson, J. J. Broglie, A. F. Adcock, and L. Yang, “Three-Dimensional Cell Culture Systems and Their Applications in Drug Discovery and Cell-Based Biosensors,” *Assay Drug Dev. Technol.*, vol. 12, no. 4, pp. 207–218, May 2014.

# CHAPTER 3

# Evaluating the Potential of iPSC-ECs to Form Microvascular Networks in 3D Cultures *in vitro*



## 3.1 Introduction

Numerous cardiovascular diseases are characterized by ischemia, a reduction/obstruction of oxygenated blood supply to tissues, which can eventually lead to necrosis [1]. Due to the increasing number of deaths and costs attributed to ischemic diseases, it is critical to create new therapies focused on rebuilding vasculature to provide cells with sufficient oxygen and nutrients to prevent additional necrosis and amputations [2-4].

Over the past decade, several therapeutic approaches have emerged to promote angiogenesis and vasculogenesis, the processes by which new blood vessels form from preexisting blood vessels or de novo respectively. One technique involves the delivery of growth factors to stimulate endothelial cell recruitment [5-7]. However, these approaches are often limited by rapid diffusion, short half-lives, and poor biostability of growth factors [8]. An alternative tissue engineering approach involves the delivery of cells to directly differentiate into capillary structures. Various cell types have been shown to create new capillary networks *in vivo* [9-11]. In addition, some strategies involve implanting engineered scaffolds or co-delivering endothelial

cells (ECs) with stromal cells to promote vessel in-growth or stable, mature vasculature formation, respectively [12-15]. Despite these advances, there are still critical challenges that plague their application, such as possible immunorejection from the host and the vast number of cells required for human translation [16-18].

Advances in cellular reprograming have led to the discovery of one particularly exciting alternative cell source for therapeutic vascularization, induced pluripotent stem cells (iPSC). These cells are derived by reprograming adult somatic cells into pluripotency, a stem-cell like state, typically with four transcription factors [Oct4, Sox2, Klf4, and cMyc (OSKM)] [19]. In this state, cells can be differentiated into many different lineages, including the mesoderm to create endothelial cells [20]. iPSCs offer numerous advantages including their potential autologous nature, which could eliminate any immunological concerns during their therapeutic delivery. Furthermore, since these cells are derived from adult somatic cells, there is little ethical concern over their use, despite their stem cell-like lineage. More importantly, these cells can be created from various sources and have an unlimited proliferation capacity, in theory, leading to a potentially large reservoir of cells for clinical applications [21].

Research has successfully demonstrated the ability to differentiate iPSCs into endothelial cells [22-24]. These induced pluripotent stem cell-derived endothelial cells (iPSC-ECs) are characterized by their ability to express endothelial cell markers. Further studies with iPSC-ECs revealed their potential to form vessel-like networks on a Matrigel supporting material both *in vitro* and *in vivo* [25-27]. While this research is promising for tissue engineering and revascularization, very little is known about how these cells behave and compare to other endothelial cell sources, specifically in the quantity, quality, and function of the vessel-like networks formed.

The present study explores whether a potentially autologous EC source derived from human induced pluripotent stem cells (iPSC-ECs) can form the same robust, stable microvasculature previously documented for other sources of ECs. Using a well-established *in vitro* model, endothelial cells were coated on dextran microcarrier beads and co-embedded in a 3D fibrin matrix with normal human lung fibroblasts (NHLFs). Fibrin was selected due to its naturally occurring presence in humans and FDA clearance for clinical use [28, 29], while NHLFs were chosen due to their aforementioned ability to aid in the formation of microvascular networks as previously reported [30-32]. We examined differences in capillary morphogenesis of iPSC-ECs and human umbilical vein endothelial cells (HUVECs) by quantifying total network lengths, number of branch points, and number of vessel-like segments and qualitatively identifying characteristics of mature capillaries.

## 3.2 Materials and Methods

### 3.2.1 HUVEC Isolation and Cell Culture

Human umbilical vein endothelial cells were either purchased (Lonza, Walkersville, MD) or harvested from fresh umbilical cords from the University of Michigan Mott Children's Hospital via an IRB-exempt protocol and isolated from methods previously described [33]. The umbilical cord was rinsed in phosphate buffer saline (PBS) and then digested with 0.1% collagenase type I (195 U/ml, Worthington Biochemical, Lakewood, NJ) for 20 mins at 37°C. The digested product was subsequently washed in PBS, collected, and centrifuged (200×G for 5 min). The pellet was resuspended in endothelial growth media (EGM-2, Lonza), and the cells were plated in tissue

culture flasks and cultured at 37°C and 5% $CO_2$. After 24 hours, HUVECs were rinsed with PBS to remove any non-adherent cells. Fresh media was changed every 48 hours. Cells from passage 3 were utilized for experiments. Normal human lung fibroblasts (NHLF, Lonza) were cultured at 37°C and 5% $CO_2$ in Dulbecco's modified eagle media (DMEM, Life Technologies, Grand Island, NY) with 10% fetal bovine serum (FBS). Culture media was replaced every 48 hours and cells from passage 6-10 were used in experiments. Two sources of iPSC-ECs were used in our experiments. iCell endothelial cells (Cellular Dynamics International, Madison, WI), referred to as iPSC-EC (1), were cultured at 37°C and 5% $CO_2$ in Vasculife VEGF endothelial media (Lifeline Cell Technology, Fredrick, MD) supplemented with iCell Endothelial Cell Medium Supplement (Cellular Dynamics International). Three different lots were used. A second source of iPSC-ECs, referred to as iPSC-EC (2), were graciously provided by Dr. Ngan Huang (Stanford University). iPSC-EC (2) were cultured at 37°C and 5% $CO_2$ in EGM-2MV (Lonza). Both iPSC-EC tissue culture flasks were coated with 35 µg/mL fibronectin (Invitrogen, Carlsbad, CA) for 1 hr at room temp prior to plating the cells. Culture media was replaced every 48 hours and cells from passage 3 were used in experiments. Microvascular endothelial cells (Lonza) were cultured at 37 °C and 5% $CO_2$ in EGM-2MV (Lonza). Culture media was replaced every 48 hours and cells from passage 5 were used in experiments.

### 3.2.2 Microcarrier Bead Assembly

Cytodex microcarrier beads (Sigma-Aldrich, St. Louis, MO) were hydrated and sterilized in phosphate buffer saline (PBS). Beads were prepared for coating by washing repeatedly with 1 mL of EGM-2, with time to settle between washes. Endothelial cells were cultured in T-75 flasks to 80% confluency and rinsed with PBS before being harvested via 0.25% trypsin incubation for

5 min at 37 °C and 5% $CO_2$. Trypsin was neutralized using DMEM supplemented with 10% FBS. The cellular suspension was centrifuged (200×G for 5 min) and supernatant was aspirated immediately. The cell pellet was re-suspended in 4 mL of fresh EGM-2. 10,000 microcarrier beads were combined with four million ECs, HUVECs or iPSC-ECs, (5 mL total) in an inverted T-25 culture flask. Over a 4 hour incubation period, the culture flask was agitated every 30 minutes to ensure EC coating of beads. After 4 hours, the cell-bead mixture was added to a new T-25 culture flask. Fresh EGM-2 (5 mL) was added to the old flask to remove any remaining beads and transferred to the new culture flask. The total volume (10 mL) was incubated overnight in standard cell culture position.

### 3.2.3 Fibrin Tissue Assembly

The next day, following bead coating, a fibrinogen (Sigma-Aldrich) solution of the desired concentration (2.5 mg/mL) was dissolved in an appropriate amount of serum-free EGM-2 and placed at 37 °C in a water bath. The solution was sterile filtered through a 0.22 μm syringe filter (Millipore, Billerica, MA). The previous day's cell-bead solution was removed from the culture flask and placed in a 15 mL centrifuge tube. After the beads settled, the remaining supernatant was used to remove any remaining beads adhering to the culture flask and added to the centrifuge tube. Upon the beads settling, the supernatant was removed and 5 mL of fresh serum-free EGM-2 was added to the cell-coated beads. The appropriate amount of bead solution (~ 50 beads per well) was added to the fibrinogen solution with 5% FBS. Fibroblasts were prepared using a similar rinsing/trypsinization procedure as described above. 25,000 NHLFs per well were added to the bead-fibrinogen solution or plated on top of each gel after polymerization in our distributed and monolayer conditions respectively. 500 μL of above mixture was added to a single well of a 24-

well tissue culture plate and polymerized with 10 µL of thrombin (50 U/mL, Sigma-Aldrich). Tissue constructs were left undisturbed for 5 min at room temperature before incubation for 30 min at 37 °C and 5% CO2. 1 mL of media [EGM-2 (Lonza), EGM-2MV (Lonza), or Vasculife VEGF media (Lifeline) + iCell endothelial cell supplement (Cellular Dynamics International) depending on the experiment was added on top of the gels following incubation and changed the following day and every other day thereafter (Fig. 3-1).

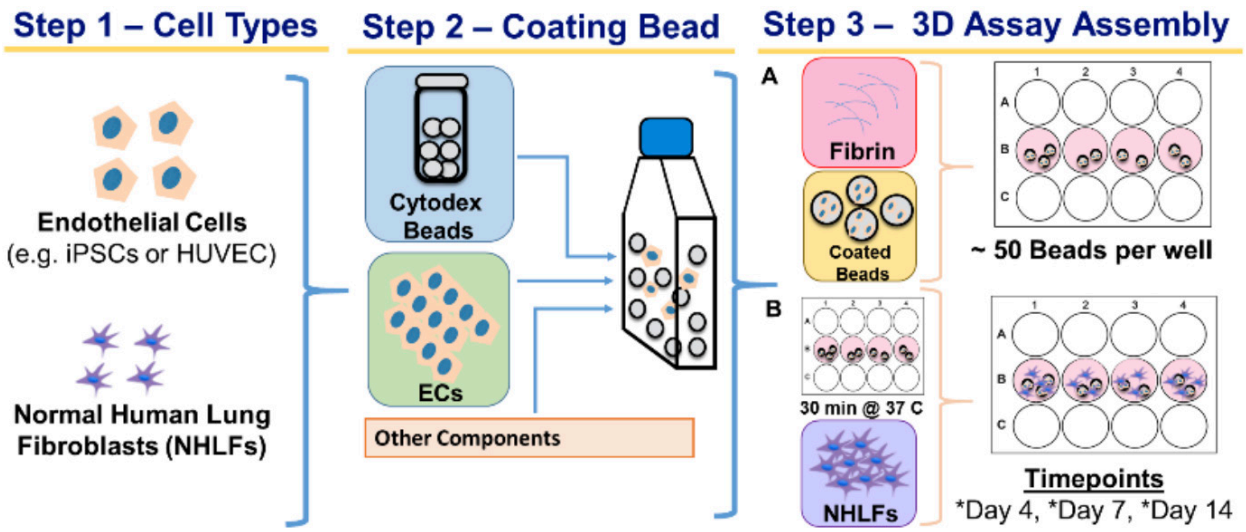


**Figure 3-1: Angiogenic Assay Fabrication Process.**
ECs are coated on microcarrier dextran beads. Cell-coated beads and NHLFs are embedded in a 2.5 mg/mL fibrin gel. Resultant tissue constructs are cultured for 4, 7, 14 days and then analyzed.

### 3.2.4 Vasculogenesis Tissue Assay Assembly

The vasculogenesis assay was prepared using a similar procedure as described above. A fibrinogen (Sigma-Aldrich) solution of the desired concentration (2.5 mg/mL) was dissolved in an appropriate amount of serum-free EGM-2 and placed at 37 °C in a water bath. The solution was sterile filtered through a 0.22 µm syringe filter (Millipore, Billerica, MA). A 1:1 ratio of endothelial cells to NHLFs was added to the fibrinogen solution with 5% FBS at varying total cell

densities (250K or 500K). Endothelial cells and fibroblasts were prepared using a similar rinsing/trypsinization procedure as described above. 500 μL of above mixture was added to a single well of a 24-well tissue culture plate and polymerized with 10 μL of thrombin (50 U/mL, Sigma-Aldrich). Tissue constructs were left undisturbed for 5 min at room temperature before incubation for 30 min at 37 °C and 5% CO2. 1 mL of EGM-2 was added on top of the gels following incubation and changed the following day and every other day thereafter.

### 3.2.5 Immunofluorescent staining

After the constructs were cultured for a specified period of time (1, 4, 7, or 14 days), gels were rinsed 3x with PBS solution for 5 min at room temperature. Gels were then fixed with 500 μL of formalin (1 mL of 36.5% Formaldehyde solution (Sigma), 1 mL of PBS, and 8 mL of d.d.H2O) for 15 min at 4 °C. Gels were rinsed again 3x with PBS for 5 min, then permeabilized with 0.5% Triton-X100 in TBS for 30 min at 4 °C. Following a rinse 3x for 5 min at room temperature with 0.1% Triton X-100 in TBS (TBS-T), samples were blocked overnight at 4 °C with a 2% Abdil solution (bovine serum albumin (Sigma) dissolved in TBS-T). The primary antibody/staining agent was dissolved in 2% Abdil at the appropriate concentration (Ulex Europaeus Lectin 1 (UEA), 1:100 (Vector Labs, Burlingame, CA); anti-CD31, 1:200 (Dako, Santa Clara, CA); collagen IV, 1:200 (Pierce Biotechnology, Waltham, MA); laminin, 1:200 (Pierce Biotechnology); alpha-smooth muscle actin (αSMA), 1:200 (Pierce Biotechnology)) and 1 mL of this solution was added to each gel for overnight incubation at 4 °C. The following day gels were rinsed 3x for 5 min with TBS-T. 1 mL of the appropriate secondary antibody (1:400, Alexa Fluor 488 Goat anti-mouse IgG, Alexa Fluor 405 Goat anti-mouse IgG, Alexa Fluor 488 Goat anti-rabbit IgG, Alexa Fluor 405 Goat anti-rabbit IgG, Invitrogen) dissolved in 2% Abdil was added to each

gel for overnight incubation at 4 °C. Following a 3x rinse for 5 min at room temperature with TBS-T, gels were incubated with TBS-T overnight at 4 °C.

### 3.2.6 Fluorescent Imaging and Vessel Quantification

Vessel formation was assessed at the aforementioned time points. Fluorescent images were captured utilizing an Olympus IX81 equipped with Disc Spinning Unit and a 100 W high-pressure mercury burner (Olympus America, Center Valley, PA), a Hamamatsu Orca II CCD camera (Hamamatsu Photonics, K.K., Hamamatsu City, Japan), and Metamorph Premier software (Molecular Devices, Sunnyvale, CA). Imaged beads were chosen at random provided vessels emanating from a given bead did not form anastomoses with vessels from adjacent beads. Images from at least 30 beads per condition were captured over three separate trials at low magnification (4×) for each independent experiment and processed using the Angiogenesis Tube Formation module in Metamorph Premier (Molecular Devices). Each image was segmented and analyzed based on any tube-like pattern that falls within a specified minimum and maximum width of each segment above a contrast threshold. The total network length, the number of branch points, and number of segments were quantified.

### 3.2.7 Statistical Analysis

Statistical analyses were performed using StatPlus (AnalystSoft Inc.,Walnut, CA). Data are reported as mean ± standard error of mean (SEM). One- or two-way analysis of variance (ANOVA) with a Bonferroni post-test was used to assess statistical significance between data sets. Statistical significance was assumed when $p<0.05$.

## 3.3 Results

### 3.3.1 iPSC-ECs exhibit deficiencies in capillary morphogenesis compared to HUVECs

In-house isolated HUVECs ("isolated HUVECs"), commercially purchased HUVECs ("commercial HUVECs"), and two different sources of iPSC-derived ECs [iPSC-ECs (1) and iPSC-ECs (2)] were characterized for the ability to sprout from microcarrier beads when co-cultured with NHLFs in a 3D fibrin matrix. Immunofluorescent staining for CD31 in these cultures demonstrated successful attachment, invasion into the ECM, and primitive sprouting across all EC types at day 1. However, on days 7 and 14, the capillary sprouting of iPSC-ECs (1) showed significant reductions in their networks compared to the two HUVEC conditions (Fig. 3-2.1A), while no capillary sprouting was evident for iPSC-ECs (2). Quantification of these networks (Fig. 3-2.2B) demonstrated a significant decrease in total network length between the two HUVEC conditions and iPSC-ECs (1) (8311 ± 2091 μm for iPSC-ECs (1) versus 29458 ± 3977 μm for the isolated HUVECs and 21794 ± 3825 μm for the commercial HUVECs on day 14). This reduced total network length was accompanied by a five-fold decrease in the number of vessel branch points and number of segments formed (Fig. 3-2.2C-D). iPSC-EC (2) was not quantified at day 7 and day 14 time points due to the lack of sprouting. There was no statistical difference between the two HUVEC conditions, despite slightly reduced total network length, number of branch points, and number of segments. Since there were no statistical differences, subsequent experiments used only in-house isolated HUVECs, and henceforth are referred to as HUVECs solely. Furthermore, due to their ability to form at least some capillary-like networks, iPSC-ECs

(1) was used as the sole iPSC-EC source in subsequent experiments and henceforth are referred to as iPSC-ECs.

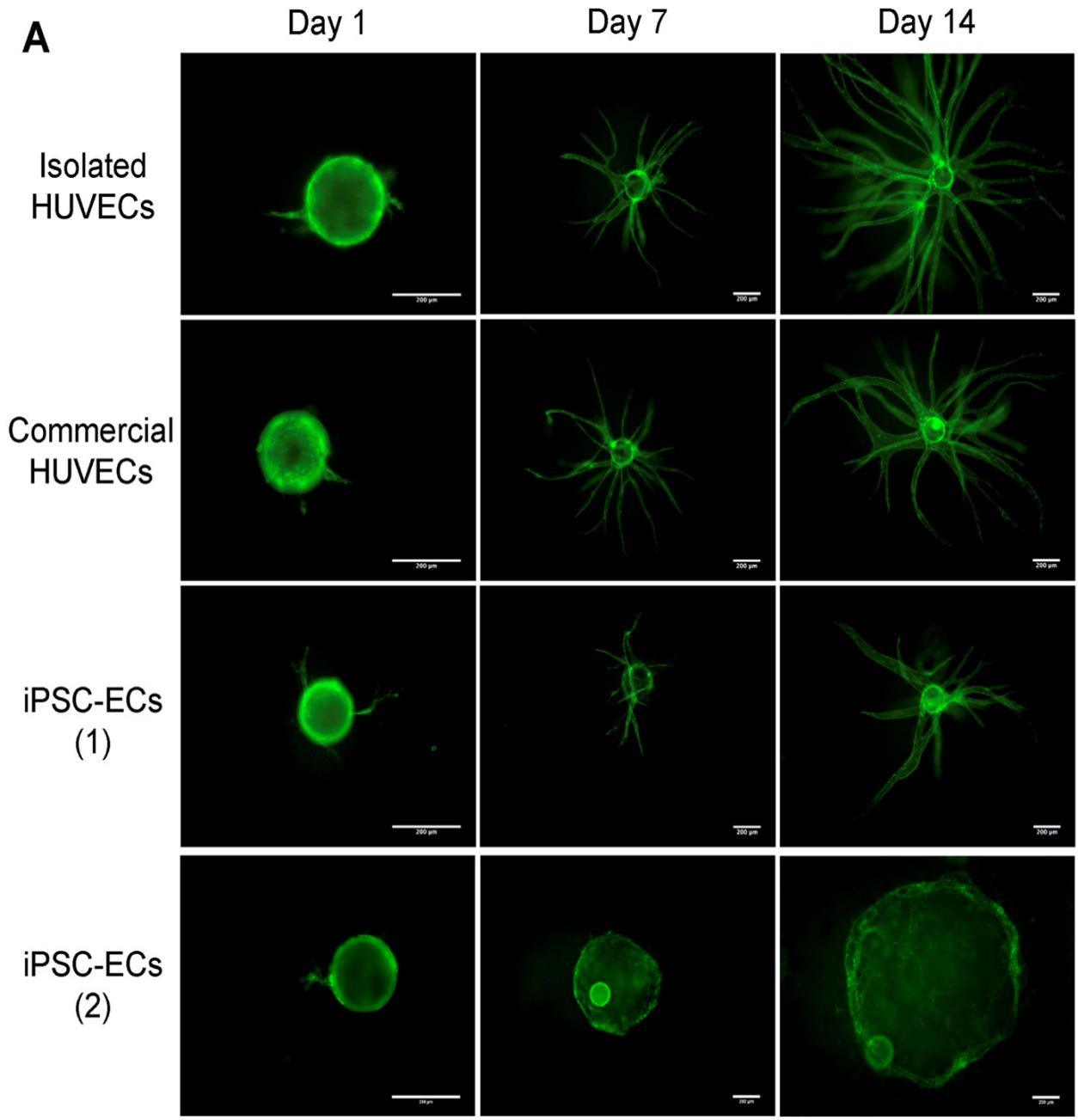


**Figure 3-2.1: iPSC-ECs exhibit deficiencies in capillary morphogenesis compared to HUVECs.** ***[Rep. Images]***
**(A)** EC-coated microbeads embedded in 2.5 mg/mL fibrin with NHLF at various time points were stained for CD31 and visualized via fluorescent microscopy. Scale bar = 200 µm.

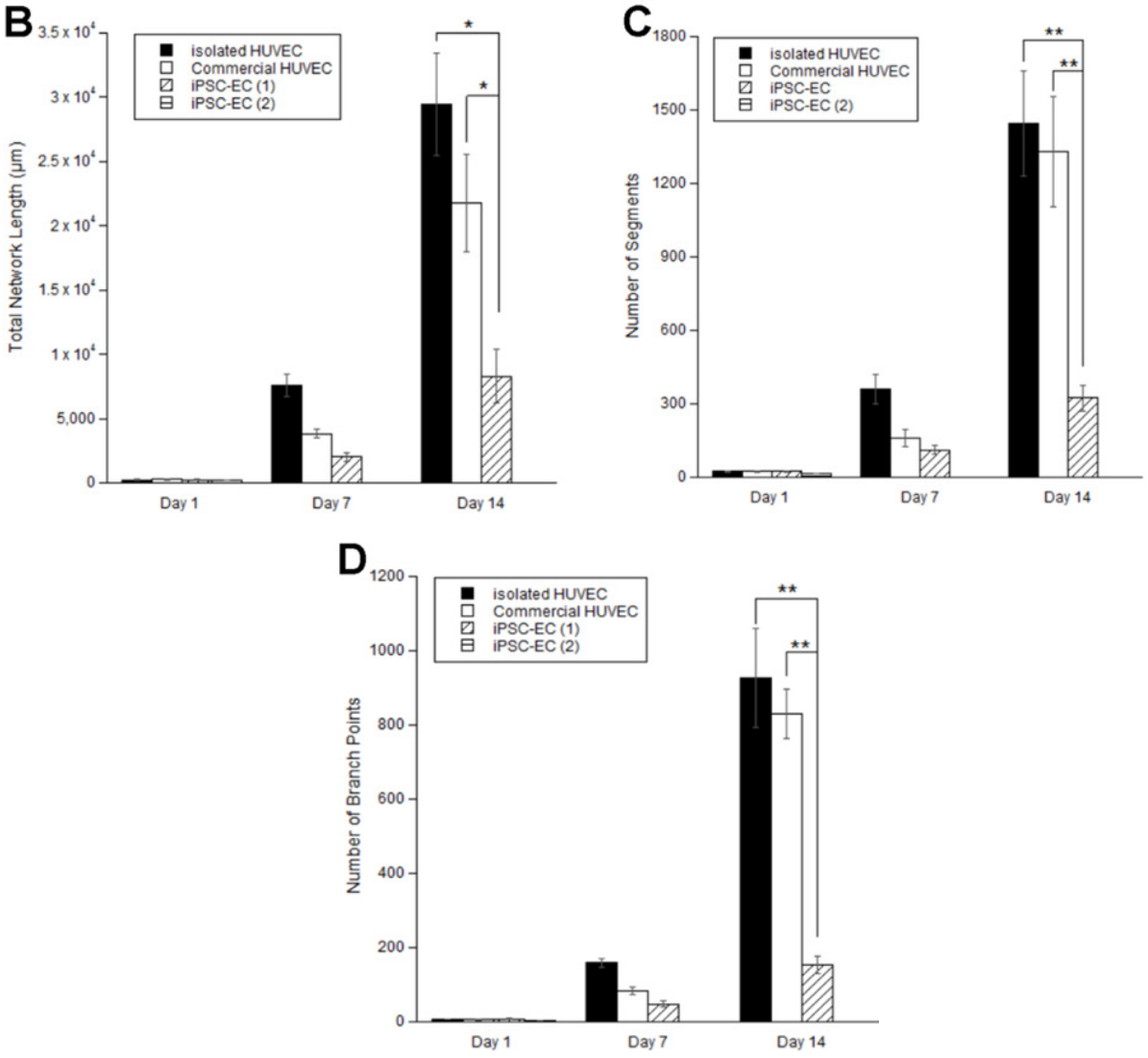


**Figure 3-2.2: iPSC-ECs exhibit deficiencies in capillary morphogenesis compared to HUVECs.** ***[Quantification]*** Over 3 separate experiments, a total of 30 beads per EC were quantified and averaged for **(B)** total capillary network length, **(C)** number of segments, and **(D)** number of branch points. *p<0.05 and **p<0.01 when comparing the indicated condition to the isolated HUVEC control at that time point. Error bars indicate ±SEM

## 3.3.2 Multiple lots of iPSC-ECs exhibit deficiencies in capillary morphogenesis.

One explanation for the attenuation of iPSC-EC sprouting seen in the prior experiment is lot-to-lot variation. While the previous experiments demonstrated attenuation across 3 independent trials, these experiments used only one lot from the commercial source. To determine if lot variation is a possible explanation for the attenuation, additional different lots were purchased from

the same vendor. Each iPSC-EC lot was characterized for the ability to sprout when embedded with NHLFs in a 3D fibrin matrix. Immunofluorescent staining for UEA in these cultures demonstrated significant reductions in their networks across all lots compared to the HUVEC condition (Fig. 3-3.1). Quantification of these networks (Fig. 3-3.2) demonstrated a significant decrease in total network length for each iPSC-EC lot in comparison to the HUVECs at every time point. This reduced total network length was accompanied by a statistically significant decrease in the number of vessel branch points and number of segments formed. Despite differences of each iPSC-EC lot to the HUVECs, there were no statistically significant differences between the iPSC-EC lots. Collectively, this data demonstrates the similarities between different iPSC-EC lots, and lot variation does not account for the attenuation of iPSC-EC capillary morphogenesis.

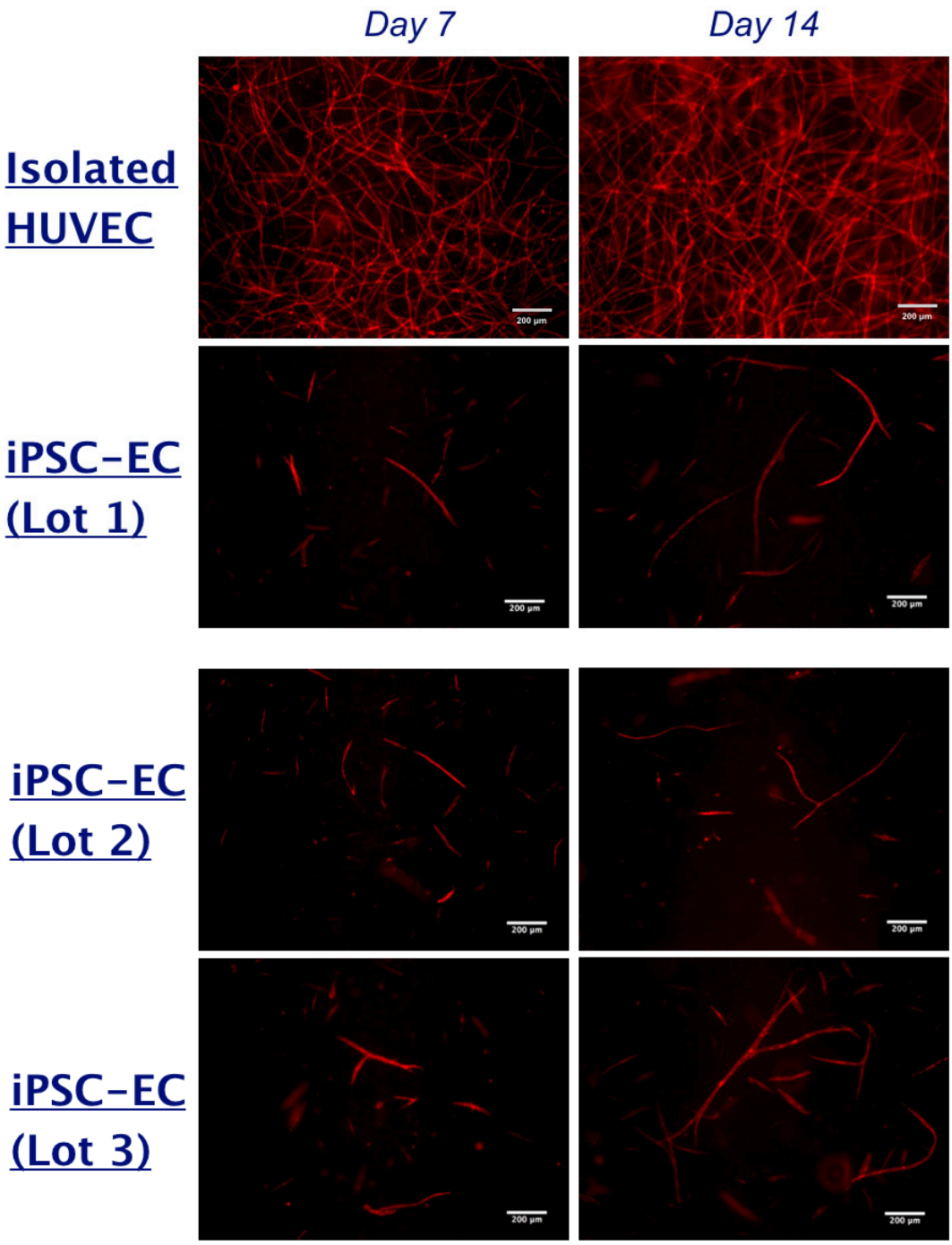


**Figure 3-3.1: Multiple lots of iPSC-ECs exhibit deficiencies in capillary morphogenesis.** ***[Rep. Images]***
ECs embedded in 2.5 mg/mL fibrin with NHLF at various time points were stained for UEA and visualized via fluorescent microscopy. Scale bar = 200 µm.

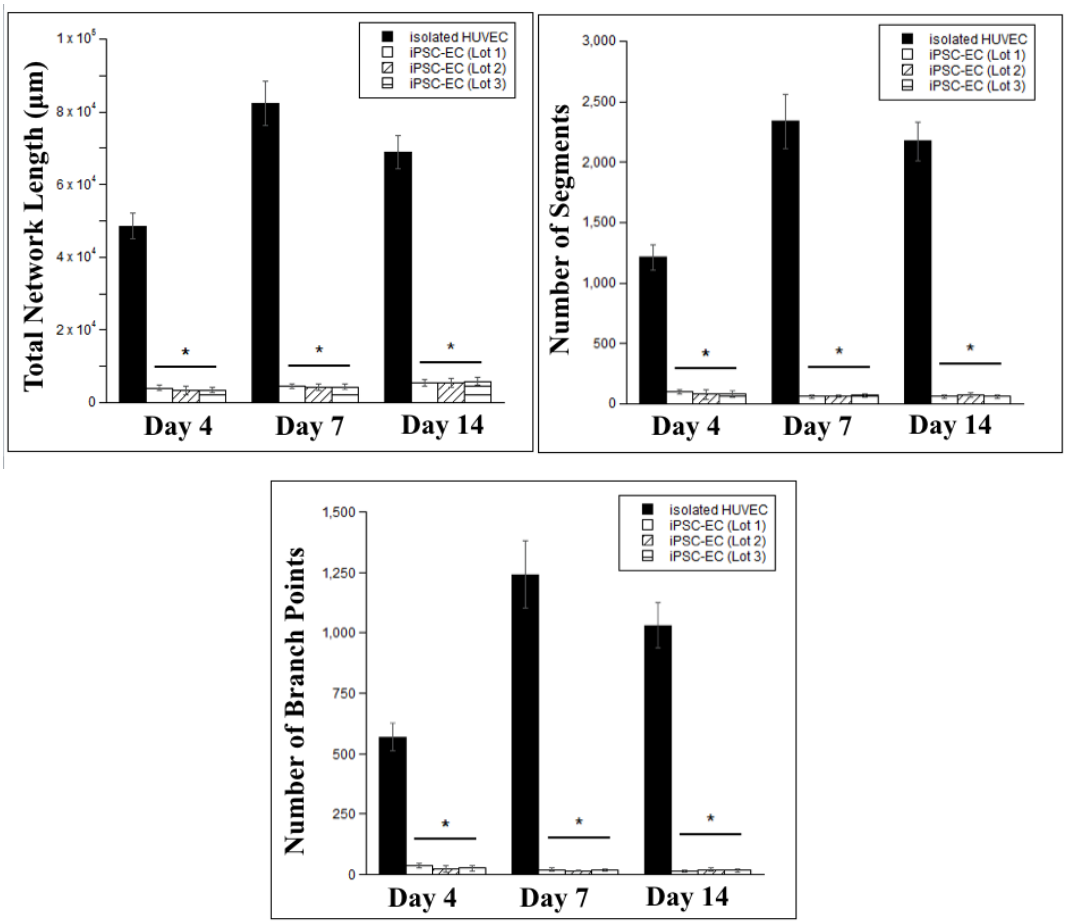


**Figure 3-3.2: Multiple lots of iPSC-ECs exhibit deficiencies in capillary morphogenesis.** ***[Quantification]*** Over 3 separate experiments, a total of 30 random locations in the fibrin gel per EC were quantified and averaged for total capillary network length, number of segments, and number of branch points. *p<0.05 and **p<0.01 when comparing the indicated condition to the HUVEC control at that time point. Error bars indicate ±SEM

### 3.3.3 Various endothelial cell lineages express differences in capillary morphogenesis

While HUVECs are a robust source of ECs with proven capability of capillary morphogenesis, particularly in the assay used here, another EC type of different origin, microvascular endothelial cells (MVECs), were also characterized for their ability to sprout from microcarrier beads when co-cultured with NHLFs in a 3D fibrin matrix and compared against iPSC-ECs. These tissue constructs were cultured with two different media conditions, EGM-2 and

EGM-2MV. Immunofluorescent staining for UEA in these cultures demonstrated successful attachment, invasion into the ECM, and primitive sprouting across all EC types and media conditions at day 1. However, on days 7 and 14, the capillary sprouting of iPSC-ECs and MVECs in both EGM-2 and EGM-2 showed significant reductions in their networks compared to the two HUVEC conditions (Fig. 3-4.1A, B). Quantification of these networks (Fig. 3-4.2) demonstrated a significant decrease in total network length in the iPSC-ECs and MVECs compared the HUVECs (2985.33 ± 757.9 μm for iPSC-EC EGM-2, 2782.83 ± 955.2 μm for iPSC-EC EGM-2MV, 1322.89 ± 135.4 μm for MVEC EGM-2, 2470.43 ± 240.4 μm for MVEC EGM-2MV, versus 15651.58 ± 2070.4 μm for the HUVEC EGM-2 and 13401.33 ± 650.8 μm for HUVEC EGM-2MV on day 14). Furthermore, there were no statistical difference between the two HUVEC conditions. There were also no statistically significant differences between the iPSC-EC conditions. Lastly, there was a 2-fold statistical difference between the two MVEC conditions.

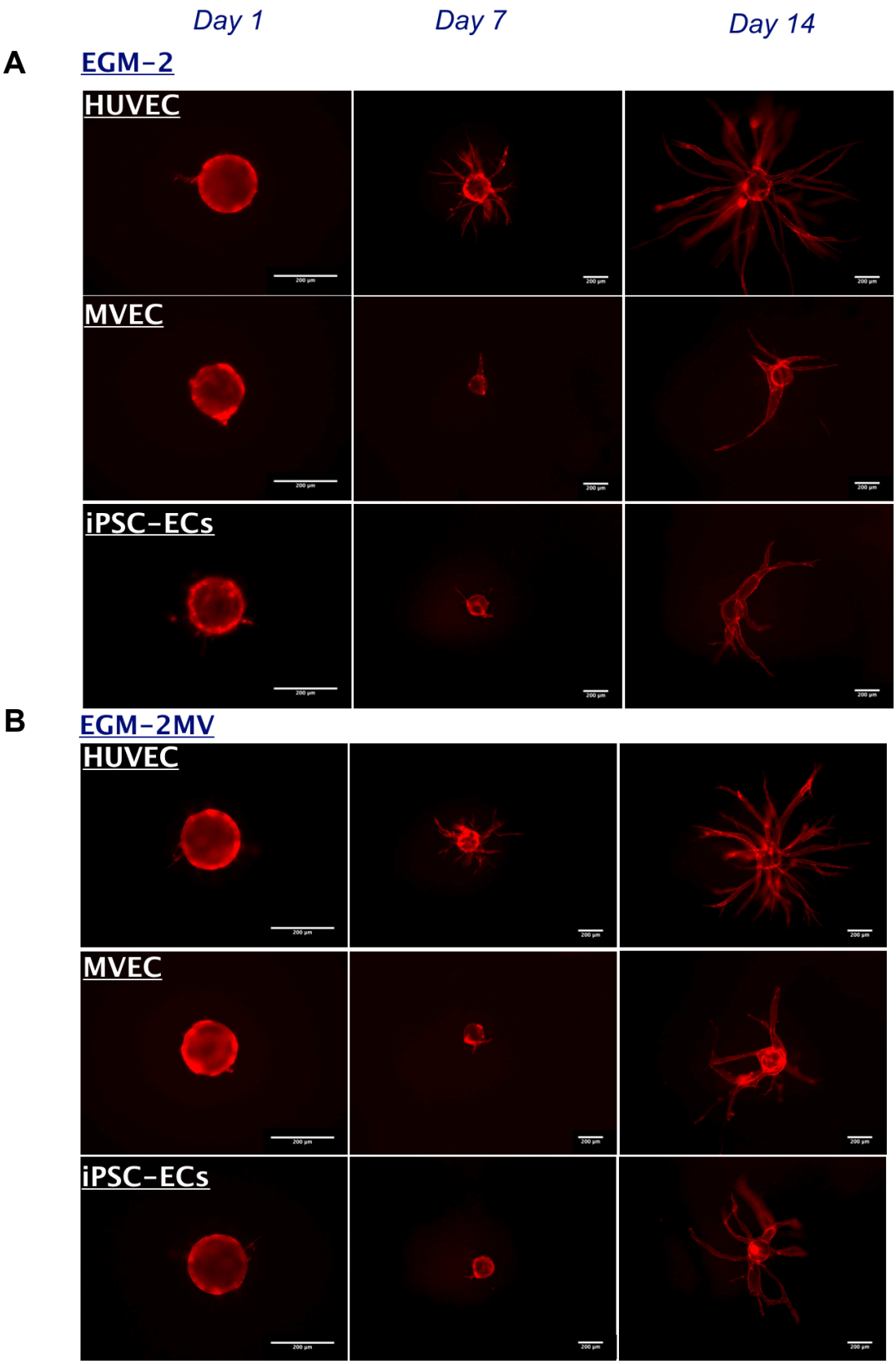


**Figure 3-3.1: Various endothelial cell lineages express differences in capillary morphogenesis *[Rep. Images]***
EC-coated microbeads embedded in 2.5 mg/mL fibrin with NHLFs cultured in either **(A)** EGM-2 or **(B)** EGM-2MV at various time points were stained for UEA and visualized via fluorescent microscopy. Scale bar = 200 µm.

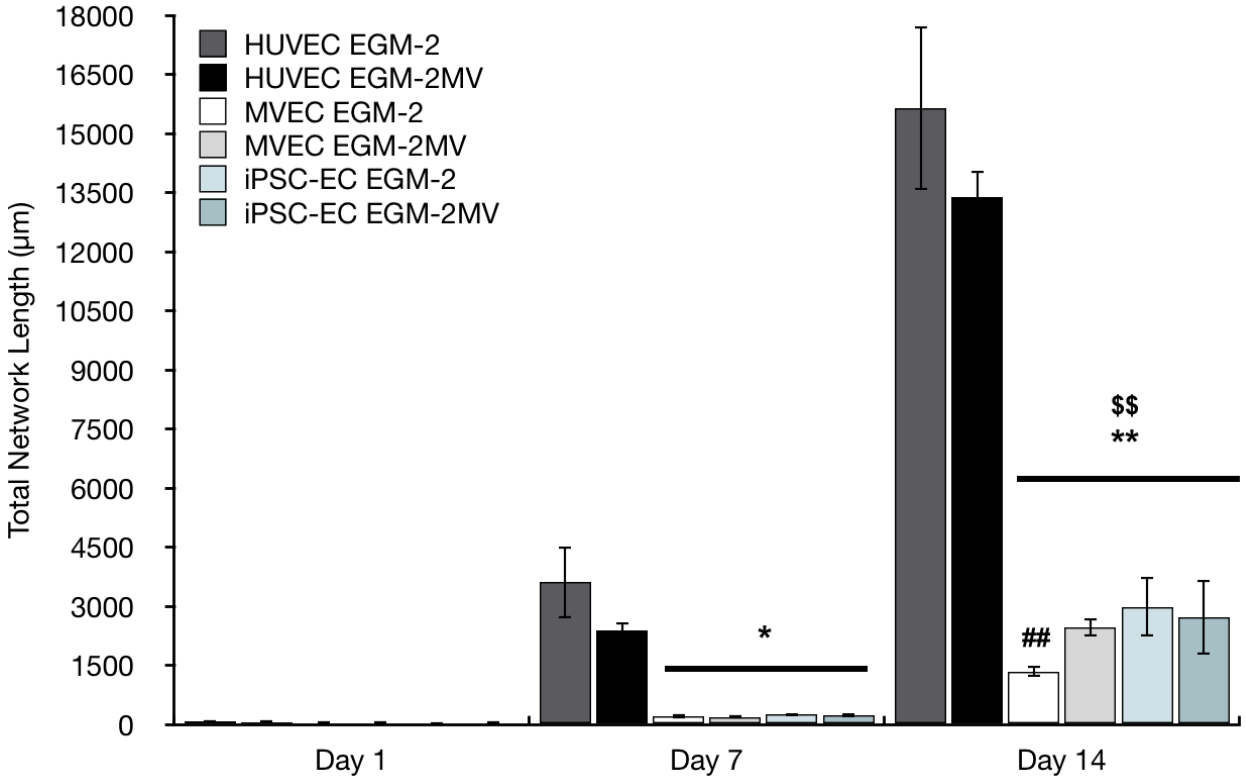


**Figure 3-3.2: Various endothelial cell lineages express differences in capillary morphogenesis *[Quantification]***
A total of 30 beads per EC were quantified and averaged for total capillary network length *p<0.05 and **p<0.01 when comparing the indicated condition to the HUVEC EGM-2 at that time point. $$ p<0.01 when comparing the indicated condition to the HUVEC EGM-2MV at that time point. ##pp<0.01 when comparing the indicated condition to the MVEC EGM-2MV at that time point. Error bars indicate ±SEM.

### 3.3.4 Differences in media composition does not account for attenuation of iPSC-EC vasculogenic attenuation

Another possible explanation for the reduction of iPSC-EC capillary morphogenesis is the culture media. The commercial vendor requires that a proprietary supplement be added to the media when culturing and passaging their iPSC-ECs. The aforementioned experiments used a general endothelial cell growth media for culturing the various tissue constructs. To assess whether media composition affects the capillary morphogenesis, ECs were coated on microcarrier beads

when co-cultured with NHLFs in a 3D fibrin matrix characterized for their ability to sprout in various media conditions, EGM-2 and Vasculife VEGF media with iCell Endothelial Cell Supplement, henceforth referred to as iPSC-EC media. Immunofluorescent staining for UEA in these cultures demonstrated reductions in the capillary sprouting of iPSC-ECs for both EGM-2 and iPSC-EC media conditions in comparison to their respective HUVEC condition (Fig. 3-5). Quantification of these networks demonstrated a significant decrease in total network length in the iPSC-ECs compared the HUVECs (1466 ± 237 μm for iPSC-ECs in EGM-2, 2092 ± 288 μm for iPSC-ECs in iPSC-EC media versus 16384 ± 3016 μm for the HUVECs in EGM-2 and 8920 ± 1596 μm for HUVECs in iPSC-EC media)**.** There was a two-fold statistical difference between the two HUVEC conditions. However, there was no statistically significant differences between the iPSC-EC conditions.

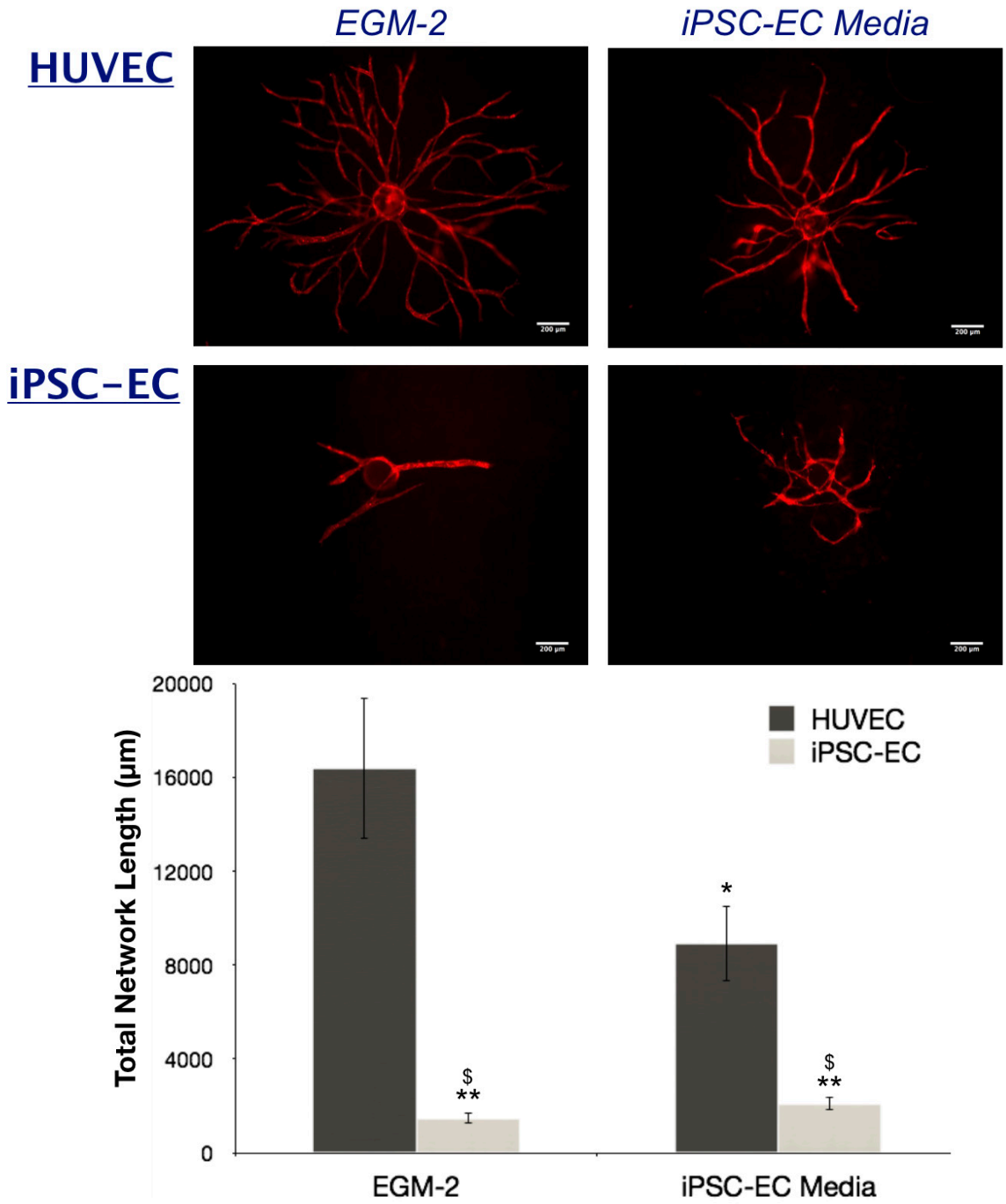


**Figure 3-5: Differences in media composition does not account for attenuation of iPSC-EC vasculogenic attenuation**
EC-coated microbeads embedded in 2.5 mg/mL fibrin with NHLF cultured in varying media formulation were stained for UEA and visualized via fluorescent microscopy at day 14. Scale bar = 200 µm. Over 3 separate experiments, a total of 30 random beads per EC were quantified and averaged for total capillary network length. *$p<0.05$ and **$p<0.01$ when comparing the indicated condition to the HUVEC EGM-2 condition. \$ $p<0.05$ when comparing the indicated condition to the HUVEC iPSC-EC media condition. Error bars indicate ±SEM

### 3.3.5 Reduced Vasculogenesis of iPSC-ECs at Constant Cell Seeding Density

In the angiogenic bead assay, endothelial cells are coated on microcarrier beads. While both endothelial cells adhere to the beads, the number of cells coated on one bead can vary. To ensure this variation in coating is not a contributor to the attenuated sprouting of iPSC-ECs, a different vasculogenesis assay was conducted. Here, ECs were characterized for their ability to sprout through directly embedding the ECs with NHLFs in a 3D fibrin matrix at a constant cell density. Immunofluorescent staining for UEA revealed significant reductions in the iPSC-EC networks compared to the HUVEC condition at both cell seeding density (Fig. 3-6.1). Quantification of these networks (Fig. 3-6.2) demonstrated a significant decrease in total network length for each iPSC-ECs condition in comparison to the HUVECs (7262.29 ± 1039 μm for iPSC-EC at 250K, 11710 ± 1587 μm for iPSC-EC at 500K, versus 73689 ± 3236 μm for the HUVEC 250K and 91327 ± 4128 μm for HUVEC 500K on day 14). This reduced total network length was accompanied by a 10-fold decrease in the number of vessel branch points and number of segments formed. Furthermore, there were no statistically significant differences between the HUVEC conditions and no differences between the iPSC-EC conditions.

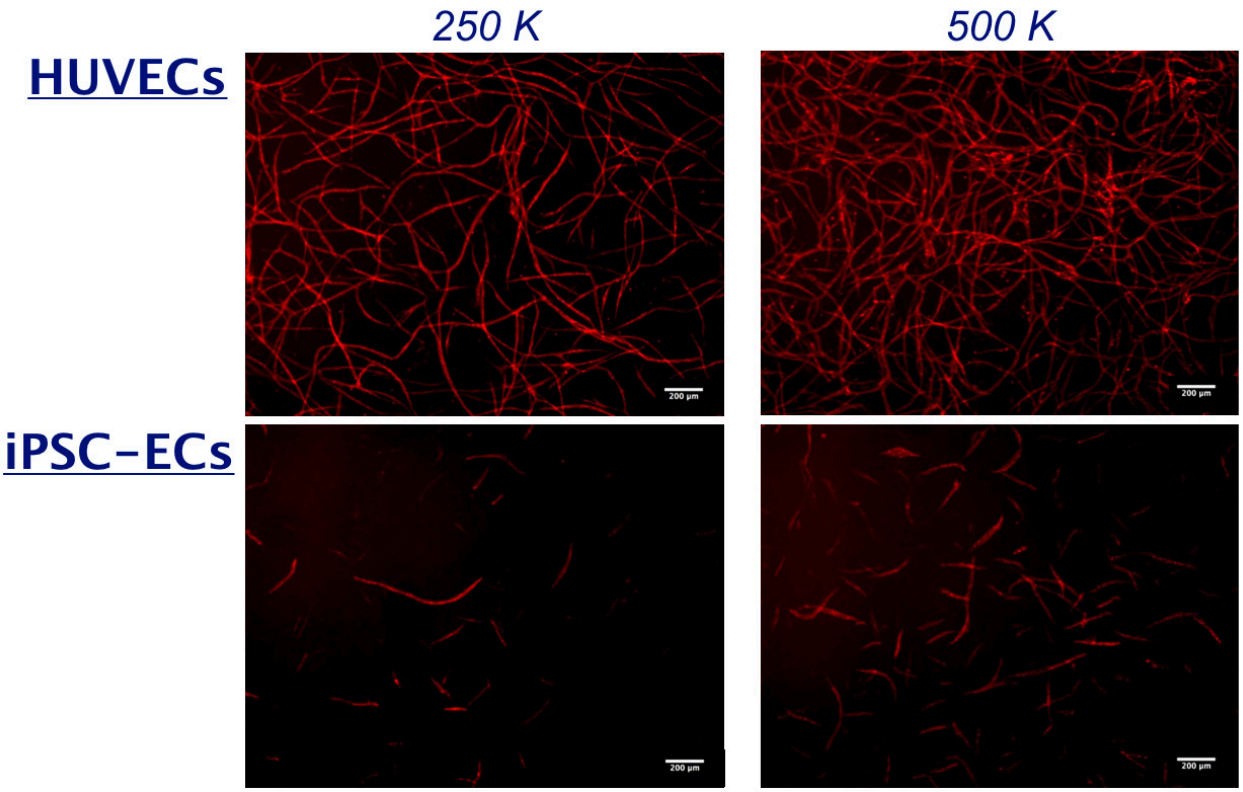


**Figure 3-6.1: Reduced Vasculogenesis of iPSC-ECs at constant cell seeding density.**
ECs embedded with NHLFs at a 1:1 ratio with a constant cell density of 250K cell or 500K cells per 2.5 mg/mL fibrin gel were stained for UEA and visualized via fluorescent microscopy on day 7. Scale bar = 200 µm.

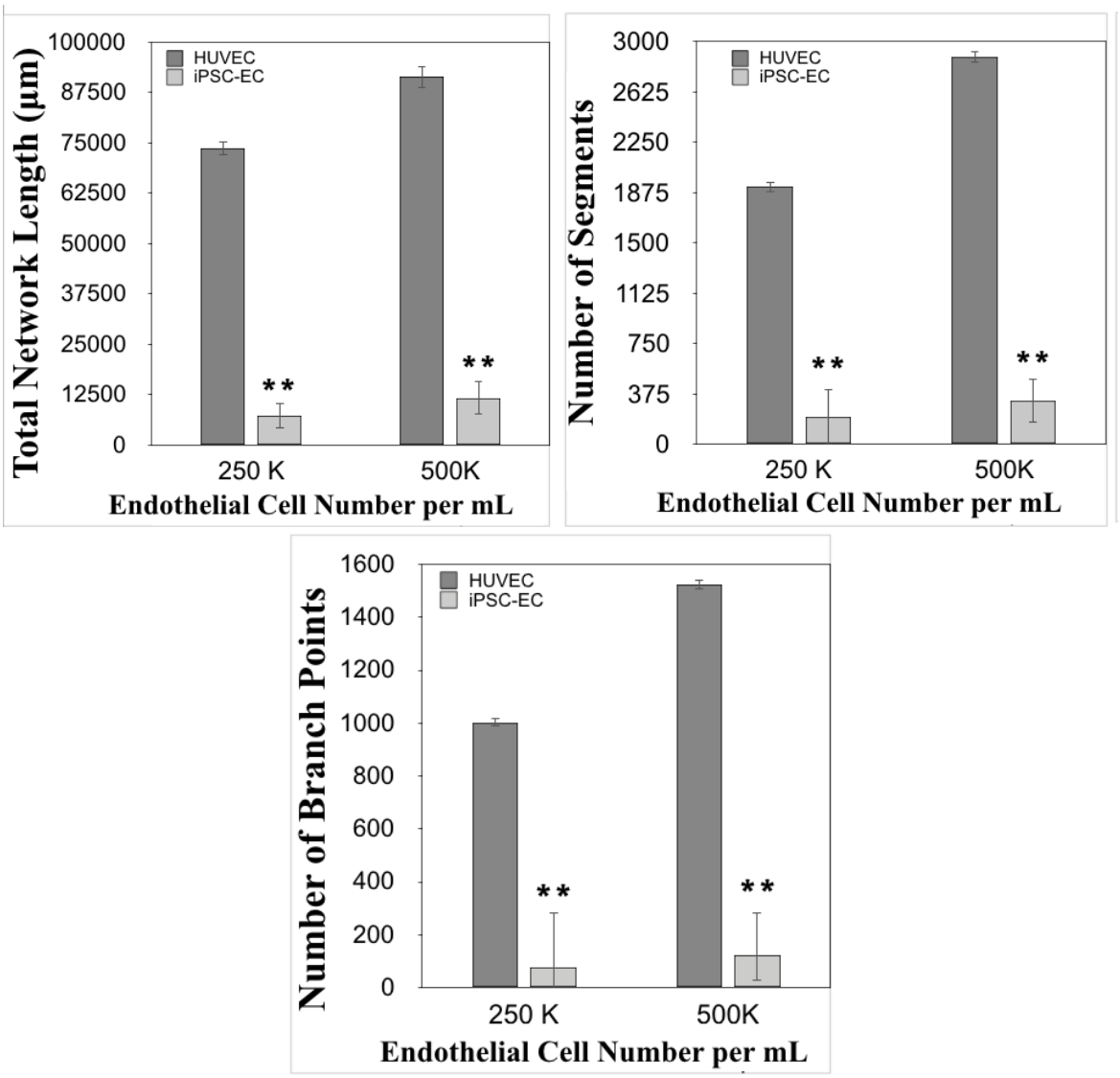


**Figure 3-6.2: Reduced Vasculogenesis of iPSC-ECs at constant cell seeding density.**
Over 3 separate experiments, a total of 30 random locations in the fibrin gel per EC were quantified and averaged for total capillary network length, number of segments, and number of branch points. *$p<0.05$ and **$p<0.01$ when comparing the indicated condition to the HUVEC control. Error bars indicate ±SEM

## 3.3.6 iPSC-EC's vessel-like structures express characteristics of mature capillaries

Despite iPSC-ECs forming vessel-like structures, the quality of the structures was also examined to determine if they exhibit qualitative characteristics of mature capillaries. In 3D fibrin

cultures, vessels of both endothelial cell types (HUVECs and iPSC-ECs), stained with UEA, were surrounded by basement membrane sleeves, as gauged by immunofluorescent staining for collagen IV (Fig. 3-7B and B') and laminin (Fig. 3-7C and C'), prominent components of native basement membranes [35]. Pericytes stabilize nascent endothelium and are characterized by physical association with ECs as well as expression of molecular markers such as αSMA [36]. IF staining revealed that NHLFs associated with vessels formed from both HUVECs (Fig. 3-7A) and iPSC-ECs (Fig. 3-7A') were positive for αSMA, suggestive of a pericyte-like phenotype when co-cultured within the fibrin matrix. Confocal analysis through multiple parallel focal planes of UEA-stained iPSC-EC and HUVEC cultures was used to verify the formation of hollow lumens. UEA staining was observed in a planar fashion in the bottom (Fig. 2-7D and D') and top slices (Fig. 3-7F and F'), but only present on the borders in the middle slice (Fig. 3-7E and E'), indicative of EC differentiation into lumen-containing structures. A full video demonstrating the hollow lumens can be seen in Appendix A along with a 3D rendering of the vasculature in Appendix B. Collectively, these results demonstrate that iPSC-ECs form vessel-like networks exhibiting characteristics of mature capillaries, similar to those formed by HUVECs in 3D co-cultures.

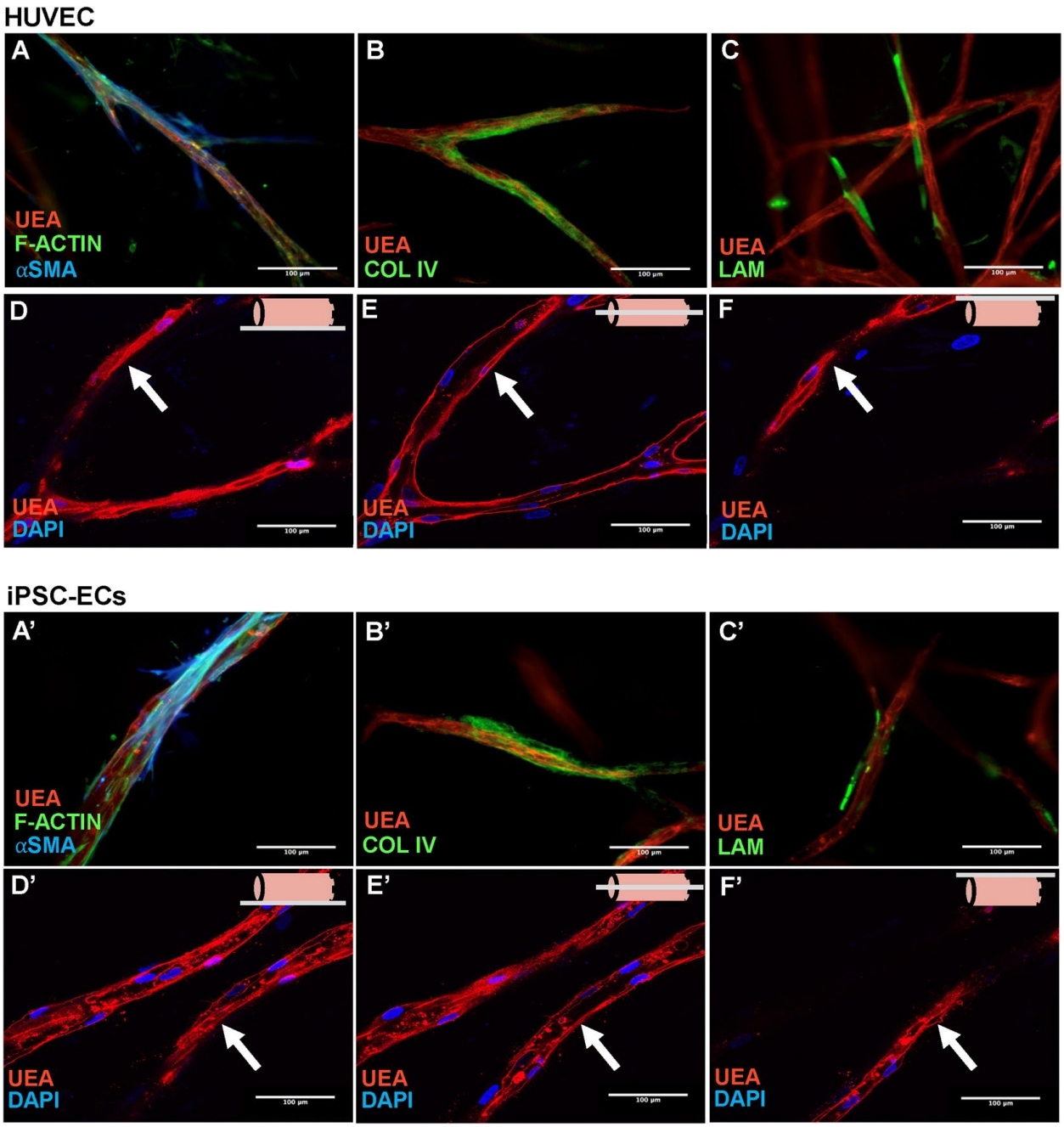


**Figure 3-6: Both HUVECs and iPSC-ECs form vessel-like structures with characteristics of mature capillaries.** HUVECs **(A-F)** or iPSC-ECs **(A'-F')** were coated on micro carrier beads and embedded in a fibrin ECM with NHLFs interspersed throughout. Beads were monitored over a 14-day period. **(A,A')** Cultures were fixed and IF stained at day 14 for UEA (red), F-Actin (green), and αSMA (blue). Pericytic association was observed for both EC types. Cultures were fixed and IF stained at day 14 for **(B,B')** UEA (red), and collagen IV (green) or **(C,C')** UEA (red), and laminin (green). Basement membrane deposition was observed for both EC types. Hollow lumen formation was demonstrated through laser confocal microscopy at the bottom **(D,D'),** middle **(E,E'),** and top **(F,F')** slice of vessel-like structures. The schematic in the upper right of each of these subsets indicates the slice relative to the vessel. Arrows indicate areas of focus. Scale bars = 100 µm.

## 3.4 Discussion

A number of different sources of endothelial cells have been explored for their ability to revascularize ischemic wounds or build microvasculature in engineered tissues. HUVECs are a robust source of ECs with proven capability of capillary morphogenesis, particularly in the assay used here, but these cells are not without their limitations. Their venous origins are often cited as a potential problem, despite evidence in the literature that ECs in the arterial circulation arise from a venous origin in development [42]. Furthermore, HUVECs and human microvascular ECs (HMVECs) have exhibited similar revascularization capacities in several studies [43, 44]. Two potentially more critical limitations of HUVECs (and also HMVECs) are their allogeneic origin and their limited proliferation potential, especially given the need to generate the large numbers of cells, on the order of billions [45, 46], for human applications.

As a consequence of the perceived limitations of existing EC populations, the vascularization potential of iPSC-ECs as a more clinically relevant cell source is increasingly of interest. Prior studies have shown that iPSC-ECs are capable of forming vessel-like structures both *in vitro* and *in vivo* within supporting Matrigel matrices [25-27], but there is little (if any) evidence comparing their potential side-by-side with more widely utilized EC sources. This study therefore explored the ability of iPSC-ECs to create functional vessel-like structures in a clinically relevant 3D *in vitro* model of angiogenesis [30, 33, 37, 40, 41, 47, 48]. We have shown iPSC-ECs coated on microcarrier beads embedded in fibrin with NHLFs yield networks with significantly shorter total network lengths (a quantitative measure of the extent of capillary morphogenesis) compared to HUVECs. If iPSC-ECs cannot efficiently yield microvascular networks of sufficient quantity, diseased or necrotic tissue may not be effectively revascularized in a timely manner, suggesting

significant technical barriers must be overcome in order for the translational potential of these cells to be realized.

In addition to the side-by-side comparisons of iPSC-ECs and HUVECs in this study, we also examined two different sources of both iPSC-ECs and HUVECs. While both iPSC-EC sources resulted in reduced capillary network formation, the variation in sprouting between the two populations demonstrates the need for standardization of iPSC-EC production. The clinical potential for iPSC-ECs is promising and could revolutionize the field of therapeutic angiogenesis. However, without a standardized approach to differentiate iPSC into an EC lineage, the success of clinical translation may vary significantly, as we observed here with the different iPSC-EC sources. As for the HUVECs, we observed only slight differences between the two sources, especially on day 7, which may be attributable to the homogeneity of the source. Our in-house isolated HUVECs were isolated from a single umbilical cord, while the commercial source was a population of cells pooled from multiple cords. Further, the commercial HUVECs were pooled from donors of more than one gender, and there are reported differences in HUVECs isolated from different sexes [49]. The in-house isolated HUVECs, from a single source, represent a more appropriate comparison to the iPSC-ECs given the expectation iPSC-ECs might be derived from a patient, i.e. a single autologous cell source.

We also examined three different lots from the selected commercial iPSC-EC source. While all lots of iPSC-ECs resulted in an attenuation of capillary network formation, there was no significant difference between each lot. This result demonstrates reproducibility in iPSC-EC manufacturing from the vendor. More importantly, lot variation as a cause of the attenuation can be eliminated. The total network formation remained relatively similar across the time points for the iPSC-ECs. This limited change over time could be attributed to the attenuation of capillary

morphogenesis. In comparison, the HUVECs increased total network length between day 4 and 7 but deceased on day 14. While expected to increase at later timepoints as cells have more time to proliferate and grow, the decrease in sprouting is an artifact of the quantification method. As the network becomes increasingly dense, the software used for quantification begins to count certain areas as nodes of origin rather than vessels.

While multiple sources and lots of cells were tested, we also investigated multiple ECs from different origin to use as a control against the iPSC-ECs. Aside from HUVECs, MVECs were also tested. While there were no significant differences between the iPSC-ECs and MVECs, there were significant differences between the MVECs and HUVECs. Previous research demonstrated similar revascularization capacities in several studies [43, 44]. The differences could be attributed to less favorable culture conditions for the MVECs. Depending on the amount of media used for culturing the tissue constructs or the ratio of endothelial cells to fibroblasts, capillary morphogenesis can vary significantly [44]. This explanation is further supported by the significant difference seen between the MVEC media conditions. MVECs culture in EGM-2MV expressed total networks lengths 2-fold greater than their EGM-2 counterparts. Per the supplier's recommendations, MVECs are best cultured in EGM-2MV, an endothelial growth media designed for microvasculature. In comparison, the optimum media for HUVECs, per the supplier's recommendation, is EGM-2. Despite lower total network formation in the EGM-2MV HUVEC condition, there were no significant difference between the two HUVEC conditions. While MVECs are still significantly different than HUVECs in the optimum media, the differences between the MVEC conditions demonstrates how sensitive MVECs can be to their environment.

Similarly, iPSC-ECs tissue constructs were cultured in their recommended media and no difference was identified between the two media conditions. HUVECs demonstrated a significant

difference when cultured in the iPSC-EC media. One or more components found in this media is affecting capillary morphogenesis in HUVECs. However, we are unable to identify the specific agents due to the proprietary nature of the supplement added to the iPSC-EC media. However, the supplement is known to contain a higher serum concentration. While serum it typically added to cell culture media to provide various growth factors and hormones required in cell proliferation [50], serum is subject to batch-to-batch variations [50]. The additional serum in the iPSC-EC media supplement could potential explain the differences seen between the HUVEC conditions. However, it is difficult to conclude a specific reason for the reduction in sprouting, as the additional serum could have a multitude of components known to inhibit not only cell growth but vasculature formation.

Ultimately, HUVECs were selected as the EC for comparison against the iPSC-ECs over MVECs. First, HUVECs have demonstrated their ability to form robust capillary networks irrelevant of culture conditions in the literature [30, 33, 37, 40, 41, 47, 48] as well as the experiments conducted in our research. Successful clinical translation will require microvascular networks of sufficient quantity to effectively revascularize tissue in a timely manner. To ensure the robustness of the iPSC-ECs, we wanted to compare their functional activity against this higher standard.

Two different assays for capillary network formation were used throughout this research. One involved coating microcarrier beads with the endothelial cells, henceforth referred to as angiogenic assay, to embed in fibrin gels, while the other directly embedded the ECs, henceforth referred to as vasculogenesis assay. As discussed previously, the variability of cell coating is an issue for the angiogenic assay. Another critique of the angiogenesis assay is whether this assay truly represents an angiogenic process. Research has shown that ECs on the microcarrier bead have

an apical-basal polarity and deposit components of a basement membrane [51, 52], indicative of an angiogenic process. On the other hand, the vasculogenic assay has its own limitations. As mentioned, high vessel density can result in improper quantification of vessels as the quantification software has difficulty distinguishing vessels from one antoher. In the constant cell density experiment, day 7 was selected to avoid this issue. The vasculogenic assay also has more macroscopic changes on the fibrin gel, as ECs are spread throughout the gel instead of being localized to a bead. The lack of difference between the various cell densities and the respective EC condition could be due to increased remodeling of the ECM [53]. Ultimately, the angiogenic assay was selected due to a zero point origin for quantification and reduced macroscopic gel changes.

While iPSC-ECs exhibit quantitative deficiencies in sprouting, the vessel-like structures formed displayed characteristics of mature capillaries. Collagen IV and laminin are components of the basement membrane of mature capillaries [35], and thus the presence of these components is indicative of iPSC-ECs' ability to form mature capillary networks. Collagen IV was observed surrounding the nascent vessels completely, while the laminin coverage was sparser. The spatial distribution may be an artifact of confocal imaging, as multiple z-plane images were flattened on top of one another to create a single image. Nevertheless, the presence of both collagen IV and laminin suggest the iPSC-ECs can deposit a basement membrane. In addition, the NHLFs associate with the vessel-like structures formed from iPSC-ECs in a pericyte-like manner, which may serve to stabilize nascent vasculature [36, 40]. Importantly, this data suggest iPSC-ECs can recruit and signal stromal cells to differentiate into pericytes. Furthermore, the presence of hollow lumens in the iPSC-EC capillary-like networks demonstrates their potential to be perfused and, once again, suggests iPSC-ECs may be capable of attaining a more mature phenotype.

One caveat to interpreting the observed differences in iPSC-ECs' vasculogenic potential is the fact only one source of iPSC-ECs was capable of capillary morphogenesis. While multiple lots and sources were tested and showed reduced network formation, it is possible variations in proprietary differentiation techniques could influence the potential of these cells. A notable difference between HUVECs and iPSC-ECs is the fact the former have been exposed to blood flow, while the latter have not. Given the role of shear stresses on vascular development [54], it seems reasonable the iPSC-ECs represent an immature EC phenotype that may require mechanobiological cues to fully differentiate into ECs capable of robust branching morphogenesis in response to angiogenic stimuli. If indeed this is true, then clearly these cues (or their absence) should be considered when interpreting data involving the use of iPSC-ECs for drug discovery and toxicity testing.

A prior study from our group has shown stromal cells of different origins induce ECs to form more mature capillaries characterized by less extravascular leakage, the expression of mature pericyte markers, and more tightly regulated permeability [56]. Stromal cells other than NHLFs may therefore be better able to induce iPSC-EC capillary morphogenesis. Similarly, it may be possible to enhance the angiogenic potential of iPSC-ECs using matrix materials other than fibrin. Synthetic hydrogels have recently been shown to support iPSC-EC capillary morphogenesis [57, 58], and controlling their mechanical properties may represent a means to increase the expression of vasculogenic and proteolytic genes as recently reported for ECs derived from human embryonic stem cells [59]. Collectively, these possibilities suggest key features of the microenvironment may be manipulated to enhance the therapeutic potential of the iPSC-ECs.

## 3.5 Conclusions

This work assessed whether iPSC-ECs form the same robust, stable microvasculature as previously documented for other sources of ECs in a well-characterized 3D fibrin-based co-culture model of angiogenic sprouting *in vitro*. Both HUVECs and iPSC-ECs formed vessel-like networks with some characteristics of mature microvasculature. However, iPSC-ECs demonstrated a significant attenuation in capillary morphogenesis. Additional experiments demonstrated lot variation, media composition, and cell number did not account for the reduction in total network length. Future *in vitro* studies are necessary to determine cause of this attenuation, discussed in the next chapter, as well as an *in vivo* investigation of the iPSC-EC vasculogenic potential, discussed in Chapter 5. Despite the promise and potential of iPSC-ECs for therapeutic revascularization, these findings suggest fundamental phenotypic differences must be understood to enable pre-clinical and clinical translation.

## 3.6 References:


1. Simons, M., & Ware, JA. Therapeutic angiogenesis in cardiovascular disease. Nat Rev Drug Discov. **2**, 863–72 (2003).

2. Tarride, J-E. et al. A review of the cost of cardiovascular disease. The Canadian Journal of Cardiology. **25(6),** e195-e202 (2009).

3. Roger, VL. et. al. Heart Disease and Stroke Statistics 2011 Update: A Report From the American Heart Association. Circulation. **123**, e18- e209 (2011).

4. Davies, M. Critical Limb Ischemia Epidemiology. Methodist DeBakey Cardiovasc J. **8(4)**, 10-14 (2012).

5. Nor, J.E., Christensen, J., Mooney, D.J., & Polverini, P.J., Vascular endothelial growth factor (VEGF)- mediated angiogenesis is associated with enhanced endothelial cell survival and induction of Bcl-2 expression. American Journal of Pathology. **154(2)** 375-84 (1999).

6. Yancopoulos, G.D. et al. Vascular-specific growth factors and blood vessel formation. Nature. **407(6801**), 242-248 (2000).

7. Kannan, R.Y., Salacinski, H.J., Sales, K., Butler, P., & Seifalian A.M. The roles of tissue engineering and vascularisation in the development of microvascular networks: a review." Biomaterials. **26(14),** 1857- 1875 (2005).

8. Sun, Q. et al. Sustained release of multiple growth factors from injectable polymeric system as a novel therapeutic approach towards angiogenesis. Pharmaceutical research. **27(2)**, 264-271 (2010).

9. Zhang, H. et al. Therapeutic Angiogenesis of Bone Marrow Mononuclear Cells (MNCs) and Peripheral Blood MNCs: Transplantation for Ischemic Hindlimb. Annals of Vascular Surgery. **22(2),** 238-247 (2008).

10. Chen, Z. et al. In vitro angiogenesis by human umbilical vein endothelial cells (HUVEC) induced by three-dimensional co-culture with glioblastoma cells. Journal of Neuro-Oncology. **92(2),** 121-128 (2009).

11. Rubina, K. et al. Adipose Stromal Cells Stimulate Angiogenesis via Promoting Progenitor Cell Differentiation, Secretion of Angiogenic Factors, and Enhancing Vessel Maturation. Tissue Eng Part A. **15(8),** 2039-2050 (2009).

12. Rouwkema, J., Rivron, N.C., & van Blitterswijk, C.A. Vascularization in tissue engineering. Trends in biotechnology. **26(8),** 434-441 (2008).

13. Koike, N. et al. Tissue engineering: creation of long-lasting blood vessels. Nature. **428(6979),** 138-139 (2004).

14. Au, P., Tam, J., Fukumura, D., & Jain, R.K. Bone marrow-derived mesenchymal stem cells facilitate engineering of long- lasting functional vasculature. Blood. **111(9),** 4551-4558 (2008).

15. Melero-Martin, J.M. et al. Engineering Robust and Functional Vascular Networks *in Vivo* with Human Adult and Cord Blood-Derived Progenitor Cells. Circulation research. **103(2),** 194–202 (2008).

16. Ikada, Y. Challenges in tissue engineering. J R Soc Interface. **3(10),** 589-601 (2006).

17. Koh, C. J. & Atala, A. Tissue Engineering, Stem Cells, and Cloning: Opportunities for Regenerative Medicine. J Am Soc Nephrol. **15(5),** 1113-1125 (2004).

18. Saigawa, T. et al. Clinical application of bone marrow implantation in patients with arteriosclerosis obliterans, and the association between efficacy and the number of implanted bone marrow cells. Circ J. **68(12),** 1189-1193 (2004).

19. Takahashi, K. & Yamanaka, S. Induction of pluripotent stem cells from mouse embryonic and adult fibroblast cultures by defined factors. Cell. **126(4),** 663–676 (2006).

20. Yee, J. Turning Somatic Cells into Pluripotent Stem Cells. Nature Education. **3(9),** 25 (2010).

21. Wong, W.T., Sayed, N., & Cooke, J.P. Induced Pluripotent Stem Cells: How They Will Change the Practice of Cardiovascular Medicine. Methodist DeBakey Cardiovasc J. **9(4),** 206-209 (2013).

22. Yoder, M.C. Differentiation of pluripotent stem cells into endothelial cells. Curr Opin Hematol. **22(3),** 252-257 (2015).

23. Ikuno, T. et al. Efficient and robust differentiation of endothelial cells from human induced pluripotent stem cells via lineage control with VEGF and cyclic AMP. PLoS One. **12(3),** e017327; 10.1371/journal.pone.0173271 (2017).

24. Di Bernardini, E. et al. Endothelial Lineage Differentiation from Induced Pluripotent Stem Cells Is Regulated by MicroRNA-21 and Transforming Growth Factor β2 (TGF-β2) Pathways. J Biol Chem. **289(6),** 3383-3393 (2014).

25. Rufaihah, A. J. et al. Human induced pluripotent stem cell-derived endothelial cells exhibit functional heterogeneity. Am J Transl Res. **5(1),** 21-35 (2013).

26. Margariti, A. et al. Direct Reprograming of Fibroblasts into Functional Endothelial Cells Capable of Enhancing Angiogenesis in Infarcted Tissues and Re-Endotheliulization in Vessel Grafts. Proc Natl Acad Sci USA. **109(34)**, 13793-13798 (2012).

27. Adams, W.J. et al. Functional Vascular Endothelium Derived from Human Induced Pluripotent Stem Cells. Stem Cell Reports. **1(2),** 105-113 (2013).

28. Rao, R.R., Peterson, A.W., Ceccarelli, J. Putnam, A.J., & Stegemann, J.P. Matrix composition regulates three-dimensional network formation by endothelial cells and mesenchymal stem cells in collagen/fibrin materials. Angiogenesis. **15(2),** 253-64 (2012).

29. Clark, R.A.F., & Henson, P.M. *The Molecular and Cellular Biology of Wound Repair*. New York: (Plenum Press, 1996).

30. Ghajar, C.M. et al. The effect of matrix density on the regulation of 3-D capillary morphogenesis. Biophys J. **94(5),** 1930-41 (2008).

31. Ghajar, C.M., et al. Mesenchymal cells stimulate capillary morphogenesis via distinct proteolytic mechanisms. Exp Cell Res. **316(5),** 813-25 (2010).

32. Grainger, S.J. & Putnam, A.J. Assessing the permeability of engineered capillary networks in a 3D culture. PLoS One. **6(7):** e22086; 10.1371/journal.pone.0022086 (2011).

33. Ghajar, C.M., Blevins, K.S., Hughes, C.C., George, S.C., & Putnam, A.J. Mesenchymal stem cells enhance angiogenesis in mechanically viable prevascularized tissues via early matrix metalloproteinase upregulation. Tissue Eng. **12(10),** 2875–88 (2006).

34. Uttamchandani M. et al. Inhibitor fingerprinting of matrix metalloproteases using a combinatorial peptide hydroxamate library. J Am Chem Soc. **129(25),** 7848–7858 (2007).

35. Li, A.C.Y., Thompson, R.P.H. Basement membrane components. J Clinical Path. **56(12),** 885-887 (2003).

36. Skalli, O., et al. Alpha-smooth muscle actin, a differentiation marker of smooth muscle cells, is present in microfilamentous bundles of pericytes. J Histochem & Cytochem. **37(3),** 315-321 (1989).

37. Kachgal, S., Carrion, B., Janson, I.A., & Putnam, A.J. Bone marrow stromal cells stimulate an angiogenic program that requires endothelial MT1-MMP. J Cell Physiol. **227(11),** 3546-3555 (2012).

38. Chun, T.H., et al. MT1-MMP-dependent neovessel formation within the confines of the three dimensional extracellular matrix. J Cell Biol. **167(4),** 757- 67 (2004).

39. Hiraoka, N., Allen, E., Apel, I.J., Gyetko, M.R., & Weiss, S.J. Matrix metalloproteinases regulate neovascularization by acting as pericellular fibrinolysins. Cell. **95(3)**, 365- 77 (1998).

40. Ghajar, C.M. et al. Mesenchymal cells stimulate capillary morphogenesis via distinct proteolytic mechanisms. Exp Cell Res. **316(5),** 813-25 (2010).

41. Kachgal, S. & Putnam, A.J. Mesenchymal stem cells from adipose and bone marrow promote angiogenesis via distinct cytokine and protease expression mechanisms. Angiogenesis. **14(1),** 47-59 (2011).

42. Red-Horse, K., Ueno, H., Weissman, I.L., & Krasnow, M.A. Coronary arteries form by developmental reprogramming of venous cells. Nature. **464(7288),** 549-53 (2010).

43. Shao, R., & Guo, X. Human microvascular endothelial cells immortalized with human telomerase catalytic protein: a model for the study of in vitro angiogenesis. Biochem Biophys Res Commun. **321(4),** 788–794 (2004).

44. Annamalai, R.T., Rioja, A.Y., Putnam, A.J., & Stegemann, J.P. Vascular Network Formation by Human Microvascular Endothelial Cells in Modular Fibrin Microtissues. ACS Biomater Sci Eng. **2(11),** 1914–1925 (2016).

45. Tateishi-Yuyama, E. et al. Therapeutic angiogenesis for patients with limb ischaemia by autologous transplantation of bone-marrow cells: a pilot study and a randomised controlled trial. Lancet. **360(9331),** 427-435 (2002).

46. Saigawa, T. et al. Clinical application of bone marrow implantation in patients with arteriosclerosis obliterans, and the association between efficacy and the number of implanted bone marrow cells. Circ J. **68(12),** 1189-1193 (2004).

47. Kniazeva, E., Kachgal, S. & Putnam, A.J. Effects of extracellular matrix density and mesenchymal stem cells on neovascularization in vivo. Tissue Eng Part A. **17(7-8),** 905-14 (2011).

48. Nehls, V. & Drenckhahn, D. A novel, microcarrier-based in vitro assay for rapid and reliable quantification of three-dimensional cell migration and angiogenesis. Microvasc Res. **50(3),** 311-22 (1995).

49. Addis, R. et al. Human umbilical endothelial cells (HUVECs) have a sex: characterisation of the phenotype of male and female cells. Biol Sex Differ. **5(1),** 18 (2014).

50. C.-Y. Fang, C.-C. Wu, C.-L. Fang, W.-Y. Chen, and C.-L. Chen, "Long-term growth comparison studies of FBS and FBS alternatives in six head and neck cell lines," *PLOS ONE*, vol. 12, no. 6, p. e0178960, Jun. 2017.

51. D.-H. T. Nguyen *et al.*, "Biomimetic model to reconstitute angiogenic sprouting morphogenesis in vitro," *Proc. Natl. Acad. Sci. U. S. A.*, vol. 110, no. 17, pp. 6712–6717, Apr. 2013.

52 H. Takahashi *et al.*, "Visualizing dynamics of angiogenic sprouting from a three-dimensional microvasculature model using stage-top optical coherence tomography," *Sci. Rep.*, vol. 7, p. 42426, Feb. 2017.

53. P. Lu, K. Takai, V. M. Weaver, and Z. Werb, "Extracellular Matrix Degradation and Remodeling in Development and Disease," *Cold Spring Harb. Perspect. Biol.*, vol. 3, no. 12, Dec. 2011.

54. Hahn, C., & Schwartz, M.A. Mechanotransduction in vascular physiology and atherogenesis. Nat Rev Mol Cell Biol. **10(1),** 53-62 (2009).

55. Newman, A.C, Nakatsu, M.N., Chou, W., Gershon, P.D., & Hughes, C.C. The requirement for fibroblasts in angiogenesis: fibroblast-derived matrix proteins are essential for endothelial cell lumen formation. Mol Biol Cell. **22(20),** 3791-3800 (2011).

56. Grainger, S.J., Carrion, B., Ceccarelli, J., & Putnam, A.J. Stromal cell identity influences the in vivo functionality of engineered capillary networks formed by co-delivery of endothelial cells and stromal cells. Tissue Eng. Part A. **19(9-10),** 1209-22 (2013).

57. Belair, D.G., Schwartz, M.P., Knudsen, T., Murphy, W.L. Human iPSC-derived endothelial cell sprouting assay in synthetic hydrogel arrays. Acta Biomater. **39,** 12–24 (2016).

58. Zanotelli, M.R. et al. Stable engineered vascular networks from human induced pluripotent stem cell-derived endothelial cells cultured in synthetic hydrogels. Acta Biomater. **35,** 32-41 (2016).

59. Zhang, J. et al. A Genome-wide Analysis of Human Pluripotent Stem Cell-Derived Endothelial Cells in 2D or 3D Culture. *Stem Cell Reports*. **8(4),** 907-918 (2017).

# CHAPTER 4

# Potential Mechanisms Involved in Vascular Network Formation by iPSC-ECs



## 4.1 Introduction

Angiogenesis is the process in which new vasculature is formed from pre-existing vessel networks [1]. Unlike vasculogenesis, where vasculature forms *de novo* from the differentiation of endothelial progenitor cells into ECs, angiogenesis is a complex process that involves various mechanisms and cues from the extracellular matrix (ECM) [1], [2]. The study of angiogenesis is of increasing interest to create vascularized tissue constructs [3]. Further understanding of this complex process may aid in development of these engineered tissues for the treatment of numerous pathologies characterized by ischemia or reduced vessel formation and maintenance [4].

There are two types of angiogenesis: sprouting angiogenesis and intussusceptive angiogenesis [1]. Sprouting angiogenesis is most common and involves a sprout of endothelial cells from a parent vessel. Intussusceptive angiogenesis is known as non-sprouting or splitting angiogenesis. This type of angiogenesis is a newly discovered process and involves the splitting of a pre-existing vessel into two different vessels [5]. While both sprouting and intussusceptive

angiogenesis occur in all types of tissues throughout the body, most angiogenic research focuses on sprouting angiogenesis [1], [5].

Sprouting angiogenesis is a multistep process that first involves activation of endothelial cells in response to angiogenic cues, such as VEGF [6]. Many factors can trigger these cues, including a lack of oxygen within a region in the body, an inflammatory response, or other changes in the ECM [7]. This activation leads to the enzymatic degradation of the basement membrane and the associated matrix surrounding the interstitial preexisting vessel [1]. The endothelial cells then begin to migrate and proliferate towards the angiogenic cue [8]. Elongation of the sprout occurs as trailing endothelial cells proliferate and fill up the gap between the non-proliferating tip cell as it migrates [9], [10]. Once two tip cells inosculate with one another, lumen formation occurs and tubulogenesis begins [11]. The newly formed vessel is stabilized by the formation of a new basement membrane and the recruitment of pericytes and vascular smooth muscle cells [12].

The ability of endothelial cells to invade the tissue space through the extracellular matrix is fundamental to angiogenesis. To achieve this invasion, the extracellular matrix needs to be degraded by proteases [8]. In particular, the family of matrix metalloproteinases (MMPs) play a pivotal role not only in degradation but regulation of angiogenesis [13]. During the initial steps of angiogenesis, MMPs degrade the vessel basement membrane and the surrounding ECM [14]. Throughout angiogenesis, MT1-MMP, MMP-2, and MMP-9 continue to facilitate EC invasion and proliferation as other MMPs such as MT2-MMP, MT3-MMP, MMP-3, MMP-7, and MMP-13 help in the release and activation of pro-angiogenic cytokines in the ECM [15]–[19]. After invading the matrix, as the new vessel forms, MMPs stabilize these capillaries through mediating cross-talk between endothelial cells and pericytes [20], [21]. After the vessel matures, MMPs aid in the pruning and regression of the vascular network [22], [23].

Over the past decade, research has further characterized the expression of MMPs and their roles in vascular development [13], [14], [16], [22], [24]–[28]. In particular, MMP-2, MMP-9, and MT1-MMP, in HUVECs, are directly related in the formation of vessel-like networks [29]–[31]. Depending on the stromal cells co-cultured with the HVUECs, sprouting is completely attenuated in BMSC-HUVEC co-cultures when MMP inhibitors are introduced. NHLF-HUVEC co-cultures exhibit a plasticity, utilizing either MMP or serine protease mediated mechanisms for capillary morphogenesis in fibrin [30]. Additional studies involving the knockdown of the expression of MMPs revealed endothelial MT1-MMP ,in particular ,is key for vessel network formation in fibrin [31].

Due to the involvement of MMPs in HUVEC capillary morphogenesis, and angiogenesis in general, the expectation is that iPSC-ECs must utilize these proteases as well, but limited research exists on the mechanisms involved in iPSC-EC capillary morphogenesis. Also, the iPSC-ECs may not utilize MMPs in the same way as bonafide ECs because that are a sort of "synthetic" cell (reprogramed) and never exposed to physiological conditions, such as blood flow. As demonstrated in the previous chapter, iPSC-EC capillary morphogenesis was significantly attenuated in comparison to HUVECs [32]. Previous studies have has shown the disruption of ECM degradation, through increased fibrin concentrations or protease inhibitors, attenuated HUVECs' microvascular formation [30], [33]. If iPSC-ECs require similar mechanisms for angiogenesis, differences in protease expression could provide one possible explanation for their attenuated response.

The present study explores whether iPSC-ECs are functionally and mechanistically similar to HUVECs. Using the aforementioned *in vitro* model, endothelial cells were coated on dextran microcarrier beads and co-embedded in a 3D fibrin matrix with normal human lung fibroblasts

(NHLFs). Functional and mechanistic differences were identified through mechanically or chemically inhibiting capillary morphogenesis with elevated fibrin concentrations or protease inhibitors respectively. We also examined key differences in matrix proteolysis and identified a potentially significant mechanistic difference between iPSC-ECs and HUVECs that may influence the translational potential of the former (Fig. 4-1).

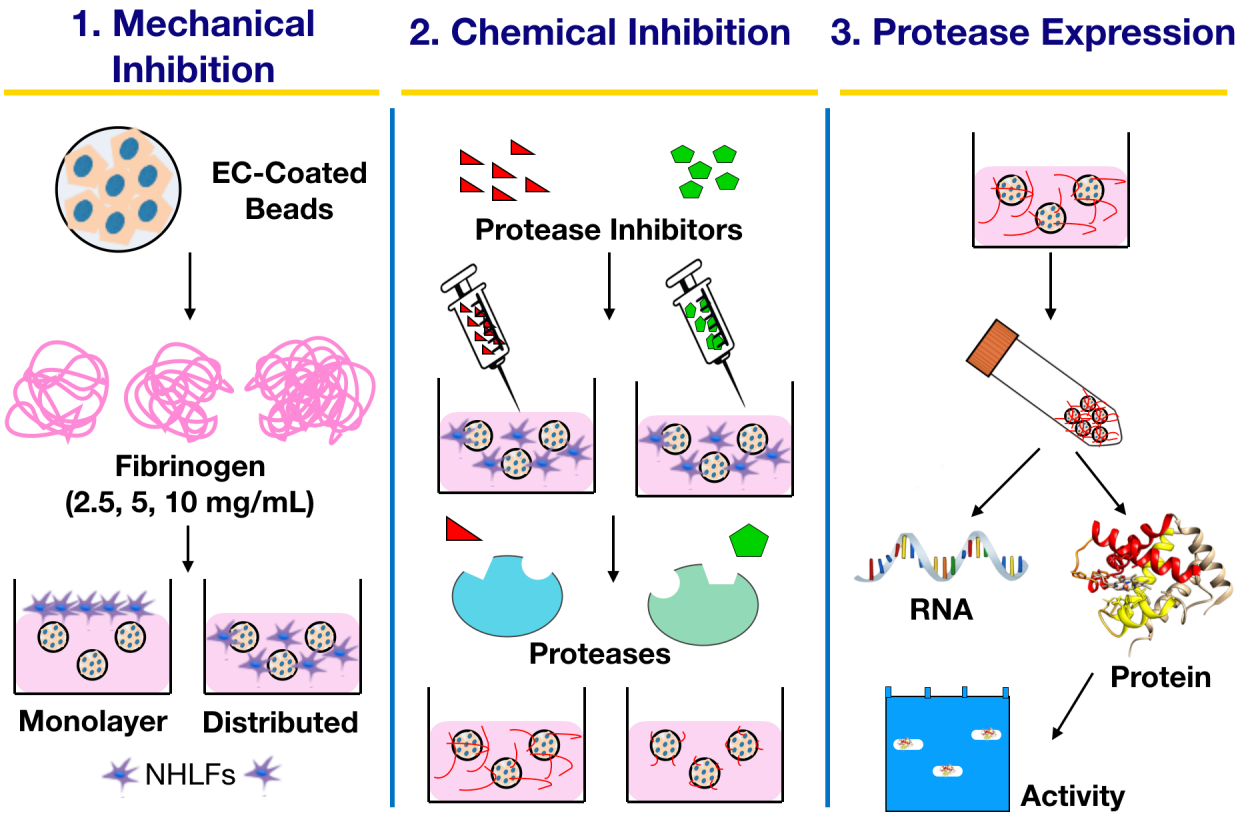


**Figure 4-1: Functional and Mechanistic Assessment Schematic**
Overview of inhibition and protease research. ECs are coated on microcarrier bead and embedded in varying fibrin concentrations with either a monolayer or distributed NHLFs throughout. Separate experiments added chemical inhibitors to tissue cultures to assess possible inhibition on capillary morphogenesis. Finally, different EC coated beads were harvested from fibrin gels and the RNA, protein, and activity levels were analyzed for specific proteases.

## 4.2 Material and Methods

### 4.2.1 HUVEC Isolation and Cell Culture

HUVECs were harvested from fresh umbilical cords obtained from the University of Michigan Mott Children's Hospital via an IRB-exempt protocol and isolated using methods previously described [29]. The umbilical cord was rinsed in phosphate buffer saline (PBS) and then digested with 0.1% collagenase type I (195 U/ml, Worthington Biochemical, Lakewood, NJ) for 20 min at 37°C. The digested product was subsequently washed in PBS, collected, and centrifuged (200×G for 5 min). The pellet was resuspended in endothelial growth media (EGM-2, Lonza), and the cells were plated in tissue culture flasks and cultured at 37°C and 5% $CO_2$. After 24 hours, HUVECs were rinsed with PBS to remove any non-adherent cells. Fresh media was changed every 48 hours. Cells from passage 3 were utilized for experiments. Normal human lung fibroblasts (NHLF, Lonza) were cultured at 37°C and 5% $CO_2$ in Dulbecco's modified eagle media (DMEM, Life Technologies, Grand Island, NY) with 10% fetal bovine serum (FBS). Culture media were replaced every 48 hours and cells from passage 6-10 were used in experiments. iCell endothelial cells (Cellular Dynamics International, Madison, WI) were cultured at 37°C and 5% $CO_2$ in Vasculife VEGF endothelial media (Lifeline Cell Technology, Fredrick, MD) supplemented with iCell Endothelial Cell Medium Supplement (Cellular Dynamics International). iPSC-EC tissue culture flasks were coated with 35 µg/mL fibronectin (Invitrogen, Carlsbad, CA) for 1 hr at room temp prior to plating the cells. Culture media were replaced every 48 hours and cells from passage 3 were used in experiments.

### 4.2.2 Microcarrier Bead Assembly

Cytodex microcarrier beads (Sigma-Aldrich, St. Louis, MO) were hydrated and sterilized in phosphate buffer saline (PBS). Beads were prepared for coating by washing repeatedly with 1 mL of EGM-2, with time to settle between washes. Endothelial cells were cultured in T-75 flasks to 80% confluency and rinsed with PBS before being harvested via 0.25% trypsin incubation for 5 min at 37 °C and 5% $CO_2$. Trypsin was neutralized using DMEM supplemented with 10% FBS. The cellular suspension was centrifuged (200×G for 5 min) and supernatant was aspirated immediately. The cell pellet was re-suspended in 4 mL of fresh EGM-2. 10,000 microcarrier beads were combined with four million ECs, HUVECs or iPSC-ECs, (5 mL total) in an inverted T-25 culture flask. Over a 4 hour incubation period, the culture flask was agitated every 30 minutes to ensure EC coating of beads. After 4 hours, the cell-bead mixture was added to a new T-25 culture flask. Fresh EGM-2 (5 mL) was added to the old flask to remove any remaining beads and transferred to the new culture flask. The total volume (10 mL) was incubated overnight in standard cell culture position.

### 4.2.3 Fibrin Tissue Assembly

The next day, following bead coating, a fibrinogen (Sigma-Aldrich) solution of the desired concentration (2.5 mg/mL, 5 mg/mL, or 10 mg/mL, based on desired experimental conditions) was dissolved in an appropriate amount of serum-free EGM-2 and placed at 37 °C in a water bath. The solution was sterile filtered through a 0.22 μm syringe filter (Millipore, Billerica, MA). The previous day's cell-bead solution was removed from the culture flask and placed in a 15 mL centrifuge tube. After the beads settled, the remaining supernatant was used to remove any remaining beads adhering to the culture flask and added to the centrifuge tube. Upon the beads

settling, the supernatant was removed and 5 mL of fresh serum-free EGM-2 was added to the cell-coated beads. The appropriate amount of bead solution (~ 50 beads per well) was added to the fibrinogen solution with 5% FBS. Fibroblasts were prepared using a similar rinsing/trypsinization procedure as described above. 25,000 NHLFs per well were added to the bead-fibrinogen solution or plated on top of each gel after polymerization in our distributed and monolayer conditions respectively. 500 μL of the above mixture was added to a single well of a 24-well tissue culture plate and polymerized with 10 μL of thrombin (50 U/mL, Sigma-Aldrich). Tissue constructs were left undisturbed for 5 min at room temperature before incubation for 30 min at 37 °C and 5% $CO_2$. For studies involving inhibitors, the appropriate vehicle or inhibitor(s) solubilized in vehicle was mixed with the media prior to addition to the culture. 1 mL of fresh EGM-2 (± protease inhibitors) was added on top of the gels following incubation and changed the following day and every other day thereafter. The medium was changed to serum free EGM-2 two days prior to harvesting for protein and RNA analysis.

### 4.2.4 Immunofluorescent staining

After the constructs were cultured for a specified period of time (1, 4, 7, or 14 days), gels were rinsed 3x with PBS solution for 5 min at room temperature. Gels were then fixed with 500 μL of formalin (1 mL of 36.5% Formaldehyde solution (Sigma), 1 mL of PBS, and 8 mL of d.d.H2O) for 15 min at 4 °C. Gels were rinsed again 3x with PBS for 5 min, then permeabilized with 0.5% Triton-X100 in TBS for 30 min at 4 °C. Following a rinse 3x for 5 min at room temperature with 0.1% Triton X-100 in TBS (TBS-T), samples were blocked overnight at 4 °C with a 2% Abdil solution (bovine serum albumin (Sigma) dissolved in TBS-T). UEA was dissolved in 2% Abdil at the appropriate concentration (Ulex Europaeus Lectin 1 (UEA), 1:100 (Vector

Labs, Burlingame, CA)) and 1 mL of this solution was added to each gel for overnight incubation at 4 °C. Following a 3x rinse for 5 min at room temperature with TBS-T, gels are incubated with TBS-T overnight at 4 °C.

### 4.2.5 Fluorescent Imaging and Vessel Quantification

Vessel formation was assessed at the aforementioned time points. Fluorescent images were captured utilizing an Olympus IX81 equipped with Disc Spinning Unit and a 100 W high-pressure mercury burner (Olympus America, Center Valley, PA), a Hamamatsu Orca II CCD camera (Hamamatsu Photonics, K.K., Hamamatsu City, Japan), and Metamorph Premier software (Molecular Devices, Sunnyvale, CA). Imaged beads were chosen at random provided that vessels emanating from a given bead did not form anastomoses with vessels from adjacent beads. Images from at least 30 beads per condition were captured over three separate trials at low magnification (4×) for each independent experiment and processed using the Angiogenesis Tube Formation module in Metamorph Premier (Molecular Devices). Each image was segmented and analyzed based on any tube-like pattern that falls within a specified minimum and maximum width of each segment above a contrast threshold. The total network length, the number of branch points, and number of segments were quantified.

### 4.2.6 Fibrin Gel Lysing

For each EC type, the spent media were collected from ten fibrin gels, each containing ~100 EC-coated beads. Each gel was then washed with PBS. The gels were dislodged from each well in the plates using a small spatula to allow for optimal dissolution of the gels. Fibrin gels were dissolved using 500 μL of Nattokinase (1000 U/mL, Japan Bio Science Laboratory Co., Osaka

City, Japan) and incubated at 37 °C for 45 min with agitation periodically. To ensure complete removal of the ECs from the microcarrier beads, the contents of each well were pipetted repeatedly. The solution was removed and centrifuged at 200 x G for 5 min to collect the ECs. Supernatant was aspirated, and cells were lysed and suspended in RIPA lysis buffer (50 mM Tris-HCl pH 7.6, 150 mM NaCl, 1% Triton X-100, 0.5% sodium deoxycholate, 0.1% SDS) before storage at -80 °C. A Bicinchoninic acid assay (Pierce Biotechnology, Rockford, IL) was utilized to determine the protein concentration of the lysed cells and supernatant.

### 4.2.7 Western Blotting Analysis

Western blot analysis of the levels of MT1-MMP was conducted on the lysed tissue samples, while the levels of MMP-2, and MMP-9 were assessed in the spent media. After boiling, equal amounts of protein (25 µg) from the respective samples were electrophoresed in a 10% Tris-glycine gel (Invitrogen) under reducing conditions and transferred to a PVDF membrane. Blots were probed in a 5% Abdil solution with mouse monoclonal antibodies for human MMP-2 (1:1000, Abcam, Cambridge, UK) and human MMP-9 (1:1000, Abcam) or rabbit monoclonal antibodies for human MT1-MMP (1:2000, Abcam). Blots were incubated for two hours at 25 °C with gentle agitation and subsequently washed 6x with TBS-T for 5 min. After washing, the membrane was incubated in TBT-T with horseradish peroxidase-conjugated anti-mouse secondary antibody (1:10,000, Pierce Biotechnology) or horseradish peroxidase-conjugated anti-rabbit secondary antibody (1:10,000, Pierce Biotechnology) and goat anti-human GAPDH (1:10000, Santa Cruz Biotechnologies, Santa Cruz, CA). Protein expression was visualized using an enhanced chemiluminescence detection system. Bands were identified by comparing to a molecular mass ladder (Pierce Biotechnology). The resulting blots were scanned and imported into

Image J (National Institutes of Health, Bethesda, MD) in order to perform densitometry. Background was subtracted using the built-in background subtraction function in Image J to normalize the background between samples. Resulting intensity values were then normalized to the HUVEC condition for each time point. Normalized values for each condition from three separate experiments were then averaged to allow for statistical comparisons.

### 4.2.8 Gelatin Zymography

For gelatin zymography, precast Novex zymogram gels (10% Tris-Glycine gel with 0.1% gelatin, Invitrogen, Carlsbad, CA) were loaded with 15 μg of protein per condition and separated under nonreducing conditions. The gels were then washed twice for 30 min in a 50 mM Tris-HCl (pH 7.5), 5 mM $CaCl_2$, and 2.5% Triton X-100 solution. After washing, gels were rinsed in incubation buffer (50 mM Tris-HCl (pH 7.5), 5 mM $CaCl_2$, and 1% Triton X-100) for 10 min at 37 °C with gentle agitation. The rinse was replaced with fresh incubation buffer and incubated for 20 h at 37 °C. Gels were then Coomassie stained for 1 h and destained for 15 min twice in 10% acetic acid and 40% methanol. MMP-2 and MMP-9 bands were identified by comparing to a molecular mass ladder (Pierce Biotechnology). The resulting blots were scanned and imported into Image J (National Institutes of Health, Bethesda, MD) in order to perform densitometry. Bands were processed as described previously for the Western Blot.

### 4.2.9 Reverse Transcription and quantitative Polymerase Chain Reaction

Total RNA was purified from RIPA buffer lysed samples using the RNeasy kit (Qiagen, Valencia, CA) per manufacturer's protocol and quantified using a Nanodrop ND-1000 (Thermo Fisher Scientific, Rochester, NY). First-strand cDNA templates were synthesized from equal

amounts of total RNA for each sample using the ImProm-II Reverse Transcription System (Promega; Madison, WI), also according to manufacturer's protocol. Quantitative PCR (qPCR) was performed using a 7500 Fast Real-Time PCR System and TaqMan Gene Expression Master Mix (Applied Biosystems, Carlsbad, CA). Predesigned qPCR primers for human MMP-2, MMP-9, MT1-MMP, and 18s rRNA were selected from the TaqMan Gene Expression Assays database (Applied Biosystems). The ΔΔCT method was used to assess the relative quantity of each target gene.

### 4.2.10 Other reagents used

The broad spectrum MMP inhibitor BB2516 (Tocris Bioscience, Ellisville, MO) was used at a concentration in 10-fold excess (0.1-0.2 μM) of its IC50 against MMP-2, MMP-9, and MT1-MMP [34]. The plasmin inhibitor aprotinin (Sigma-Aldrich) was used at a concentration greater than two-fold excess (22 nM) of its IC50 against plasmin. Equal volumes of dimethyl sulfoxide (DMSO, Sigma-Aldrich) were used as the vehicle control for these experiments.

### 4.2.11 Statistical Analysis

Statistical analyses were performed using StatPlus (AnalystSoft Inc.,Walnut, CA). Data are reported as mean ± standard error of mean (SEM). One- or two-way analysis of variance (ANOVA) with a Bonferroni post-test was used to assess statistical significance between data sets. Statistical significance was assumed when $p<0.05$.

## 4.3 Results

### 4.3.1 Distributing stromal cells throughout matrix abrogates sprouting decreases for iPSC-EC capillary network formation in elevated fibrin concentrations.

Previous research has shown that elevated fibrin concentrations have an inhibitory effect on HUVEC capillary morphogenesis [33]. To investigate any functional similarities between iPSC-EC vasculature, ECs were cultured on microcarrier beads within 2.5 mg/mL, 5 mg/mL, or 10 mg/ml fibrin gels overlaid with a NHLF monolayer. Extensive capillary networks stained for UEA were formed with either HUVECs (Fig. 4-2.1A) and iPSC-ECs (Fig. 4-2.1D) by day 14. Increasing matrix density to 5 mg/mL inhibited network formation slightly for both ECs (Fig. 4-1.2B, E), while greatly inhibiting sprouting for both ECs in 10 mg/mL matrices (Fig. 4-2.1C and 2.1F). Quantification of these networks, normalized to their respective 2.5 mg/mL condition, demonstrated a significant decrease in total network length (Fig. 4-2.2G), number of vessel segments (Fig. 4-2.2H), and number of vessel branch points (Fig 4-2.2I) between both ECs 2.5 mg/mL conditions and their respective 10 mg/mL condition. Research suggests that for HUVECs distributing the fibroblasts throughout the matrix abrogated the inhibitory effect of increased fibrin concentration, primarily by overcoming diffusion limitations imposed on ECs in denser matrices with stromal cell monolayers [33]. Thus, to assess whether the same effect is seen with iPSC-ECs undergoing capillary morphogenesis, we distributed fibroblasts throughout the matrix embedded with EC-coated microcarrier beads. IF staining for UEA revealed a notable increase in network formation for both EC types across all matrix densities (Fig. 4-2.1A'-F'). Quantification of total network length (Fig. 4-2.2G), number of vessel segments (Fig. 4-2.2H), and number of vessel

branch points (Fig. 4-2.2I), normalized to their respective 2.5 mg/mL condition, no longer decreased significantly with increasing fibrin densities. Collectively, the inhibition of morphogenesis through elevated matrix density, and the subsequent abrogation of inhibition by direct co-culture of ECs with stromal fibroblasts, demonstrates iPSC-EC vascular networks are functionally regulated in a manner similar to HUVEC networks.

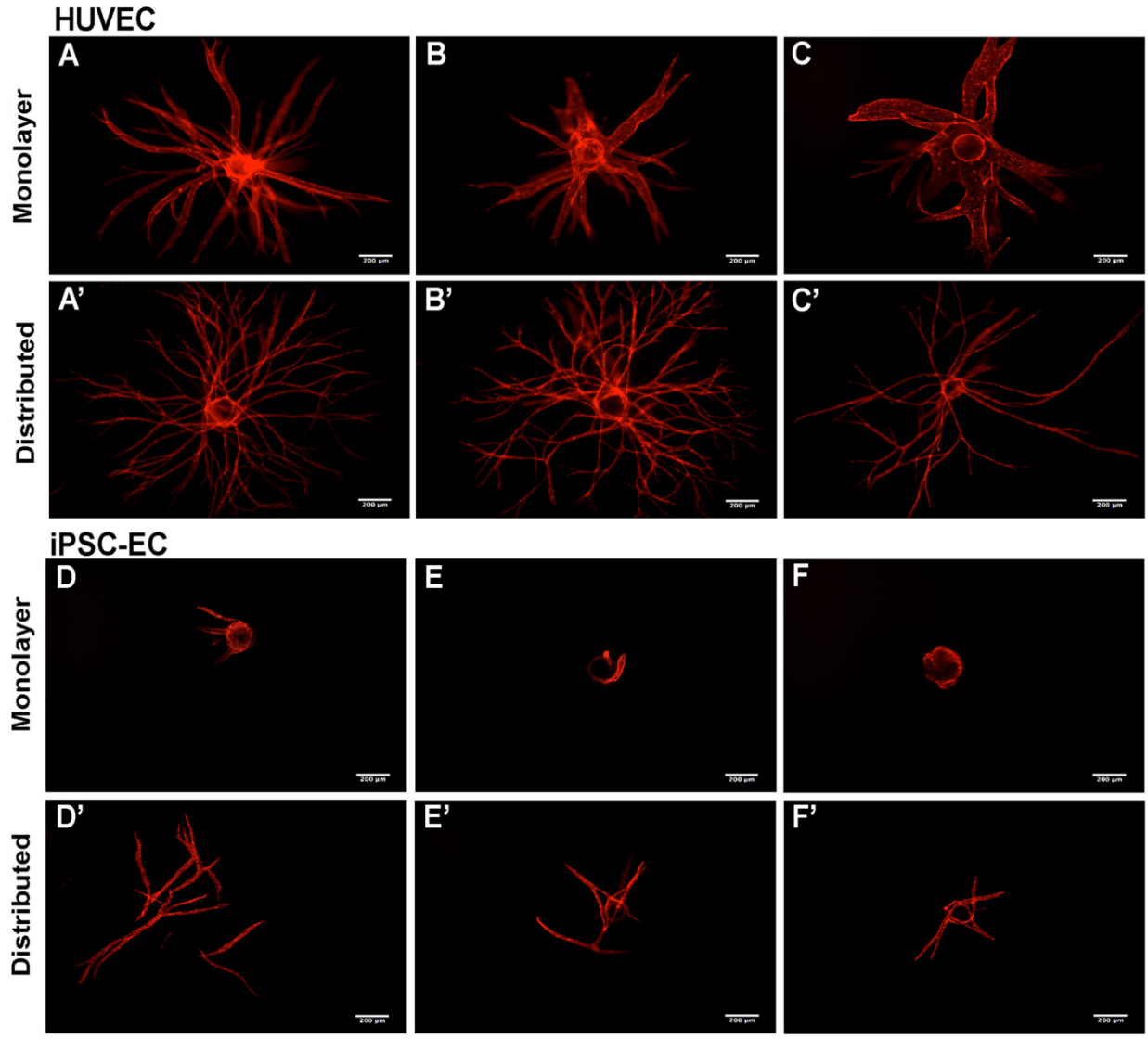


**Figure 4-2.1: Distributing stromal cells throughout the matrix abrogates reductions in EC sprouting caused by elevated fibrin concentrations for both HUVECs and iPSC-ECs.** ***[Rep. Images]***

Fluorescent images of UEA-stained HUVEC **(A-C,A-C')** or iPSC-EC **(D-F,D'-F')** coated microcarrier beads with **(A-F)** overlaying monolayer or **(A'-F')** distributed NHLFs. Beads are embedded in **(A,A',D,D')** 2.5 mg/mL, **(B,B',E,E')** 5 mg/mL, **(C,C',F,F')** 10 mg/mL fibrin matrices. Scale bar = 200 μm.

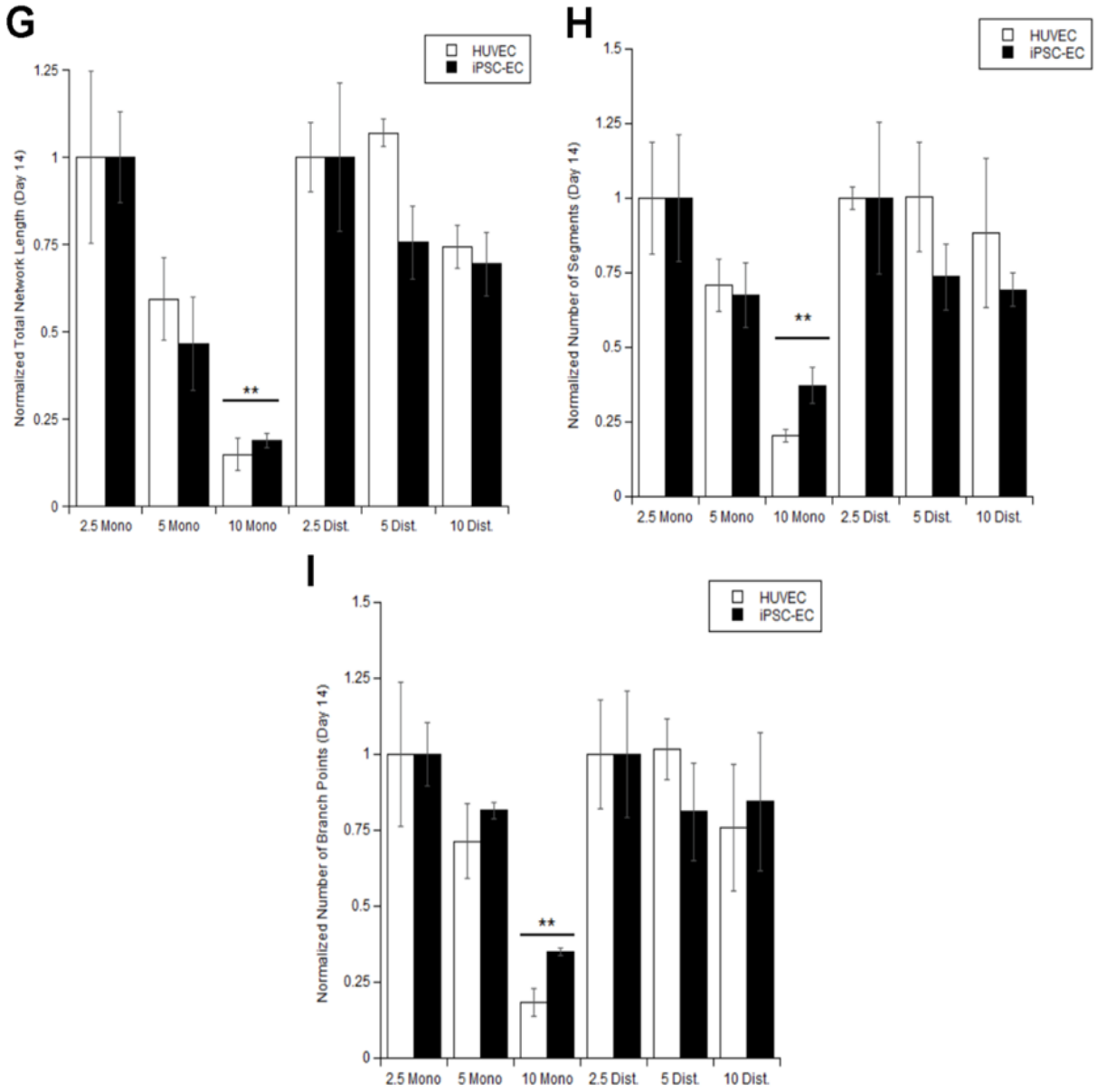


**Figure 4-2.2: Distributing stromal cells throughout the matrix abrogates reductions in EC sprouting caused by elevated fibrin concentrations for both HUVECs and iPSC-ECs.** ***[Quantification]***
A total of 30 beads over three separate experiments at day 14 were quantified, averaged, and normalized to the respective 2.5 mg/mL stromal cell distribution of each EC type for **(G)** total capillary network length, **(H)** number of segments, and **(I)** number of branch points. *$p<0.05$ and **$p<0.01$ when comparing the indicated condition to the 2.5 mg/mL monolayer condition. Error bars indicate ±SEM

### 4.3.2 Capillary morphogenesis by iPSC-ECs involves both plasmin-mediated and MMP-mediated mechanisms.

Proteases play a key role in degrading and remodeling the ECM in capillary morphogenesis [37-39]. Our prior findings demonstrate capillary morphogenesis of HUVEC-NHLF co-cultures in fibrin gels proceeds in a manner that involves both MMP- and plasmin-mediated fibrinolysis [30]. To assess the involvement of these proteases in iPSC-EC capillary morphogenesis, protease inhibitors dissolved in a vehicle (DMSO) were added to cultures of 2.5 mg/mL fibrin gels embedded with EC-coated microcarrier beads and distributed fibroblasts. Gels were fixed, stained for UEA, and imaged at day 14 for both HUVECs (Fig. 4-3.1A-E) and iPSC-ECs (Fig. 4-3.1A'-E'). The addition of a broad spectrum MMP inhibitor, BB2516, at concentrations of 0.1 μM or 0.2 μM, did not significantly reduce sprouting in iPSC-EC cultures compared to the vehicle control (Fig. 4-3.2F). The resulting similarities in network formation is primarily attributed to no significant change in the number of branch points (Fig. 4-3.2G) or number of segments (Fig. 4-3.2H). While spouting was significantly reduced with 0.2 μM of BB2516 in HUVEC cultures (Fig. 4-3.2F), spouting was not completely eliminated, which is consistent with our previous findings [40]. For both HUVECs and iPSC-ECs, the serine protease inhibitor aprotinin, also did not alter network formation. However, the dual application of BB2516 (0.1 μM) and aprotinin (22 nM) completely eliminated network formation (Fig. 4-3.2E,E',F), branching (Fig. 4-3.2G), and segmentation (Fig. 4-3.2H) in both EC types. In sum, these data demonstrate iPSC-ECs undergoing capillary morphogenesis stimulated by fibroblasts in 3D fibrin gels with similar proteolytic dependencies as HUVECs.

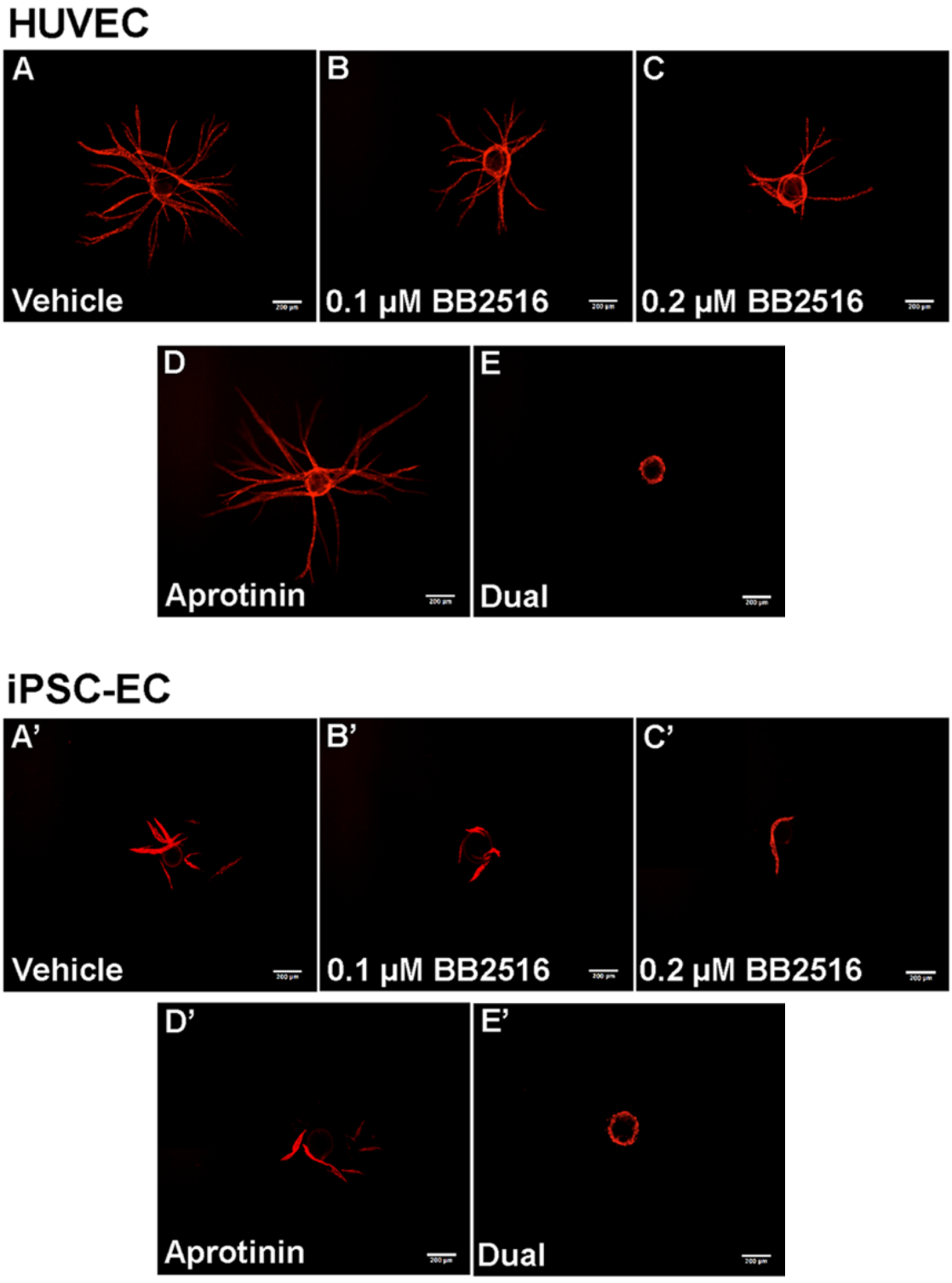


**Figure 4-3.1: Capillary morphogenesis by iPSC-ECs and HUVECs proceed via similar preoteolytic mechanisms.** ***[Rep. Images]***

HUVEC **(A-E)** or iPSC-EC **(A'-E')** coated microcarrier beads were embedded in a fibrin matrix dispersed with NHLFs. Shown are fluorescent images stained for UEA at day 14 of the capillary network formation from cultures treated with **(A,A')** vehicle (DMSO), **(B,B')** 0.1 µM, or **(C,C')** 0.2 µM of the broad spectrum MMP inhibitor BB2516, **(D,D)** 22 nM of the serine protease inhibitor aprotinin, or with a combination of BB2516 (0.1 µM) and aprotinin (22 nM) ("dual"). Scale = 200 µm.

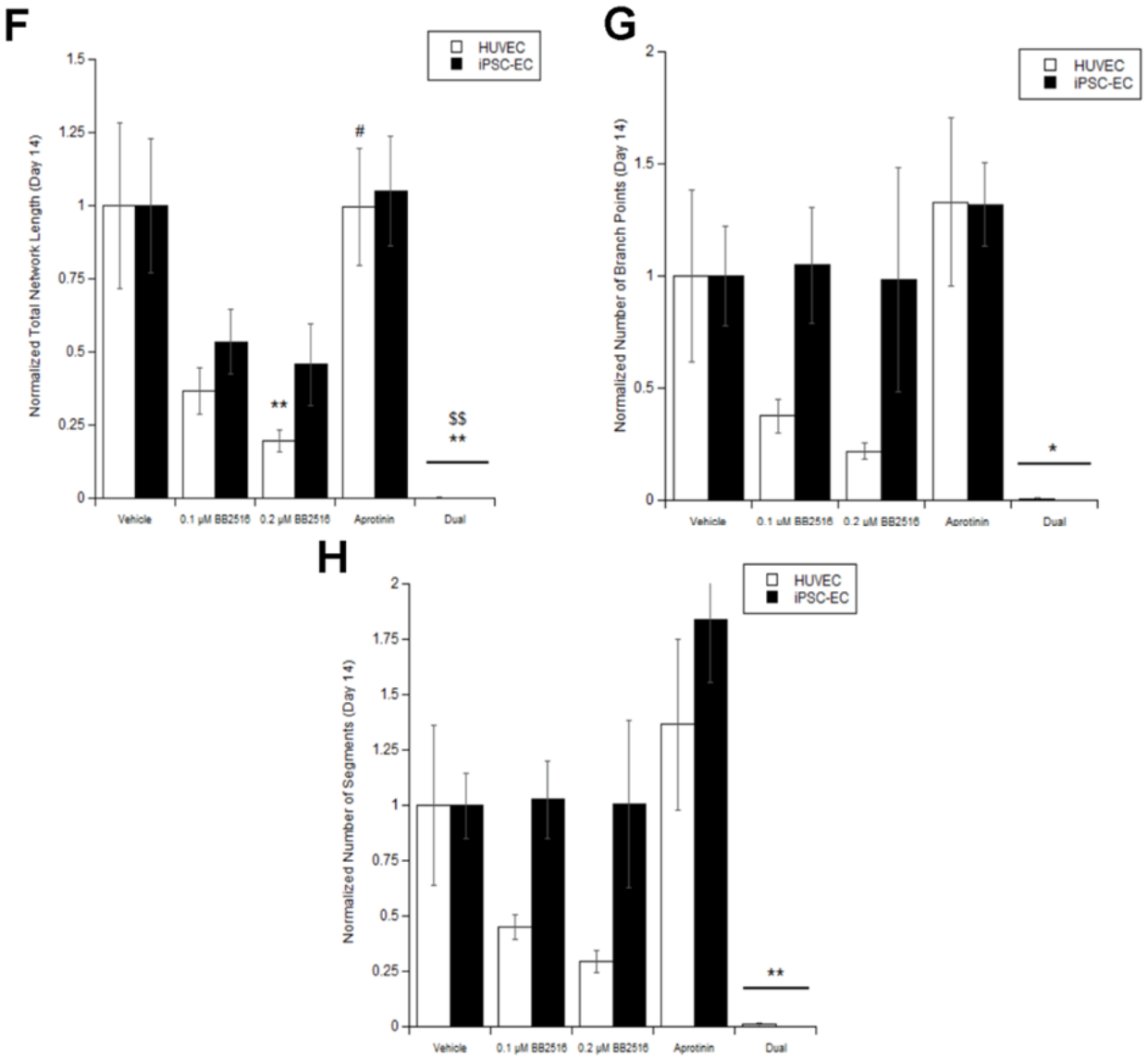


**Figure 4-3.2: Capillary morphogenesis by iPSC-ECs and HUVECs proceed via similar preoteolytic mechanisms.** ***[Quantifacation]***

**(F)** Total capillary network length, **(G)** number of segments, and **(H)** number of branch points from a minimum of 30 beads over three separate experiments at day 14 were quantified, averaged, and normalized to the respective EC vehicle control. * $p<0.05$ and ** $p<0.01$ when comparing the indicated condition to the vehicle control. @ $p<0.05$ and @@ $p<0.01$ when comparing the indicated condition to the 0.1 µM BB2516 condition. # $p<0.05$ and ## $p<0.01$ when comparing the indicated condition to the 0.2 µM BB2516 condition. $ $p<0.05$ and $$ $p<0.01$ when comparing the indicated condition to the aprotinin condition. Error bars indicate ±SEM.

### 4.3.3 iPSC-EC/NHLF co-cultures show differences in MMP RNA expression, compared to HUVEC/NHLF co-cultures.

The expression of MMPs, specifically MMP-2, MMP-9, and MT1-MMP, in HUVECs is directly related to the formation of vessel-like networks [29]–[31]. Knockdown of MT1-MMP expression, in particular, attenuates sprouting for HUVECs in fibrin [31]. Despite similar dependencies on MMP- and plasmin-mediated mechanisms revealed through the use of protease inhibitors, we sought to compare the expression levels of MMPs between iPSC-EC and HUVEC co-cultures as a potential explanation for the attenuated sprouting in the case of the former. qPCR demonstrated no significant differences in the RNA expression levels of MMP-2 (Fig. 4-4A) and MT1-MMP (Fig. 4-4B) across all time points. However, MMP-9 levels (Fig. 4-4C) were significantly different in iPSC-EC co-cultures. At earlier times points (day 4), iPSC-EC co-cultures show a ~3.5 fold increase in RNA expression, while at later time points (day 14), a ~4 fold reduction in RNA expression.

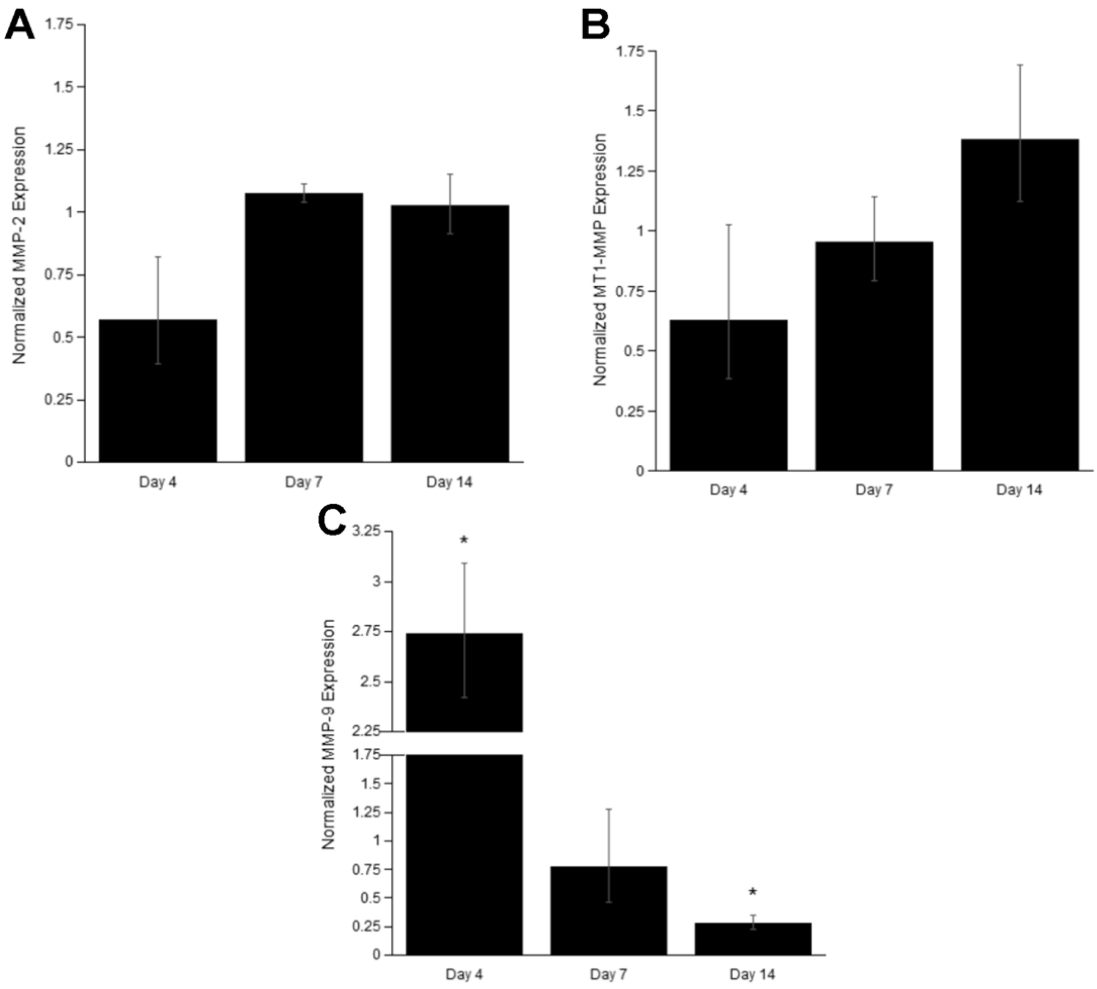


**Figure 4-4: iPSC-ECs co-cultures show differences in MMP RNA expression levels compared to HUVEC co-cultures.** The expression levels of key matrix metalloproteases [**(A)** MMP-2, **(B)** MT1-MMP, and **(C)** MMP-9] involved in capillary morphogenesis were quantified from iPSC-EC/NHLF co-cultures via qPCR. Expression levels were averaged across three separate experiments at the indicated time points and normalized to HUVEC/NHLF co-culture controls. * $p<0.05$ when comparing the indicated time point to the HUVEC control. Error bars indicate ±SEM.

### 4.3.4 iPSC-EC/NHLF co-cultures show differences in MMP protein expression, compared to HUVEC/NHLF co-cultures.

We next characterized MMP protein expression levels by Western blotting. MMP-2 (Fig. 4-5A), MT1-MMP (Fig. 4-5B), and MMP-9 (Fig. 4-5C) were all expressed at the protein level in iPSC-EC co-cultures. Full Western Blot images with loading controls can be seen in Supplemental Fig. 4-S1. Semi-quantification, normalized to a GAPDH loading control, of the band intensities revealed no significant differences in protein expression for MMP-2 (Fig. 4-5D), MT1-MMP (Fig. 4-5E), and at day 4 for MMP-9 (Fig. 4-5F). However, at later time points (day 7 and day 14), the protein expression levels of MMP-9 were significantly reduced in iPSC-EC co-cultures (~25% in both conditions), consistent with the qPCR results.

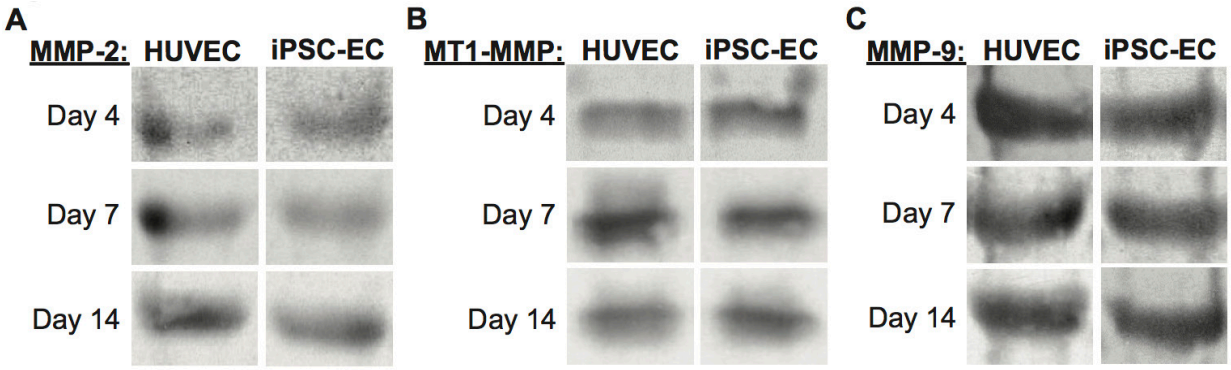


**Figure 4-5.1: iPSC-EC/NHLF co-cultures show differences in MMP protein expression levels compared to HUVEC/NHLF co-cultures. [Rep. Images]**
Representative images of Western blots for (A) MMP-2, (B) MT1-MMP, (C) MMP-9 from HUVEC or iPSC-EC coated microcarrier beads co-cultured with NHLFS at various time points

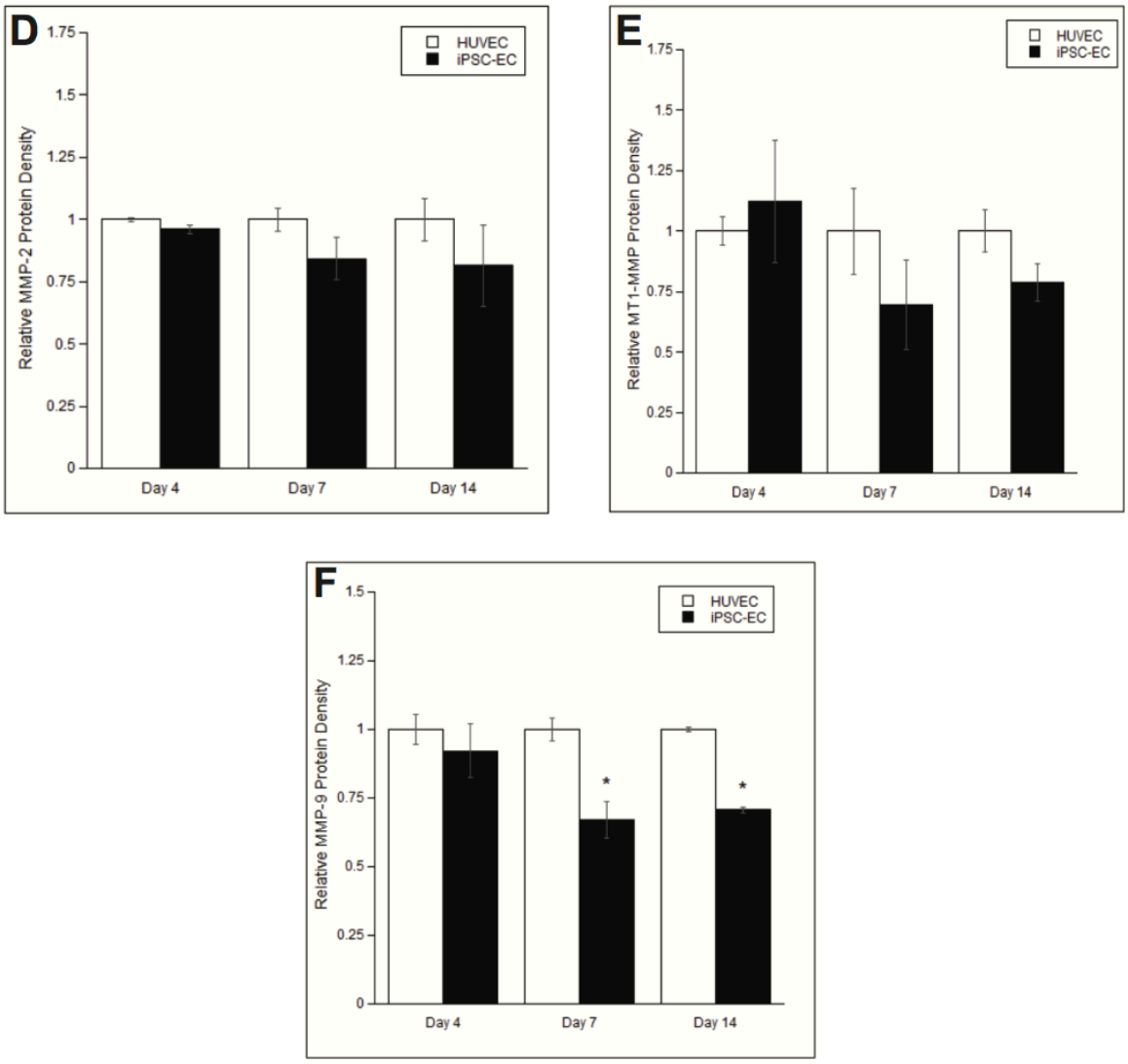


**Figure 4-5.2: iPSC-EC/NHLF co-cultures show differences in MMP protein expression levels compared to HUVEC/NHLF co-cultures. [Quantification]**
Images were quantified and averaged across three separate experiments via scanning densitometry. Protein levels for **(D)** MMP-2, **(E)** MT1-MMP, and **(F)** MMP-9 were normalized to their respective HUVEC co-culture controls. * $p<0.05$ when comparing the indicated time point to the HUVEC control. Error bars indicate ±SEM. Full (uncropped) Western blot images are shown in supplemental information (Fig. 4-S1).

### 4.3.5 iPSC-EC/NHLF co-cultures show differences in MMP activity levels, compared to HUVEC/NHLF co-cultures.

Finally, the proteolytic activities of the MMPs in question were investigated using gelatin zymography. MMP-2 (Fig. 4-6A) and MMP-9 (Fig. 4-6B) both degraded a gelatin matrix across all time points in iPSC-EC co-cultures and HUVEC co-cultures. Full gelatin zymography can be seen in Supplemental Fig. 4-S2. Semi-quantification via densitometry indicated no discernible differences in both pro- (Fig. 4-6C) and active- (Fig. 4-6E) forms of MMP-2. While there were no significant differences in pro- (Fig. 4-6D) and active- (Fig. 4-6F) forms of MMP-9 at earlier time points (day 4 and day 7), both forms of MMP-9 were significantly less active at day 14 in iPSC-EC co-cultures. Collectively, these data not only demonstrate the expression and activity of MMP-9 is significantly different in iPSC-EC co-cultures, but offers one potential mechanism to explain the attenuated capillary morphogenesis by iPSC-ECs.

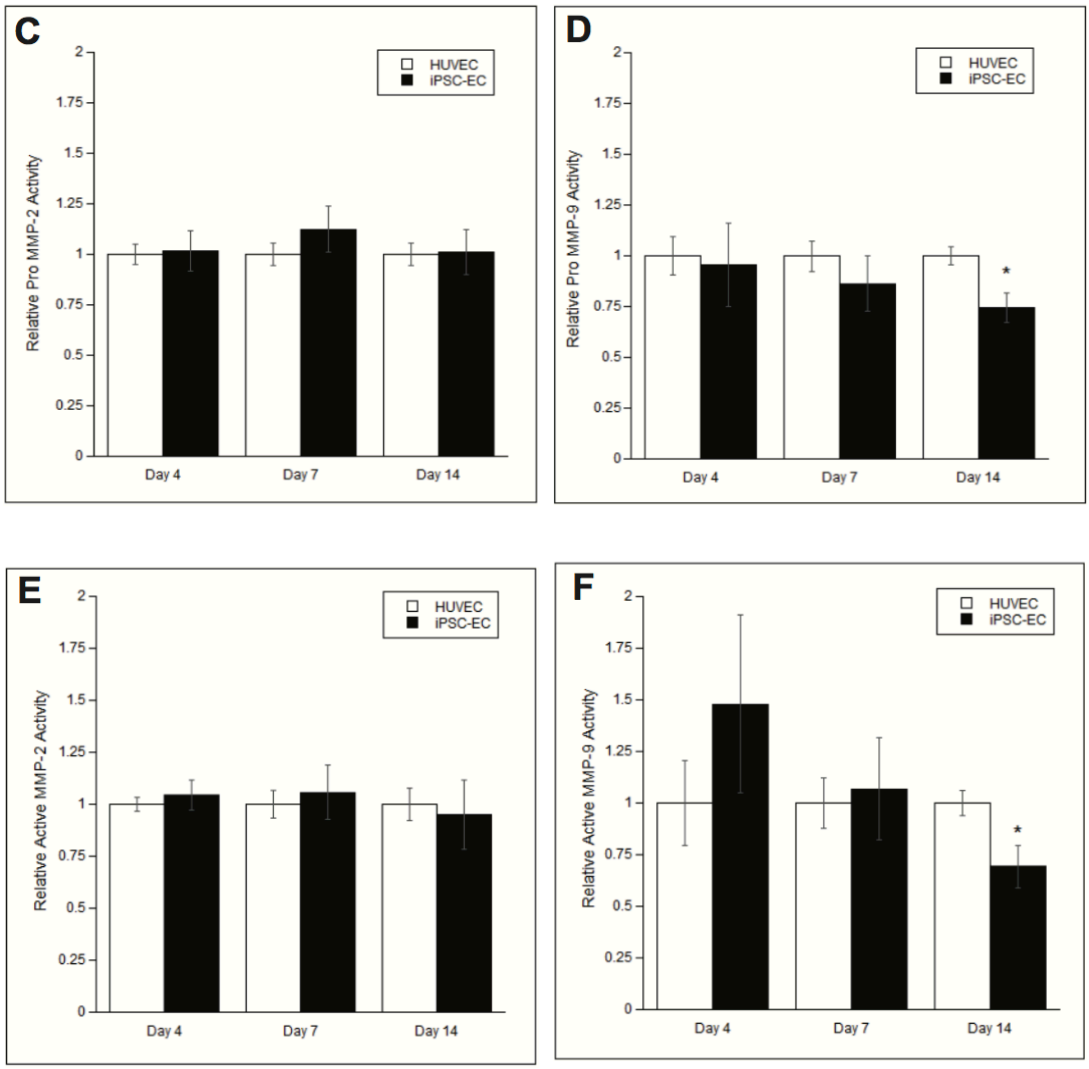


**Figure 4-6: iPSC-EC/NHLF co-cultures show differences in the levels of MMP activity compared to HUVEC/NHLF co-cultures.**
HUVEC or iPSC-EC coated microcarrier beads co-cultured with NHLFs were digested and pooled to assay for activity via gelatin zymography. Representative images of zymograms performed at various time points for **(A)** MMP-2, and **(B)** MMP-9. A standard for MMP-2 and -9 was used to identify bands for pro-MMP-9 (92kDa), active MMP-9 (88kDa), pro-MMP-2 (72kDa), intermediate MMP-2 (64kDa), and active MMP-2 (62kDa). Images were quantified and averaged across three separate experiments via scanning densitometry. The levels for **(C)** pro-MMP-2, **(D)** pro-MMP-9, **(E)** active-MMP-2, and **(F)** active-MMP-9 were normalized to their respective HUVEC/NHLF co-culture controls. * $p<0.05$ when comparing the indicated condition to the HUVEC control. Error bars indicate ±SEM. Images were set to 8-bit color and contrast enhanced in an identical manner for each gel prior to quantification. Representative enhanced images are shown here. Full unedited gelatin images are shown in supplemental information (Fig. 4-S2)

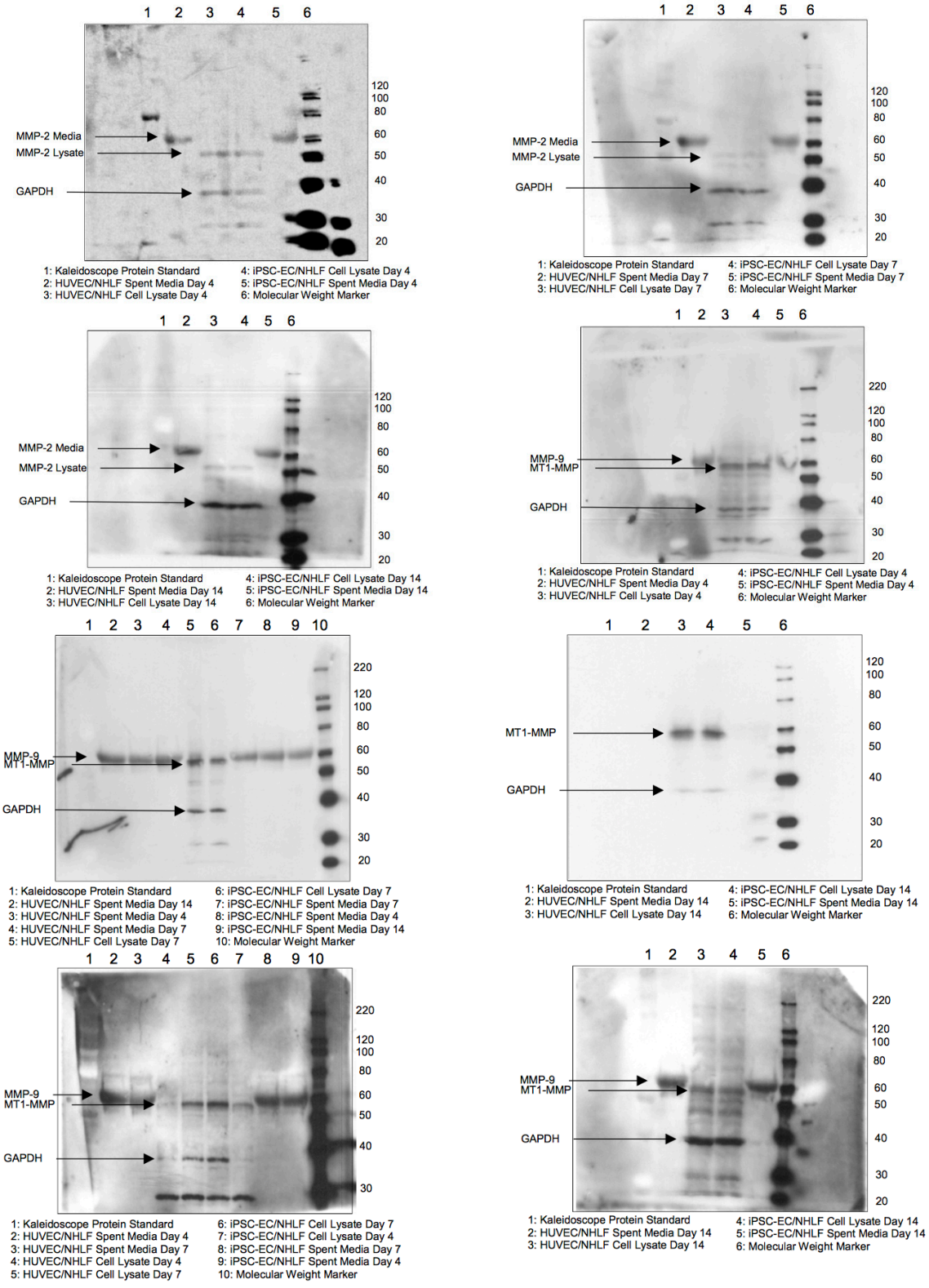


**Supplemental Fig. 4-S1:**
Full Western blot images of protein transcript levels of MMP-2, MT1-MMP, MMP-9 from HUVEC or iPSC-EC coated microcarrier beads co-cultured with NHLFS at various time points. Two protein standards were used, one for visualization during transfer and the other for visualization via chemiluminescence.

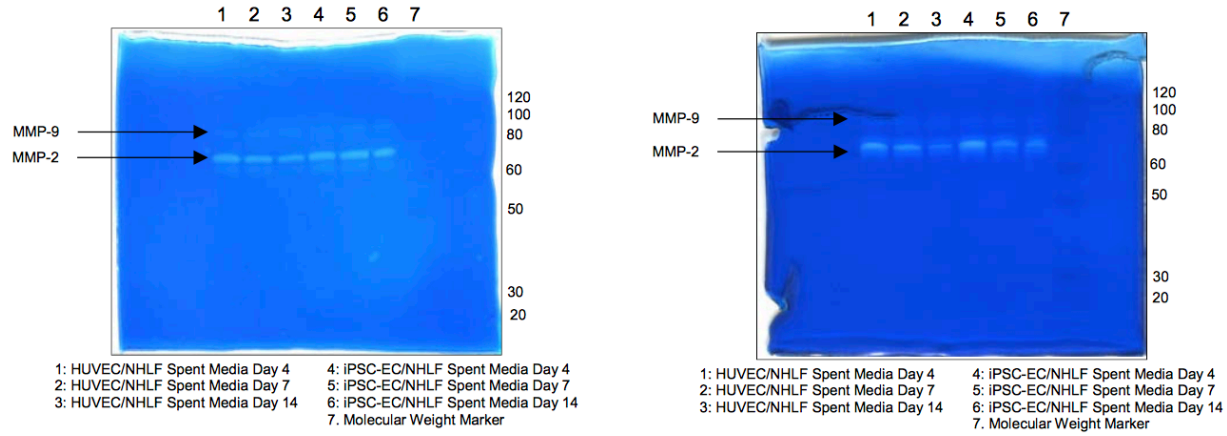


**Supplemental Fig. 4-S2:**
Full Gelatin Zymograpy images of protein activity levels of MMP-2, MT1-MMP, MMP-9 from HUVEC or iPSC-EC coated microcarrier beads co-cultured with NHLFS at various time points

## 4.4 Discussion

Although current tissue engineering approaches have potential to revascularize ischemic regions, limitations of abundant sourcing and immunorejection inhibit their clinical translation. iPSC-ECs are of increasing interest because of their potentially limitless sourcing and autologous nature. In chapter 3, using a 3D fibrin-based *in vitro* model, we demonstrated that capillary morphogenesis by iPSC-ECs was significantly attenuated when compared to HUVECs [32]. While prior studies have shown that iPSC-ECs are capable of forming vessel-like structures [34], [35], there is little evidence regarding possible differences in vessel formation in comparison to widely utilized EC sources. Furthermore, there is little to no research on the iPSC-ECs' functional abilities and mechanisms involved in capillary morphogenesis. This study explored the functional and mechanistic similarities *in vitro* between iPSC-ECs and HUVECs in the formation of capillary networks as a potential explanation for the iPSC-ECs' reduced sprouting capability. Despite similar functional phenotypes and proteolytic remodeling mechanisms, we have shown that MMP-

9 expression is significantly reduced for iPSC-ECs co-cultured with NHLFs in comparison to HUVECs.

The inhibition, and subsequent abrogation of inhibition, of iPSC-EC capillary morphogenesis in fibrin gels of elevated concentrations demonstrates the mechanistic similarities in the ways both HUVECs and iPSC-ECs form vessel-like structures. In ECMs of higher density, transport of proangiogenic cues from stromal fibroblasts to ECs is inhibited, which significantly affects capillary morphogenesis when the fibroblasts are cultured atop gels at a fixed distance from the underlying ECs [24]. Distributing the stromal cells throughout the gel reduces these transport limitations, allowing for greater network formation. The data were normalized to their respective 2.5 mg/mL condition to highlight the similarities between iPSC-ECs and HUVECs, since the response of iPSC-ECs was otherwise dwarfed in magnitude relative to that of HUVECs on a non-normalized scale. Qualitatively, we also observed wider vessels formed with increased fibrin concentrations, a response that may be attributable to the reduced porosity of the matrix as increased densities are less porous [29]. Decreased pore size may cause cells to proliferate radially expanding laterally into the matrix. Another possibility is that an increase in ligand binding density can exert morphogenetic effects on these cells that are abrogated by signaling from the stromal cells [36]. Regardless, the effects of fibrin concentration and stromal cell distribution on network formation demonstrate the phenotypic similarities between the two EC populations.

Broad spectrum protease inhibition revealed iPSC-EC/NHLF co-cultures utilize proteolytic mechanisms similar to those employed by HUVEC/NHLF co-cultures. The fibroblast-mediated sprouting was only completely attenuated through dual inhibition of both MMPs and serine proteases, which is consistent with findings we previously reported for HUVEC/NHLF co-cultures [30]. This proteolytic plasticity could be explained by the relationship between plasmin

and MMPs [37] or possibly a third type of extracellular protease involved in the morphogenic process [13]. Of the two doses of MMP inhibitor (BB2516) we tested, the higher dose (0.2 μM) did significantly reduce total network lengths in the HUVEC/NHLF co-cultures compared to vehicle controls, consistent with our prior findings [13], but did not significantly affect the iPSC-EC/NHLF co-cultures. Of course, the overall sprouting of the latter cultures is significantly less than the former, and thus any subtle effects of the protease inhibitors would be more difficult to detect.

The experiments performed with elevated fibrin concentration and the effect of protease inhibitors suggested that iPSC-ECs and HUVECs utilize similar fibrinolytic mechanisms. However, we hypothesized that differential quantities and/or activities of key MMPs may underlie the attenuated iPSC-ECs sprouting relative to HUVECs. qPCR showed the expression levels of mRNAs encoding for MMP-2 and MT1-MMP were similar between HUVEC and iPSC-EC cultures and did not vary significantly with time. By comparison, MMP-9 mRNA levels were significantly higher in iPSC-EC than HUVEC cultures initially, but then dropped off dramatically over the time course of the sprouting assay to become significantly lower than the HUVEC expression level by day 14. These findings were mirrored in terms of protein levels and enzymatic activities, with the levels and activities of MMP-9 significantly less in iPSC-EC cultures by day 14 relative to HUVECs. While there is compelling evidence that the MT-MMPs may be the only essential MMPs for capillary morphogenesis [38], multiple MMP family members, including MMP-9, have been implicated in capillary invasion in fibrin gels [39] and there is evidence MT1-MMP regulates MMP-9 specifically [40]. Therefore, it is entirely plausible the reduced MMP-9 expression and/or activity contributes to the inability of the iPSC-ECs to form capillary-like networks of the same magnitude as HUVECs. While molecular genetics tools to knock-down

and/or over-express MMP-9 in iPSC-EC may offer a more definitive interpretation of our findings here, the key focus of this study was to compare iPSC-ECs head-to-head with an established EC source.

It is also important to note our assessment of differences in the repertoire of proteolytic enzymes was performed in EC/NHLF co-cultures. While it is possible, though technically challenging, to separate the relative contributions of these two populations of cells, we elected not to do so given the importance of reciprocal cross-talk between ECs and their stromal support cells [41] and our intention to co-deliver both cell types in vivo for revascularization applications. Finally, while we focused on proteolytic differences between iPSC-ECs and HUVECs to partially explain the attenuation of sprouting, we of course cannot rule out other possibilities.

## 4.5 Conclusions

In summary, these studies assessed whether iPSC-ECs utilize similar mechanistic pathways previously documented for other sources of ECs in a well-characterized 3D fibrin-based co-culture model of angiogenic sprouting *in vitro*. Both HUVECs and iPSC-ECs capillary network formation were attenuated in elevated fibrin concentrations. Subsequent abrogation of spouting through distributing stromal cells throughout the matrix demonstrated functional similarities between the two populations. Proteolytic inhibition revealed iPSC-ECs utilized similar proteolytic invasion mechanisms. Furthermore, we identified differences in the RNA, protein, and activity expression levels of MMP-9 as a possible mechanistic explanation for the iPSC-EC attenuation documented in earlier chapters. Future *in vivo* studies, discussed in the next chapter, are necessary to determine if this attenuation is only an *in vitro* phenomenon. Ultimately, these findings suggest

an additional understanding of the fundamental mechanistic functions and phenotypic differences is necessary to reach the full potential of the iPSC-ECs.

## 4.6 References:


[1] T. H. Adair and J.-P. Montani, *Overview of Angiogenesis*. Morgan & Claypool Life Sciences, 2010.

[2] N. Kubis and B. I. Levy, "Vasculogenesis and Angiogenesis: Molecular and Cellular Controls," *Interv. Neuroradiol.*, vol. 9, no. 3, pp. 227–237, Sep. 2003.

[3] J. Rouwkema and A. Khademhosseini, "Vascularization and Angiogenesis in Tissue Engineering: Beyond Creating Static Networks," *Trends Biotechnol.*, vol. 34, no. 9, pp. 733–745, Sep. 2016.

[4] H. M. Nugent and E. R. Edelman, "Tissue Engineering Therapy for Cardiovascular Disease," *Circ. Res.*, vol. 92, no. 10, pp. 1068–1078, May 2003.

[5] P. H. Burri, R. Hlushchuk, and V. Djonov, "Intussusceptive angiogenesis: its emergence, its characteristics, and its significance," *Dev. Dyn. Off. Publ. Am. Assoc. Anat.*, vol. 231, no. 3, pp. 474–488, Nov. 2004.

[6] I. Buschmann and W. Schaper, "Arteriogenesis Versus Angiogenesis: Two Mechanisms of Vessel Growth," *News Physiol. Sci. Int. J. Physiol. Prod. Jointly Int. Union Physiol. Sci. Am. Physiol. Soc.*, vol. 14, pp. 121–125, Jun. 1999.

[7] D. C. Felmeden, A. D. Blann, and G. Y. H. Lip, "Angiogenesis: basic pathophysiology and implications for disease," *Eur. Heart J.*, vol. 24, no. 7, pp. 586–603, Apr. 2003.

[8] P. A. D'Amore and R. W. Thompson, "Mechanisms of angiogenesis," *Annu. Rev. Physiol.*, vol. 49, pp. 453–464, 1987.

[9] "VEGF guides angiogenic sprouting utilizing endothelial tip cell filopodia." [Online]. Available: https://www.ncbi.nlm.nih.gov/pmc/articles/PMC2172999/. [Accessed: 09-Jun-2018].

[10] M. S. Pepper, "Manipulating angiogenesis. From basic science to the bedside," *Arterioscler. Thromb. Vasc. Biol.*, vol. 17, no. 4, pp. 605–619, Apr. 1997.

[11] D. H. Ausprunk and J. Folkman, "Migration and proliferation of endothelial cells in preformed and newly formed blood vessels during tumor angiogenesis," *Microvasc. Res.*, vol. 14, no. 1, pp. 53–65, Jul. 1977.

[12] M. M. Sholley, G. P. Ferguson, H. R. Seibel, J. L. Montour, and J. D. Wilson, "Mechanisms of neovascularization. Vascular sprouting can occur without proliferation of endothelial cells," *Lab. Investig. J. Tech. Methods Pathol.*, vol. 51, no. 6, pp. 624–634, Dec. 1984.

[13] C. M. Ghajar, S. C. George, and A. J. Putnam, "Matrix metalloproteinase control of capillary morphogenesis," *Crit. Rev. Eukaryot. Gene Expr.*, vol. 18, no. 3, pp. 251–278, 2008.

[14] J. E. Rundhaug, "Matrix metalloproteinases and angiogenesis," *J. Cell. Mol. Med.*, vol. 9, no. 2, pp. 267–285, Jun. 2005.

[15] C.-L. E. Helm, M. E. Fleury, A. H. Zisch, F. Boschetti, and M. A. Swartz, "Synergy between interstitial flow and VEGF directs capillary morphogenesis in vitro through a gradient amplification mechanism," *Proc. Natl. Acad. Sci.*, vol. 102, no. 44, pp. 15779–15784, Nov. 2005.

[16] T.-K. Ito, G. Ishii, H. Chiba, and A. Ochiai, "The VEGF angiogenic switch of fibroblasts is regulated by MMP-7 from cancer cells," *Oncogene*, vol. 26, no. 51, pp. 7194–7203, Nov. 2007.

[17] S. Lee, S. M. Jilani, G. V. Nikolova, D. Carpizo, and M. L. Iruela-Arispe, "Processing of VEGF-A by matrix metalloproteinases regulates bioavailability and vascular patterning in tumors," *J. Cell Biol.*, vol. 169, no. 4, pp. 681–691, May 2005.

[18] J. M. Whitelock, A. D. Murdoch, R. V. Iozzo, and P. A. Underwood, "The degradation of human endothelial cell-derived perlecan and release of bound basic fibroblast growth factor by stromelysin, collagenase, plasmin, and heparanases," *J. Biol. Chem.*, vol. 271, no. 17, pp. 10079–10086, Apr. 1996.

[19] A. Zijlstra *et al.*, "Collagenolysis-dependent angiogenesis mediated by matrix metalloproteinase-13 (collagenase-3)," *J. Biol. Chem.*, vol. 279, no. 26, pp. 27633–27645, Jun. 2004.

[20] K. Lehti *et al.*, "An MT1-MMP-PDGF receptor-beta axis regulates mural cell investment of the microvasculature," *Genes Dev.*, vol. 19, no. 8, pp. 979–991, Apr. 2005.

[21] M. Hellström *et al.*, "Lack of pericytes leads to endothelial hyperplasia and abnormal vascular morphogenesis," *J. Cell Biol.*, vol. 153, no. 3, pp. 543–553, Apr. 2001.

[22] G. E. Davis, K. A. Pintar Allen, R. Salazar, and S. A. Maxwell, "Matrix metalloproteinase-1 and -9 activation by plasmin regulates a novel endothelial cell-mediated mechanism of collagen gel contraction and capillary tube regression in three-dimensional collagen matrices," *J. Cell Sci.*, vol. 114, no. Pt 5, pp. 917–930, Mar. 2001.

[23] W. B. Saunders, K. J. Bayless, and G. E. Davis, “MMP-1 activation by serine proteases and MMP-10 induces human capillary tubular network collapse and regression in 3D collagen matrices,” *J. Cell Sci.*, vol. 118, no. Pt 10, pp. 2325–2340, May 2005.

[24] T.-H. Chun *et al.*, “MT1-MMP-dependent neovessel formation within the confines of the three-dimensional extracellular matrix,” *J. Cell Biol.*, vol. 167, no. 4, pp. 757–767, Nov. 2004.

[25] K. B. Hotary *et al.*, “Matrix metalloproteinases (MMPs) regulate fibrin-invasive activity via MT1-MMP-dependent and -independent processes,” *J. Exp. Med.*, vol. 195, no. 3, pp. 295–308, Feb. 2002.

[26] C. Lu, X.-Y. Li, Y. Hu, R. G. Rowe, and S. J. Weiss, “MT1-MMP controls human mesenchymal stem cell trafficking and differentiation,” *Blood*, vol. 115, no. 2, pp. 221–229, Jan. 2010.

[27] Y. Tang *et al.*, “MT1-MMP-dependent control of skeletal stem cell commitment via a β1-integrin/YAP/TAZ signaling axis,” *Dev. Cell*, vol. 25, no. 4, pp. 402–416, May 2013.

[28] I. Yana *et al.*, “Crosstalk between neovessels and mural cells directs the site-specific expression of MT1-MMP to endothelial tip cells,” *J. Cell Sci.*, vol. 120, no. Pt 9, pp. 1607–1614, May 2007.

[29] C. M. Ghajar, K. S. Blevins, C. C. W. Hughes, S. C. George, and A. J. Putnam, “Mesenchymal stem cells enhance angiogenesis in mechanically viable prevascularized tissues via early matrix metalloproteinase upregulation,” *Tissue Eng.*, vol. 12, no. 10, pp. 2875–2888, Oct. 2006.

[30] C. M. Ghajar *et al.*, “Mesenchymal cells stimulate capillary morphogenesis via distinct proteolytic mechanisms,” *Exp. Cell Res.*, vol. 316, no. 5, pp. 813–825, Mar. 2010.

[31] S. Kachgal, B. Carrion, I. A. Janson, and A. J. Putnam, “Bone marrow stromal cells stimulate an angiogenic program that requires endothelial MT1-MMP,” *J. Cell. Physiol.*, vol. 227, no. 11, pp. 3546–3555, Nov. 2012.

[32] J. R. Bezenah, Y. P. Kong, and A. J. Putnam, “Evaluating the potential of endothelial cells derived from human induced pluripotent stem cells to form microvascular networks in 3D cultures,” *Sci. Rep.*, vol. 8, no. 1, p. 2671, Feb. 2018.

[33] C. M. Ghajar *et al.*, “The Effect of Matrix Density on the Regulation of 3-D Capillary Morphogenesis,” *Biophys. J.*, vol. 94, no. 5, pp. 1930–1941, Mar. 2008.

[34] A. Margariti *et al.*, “Direct reprogramming of fibroblasts into endothelial cells capable of angiogenesis and reendothelialization in tissue-engineered vessels,” *Proc. Natl. Acad. Sci. U. S. A.*, vol. 109, no. 34, pp. 13793–13798, Aug. 2012.

[35] W. J. Adams *et al.*, “Functional Vascular Endothelium Derived from Human Induced Pluripotent Stem Cells,” *Stem Cell Rep.*, vol. 1, no. 2, pp. 105–113, Jul. 2013.

[36] M. D. Sternlicht and Z. Werb, “HOW MATRIX METALLOPROTEINASES REGULATE CELL BEHAVIOR,” *Annu. Rev. Cell Dev. Biol.*, vol. 17, pp. 463–516, 2001.

[37] V. W. M. van Hinsbergh, M. A. Engelse, and P. H. A. Quax, “Pericellular proteases in angiogenesis and vasculogenesis,” *Arterioscler. Thromb. Vasc. Biol.*, vol. 26, no. 4, pp. 716–728, Apr. 2006.

[38] S. Kachgal and A. J. Putnam, “Mesenchymal stem cells from adipose and bone marrow promote angiogenesis via distinct cytokine and protease expression mechanisms,” *Angiogenesis*, vol. 14, no. 1, pp. 47–59, Mar. 2011.

[39] M. Toth, I. Chvyrkova, M. M. Bernardo, S. Hernandez-Barrantes, and R. Fridman, “Pro-MMP-9 activation by the MT1-MMP/MMP-2 axis and MMP-3: role of TIMP-2 and plasma membranes,” *Biochem. Biophys. Res. Commun.*, vol. 308, no. 2, pp. 386–395, Aug. 2003.

[40] C. Hahn and M. A. Schwartz, “Mechanotransduction in vascular physiology and atherogenesis,” *Nat. Rev. Mol. Cell Biol.*, vol. 10, no. 1, pp. 53–62, Jan. 2009.

[41] A. C. Newman, M. N. Nakatsu, W. Chou, P. D. Gershon, and C. C. W. Hughes, “The requirement for fibroblasts in angiogenesis: fibroblast-derived matrix proteins are essential for endothelial cell lumen formation,” *Mol. Biol. Cell*, vol. 22, no. 20, pp. 3791–3800, Oct. 2011

# CHAPTER 5

# Assessing the Ability of iPSC-ECs to Form Functional Microvasculature *in vivo*

## 5.1 Introduction

Cardiovascular diseases (CVDs) are the leading cause of death worldwide with total yearly health expenditures and costs associated with lost productivity exceeding $300 billion and rising [1]. Many of these patients suffer from atherosclerosis, characterized by hardening of the vessels and typically caused by buildup of a cholesterol-rich plaque in an artery [2]. Atherosclerotic lesions can cause ischemia, a reduction/obstruction of oxygenated blood supply to tissues, which can lead to tissue damage and eventually necrosis [3]. With the number of deaths and costs attributed to CVD expected to rise over the next decade, there is an urgent clinical need for new approaches to revascularize ischemic tissues to prevent necrosis, amputations, and ultimately death [4], [5].

A variety of therapeutic strategies have been investigated in recent years to direct angiogenesis. Growth factor delivery has been extensively studied to promote endothelial cell recruitment and eventually increase vessel formation [6], [7]. However, various challenges plague growth factor delivery therapies, including protein instability, the need for precision delivery, and rapid degradation [8]. Alternative tissue engineering approaches have attempted to revascularize

ischemic tissues using cell transplantation [9], [10]. Co-delivering endothelial cells (ECs) with stromal cells embedded in a hydrogel biomaterial promotes the formation of stable, mature microvasculature [11]–[14]. However, cell-based approaches have their own set of limitations, including potential immunorejection by the host. Perhaps the most critical challenge that must be overcome is the need for a plentiful cell source to supply the billions of cells required for clinical translation [15], [16].

A great deal of enthusiasm emerged with the creation of induced pluripotent stem cells (iPSC). Using four transcription factors [Oct4, Sox2, Klf4, and cMyc (OSKM)], adult somatic cells can be reprogramed into a pluripotent stem-cell like state [17]. Because iPSCs are dedifferentiated from a potentially autologous somatic cell type, using them as a cell source not only minimizes ethical concerns associated with other pluripotent cell sources but may also potentially bypass immunological concerns in clinical applications [18]. Even if derived from allogeneic sources, iPSCs and their theoretical ability to proliferate indefinitely could ultimately overcome biomanufacturing hurdles by providing a large reservoir of cells necessary for human translation [19].

Endothelial-like cells, characterized by their expression of endothelial cell markers, can be differentiated from iPSCs [20], [21]. Their functional abilities to form vessel-like networks both *in vitro* and *in vivo* have also been described [22]–[24]. However, because the potential of these cells has been lauded without appropriate benchmarking against other endothelial cell sources, we recently investigated the vasculogenic potential of iPSC-ECs in a well-established 3D cell culture model of sprouting angiogenesis [25]. The quantity, quality, and function of the vessel-like networks formed by these cells were compared to human umbilical vein endothelial cells (HUVECs), another endothelial cell source with a proven capability of capillary morphogenesis.

Our worked, seen in Chapter 4, revealed sprouting by iPSC-ECs was significantly reduced (vs. HUVECs) and identified differences in MMP-9 expression as a possible mechanistic explanation [25]. Despite highlighting these differences, the question remains if this attenuation is only an *in vitro* phenomenon.

In this present study, we compared the *in vivo* vascularization potential of iPSC-ECs head-to-head with HUVECs. Endothelial cells (either iPSC-ECs or HUVECs) and normal human lung fibroblasts (NHLFs) were co-injected subcutaneously within a fibrin matrix into the dorsal flank of SCID mice. Vessel formation was characterized by quantifying vessel density, vessel perfusion, and markers of vessel maturity. Our findings demonstrate iPSC-ECs are unable to form vessels of equal quality and quantity compared to an established EC source.

## 5.2 Methods

### 5.2.1 Cell culture

Human umbilical vein endothelial cells (HUVECs) were harvested from fresh umbilical cords following a previously established protocol [26]. HUVECs were plated with endothelial growth media (EGM-2, Lonza, Walkersville, MD) in tissue culture flasks and cultured at 37 °C and 5% $CO_2$. Media were changed every 48 hours and cells were used at passage 3. Normal human lung fibroblasts (NHLFs, Lonza) were cultured at 37 °C and 5% $CO_2$ in Dulbecco's modified eagle media (DMEM, Life Technologies, Grand Island, NY) with 10% fetal bovine serum (FBS). Culture media were replaced every 48 hours and cells from passage 6–10 were used in experiments. iCell endothelial cells (Cellular Dynamics International, Madison, WI), referred to

as iPSC-ECs, were cultured at 37 °C and 5% $CO_2$ in Vasculife VEGF endothelial medium (Lifeline Cell Technology, Fredrick, MD) supplemented with iCell Endothelial Cell Medium Supplement (Cellular Dynamics International), per the manufacturer's instructions. iPSC-EC tissue culture flasks were coated with 35 µg/mL fibronectin (Invitrogen, Carlsbad, CA) for 1 hr at room temperature prior to plating the cells. Culture media were replaced every 48 hours and cells from passage 3 were used in experiments.

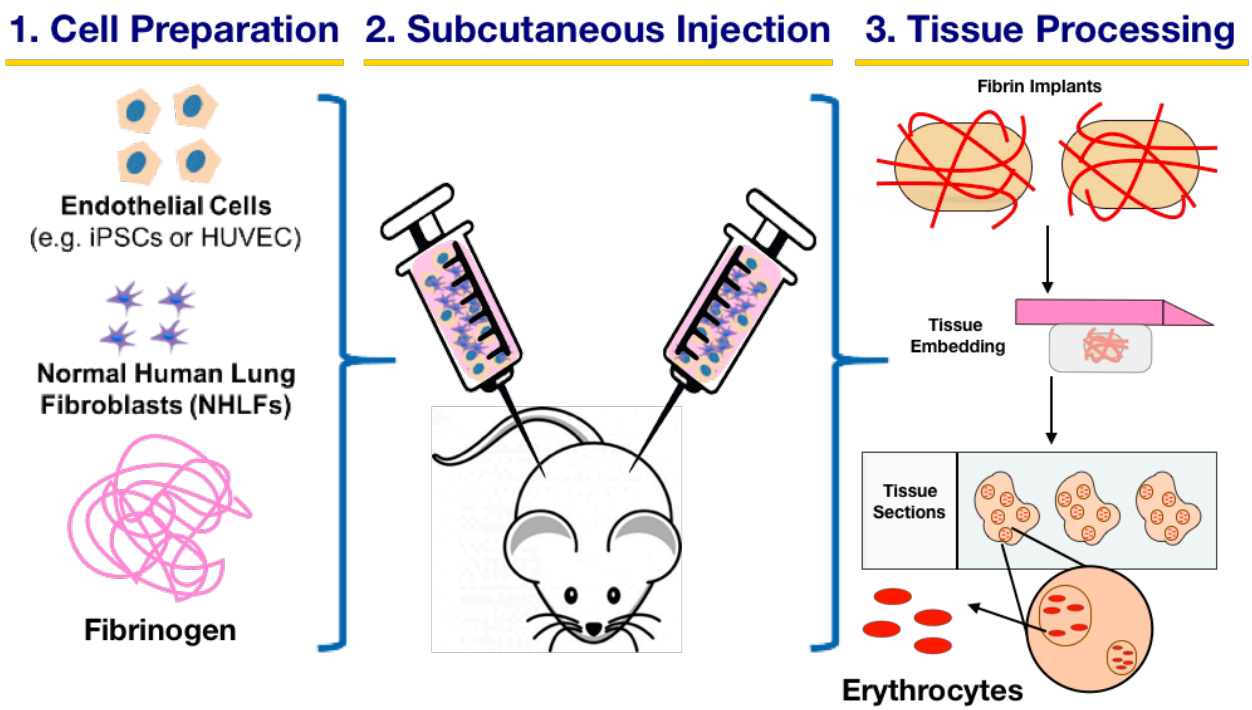


**Figure 5-1: in Vivo Subcutaneous Schematic**
ECs are co-injected with NHLFs in a 2.5mg/mL fibrin solution into the dorsa flank of SCID mice. Implants are harvested, processed, and embedded in paraffin for sectioning, Tissue sections are IHC stained for CD31 to visualize vessel formation

## 5.2.2 Sample Preparation for Subcutaneous Injection

A 2.5 mg/mL bovine fibrinogen (92% clottable, Sigma-Aldrich, St. Louis, MO) solution was prepared by dissolving the protein in an appropriate amount of serum-free EGM-2 and placed

in a water bath at 37 °C. The solution was sterile filtered through a 0.22 µm syringe filter (Millipore, Billerica, MA). Cells were cultured in T-75 flasks to 80% confluency and rinsed with PBS before being harvested via 0.25% trypsin incubation for 5 min at 37 °C and 5% $CO_2$. Trypsin was neutralized using DMEM supplemented with 10% FBS. The cellular suspension was centrifuged (200 × G for 5 min) and supernatant was aspirated immediately. Cells were resuspended at a 1:1 ratio of ECs:NHLFs in the previously prepared fibrinogen solution at a final concentration of 4 million cells/mL, totaling 2 million cells per injection (500 µL). Immediately before injection, 5% FBS and 12 µL of thrombin solution (50 U/mL; Sigma-Aldrich) were added to the 500 µL of fibrinogen–cell solution. Acellular controls containing fibrinogen, FBS, and thrombin were also prepared.

### 5.2.3 Subcutaneous Injections

All animal procedures were performed in accordance with the NIH guidelines for laboratory animal usage and approved by the University of Michigan's Institutional Animal Care and Use Committee (IACUC). Male CB17/SCID mice (6-8 weeks old; Taconic Labs, Hudson, NY) were used for all experiments. The mice were allowed to acclimate for ≥72 hours after arrival. Prior to surgery, mice were weighed and marked with permanent marker to identify experimental conditions. The mice were then anesthetized in an induction chamber with 5% isoflurane at 1L/min $O_2$ (Cyogenic Gases) using a V-1 Tabletop isoflurane vaporizer system equipped with an Active Scavenging Unit (VetEquipt, Livermore, CA). Once mice were fully anesthetized, they were moved to a surgery bench and fitted with an active scavenging nose cone. The isoflurane level was reduced to 1-1.5%, depending on weight, during surgery to maintain anesthesia. Ophthalmic ointment (Puralube® 499 vet ointment, Dechra, Overland Park, KS) was added to the eyes of each

mouse. An analgesic, carprofen (5 mg/kg), was then administered to each animal via intraperitoneal injection. The dorsal flanks of each mouse were shaved and depilatory agent (Nair, Fisher Scientific, Pittsburg, PA) was applied to remove any remaining hair. Ethanol and betadine (Thermo Fisher Scientific, Fremont, CA) were applied alternating three times each to sterilize the injection site. The injection samples were then prepared, as described above. Each solution was rapidly mixed and drawn into a 1-mL syringe fitted with a BD PrecisionGlideTM 20G needle. The mixture (500 μL) was immediately injected subcutaneously on the dorsal flank of the mouse, with two implants per animal, one on each flank. The needle was left in the injection site for 1 min to allow for the solution to polymerize. Mice were then placed in a recovery cage to recover from the anesthesia, and then returned to their normal housing environment. Mice were monitored daily post-surgery. A total of 18 mice (4 implants/ cell condition x 3 time points x 3 cell conditions x 2 implants/mouse) were used for this study. Bilateral implants were injected per animal, one on each flank in a randomized fashion.

### 5.2.4 Implant retrieval post-processing

Animals were euthanized on day 4, day 7, or day 14 after implants were injected. The implants were surgically excised from each mouse via gross dissection and placed immediately in Z-fix (Fisher Scientific). After a 24 hour fixation, implants were washed 3x in PBS and stored in 70% ethanol at 4 °C until further processing. Excess tissue was then removed from the implant using forceps and scissors, and samples were placed in embedding cassettes (UNISETTE cassette with lid, Simport, Canada), dehydrated, and embedded in paraffin using a KD-BMII tissue embedding center (IHC World, Ellicott City, MD). For further analysis, embedded samples were

sectioned (6 μm thick sections) with a Thermo Scientific HM 325 rotary microtome and placed on glass slides with 6 sections per slide.

### 5.2.5 Hematoxylin and Eosin Staining

Paraffin sections on glass slides were dewaxed in xylene baths 2x for 5 minutes. Slides were then washed 2x in each decreasing ethanol concentration (100%, 95%, 70%) bath for 3 minutes. Lastly, slides were rehydrated in deionized water for 3 minutes prior to staining with Mayer's hematoxylin (Electron Microscopy Sciences) for 15 minutes. Slides were then rinsed in tap water for 15 minutes and briefly placed in 95% ethanol for 30 seconds. Following, slides were immersed in Eosin Y (Sigma) for 1 minute and dehydrated twice in each increasing ethanol concentration (95%, 100%) bath for 1 minute. Samples were cleared by washing in xylene baths 2x for 3 minutes. Toluene mounting solution (Permount, Thermo Fisher Scientific) was added to cover slips prior to placing on top of each slide. Slides were left to dry before imaging.

### 5.2.6 Immunohistochemical Staining

Implant region locations were first approximated with the aforementioned H&E staining. Serial sections were deparaffinized and rehydrated following the same protocol described for hematoxylin and eosin staining. Slides were then steamed in a vegetable steamer (95-99 °C) for 35 minutes in an antigen retrieval solution (Dako, Carpinteria, CA) and equilibrated to room temperature for 30 minutes. Slides were washed 3x in 0.1% Tween 20 tris-buffered saline (TBS-T) for 2 minutes/wash while changing the baths for every wash. Excess moisture was removed from each slide and the area around the tissue was marked with an ImmEdge pen (Vector Laboratories, Inc., Burlingame, CA). The Dako EnVision System-HRP (DAB) kit (Dako) was

utilized to detect labeled antigens in the sections. First, peroxidase blocking solution was added to each tissue section for 5 minutes. Slides were subsequently washed 3x in 0.1% Tween 20 tris-buffered saline (TBS-T) for 2 minutes/wash (changing baths between washes). Mouse anti-human CD31 primary antibody (1:50, Dako), mouse anti-human smooth muscle actin antibody (1A4 (asm-1)) (1:200, Thermo Fisher Scientific), or mouse anti-human collagen IV monoclonal antibody (COL-94) (1:500, Thermo Fisher Scientific) were diluted in TBS-T and added to each tissue sample. Primary antibodies were incubated for 16 hours at 4 °C for both CD31 and COL-IV and 2 hours at room temperature for αSMA. After incubations, samples were rinsed 3x with TBS-T at 2 min/wash. The HRP-labeled polymer solution was then added to each sample and incubated for 30 minutes at room temperature. Samples were washed once again as described above. DAB+ substrate-chromogen buffer solution was then added to each tissue section for 5 minutes, and immediately rinsed in deionized water for 30 seconds. Samples were counterstained with hematoxylin for 15 minutes, followed by a 15 minute wash in tap water. Slides were then washed, as described for H&E staining, with 95% ethanol, 100% ethanol, and xylene to dehydrate the samples. Lastly, toluene mounting solution was added to each slide prior to covering the samples with coverslips. Slides were left to dry before imaging.

### 5.2.7 Vessel quantification

After staining, slides were imaged using an Olympus IX81 microscope with a DP2-Twain color camera (Olympus America, Center Valley, PA) and CellSens Imagining Software (Olympus) for visualizing stained slides. Brightfield images were taken at 4x and 20x for each of the various positively stained marker region of the sections. A 40x objective was used to image individual vessels. Positively stained sections from 3 separate implants for each condition, with 5 random

20x images per section, were then quantified to determine average vessel density on a per $mm^2$ basis for each of the indicated expression markers. Structures were considered a blood vessel if they exhibited a hollow lumen surrounded by a complete brown rim of positive stain. Quantification of vessels derived from the transplanted human cells was conducted by two independent evaluators via a one-side blinded study for hCD31. Lumen diameter was also quantified by each evaluator using Image J (National Institutes of Health, Bethesda, MD). Quantification of vessels expressing αSMA and COL-IV proceeded via the same methods described above but were unblinded. Acellular fibrin controls were not analyzed or shown because they did not contain any human EC-derived vessels.

### 5.2.8 Statistical analysis

Statistical analyses were performed using StatPlus (AnalystSoft Inc.,Walnut, CA). One-way analysis of variance (ANOVA) with a Bonferroni post-test was used to assess statistical significance between data sets. Data are reported as mean ± standard error of mean (SEM). Statistical significance was assumed when $p < 0.05$.

## 5.3 Results

### 5.3.1 iPSC-ECs/NHLF fibrin implants capable of vascular morphogenesis *in vivo*

In this study, HUVECs and iPSC-derived ECs were characterized for their abilities to form microvasculature when co-injected with NHLFs in a 3D fibrin matrix into subcutaneous pockets *in vivo*. Hematoxylin and eosin (H&E) staining of tissue sections from these implants demonstrated the presence of vessel structures across all time points (Fig. 5-2A). Despite the evidence of vessel formation and the presence of lumens for both EC types at each time point, the vessels formed by day 4 were comparatively smaller relative to the later time points (Fig. 5-2A, D). Vessels identified in day 4 sections also showed minimal evidence of inosculation with host microvasculature due to relative absence of host erythrocytes observed within the lumens or in the surrounding matrix. However, by days 7 and 14, constructs exhibited larger vessel morphologies and host erythrocytes were increasingly apparent throughout the implant region (Fig. 5-2B, C, E, F). Sections from both day 7 and day 14 show evidence of vessel perfusion. The erythrocytes were largely contained within the lumens of the neovessels formed by both EC types (as opposed to leaking into the interstitial tissue space) at the day 14 time point. Collectively, these results suggest the iPSC-ECs and HUVECs form functional microvasculature with similar qualities *in vivo*.

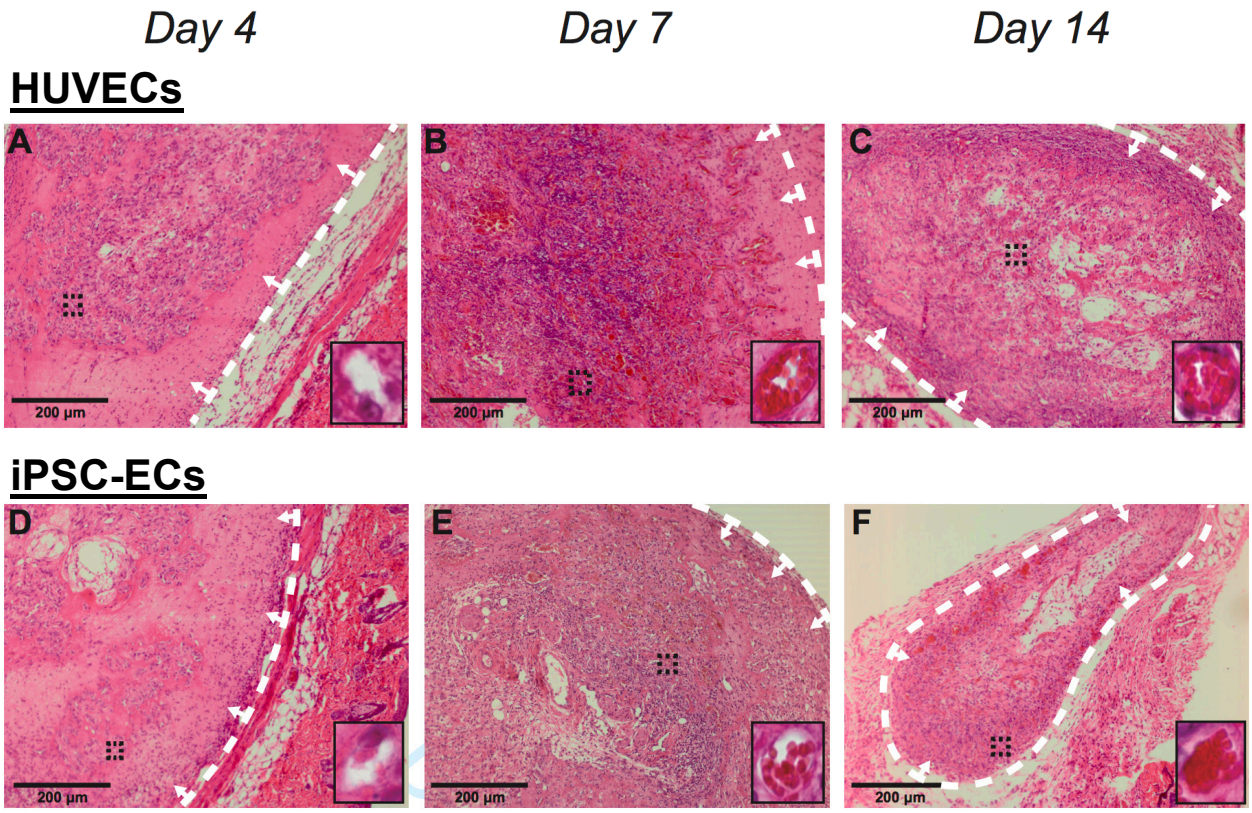


**Figure 5-2: Histological staining illustrates in vivo vessel formation and similar phenotypes across cell types**
Representative images of subcutaneous implants stained with hematoxylin and eosin. Implants were formed by co-injecting HUVECs **(A-C)** or iPSC-ECs **(C-F)** with NHLFs in 2.5 mg/mL fibrin. Implants were harvested at day 4 **(A,D)**, day 7 **(B,E)**, and day 14 **(C,F)**. Insets are images from a 40x objective lens, taken from the region indicated with black dashed lines, to more clearly show vessel morphologies and the presence of host erythrocytes. The white dashed lines are to indicate the boundary between the implant and mouse tissue, while arrows point to the implant region (*Scale bar = 200 µm)*

### 5.3.2 iPSC-ECs produce vessels with comparable morphologies and similar diameters

To validate the observations from the H&E-stained sections and confirm the human origins of the neovasculature, human ECs were identified in explanted tissue constructs via immunohistochemical staining of human CD31 (Fig. 5-3.1A-F). Both EC types demonstrated hollow lumens surrounded by a brown rim of positive staining at each time point, confirming successful vessel formation by the implanted human cells as suggested by the H&E stain. Vessels

also demonstrated morphological similarities with both cell conditions. Furthermore, vessel lumens demonstrated similarities in size. Quantification of the inner lumen diameter supported these qualitative observations (Fig. 5-3.2G-I) demonstrating no significant differences between the HUVEC and iPSC-EC condition across all time points ($12.03 \pm 1.45$ µm, $16.33 \pm 1.19$ µm, $14.04 \pm 1.15$ µm for iPSC-ECs versus $12.30 \pm 0.38$ µm, $17.58 \pm 1.32$ µm, $15.59 \pm 2.01$ µm for HUVECs on days 4, 7, and 14 respectively). Despite slightly smaller lumens at the day 4 time point, there were also no significant differences between time points for each of the cell conditions.

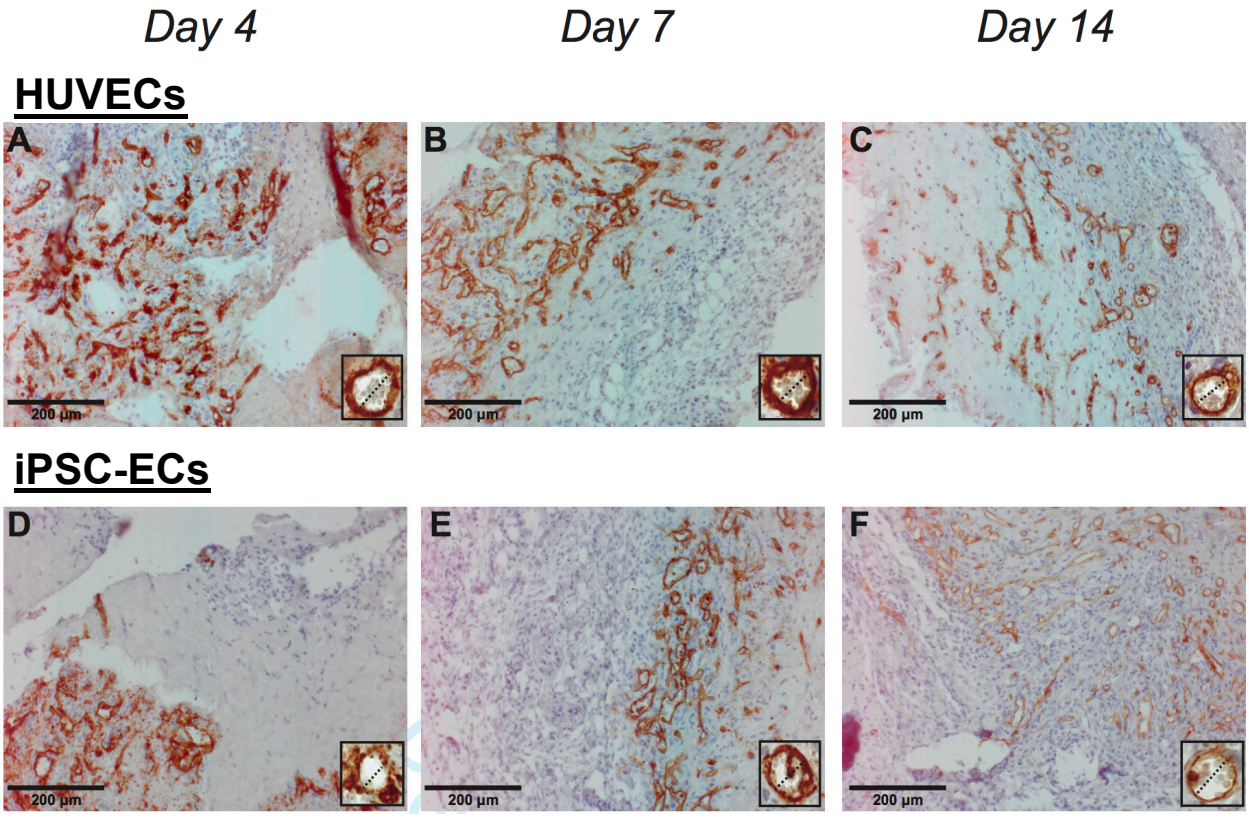


**Figure 5-3.1: Both iPSC-ECs and HUVECs express comparable vessel morphologies with similar vessel diameters *[Rep. Images]***
Representative images of human CD31-stained HUVECs **(A-C)** or iPSC-ECs **(D-F)** subcutaneous implants at various time points. All images were counterstained with hematoxylin. Implants were harvested at day 4 **(A,D)**, day 7 **(B,E)**, and day 14 **(C,F)**. Insets are images from a 40x objective lens and dashed lines are present to more clearly show similarities between vessel diameters. (*Scale bar = 200 µm)*

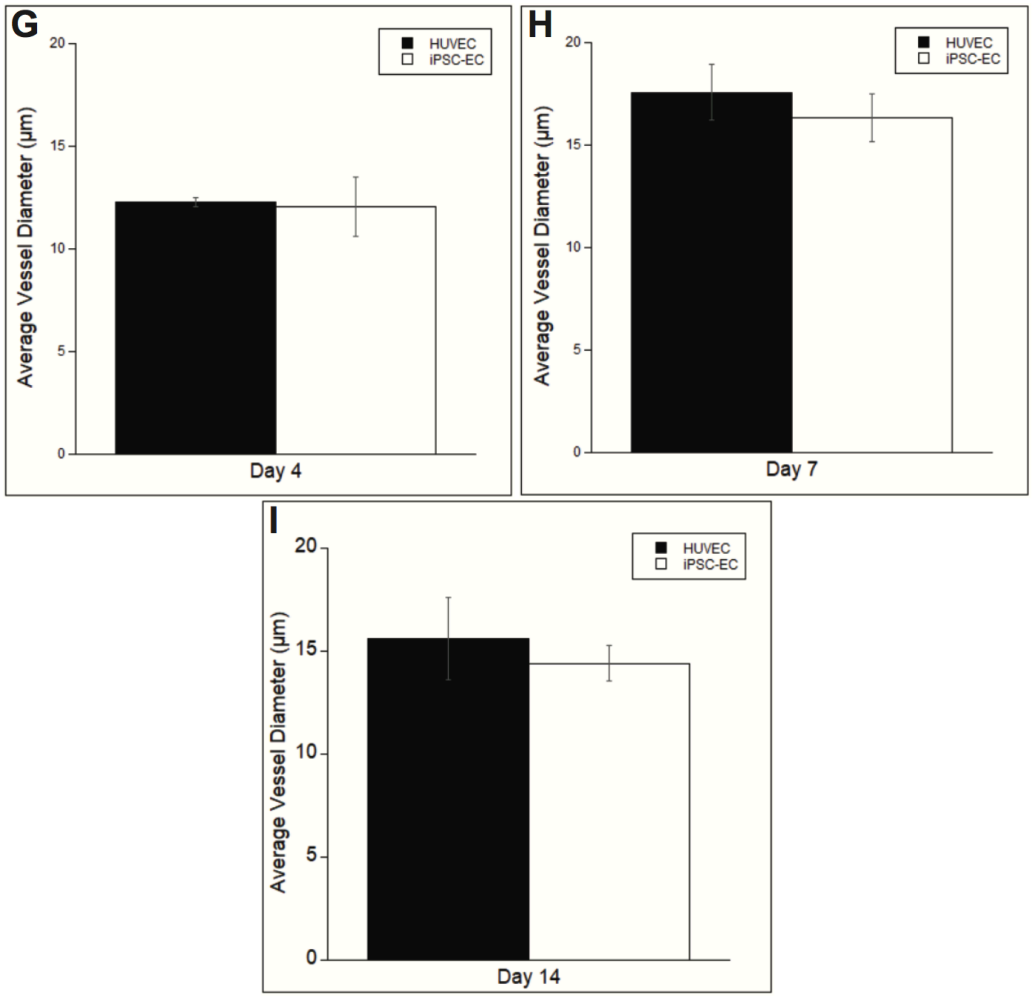


**Figure 5-3.2: Both iPSC-ECs and HUVECs express comparable vessel morphologies with similar vessel diameters *[Quantification]***
Vessel diameters, both with or without erythrocytes, were measured and quantified over a total of 5 random images per selected section across three separate animals. Quantifications were single-blinded and averaged at the given time points **(G-I)**. Error bars indicate ± SEM.

### 5.3.3 iPSC-ECs exhibit deficiencies in vessel lumen formation compared to HUVECs *in vivo*

Our previous study demonstrated that iPSC-ECs are quantitatively deficient in vascular network formation *in vitro* compared to HUVECs [25]. To investigate the extent of network formation *in vivo,* sections from subcutaneous implants were stained with an endothelial cell marker, hCD31, and the number of vessels throughout a given area were quantified. Vessels with clearly identifiable lumens surrounded by a positive hCD31 brown rim were counted. Representative images of average vessel density for both HUVECs and iPSC-ECs at varying time points are shown (Fig. 5-4.1A-F). Quantification of the vessel density (Fig. 5.4.2G-I) revealed significant differences in the average number of vessels per $mm^2$ at day 4 and day 7 ($42.27 \pm 4.82$ μm and $86.43 \pm 21.86$ μm for HUVECs versus $25.48 \pm 4.41$ μm and $35.58 \pm 7.62$ μm for iPSC-ECs on day 4 and day 7 respectively). However, at later time points, i.e. day 14, there were no significant differences between the iPSC-EC and HUVEC implants with a relatively equal average number of vessels per $mm^2$ ($37.61 \pm 13.61$ μm for HUVECs versus $36.46 \pm 3.76$ μm for iPSC-ECs on day 14 respectively). Vessel density peaked for the HUVECs at day 7 and regressed by day 14, while iPSC-EC vessel density increased over time.

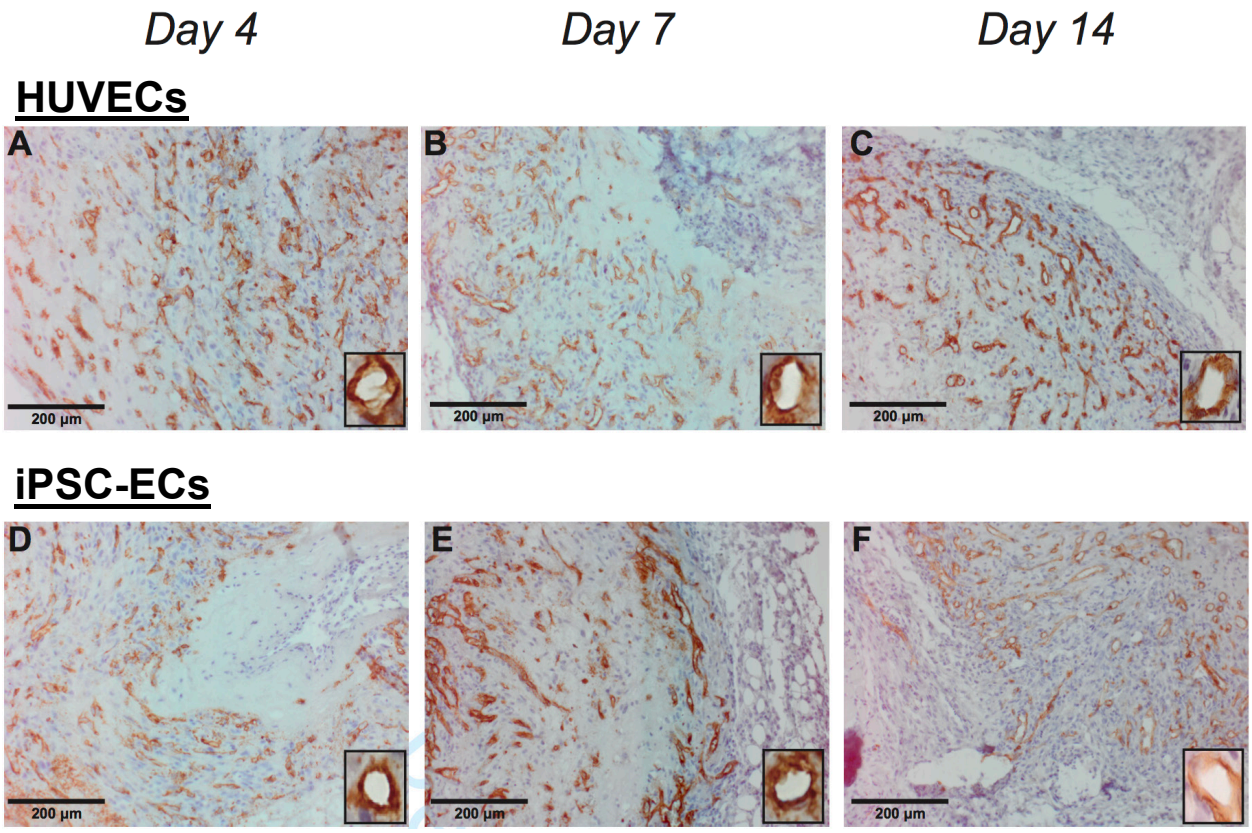


**Figure 5-4.1: iPSC-ECs exhibit deficiencies in vessel lumen formation compared to HUVECs *[Rep. Images]***
Representative images of non-perfused (without erythrocytes) vessel formation from human CD31-stained HUVECs **(A-C)** or iPSC-ECs **(D-F)** in subcutaneous implants at various time points. All images were counterstained with hematoxylin. Implants were harvested at day 4 **(A,D)**, day 7 **(B,E)**, and day 14 **(C,F)**. Insets are images from a 40x objective lens to more clearly show vessel lumens. (*Scale bar = 200 µm).*

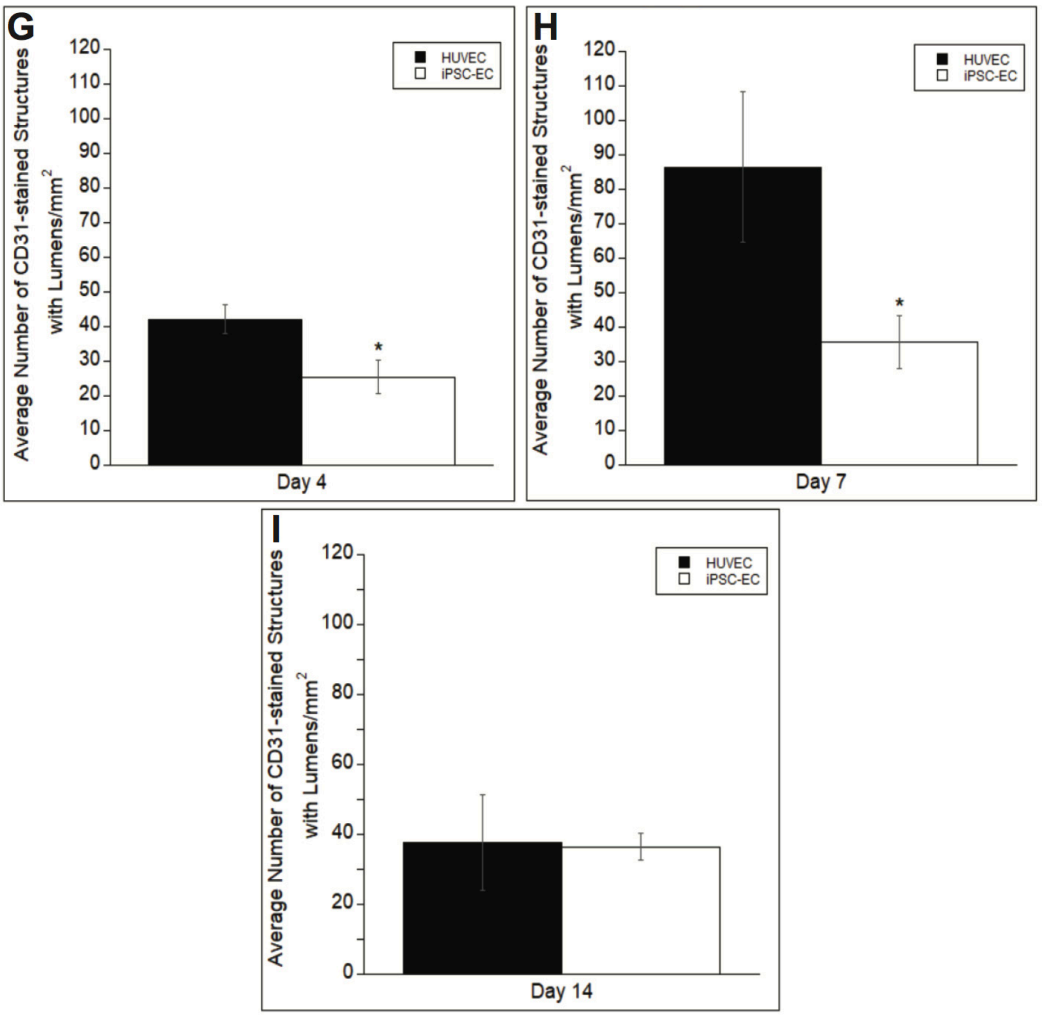


**Figure 5-4.2: iPSC-ECs exhibit deficiencies in vessel lumen formation compared to HUVECs**
A total of 5 random images per selected section across three separate animals were quantified for +hCD31 vessels with lumens. Quantifications were single-blinded, averaged, and normalized to the respective +hCD31 implant area of each EC type at the given time points **(G-I)**. * $p < 0.05$ and comparing the indicated condition to the HUVEC condition. Error bars indicate ± SEM

## 5.3.4 iPSC-ECs vessels exhibit less perfusion compared to HUVECs

Once the baseline density of vessels formed by the implanted cell types was established, potential differences in functionality of these newly formed vessels were examined. To evaluate functional anastomoses with the host vasculature, the numbers of vessel lumens perfused with erythrocytes were quantified. Once again, vessels were quantified only if lumens surrounded by a positive hCD31 brown rim were clearly present and erythrocytes were clearly visible within the

lumen. Representative images of average number of perfused vessels for both HUVECs and iPSC-ECs at varying time points are shown (Fig. 5-5.1A-F). Erythrocytes can clearly be seen in higher magnification inserts. Quantification of these vessels (Fig. 5.5.2G-I) demonstrated no significant differences in the average number of perfused vessels per $mm^2$ at day 4 ($4.54 \pm 1.89$ µm for iPSC-ECs versus $2.39 \pm 2.25$ µm for HUVECs). However, at day 7, iPSC-ECs exhibited a statistical significant reduction in perfused vessel density compared to HUVECs ($22.83 \pm 4.06$ µm versus $72.81 \pm 21.72$ respectively). No significant differences were seen once again by day 14. While iPSC-EC vessel perfusion increased over time, HUVEC vessel perfusion peaked at day 7, but decreased to similar levels as iPSC-ECs by day 14.

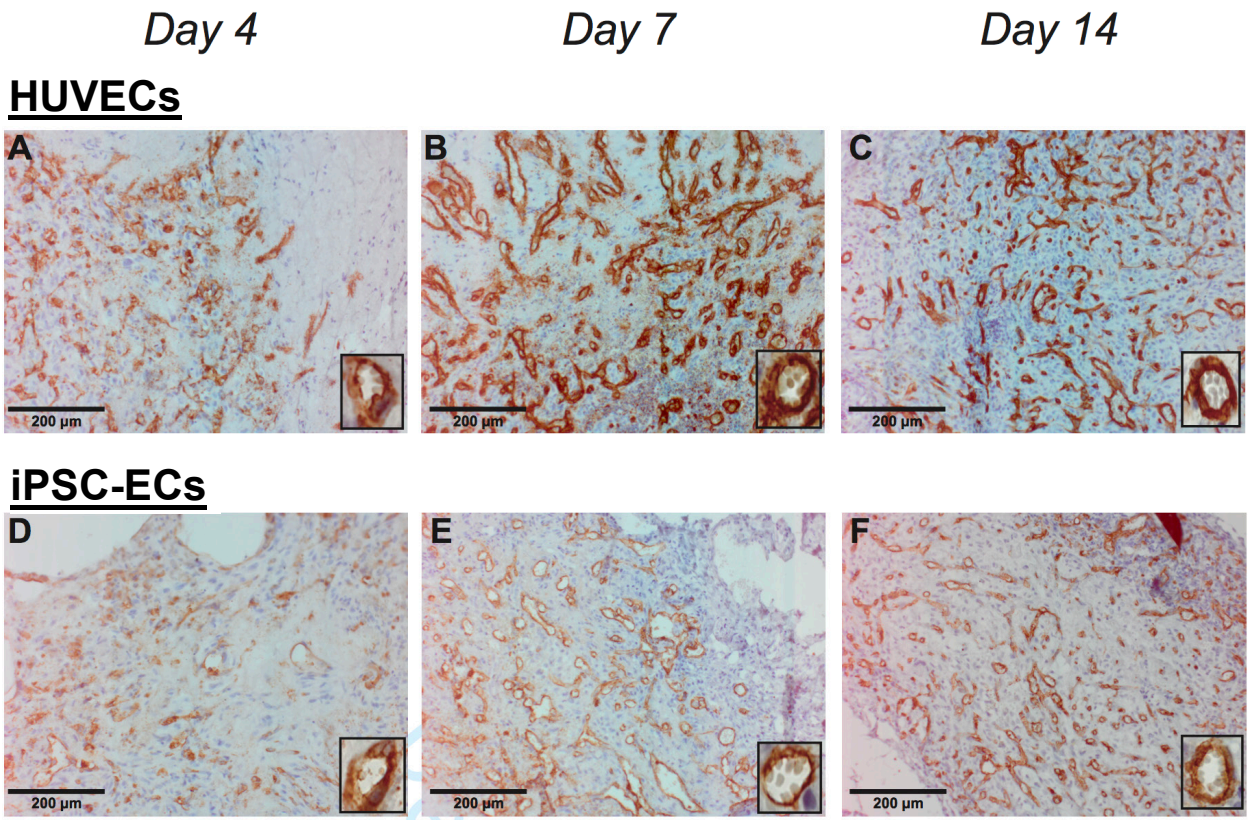


**Figure 5-5.1: iPSC-ECs vessels exhibit less perfusion compared to HUVECs *[Rep. Images]***
Representative images of perfused (with erythrocytes) vessel formation from human CD31-stained HUVECs **(A-C)** or iPSC-ECs **(D-F)** in subcutaneous implants at various time points. All images were counterstained with hematoxylin. Implants were harvested at day 4 **(A,D)**, day 7 **(B,E)**, and day 14 **(C,F)**. Insets are images from a 40x objective lens to more clearly show vessel lumens. (*Scale bar = 200 µm).*

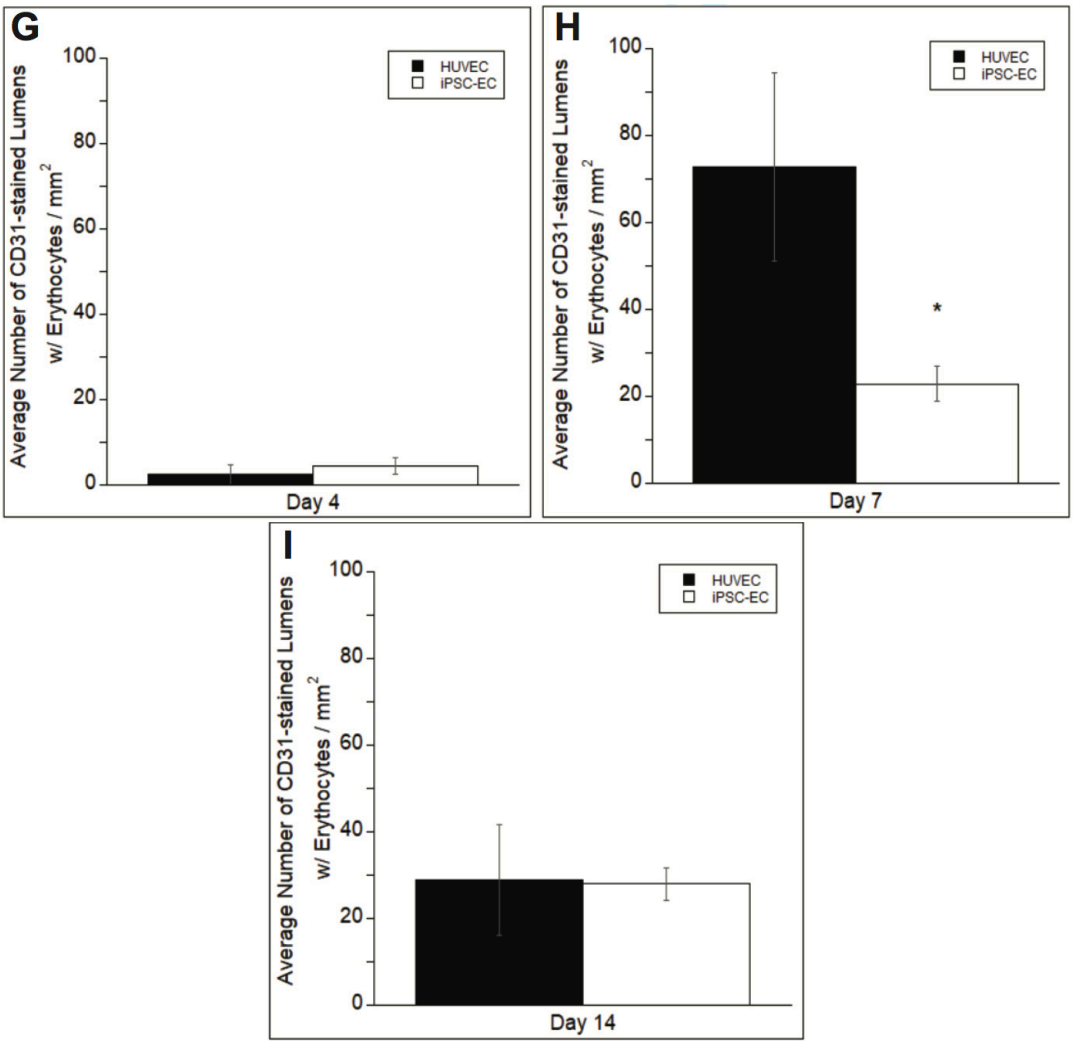


**Figure 5-5.2: iPSC-ECs exhibit deficiencies in vessel lumen formation compared to HUVECs *[Quantification]***
A total of 5 random images per selected section across three separate animals were quantified for +hCD31 vessels with lumens. Quantifications were single-blinded, averaged, and normalized to the respective +hCD31 implant area of each EC type at the given time points **(G-I)**. * $p < 0.05$ and comparing the indicated condition to the HUVEC condition. Error bars indicate ± SEM.

## 5.3.5 iPSC-ECs express differences in αSMA in vivo compared to HUVECs

Despite the iPSC-ECs' ability to form vessel-like structures *in vivo*, the quality of the structures was also examined to determine if they exhibit qualitative characteristics of mature capillaries *in vivo*. To assess vessel development and maturity, sections serial to the positively-stained hCD31 samples in the previous experiments were IHC stained and quantified for various

maturity markers to identify pericytic association of the co-implanted NHLFs and basement membrane deposition by the ECs. Vessels were quantified only if they were previously identified as human origin through hCD31 staining in former tissue section, and erythrocytes were present in the lumen. Representative images reveal the presence of alpha smooth muscle actin, αSMA, across all time points for both iPSC-ECs and HUVECs, suggesting recruitment and a pericyte-like phenotype of the co-implanted NHLFs (Fig. 5-6A-D). Pericytes stabilize nascent endothelium and are characterized by physical association with ECs as well as expression of molecular markers such as αSMA [27]. Quantification of the vessel density indicated significant differences in αSMA at both time points between iPSC-ECs and HUVECs (Fig. 5-6E, F). The number of vessels surrounded by αSMA also increased from day 7 to day 14 for both cell conditions.

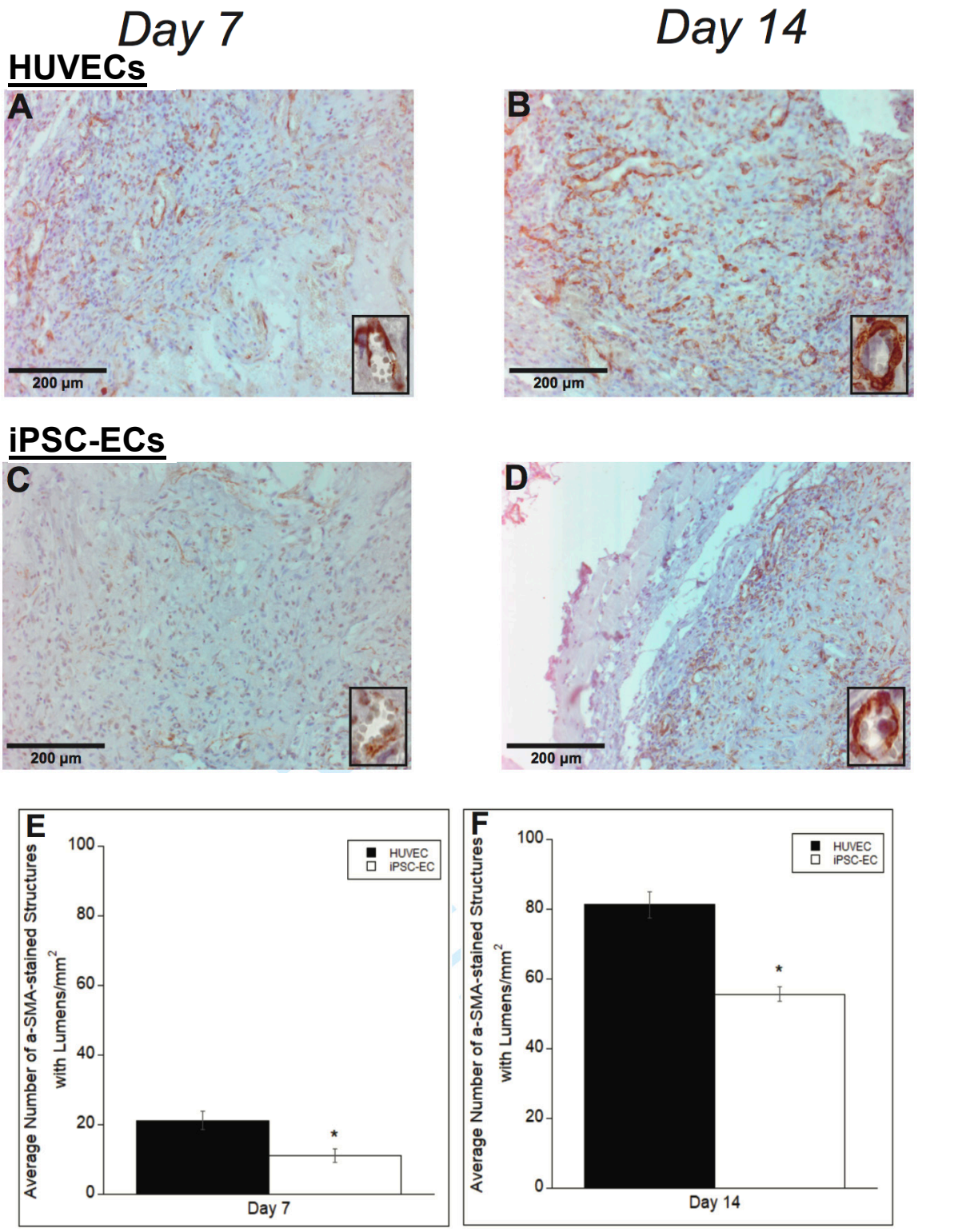


**Figure 5-6: α-SMA staining of iPSC-ECs show differences in vessel maturity compared to HUVECs**
Representative images of αSMA-stained HUVEC **(A,B)** or iPSC-ECs **(C,D)** subcutaneous implants at various time points. All images were counter stained with hematoxylin. Implants were harvested at day 7 **(A,C)** and day 14 **(B,D)**. Insets are images from a 40x objective lens to more clearly show smooth muscle actin surrounding vessel lumens. *Scale bar = 200 µm* Vessel lumens surrounded by αSMA were quantified over a total of 5 random images per selected section across three separate animals. Quantifications were averaged and normalized to the respective + human αSMA implant area of each EC type at the given time points **(E,F)**. * $p < 0.05$ and comparing the indicated condition to the HUVEC condition. Error bars indicate ± SEM.

### 5.3.6 iPSC-ECs express differences in COL-IV in vivo compared to HUVECs

We next characterized basement membrane deposition by immunohistochemical staining for type IV collagen, a prominent component of this specialized form of ECM [28]. Representative images reveal the presence of collagen-IV across all time points for both iPSC-ECs and HUVECs (Fig. 5-7A-D). While there was no significant change in type IV collagen staining between day 7 and day 14 for either iPSC-ECs or HUVECs, type IV collagen levels were decreased by roughly 25% in iPSC-ECs at both day 7 and day 14 (Fig. 5-7E, F). Collectively, this data demonstrates that are iPSC-ECs vessels lack maturity in comparison to HUVECs.

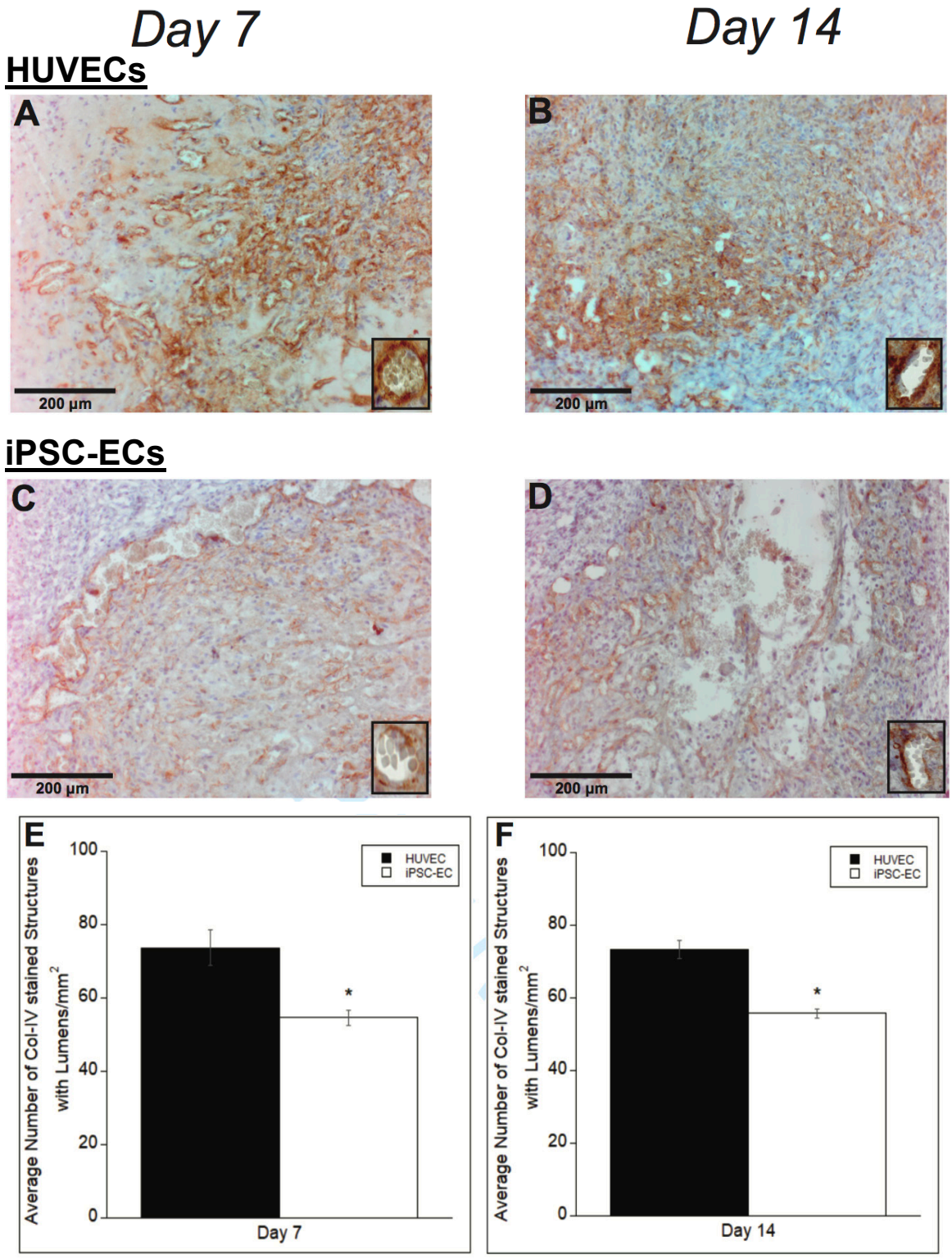


**Figure 5-7: COL-IV staining of iPSC-ECs show differences in vessel maturity compared to HUVECs**
Representative images of COL-IV-stained HUVEC **(A,B)** or iPSC-ECs **(C,D)** subcutaneous implants at various time points. All images were counter stained with hematoxylin. Implants were harvested at day 7 **(A,C)** and day 14 **(B,D)**. Insets images from a 40x objective lens to more clearly show collagen IV surrounding vessel lumens. *Scale bar = 200 µm.* Vessel lumens surrounded by COL-IV were quantified over a total of 5 random images per selected section across three separate animals. Quantifications were averaged and normalized to the respective + human COL-IV implant area of each EC type at the given time points **(E,F)**. * $p < 0.05$ and comparing the indicated condition to the HUVEC condition. Error bars indicate ± SEM.

## 5.4 Discussion

Due to a critical need for a more sustainable and abundant clinically relevant cell source, the vascularization potential of iPSC-ECs is of increasing interest. In previous studies, using a 3D fibrin-based in vitro model, we demonstrated that iPSC-ECs' capillary morphogenesis was significantly attenuated, with reduced MMP-9 expression as one possible candidate for such phenomena [25]. While prior studies have shown that iPSC-ECs are capable of forming vessel-like structures *in vivo* within supporting Matrigel matrices [22], [23], there is little evidence comparing their in vivo potential with more widely utilized EC sources. Therefore, this study explored the ability of iPSC-ECs to create functional vessel-like structures in a fibrin-based subcutaneous implant and compared the quantity and quality of such vessels formed against HUVECs. When co-delivered with stromal fibroblasts (NHLFs), iPSC-ECs formed functional microvessels that inosculated with host vasculature; however, the resultant vasculature was of significantly lower density quantitatively and less mature qualitatively when compared to that formed by HUVECs.

Fibrin was selected as the material for implantation because it is a naturally occurring biopolymer that promotes wound healing and neovascularization [29] and is FDA cleared for some uses in humans [30]. In addition, fibrin was selected for these studies due to its track record of supporting neovascularization *in vivo* [29]–[31] and to match our prior *in vitro* study in which we evaluated the potential of iPSC-ECs relative to HUVECs [25]. NHLFs were chosen due to their ability to aid in the formation of microvascular networks, adopt a mural cell-like localization around the vessel-like structures, and express a subset of pericyte markers as previously reported [26], [32]–[34]. We selected a 1:1 ratio of ECs to stromal cells based on previous studies from our group and others [11], [34], [35]. HUVECs are a robust EC source and were selected for their

proven capability of capillary morphogenesis not only in the model used for this study, but in other *in vivo* models as well [34], [36], [37]. The animal model used here has been widely explored in the literature to approximate wound healing and test the ability of transplanted human cells to form vasculature [11], [38], [39], [40]. This model also avoids potential immunorejection of the human cells injected into SCID mice.

H&E staining of the retrieved implants suggested some similarities, in terms of morphology and phenotype, across the different EC conditions. Both iPSC-ECs and HUVECs formed vessels with similar lumen diameters and shapes across all time points. Capillary diameters are typically around 4 μm [41]. While our results reveal 3-to-4 fold larger lumen diameters, capillary diameters can range much larger depending on the tissue [42]. The larger diameters could also indicate less mature vessel formation. As the neovasculature matures, ECs form tightly regulated junctions to each other [43]. The ECs in our study may not yet have formed these tight boundaries leading to increased extracellular space between each cell and therefore causing the larger than expected diameters. The vessels formed also exhibit a slightly irregular morphology and lacked a definitive circumscribed geometry. Vessel cross-sections typically yield lumens with an orbicular shape [44]. While, once again, this could be indicative of less mature vasculature that has yet to form a more robust geometry, these results are consistent with our previous studies [34]. Vessels formed by both types of ECs contained few, if any, erythrocytes at day 4 within their lumens. Their presence at later time points suggests inosculation with the host vasculature occurred between days 4 and 7. Qualitatively, extravascular erythrocytes decreased by day 14, similar to a previous study [34], suggesting stabilization and maturation of vessels. However, free erythrocytes still remained in the interstitial space of constructs containing iPSC-ECs, further supporting the aforementioned lack of vessel maturity.

Despite morphologic and phenotypic similarities in vessels formed from both EC types, IHC staining for hCD31 demonstrated quantitative differences in the vasculogenic abilities of iPSC-ECs. This may be due to reduced abilities of iPSC-ECs (relative to HUVECs) to proteolytically degrade the fibrin matrix, as they exhibit reduced expression of MMP-9 [25]. However, while vessel density was significantly reduced at day 4 and day 7, there were no significant differences between iPSC-ECs and HUVECs at later time points. Quantification of vessels containing erythrocytes further revealed iPSC-EC vasculature was less perfused. Early time points showed no difference between the two cell conditions, but the relatively low vessel density indicates the neovascualture formed did not sufficiently inosculate with the host's vasculature at this time. The large increase in vessel diameter by day 7 suggests inosculation sometime between day 4 and day 7. We attributed the observed significant differences in vessel density (both total and perfused vessels) to the reduced abilities of iPSC-ECs to undergo capillary morphogenesis. By day 14, densities of perfused vessels in implants containing either HUVECs or iPSC-ECs were similar due to significant reduction in vessel density for the HUVEC group. This regression in the HUVEC group is consistent with a previous study from our group [34]. Vessels undergo selective branch regression and pruning during the normal process of wound healing angiogenesis, changing network architecture over time as tissue metabolic demands change [45]. This could be a result of increased tissue oxygenation by the HUVEC group at earlier time points, causing a down-regulation of VEGF expression, a key signal involved in EC proliferation and invasion during vessel formation, and EC apoptosis in the newly established vessels [46].

In addition to the observed differences in vessel quantity, vessels formed by the iPSC-ECs showed lower levels of COL-IV and αSMA staining, which may be indicative of a reduced

maturity. Collagen-IV is a prominent component of the basement membrane of mature capillaries [28], and thus the presence of this component is indicative of ECs' ability to form mature capillary networks. In addition, smooth muscle α-actin is commonly used as a pericyte marker [27], albeit not a very selective one as it also stains myofibroblasts [47]. Pericytes stabilize nascent vasculature and their presence suggests mature capillary networks [27], [48]. As revealed by positive αSMA staining, the co-implanted NHLFs associated with the vessels formed in a pericyte-like manner. However, whether these NHLFs are capable of becoming bona fide pericytes in either EC condition is difficult to prove given the limited availability of bona fide pericyte markers [49], [50]. Although still significantly different to the HUVECs, iPSC-ECs demonstrated an increase in αSMA presence at day 14, perhaps indicating more recruitment of the NHLFs over time. Collectively, these data suggest iPSC-ECs are capable of recruiting and signaling stromal cells to differentiate into pericytes and depositing the components necessary for a basement membrane *in vivo*, but to a lesser degree than HUVECs.

Despite these differences in comparison to HUVECs, the iPSC-ECs performed better *in vivo* than expected relative to our previous *in vitro* findings [25]. This perhaps suggests the *in vivo* microenvironment is able to induce the iPSC-ECs to attain a more mature phenotype. As the iPSCs from which the iPSC-ECs were differentiated were themselves generated from fibroblasts via an artificial reprogramming process, the iPSC-ECs have never been exposed to physiologic conditions, including blood flow. Shear stresses play a critical role in vascular development and EC phenotype [51], and one avenue for future studies would be to explore the ability to induce maturation of the iPSC-ECs through exposure to fluid flow. Additionally, while this experiment chose to use NHLFs as the stromal cells for co-injection, different stromal cells may better support iPSC-ECs vessel formation. Recent research has demonstrated differences in vascular

morphogenesis of iPSC-ECs *in vitro* when co-cultured with stromal cells of varying identities [52]. Co-injecting different stromal cells may aid in the maturation of the iPSC-ECs and as a result, increase the number of vessels formed. Furthermore, while the subcutaneous implant model used here is relatively simple and effectively demonstrated differences in vessel formation, evaluating iPSC-ECs in more advanced *in vivo* models is critical to aid clinical translation. For example, a window-chamber model has enabled real-time visualization of vessel formation and anastomosis [53] and may be useful to understand the abilities of iPSC-ECs to inosculate with host vessels. Similarly, hind limb ischemia models, where the lack of oxygen and nutrients may be more challenging (or more stimulatory) for vessel formation, have already been used to demonstrate the ability of iPSC-ECs to rescue ischemic tissue in a situation that better replicates the clinical target [24]. Our data here underscore the importance of comparing the efficacy of iPSC-ECs head-to-head with HUVECs (and other sources of ECs) in these more advanced models as well.

## 5.5 Conclusions

In summary, this work assessed whether iPSC-ECs form the same robust, stable microvasculature as previously documented for other sources of EC in a well-characterized 3D fibrin-based co-culture model of vasculogenesis *in vivo*. Both iPSC-ECs and HUVECs formed vessels with similar phenotypes and morphologies and demonstrated some characteristics of vessel maturation. However, the iPSC-ECs expressed significantly reduced vessel density, perfusion, and maturation in comparison to HUVECs. Ultimately, these findings suggest iPSC-ECs must be better understood to enable pre-clinical and clinical translation and achieve their promise and potential for therapeutic revascularization.

## 5.6 References


[1] D. Mozaffarian *et al.*, "Executive Summary: Heart Disease and Stroke Statistics—2015 Update: A Report From the American Heart Association," *Circulation*, vol. 131, no. 4, pp. 434–441, Jan. 2015.

[2] S. Taleb, "Inflammation in atherosclerosis," *Arch. Cardiovasc. Dis.*, vol. 109, no. 12, pp. 708–715, Dec. 2016.

[3] M. G. Davies, "Criticial Limb Ischemia: Epidemiology," *Methodist DeBakey Cardiovasc. J.*, vol. 8, no. 4, pp. 10–14, 2012.

[4] J.-E. Tarride *et al.*, "A review of the cost of cardiovascular disease," *Can. J. Cardiol.*, vol. 25, no. 6, pp. e195-202, Jun. 2009.

[5] V. L. Roger *et al.*, "Heart Disease and Stroke Statistics—2011 Update," *Circulation*, vol. 123, no. 4, pp. e18–e209, Feb. 2011.

[6] R. Y. Kannan, H. J. Salacinski, K. Sales, P. Butler, and A. M. Seifalian, "The roles of tissue engineering and vascularisation in the development of micro-vascular networks: a review," *Biomaterials*, vol. 26, no. 14, pp. 1857–1875, May 2005.

[7] G. D. Yancopoulos, S. Davis, N. W. Gale, J. S. Rudge, S. J. Wiegand, and J. Holash, "Vascular-specific growth factors and blood vessel formation," *Nature*, vol. 407, no. 6801, pp. 242–248, Sep. 2000.

[8] Q. Sun *et al.*, "Sustained release of multiple growth factors from injectable polymeric system as a novel therapeutic approach towards angiogenesis," *Pharm. Res.*, vol. 27, no. 2, pp. 264–271, Feb. 2010.

[9] K. Rubina *et al.*, "Adipose stromal cells stimulate angiogenesis via promoting progenitor cell differentiation, secretion of angiogenic factors, and enhancing vessel maturation," *Tissue Eng. Part A*, vol. 15, no. 8, pp. 2039–2050, Aug. 2009.

[10] H. Zhang *et al.*, "Therapeutic angiogenesis of bone marrow mononuclear cells (MNCs) and peripheral blood MNCs: transplantation for ischemic hindlimb.," *Ann. Vasc. Surg.*, vol. 22, no. 2, pp. 238–247, Mar. 2008.

[11] J. M. Melero-Martin *et al.*, "Engineering robust and functional vascular networks in vivo with human adult and cord blood-derived progenitor cells," *Circ. Res.*, vol. 103, no. 2, pp. 194–202, Jul. 2008.

[12] N. Koike, D. Fukumura, O. Gralla, P. Au, J. S. Schechner, and R. K. Jain, "Tissue engineering: creation of long-lasting blood vessels," *Nature*, vol. 428, no. 6979, pp. 138–139, Mar. 2004.

[13] J. Rouwkema and A. Khademhosseini, “Vascularization and Angiogenesis in Tissue Engineering: Beyond Creating Static Networks,” *Trends Biotechnol.*, vol. 34, no. 9, pp. 733–745, Sep. 2016.

[14] P. Au, J. Tam, D. Fukumura, and R. K. Jain, “Bone marrow-derived mesenchymal stem cells facilitate engineering of long-lasting functional vasculature,” *Blood*, vol. 111, no. 9, pp. 4551–4558, May 2008.

[15] T. Saigawa *et al.*, “Clinical application of bone marrow implantation in patients with arteriosclerosis obliterans, and the association between efficacy and the number of implanted bone marrow cells,” *Circ. J. Off. J. Jpn. Circ. Soc.*, vol. 68, no. 12, pp. 1189–1193, Dec. 2004.

[16] Y. Ikada, “Challenges in tissue engineering,” *J. R. Soc. Interface*, vol. 3, no. 10, pp. 589–601, Oct. 2006.

[17] K. Takahashi and S. Yamanaka, “Induction of pluripotent stem cells from mouse embryonic and adult fibroblast cultures by defined factors,” *Cell*, vol. 126, no. 4, pp. 663–676, Aug. 2006.

[18] J. Yu *et al.*, “Induced pluripotent stem cell lines derived from human somatic cells,” *Science*, vol. 318, no. 5858, pp. 1917–1920, Dec. 2007.

[19] W. T. Wong, N. Sayed, and J. P. Cooke, “Induced pluripotent stem cells: how they will change the practice of cardiovascular medicine,” *Methodist DeBakey Cardiovasc. J.*, vol. 9, no. 4, pp. 206–209, Dec. 2013.

[20] M. C. Yoder, “Differentiation of pluripotent stem cells into endothelial cells,” *Curr. Opin. Hematol.*, vol. 22, no. 3, pp. 252–257, May 2015.

[21] T. Ikuno *et al.*, “Efficient and robust differentiation of endothelial cells from human induced pluripotent stem cells via lineage control with VEGF and cyclic AMP,” *PLOS ONE*, vol. 12, no. 3, p. e0173271, Mar. 2017.

[22] A. Margariti *et al.*, “Direct reprogramming of fibroblasts into endothelial cells capable of angiogenesis and reendothelialization in tissue-engineered vessels,” *Proc. Natl. Acad. Sci. U. S. A.*, vol. 109, no. 34, pp. 13793–13798, Aug. 2012.

[23] W. J. Adams *et al.*, “Functional Vascular Endothelium Derived from Human Induced Pluripotent Stem Cells,” *Stem Cell Rep.*, vol. 1, no. 2, pp. 105–113, Jul. 2013.

[24] A. J. Rufaihah *et al.*, “Human induced pluripotent stem cell-derived endothelial cells exhibit functional heterogeneity,” *Am. J. Transl. Res.*, vol. 5, no. 1, pp. 21–35, Jan. 2013.

[25] J. R. Bezenah, Y. P. Kong, and A. J. Putnam, “Evaluating the potential of endothelial cells derived from human induced pluripotent stem cells to form microvascular networks in 3D cultures,” *Sci. Rep.*, vol. 8, no. 1, p. 2671, Feb. 2018.

[26] C. M. Ghajar, K. S. Blevins, C. C. W. Hughes, S. C. George, and A. J. Putnam, “Mesenchymal stem cells enhance angiogenesis in mechanically viable prevascularized tissues via early matrix metalloproteinase upregulation,” *Tissue Eng.*, vol. 12, no. 10, pp. 2875–2888, Oct. 2006.

[27] O. Skalli *et al.*, “Alpha-smooth muscle actin, a differentiation marker of smooth muscle cells, is present in microfilamentous bundles of pericytes,” *J. Histochem. Cytochem. Off. J. Histochem. Soc.*, vol. 37, no. 3, pp. 315–321, Mar. 1989.

[28] A. C. Y. Li and R. P. H. Thompson, “Basement membrane components,” *J. Clin. Pathol.*, vol. 56, no. 12, pp. 885–887, Dec. 2003.

[29] K. L. Christman, A. J. Vardanian, Q. Fang, R. E. Sievers, H. H. Fok, and R. J. Lee, “Injectable fibrin scaffold improves cell transplant survival, reduces infarct expansion, and induces neovasculature formation in ischemic myocardium,” *J. Am. Coll. Cardiol.*, vol. 44, no. 3, pp. 654–660, Aug. 2004.

[30] J. Ceccarelli and A. J. Putnam, “Sculpting the blank slate: how fibrin’s support of vascularization can inspire biomaterial design,” *Acta Biomater.*, vol. 10, no. 4, pp. 1515–1523, Apr. 2014.

[31] U. Blache and M. Ehrbar, “Inspired by Nature: Hydrogels as Versatile Tools for Vascular Engineering,” *Adv. Wound Care*, vol. 7, no. 7, pp. 232–246, Jul. 2018.

[32] C. M. Ghajar *et al.*, “The Effect of Matrix Density on the Regulation of 3-D Capillary Morphogenesis,” *Biophys. J.*, vol. 94, no. 5, pp. 1930–1941, Mar. 2008.

[33] A. W. Peterson, D. J. Caldwell, A. Y. Rioja, R. R. Rao, A. J. Putnam, and J. P. Stegemann, “Vasculogenesis and Angiogenesis in Modular Collagen-Fibrin Microtissues,” *Biomater. Sci.*, vol. 2, no. 10, pp. 1497–1508, Oct. 2014.

[34] S. J. Grainger, B. Carrion, J. Ceccarelli, and A. J. Putnam, “Stromal cell identity influences the in vivo functionality of engineered capillary networks formed by co-delivery of endothelial cells and stromal cells,” *Tissue Eng. Part A*, vol. 19, no. 9–10, pp. 1209–1222, May 2013.

[35] R. R. Rao, A. W. Peterson, J. Ceccarelli, A. J. Putnam, and J. P. Stegemann, “Matrix Composition Regulates Three-Dimensional Network Formation by Endothelial Cells and Mesenchymal Stem Cells in Collagen/Fibrin Materials,” *Angiogenesis*, vol. 15, no. 2, pp. 253–264, Jun. 2012.

[36] E. Kniazeva, S. Kachgal, and A. J. Putnam, “Effects of extracellular matrix density and mesenchymal stem cells on neovascularization in vivo,” *Tissue Eng. Part A*, vol. 17, no. 7–8, pp. 905–914, Apr. 2011.

[37] D.-Y. Chen *et al.*, “Three-dimensional cell aggregates composed of HUVECs and cbMSCs for therapeutic neovascularization in a mouse model of hindlimb ischemia,” *Biomaterials*, vol. 34, no. 8, pp. 1995–2004, Mar. 2013.

[38] X. Chen, A. S. Aledia, S. A. Popson, L. Him, C. C. W. Hughes, and S. C. George, “Rapid anastomosis of endothelial progenitor cell-derived vessels with host vasculature is promoted by a high density of cotransplanted fibroblasts,” *Tissue Eng. Part A*, vol. 16, no. 2, pp. 585–594, Feb. 2010.

[39] D. O. Traktuev *et al.*, “Robust functional vascular network formation in vivo by cooperation of adipose progenitor and endothelial cells,” *Circ. Res.*, vol. 104, no. 12, pp. 1410–1420, Jun. 2009.

[40] P. Allen, J. Melero-Martin, and J. Bischoff, “Type I collagen, fibrin and PuraMatrix matrices provide permissive environments for human endothelial and mesenchymal progenitor cells to form neovascular networks,” *J. Tissue Eng. Regen. Med.*, vol. 5, no. 4, pp. e74-86, Apr. 2011.

[41] R. F. Potter and A. C. Groom, “Capillary diameter and geometry in cardiac and skeletal muscle studied by means of corrosion casts,” *Microvasc. Res.*, vol. 25, no. 1, pp. 68–84, Jan. 1983.

[42] M. P. Wiedeman, “Dimensions of Blood Vessels from Distributing Artery to Collecting Vein,” *Circ. Res.*, vol. 12, no. 4, pp. 375–378, Apr. 1963.

[43] K. Xu and O. Cleaver, “Tubulogenesis during blood vessel formation.,” *Semin. Cell Dev. Biol.*, vol. 22, no. 9, pp. 993–1004, Dec. 2011.

[44] Y.-R. Gao and P. J. Drew, “Determination of vessel cross-sectional area by thresholding in Radon space,” *J. Cereb. Blood Flow Metab. Off. J. Int. Soc. Cereb. Blood Flow Metab.*, vol. 34, no. 7, pp. 1180–1187, Jul. 2014.

[45] C. Korn and H. G. Augustin, “Mechanisms of Vessel Pruning and Regression,” *Dev. Cell*, vol. 34, no. 1, pp. 5–17, Jul. 2015.

[46] N. Simonavicius *et al.*, “Pericytes promote selective vessel regression to regulate vascular patterning,” *Blood*, vol. 120, no. 7, pp. 1516–1527, Aug. 2012.

[47] B. Hinz, “Formation and function of the myofibroblast during tissue repair,” *J. Invest. Dermatol.*, vol. 127, no. 3, pp. 526–537, Mar. 2007.

[48] C. M. Ghajar *et al.*, “Mesenchymal cells stimulate capillary morphogenesis via distinct proteolytic mechanisms,” *Exp. Cell Res.*, vol. 316, no. 5, pp. 813–825, Mar. 2010.

[49] D. Bexell *et al.*, “Bone Marrow Multipotent Mesenchymal Stroma Cells Act as Pericyte-like Migratory Vehicles in Experimental Gliomas,” *Mol. Ther. J. Am. Soc. Gene Ther.*, vol. 17, no. 1, pp. 183–190, Jan. 2009.

[50] S. Shi and S. Gronthos, “Perivascular Niche of Postnatal Mesenchymal Stem Cells in Human Bone Marrow and Dental Pulp,” *J. Bone Miner. Res.*, vol. 18, no. 4, pp. 696–704.

[51] D. Della-Morte and T. Rundek, “The role of shear stress and arteriogenesis in maintaining vascular homeostasis and preventing cerebral atherosclerosis,” *Brain Circ.*, vol. 1, no. 1, p. 53, Jan. 2015.

[52] O. V. Halaidych *et al.*, “Inflammatory Responses and Barrier Function of Endothelial Cells Derived from Human Induced Pluripotent Stem Cells,” *Stem Cell Rep.*, vol. 10, no. 5, pp. 1642–1656, May 2018.

[53] G. Cheng *et al.*, “Engineered blood vessel networks connect to host vasculature via wrapping-and-tapping anastomosis,” *Blood*, vol. 118, no. 17, pp. 4740–4749, Oct. 2011.

# CHAPTER 6

# Conclusions and Future Directions

## 6.1 Conclusions

The overall goal of this work was to examine an alternative endothelial cell source for potential revascularization therapy in the treatment of ischemic disease, the leading cause of death worldwide with rising rates. Current solutions involving pharmaceutical and surgical interventions are limited and not suitable for every patient, especially those with more serve progression of the disease, such as critical limb ischemia (CLI).

Various tissue engineering therapies have emerged to engineer new vasculature to replace those damaged or diseased within body. Although many different approaches, including growth factor delivery or cell-based therapies, have demonstrated the potential to revascularize tissue both *in vitro* and *in vivo,* there is currently no FDA approved tissue engineering approach for the treatment of ischemic diseases, such as PAD. While cell-based approaches offer additional control over microvessel formation, these methods may be critically limited by potential immunorejection and most importantly, the lack of an abundant cell source.

This dissertation investigated an alternative cell source, endothelial cells derived from induced pluripotent stem cells (iPSC-ECs). Aside from their potentially autologous nature, iPSC-ECs are differentiated from a theoretically unlimited cell source. Prior to this work, studies

demonstrated iPSC-ECs' abilities to form vessel-like networks *in vitro* when seeded on 2D Matrigel and *in vivo* in Matrigel plugs [1], [2]. Despite the iPSC-ECs' abilities to form vessels, there is limited research on iPSC-ECs in more physiologically relevant models, especially in comparison to established EC lineages.

This work began by first characterizing the endothelial nature of iPSC-ECs in 2D (Chapter 2). Both HUVECs and iPSC-ECs were cultured in flasks or plates and their expression of key endothelial cell markers was analyzed via immunofluorescent microscopy and fluorescent activated cell sorting (FACS). This study found no difference between the phenotypic expression of CD31, VE-Cadherin, and vWF. We also demonstrated both ECs have similar proliferation rates on varying substrate stiffnesses. In addition to similar phenotypic characteristics, the gene expression profile assessment identified various expression similarities between iPSC-ECs and HUVECs, including key endothelial cell and pluripotency genes.

Next, this dissertation established iPSC-ECs could form vessel-like structures when coated on microcarrier beads and co-embedded with normal human lung fibroblasts (NHLFs) in a fibrin matrix (Chapter 3). However, this study found iPSC-ECs produced quantitatively lower total networks lengths in comparison to HUVECs after 14 days of culture [3]. While the sources of cells, lots of cells, media formulations, and assay format were varied, iPSC-EC capillary morphogenesis was attenuated in each condition in comparison to HUVECs. We also investigated the maturity of the vessel-like structures formed, showing similar levels of basement membrane deposition, hollow lumen formation, and pericyte association.

To provide a possible explanation for the iPSC-EC attenuation, we characterized the mechanisms iPSC-ECs use to remodel the fibrin-based ECM during capillary morphogenesis in our experimental model systems (Chapter 4). EC-coated microcarrier beads were first embedded

in fibrin gels of increasing concentrations to mechanically inhibit sprouting. The iPSC-ECs were functionally similar to HUVECs, with elevated fibrin concentrations inhibiting sprouting of both EC types and distributing stromal cells through the entire 3D matrix largely abrogating this effect [3]. Chemical inhibition of both MMPs and serine-proteases revealed complete inhibition of sprouting morphogenesis occurring only under dual inhibition, demonstrating iPSC-ECs' proteolytic plasticity in fibrin as seen similarly with prior studies on HUVECs [4].

In addition to these inhibition studies, we characterized the iPSC-ECs' expression of key matrix metalloproteases implicated in capillary morphogenesis (Chapter 4) [5], [6]. Both RNA and protein were harvested from microcarrier beads coated with iPSC-ECs and embedded with NHLFs in fibrin at varying time points. Quantitative PCR demonstrated a significant over expression at day 4 and significant under expression at day 14 of MMP-9 in comparison to HUVECs. Western blot analysis further identified differences in MMP-9 expression at day 7 and day 14. Last, gel zymography analysis revealed significant differences in activity levels of MMP-9 on day 14. By contract. no differences in the expression levels and/or activity of MMP-2 and MT1-MMP were seen throughout all experiments.

Last, we established the *in vivo* vasculogenic potential of iPSC-ECs and determined the sprouting attenuation is not only an *in vtiro* phenomena (See Chapter 5). A subcutaneous model was used where ECs and NHLFs were embedded in fibrin and injected into the dorsal flank of SCID mice. iPSC-ECs demonstrated successful vessel formation, inosculation with the host vasculature, and morphologies comparable to HUVECs. However, the vessel density was significantly reduced at early time points compared to HUVECs. Additionally, the iPSC-EC vasculature was less perfused at day 7. Vessel maturity was also assessed through the deposition of a component in the basement membrane and pericyte association. Despite similar levels of

vessel density and perfusion between the two EC conditions at day 14, immunohistochemical staining revealed reduced expression of COL-IV and α -SMA for microvasculature derived from iPSC-ECs, demonstrating *in vivo* differences in vessel maturity compared to HUVECs.

While iPSC-ECs generated microvasculature with some characteristics of mature capillaries, the vessel networks formed by HUVECs were quantitatively superior both *in vitro* and *in vivo* to the iPSC-ECs, as well as MVECs. Although the focus of this research was to assess iPSC-ECs, an underlying outcome of this work is the HUVECs' vasculogenic potential. Despite critiques that HUVECs are not suitable to form microvascular networks due to their origin from a large vein, the data presented here argues HUVECs are able to form vessels comparable to microvasculature and at a greater extent than other ECs, demonstrating their potential for clinical translation. However, additional research is necessary as HUVEC delivery will likely be allogeneic and the EC phenotype of HUVECs may not be relevant for the target tissue [7].

Collectively, this dissertation assessed the potential of iPSC-ECs to from microvascular networks in comparison to an established EC, HUVECs. Despite all deficiencies of capillary morphogenesis compared to HUVECs in a fibrin based *in vitro* model co-cultured with NHLFs, iPSC-ECs performed to a much higher degree than expected in a clinically relevant subcutaneous *in vivo* model and were capable of vasculature formation, perfusion, and vessel maturation. This work also established potential mechanisms for iPSC-EC capillary morphogenesis. While other ECs, such as HUVECs, are quantitatively better for revascularization, the work presented here, along with the autologous and unlimited sourcing potential, argues for continued research in the clinical translation of iPSC-ECs. Future studies, discussed in the next section, need to further investigate iPSC-EC vasculature differences and new approaches to create quantitatively and

qualitatively comparable iPSC-EC vessel networks prior to the successful translation and treatment of PAD with iPSC-ECs.

## 6.2 Future Directions/Work

The data present in this work open several avenues for iPSC-EC revascularization research. There are numerous *in vitro* and *in vivo* experiments described below to provide additional understanding of iPSC-ECs, to enhance iPSC-EC vasculature formation, and to further demonstrate iPSC-ECs' therapeutic potential.

### 6.2.1 Main Focus

The primary focus of future research, discussed in more detail in the following subsections, should prioritize understanding the iPSC-ECs and enhancing their vasculogenic potential as demonstration of extensive, robust network formation is necessary prior to clinical translation. Specifically, this work demonstrated MMP differences along with other genetic expression differences in the iPSC-ECs, resulting in possible avenues to explore as an approach to strengthen the iPSC-ECs. Additionally, iPSC-ECs vessel formation *in vivo* was higher than expected possibly due to the exposure of physiological relevant conditions, suggesting prior *in vitro* shear stimulation could lead to iPSC-ECs' maturation.

Other MMP Expression, MMP Knockdown, and MMP Overexpression

MMPs are critical for ECs to remodel the ECM during angiogenesis. The expression of various MMP, specifically MMP-2, MMP-9 and MT1-MMP, were investigated during this work, concluding differences in MMP-9 expression as one possible explanation for iPSC-EC attenuation.

One caveat to these experiments is NHLFs were co-cultured with the iPSC-ECs to induce angiogenic sprouting. As a result, the MMP-9 expression differences are not solely from the iPSC-ECs, but a combination from both populations of cells. This expression is further complicated as ECs and stromal cells signal each other during angiogenesis, regulating the expression of angiogenic genes, including MMPs [8]. Methods described in Kachgal et al. can be employed to knockdown the expression of MMP-2, -9, and MT1-MMP in a cell-type selective manner [6]. In addition to eliminating any stromal cell MMP contribution while still providing instructive cues to the ECs, knockdown of iPSC-ECs' MMPs can be explored to further establish the role of specific MMPs in iPSC-EC capillary morphogenesis. On the other hand, these genes could also be overexpressed. Using a similar approach, MMPs, specifically MMP-9, can be overexpressed in iPSC-ECs to possibly rescue the iPSC-ECs sprouting deficiencies. Not only could this method enhance the vasculogenic potential of iPSC-ECs but formalize or overturn the conclusions that lower MMP-9 expression may be responsible for the attenuated angiogenesis properties of stem-cell derived ECs.

Finally, while these three MMPs were selected based on prior research implicating their importance in angiogenesis [6], the expression of other MMPs could also be investigated using similar methods described in Chapter 4. The gene expression profiles show no differences between HUVECs and iPSC-ECs for various MMPs (Fig. 6-1). However, the RNA was harvested from a monolayer of cells cultured in 2D. Despite these similarities, MMP expression will differ when cultured in 3D when the ECs are actively undergoing angiogenesis.

| Symbol | ID | LogFC | p-value |
|---|---|---|---|
| MMP | | | |
| MMP1 | 4312 | -0.166 | 1.000 |
| MMP2 | 4313 | -0.407 | 1.000 |
| MMP9 | 4318 | 0.811 | 1.000 |
| MMP10 | 4319 | 0.820 | 1.000 |
| MMP11 | 4320 | 0.014 | 1.000 |
| MMP14 | 4323 | 0.336 | 1.000 |
| MMP15 | 4324 | 0.559 | 1.000 |
| MMP17 | 4326 | -0.500 | 1.000 |
| MMP19 | 4327 | 0.638 | 1.000 |
| MMP25-AS1 | 100507419 | 0.471 | 1.000 |

**Figure 6-1: Expression fold change between 2D cultures of HUVECs and iPSC-ECs for various MMPs**

Gene Expression Studies

Angiogenesis is a highly regulated process depending on growth factors, proteases, integrins, cell adhesion receptors, and many other components [8], [9]. This work investigated the role of MMPs in iPSC-EC mechanisms to potentially explain the sprouting attenuation. However, there are a multitude of other cellular components that promote or inhibit angiogenesis which could explain the attenuated response of iPSC-ECs as well. The gene expression profile results indicated there are over 800 genes that display a 2-fold or greater difference in expression, between HUVECs and iPSC-ECs. These results are based on 2D cultures and expression profiles can change when cultured in 3D [10]. This experiment provides multiple avenues to further investigate differences between iPSC-ECs and other ECs lineages.

One possible avenue is to investigate tissue inhibitor of metalloproteinases 3 (TIMP-3) differences. TIMPs are a family of proteins that act as natural inhibitors to MMPs [11]. TIMP-3 is unique from other TIMPs as it is not freely diffusible; it blocks the binding of VEGF to its receptor VEGF2. In addition to inhibiting MMPs, it also acts on another class of metalloproteinases, the a disintegrin and metalloproteinase domain (ADAM) family [37], [38]. The gene expression profile analysis revealed a 16-fold overexpression of TIMP-3 in iPSC-ECs over HUVECs. Increased TIMP-3 expression could explain the sprouting attenuations as the MMPs are readily inhibited and unable to remodel the ECM for capillary morphogenesis. Experiments can be conducted to assess TIMP-3 RNA and protein level expression in the 3D fibrin assay.

Another area to explore is differences in interleukin 6 (IL-6). IL-6 is a part of a family of cytokines involved in inflammatory response [14]. While IL-6 is typically secreted by T cells and macrophages to stimulate immune response during infection and after trauma, IL-6 is also implicated in stimulating angiogenesis [15]–[18]. Specifically, IL-6 upregulates the expression of various MMPs, including MMP-9 [19]. The gene expression profile analysis revealed a 4-fold lower expression of IL-6 in iPSC-ECs over HUVECs. Lower IL-6 expression levels could indirectly affect MMP-9 expression explaining the differences seen in this work. As with TIMP-3, experiments can be conducted to assess IL-6 RNA and protein level expression in the 3D fibrin assay.

Mechanical Shear Stress

Shear stress plays a critical role in vascular development and EC phenotype. Shear stress, caused by blood flow, activates integrins on the endothelial cell's surface to upregulate eNOS activity through the PECAM-1 complex [20]. eNOS is responsible for NO generation which

regulates EC tone and proliferation as well as platelet aggregation [21]. While the HUVECs have been exposed to blood flow, the iPSC-ECs have never been exposed to any physiological conditions, including blood flow. Given the role of shear stresses on vascular development, the iPSC-ECs may represent an immature EC phenotype, which in turn could explain the sprouting attenuation seen in this work. A simple parallel plate flow chamber can be employed to expose the iPSC-ECs to flow. The capillary morphogenesis of flow-exposed iPSC-ECs can then be compared to unexposed iPSC-ECs and HUVECs in the angiogenic bead assay. Research has shown differences in the expression of various arterial and venous markers of iPSC-ECs exposed to flow [2], [22]–[24].

Stromal Cell Identity

Stromal cells play a key role in vasculature development and help stabilize new vessels [9]. NHLFs were cultured with the ECs in all experiments to promote the formation of a stable, mature vasculature. However, research has demonstrated stromal cell identity can influence capillary morphogenesis as HUVEC-NHLF co-cultures, in particular, produce large networks of leaky vasculature while HUVEC-BMSC (bone marrow mesenchymal stem cells) co-cultures produce less extensive networks with more mature vasculature [25], [26]. Similarly, one study with iPSC-ECs-BMSC co-cultures showed poor sprouting compared to HUVECs both *in vitro* and *in vivo* [27]. This study showed the ratio of ECs to stromal cells may affect efficient vascularization, which could imply the attenuation differences in iPSC-ECs sprouting is due to a less suitable ratio of ECs to stromal cells. Different types of stromal cells, such as normal human dermal fibroblasts (NHDFs), adipose derived stem cells (AdSC), and bone marrow stromal cells (BMSCs), can be cultured with the iPSC-ECs to assess their effect on vasculature formation, both quantitatively and

qualitatively. These studies could determine the appropriate stromal cell type and concentration to produce comparable levels of capillary morphogenesis to HUVECs.

### 6.2.2 Auxiliary Focus

The secondary focus of any future studies, discussed in the following subsections, should continue the evaluation of iPSC-ECs' vasculogenic potential. While this work established the iPSC-ECs' ability to form microvascular networks, our comparisons were largely limited to only one other EC source, suggesting an assessment to other ECs to formalize our conclusions about iPSC-ECs' sprouting attenuation. In addition, other iPSC-ECs source should be examined, including an in-house reprogrammed and differentiated iPSC-EC source, as only one iPSC-EC source was largely tested during this work. Lastly, additional characterization of the iPSC-ECs' ability to regulate permeability and form vasculature in ischemic regions would further establish their potential for clinical translation.

Additional EC Sources

HUVECs were used as the main EC source for comparison during this work due to their proven ability to form robust microvasculature networks. While HMVECs were also compared against iPSC-ECs in the angiogenic assay, all other studies were only compared against HUVECs. Although many differences were established between HUVECs and iPSC-ECs, these differences may not be present when compared to other ECs, i.e. iPSC-ECs may be more similar to other ECs lines. As seen with this study, HMVECs and iPSC-ECs exhibited similar levels of capillary morphogenesis. Additional studies should characterize the iPSC-ECs vessel formation, genetic expression profile, mechanisms, and protease expression against many types of ECs. Not only can

different sources of ECs help to more thoroughly compare and contrast the vasculogenic potential of iPSC-ECs but expanding further to other sources may also provide additional mechanistic insights to explain the observed attenuation in vascular morphogenesis of iPSC-ECs compared to HUVECs.

Additional iPSC-ECs Sources

Similar to the limitations of using only HUVECs, limited iPSC-ECs sources were tested throughout the course of this work. While two different sources of iPSC-ECs were investigated, only one source was capable of undergoing capillary morphogenesis. Although the data demonstrate a reduced vasculogenic potential of iPSC-ECs to HUVECs, there is a possibility the source of iPSC-ECs could be the cause of the sprouting attenuation. An experimental study using many sources of iPSC-ECs capable of sprouting in both the vasculogenic and angiogenic assay can be utilized to determine whether the capillary morphogenesis attenuation affects the whole lineage or specific sources. In addition, genetic expression profiles of the various iPSC-EC sources would aid not only in characterizing similarities and differences between the iPSC-ECs, but aid in characterization of other ECs as well.

Reprograming and Differentiation of iPSC-ECs

One possibility to generate an additional iPSC-EC source is through in-house reprograming and differentiation. Research has demonstrated the ability to successfully reprogram fibroblasts into iPSCs and then differentiate the iPSCs to an EC lineage [1], [28]–[30]. Currently, there is no standardization for iPSC generation or differentiation into ECs. While most protocols use the OSKM genes for reprogramming and a VEGF-based media for differentiation, variations in the

methods could lead to varying clinical results. For the successful translation of iPSC-ECs, a consistent, robust differentiation approach is necessary to ensure efficacy. Preliminary studies for iPSC-EC generation can be found in Appendix A. Briefly, mouse embryonic fibroblasts were reprogrammed into a pluripotent state using lentiviruses, and then an attempt to differentiate these cells was conducted using EGM-2 media. IF staining for CD31 revealed little to no expression, indicating unsuccessful reprograming. Additional studies should follow the protocols established in the literature to successfully create an in-house source of iPSC-ECs from human fibroblasts. Not only would this provide an additional source of iPSC-ECs for comparison in all future vasculogenic experiments, but further the clinical translation of our work through establishing an approach to make autologous iPSC-ECs. The main source of iPSC-ECs used in our experiments is allogeneic, therefore, limiting the success for FDA approval and acceptance by the patient's immune system.

Perfusion and Permeability

The ultimate goal of this work is to create functional vasculature capable of supplying oxygen and nutrients to ischemic regions. As vessels mature through pericyte stabilization, basement membrane formation, and tight junction regulation, blood can be successfully perfused to the target tissue. While evidence of vessel maturity was present both *in vitro* and *in vivo*, the vessels may still be immature, resulting in leakiness and the inability to regulate permeability. To further assess the ability of IPSC-ECs to form stable capillaries *in vitro*, the functional properties of these engineered vessel structures can be quantified using an inverse permeability assay developed previously by Grainger et al [25]. The rationale behind this experiment is immature capillaries are unable to regulate permeability due to incomplete cell junctions [31]. Previous

research showed HUVEC-NHLFs co-cultures resulted in leaky vasculature in comparison to other stromal cells [25], demonstrating the need to assess permeability with a variety of stromal cells. Additionally, tail vein injections can be employed in the subcutaneous mouse model to assess *in vivo* permeability and inosculation. Not only could a dextran tracer determine vessel maturity at varying time points but also determine exactly when the neovasculature inosculates with the host's vasculature, providing a timeframe for restored perfusion.

Advanced Animal Models

Since the iPSC-ECs are capable of vasculature formation *in vivo,* it is important to study more advanced *in vivo* models to aid in clinical translation. The model used in this work used young healthy mice and healthy tissue to assess vasculature formation, which does not appropriately replicate the clinical conditions of a diseased patient. Research has demonstrated young, healthy animals recover from ischemia easier than animals that more closely match the patient demographic [32], [33]. Non-obese diabetic (NOD)-SCID mice have been extensively studied for diabetes and CVD research and could be used as a more appropriate mouse model to better replicate the intended patients.

A hind-limb ischemia model can also be employed to evaluate iPSC-EC vasculature formation in an ischemic region and determine whether iPSC-ECs can re-vascularize and stabilize the network in a similar time frame to HUVECs. An adaptation of the murine model of hind-limb ischemia described by Niiyama et al. 2009 can be used to assess blood flow restoration in SCID mice first and then (NOD)-SCID mice [34]. In brief, this model consists of surgically ligating one of the mouse's femoral arteries. ECs and stromal cells would be embedded in a fibrin matrix and injected into the ligated region of the mouse to revascularize the region and restore blood perfusion

to the limb. Laser Doppler perfusion imaging (LDPI) can be used to measure blood vessel perfusion during the study.

## 6.3 References


[1] A. Margariti *et al.*, "Direct reprogramming of fibroblasts into endothelial cells capable of angiogenesis and reendothelialization in tissue-engineered vessels," *Proc. Natl. Acad. Sci. U. S. A.*, vol. 109, no. 34, pp. 13793–13798, Aug. 2012.

[2] W. J. Adams *et al.*, "Functional Vascular Endothelium Derived from Human Induced Pluripotent Stem Cells," *Stem Cell Rep.*, vol. 1, no. 2, pp. 105–113, Jul. 2013.

[3] J. R. Bezenah, Y. P. Kong, and A. J. Putnam, "Evaluating the potential of endothelial cells derived from human induced pluripotent stem cells to form microvascular networks in 3D cultures," *Sci. Rep.*, vol. 8, no. 1, p. 2671, Feb. 2018.

[4] C. M. Ghajar *et al.*, "The Effect of Matrix Density on the Regulation of 3-D Capillary Morphogenesis," *Biophys. J.*, vol. 94, no. 5, pp. 1930–1941, Mar. 2008.

[5] C. M. Ghajar, K. S. Blevins, C. C. W. Hughes, S. C. George, and A. J. Putnam, "Mesenchymal stem cells enhance angiogenesis in mechanically viable prevascularized tissues via early matrix metalloproteinase upregulation," *Tissue Eng.*, vol. 12, no. 10, pp. 2875–2888, Oct. 2006.

[6] S. Kachgal, B. Carrion, I. A. Janson, and A. J. Putnam, "Bone marrow stromal cells stimulate an angiogenic program that requires endothelial MT1-MMP," *J. Cell. Physiol.*, vol. 227, no. 11, pp. 3546–3555, Nov. 2012.

[7] W. C. Aird, "Endothelial Cell Heterogeneity," *Cold Spring Harb. Perspect. Med.*, vol. 2, no. 1, Jan. 2012.

[8] Z. Ahmed and R. Bicknell, "Angiogenic signalling pathways," *Methods Mol. Biol. Clifton NJ*, vol. 467, pp. 3–24, 2009.

[9] T. H. Adair and J.-P. Montani, *Overview of Angiogenesis*. Morgan & Claypool Life Sciences, 2010.

[10] K. Duval *et al.*, "Modeling Physiological Events in 2D vs. 3D Cell Culture," *Physiology*, vol. 32, no. 4, pp. 266–277, Jul. 2017.

[11] R. Chirco, X.-W. Liu, K.-K. Jung, and H.-R. C. Kim, "Novel functions of TIMPs in cell signaling," *Cancer Metastasis Rev.*, vol. 25, no. 1, pp. 99–113, Mar. 2006.

[12] J. H. Qi *et al.*, "A novel function for tissue inhibitor of metalloproteinases-3 (TIMP3): inhibition of angiogenesis by blockage of VEGF binding to VEGF receptor-2," *Nat. Med.*, vol. 9, no. 4, pp. 407–415, Apr. 2003.

[13] W. H. Yu, S. Yu, Q. Meng, K. Brew, and J. F. Woessner, "TIMP-3 binds to sulfated glycosaminoglycans of the extracellular matrix," *J. Biol. Chem.*, vol. 275, no. 40, pp. 31226–31232, Oct. 2000.

[14] M. Akdis *et al.*, "Interleukins, from 1 to 37, and interferon-γ: receptors, functions, and roles in diseases," *J. Allergy Clin. Immunol.*, vol. 127, no. 3, pp. 701-721.e1–70, Mar. 2011.

[15] T. Tanaka, M. Narazaki, and T. Kishimoto, "IL-6 in Inflammation, Immunity, and Disease," *Cold Spring Harb. Perspect. Biol.*, vol. 6, no. 10, Oct. 2014.

[16] G. Gopinathan *et al.*, "Interleukin-6 Stimulates Defective Angiogenesis," *Cancer Res.*, vol. 75, no. 15, pp. 3098–3107, Aug. 2015.

[17] T. Cohen, D. Nahari, L. W. Cerem, G. Neufeld, and B.-Z. Levi, "Interleukin 6 Induces the Expression of Vascular Endothelial Growth Factor," *J. Biol. Chem.*, vol. 271, no. 2, pp. 736–741, Jan. 1996.

[18] R. Catar *et al.*, "IL-6 Trans–Signaling Links Inflammation with Angiogenesis in the Peritoneal Membrane," *J. Am. Soc. Nephrol.*, p. ASN.2015101169, Nov. 2016.

[19] J. S. Yao, W. Zhai, W. L. Young, and G.-Y. Yang, "Interleukin-6 triggers human cerebral endothelial cells proliferation and migration: the role for KDR and MMP-9," *Biochem. Biophys. Res. Commun.*, vol. 342, no. 4, pp. 1396–1404, Apr. 2006.

[20] D. Lu and G. S. Kassab, "Role of shear stress and stretch in vascular mechanobiology," *J. R. Soc. Interface*, vol. 8, no. 63, pp. 1379–1385, Oct. 2011.

[21] U. Förstermann and T. Münzel, "Endothelial nitric oxide synthase in vascular disease: from marvel to menace," *Circulation*, vol. 113, no. 13, pp. 1708–1714, Apr. 2006.

[22] R. Ohtani-Kaneko, K. Sato, A. Tsutiya, Y. Nakagawa, K. Hashizume, and H. Tazawa, "Characterisation of human induced pluripotent stem cell-derived endothelial cells under shear stress using an easy-to-use microfluidic cell culture system," *Biomed. Microdevices*, vol. 19, no. 4, p. 91, Dec. 2017.

[23] A. Sivarapatna, M. Ghaedi, A. V. Le, J. J. Mendez, Y. Qyang, and L. E. Niklason, "Arterial specification of endothelial cells derived from human induced pluripotent stem cells in a biomimetic flow bioreactor," *Biomaterials*, vol. 53, pp. 621–633, Jun. 2015.

[24] J. G. DeStefano, Z. S. Xu, A. J. Williams, N. Yimam, and P. C. Searson, "Effect of shear stress on iPSC-derived human brain microvascular endothelial cells (dhBMECs)," *Fluids Barriers CNS*, vol. 14, Aug. 2017.

[25] S. J. Grainger and A. J. Putnam, “Assessing the permeability of engineered capillary networks in a 3D culture,” *PloS One*, vol. 6, no. 7, p. e22086, 2011.

[26] S. J. Grainger, B. Carrion, J. Ceccarelli, and A. J. Putnam, “Stromal cell identity influences the in vivo functionality of engineered capillary networks formed by co-delivery of endothelial cells and stromal cells,” *Tissue Eng. Part A*, vol. 19, no. 9–10, pp. 1209–1222, May 2013.

[27] O. V. Halaidych *et al.*, “Inflammatory Responses and Barrier Function of Endothelial Cells Derived from Human Induced Pluripotent Stem Cells,” *Stem Cell Rep.*, vol. 10, no. 5, pp. 1642–1656, May 2018.

[28] T. Ikuno *et al.*, “Efficient and robust differentiation of endothelial cells from human induced pluripotent stem cells via lineage control with VEGF and cyclic AMP,” *PLOS ONE*, vol. 12, no. 3, p. e0173271, Mar. 2017.

[29] Y. Lin, C.-H. Gil, and M. C. Yoder, “Differentiation, Evaluation, and Application of Human Induced Pluripotent Stem Cell–Derived Endothelial Cells,” *Arterioscler. Thromb. Vasc. Biol.*, vol. 37, no. 11, pp. 2014–2025, Nov. 2017.

[30] X. Liu, J. Qi, X. Xu, M. Zeisberg, K. Guan, and E. M. Zeisberg, “Differentiation of functional endothelial cells from human induced pluripotent stem cells: A novel, highly efficient and cost effective method,” *Differentiation*, vol. 92, no. 4, pp. 225–236, Oct. 2016.

[31] K. M. Chrobak, D. R. Potter, and J. Tien, “Formation of perfused, functional microvascular tubes in vitro,” *Microvasc. Res.*, vol. 71, no. 3, pp. 185–196, May 2006.

[32] S. Lotfi, A. S. Patel, K. Mattock, S. Egginton, A. Smith, and B. Modarai, “Towards a more relevant hind limb model of muscle ischaemia,” *Atherosclerosis*, vol. 227, no. 1, pp. 1–8, Mar. 2013.

[33] P. Madeddu *et al.*, “Murine models of myocardial and limb ischemia: diagnostic end-points and relevance to clinical problems.,” *Vascul. Pharmacol.*, vol. 45, no. 5, pp. 281–301, Nov. 2006.

[34] H. Niiyama, N. F. Huang, M. D. Rollins, and J. P. Cooke, “Murine model of hindlimb ischemia,” *J. Vis. Exp. JoVE*, no. 23, Jan. 2009.

# Appendix A – Videos of Vessel Hollow Lumens

NOTE: Videos will play in electronic format via Adobe Acrobat with Flash. Videos are also available upon request from the author.

## HUVECs

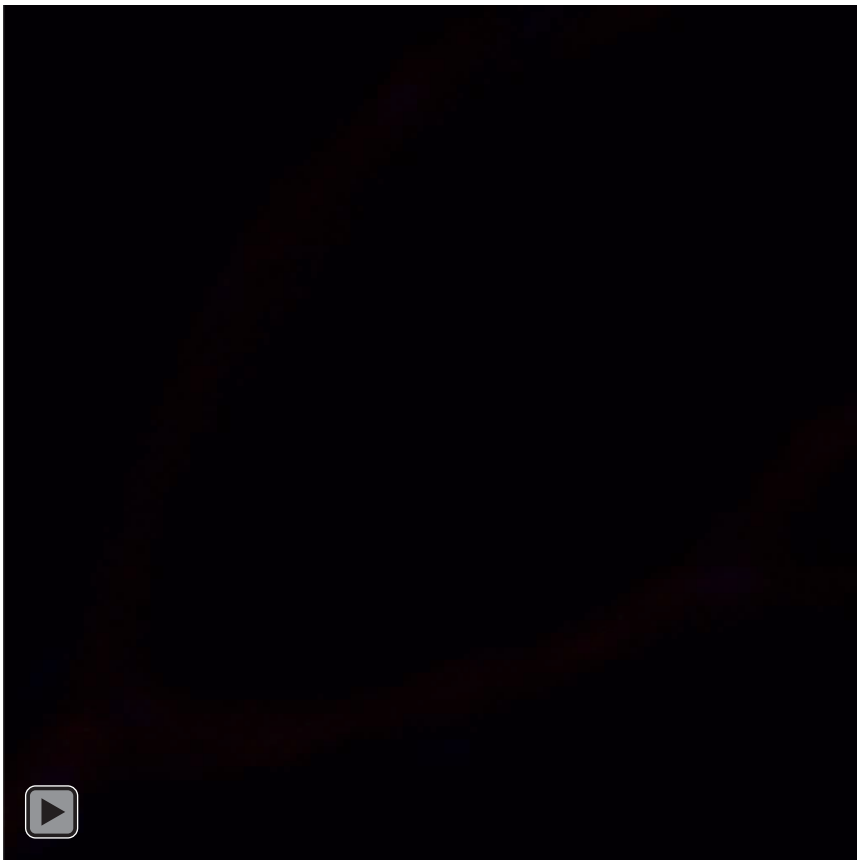

**Video 1: Hollow Lumens of HUVEC vessels *in vitro***

# iPSC-ECs

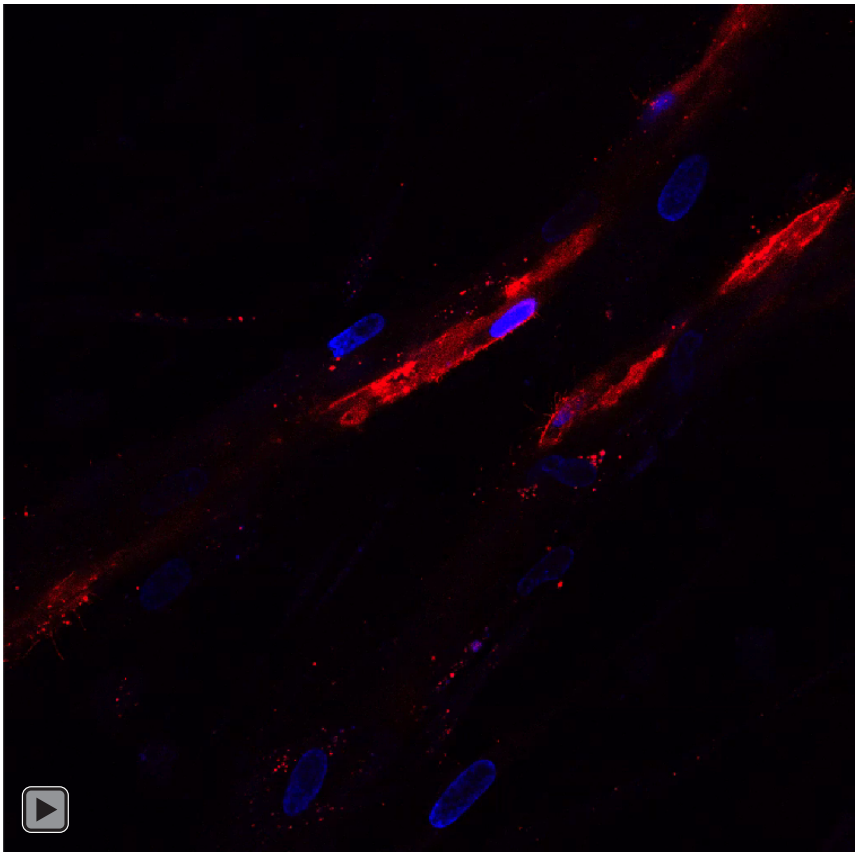

**Video 2: Hollow Lumens of iPSC-EC vessels** ***in vitro***

# Appendix B – Video of 3D Vessel Reconstruction

NOTE: Videos will play in electronic format via Adobe Acrobat with Flash. Videos are also available upon request from the author.

## HUVECs

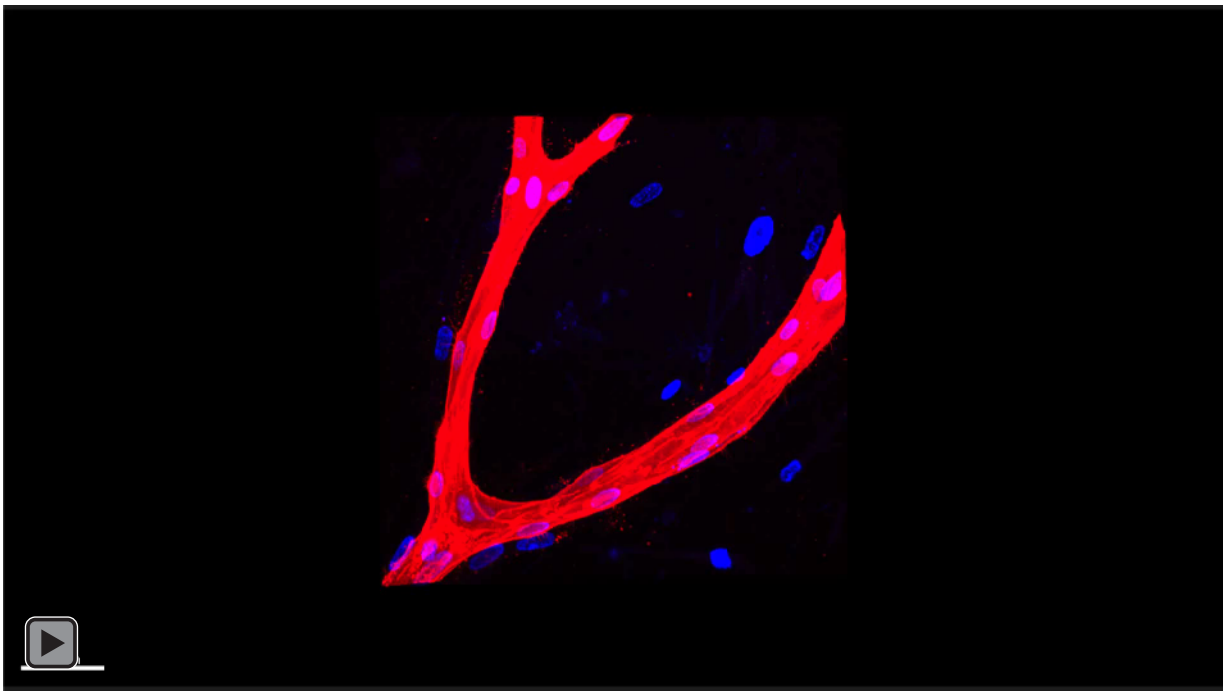

**Video 3: 3D Reconstruction of HUVEC vessel *in vitro***

# iPSC-ECs

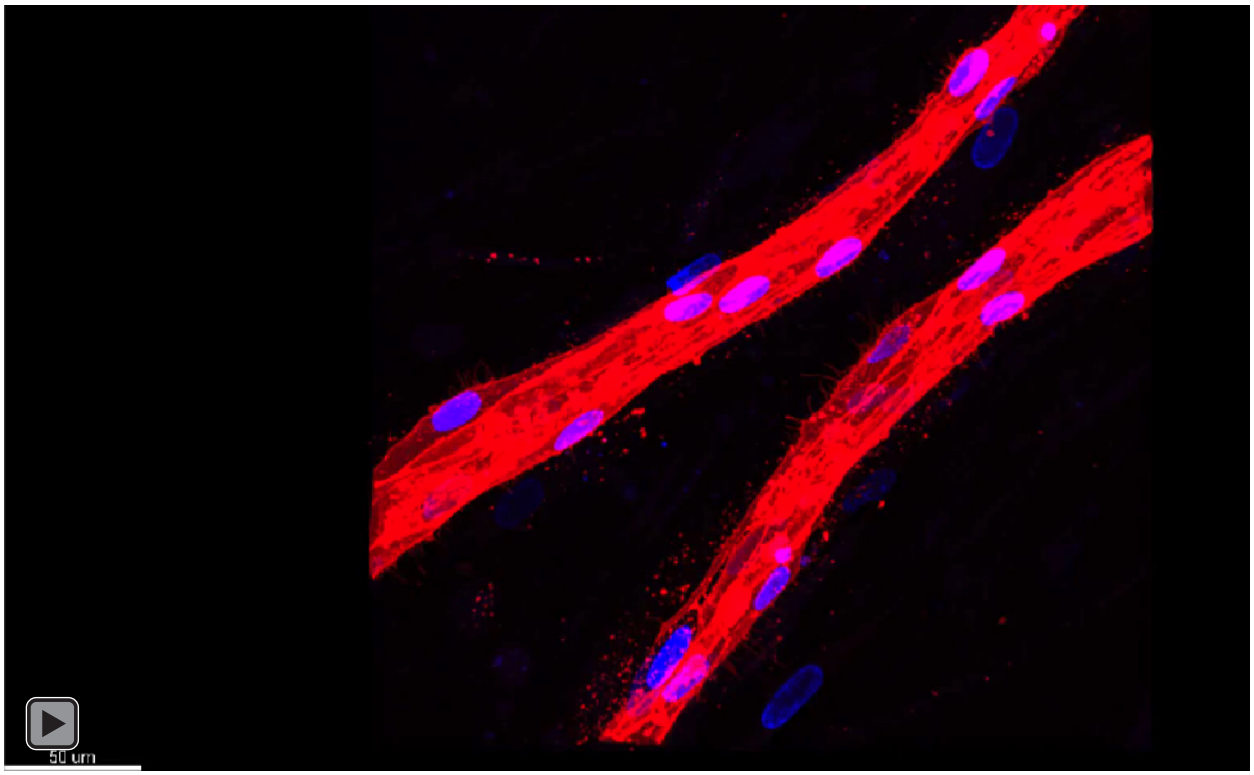


**Video 4: 3D Reconstruction of iPSC-EC vessel *in vitro***

# Appendix C – Reprogramming MEFs to ECs

## AC.1 Introduction

iPSCs were first generated over a decade ago by using a combination of 4 reprogramming factors, including Oct4 (Octamer binding transcription factor-4), Sox2 (Sex determining region Y-box 2), Klf4 (Kruppel Like Factor-4), and c -Myc [1]. iPSCs are an alternative self-renewing pluripotent cell that can be differentiated in many lineages including ECs [2]. Throughout this work, we investigated various sources of iPSC-ECs and assessed their vasculogenic potential. However, these sources were either commercially purchased or donated from other labs, so little is known about the original origin of the cells or the methods for reprogramming and differentiation. Furthermore, the iPSC-ECs used in this work are not autologous, a potential requirement for successful clinical translation.

The present study explores whether mouse embryonic fibroblasts (MEFs) can be reprogramed into an endothelial cell lineage. The overall goal of this study is to 1) create an alternative source of iPSC-ECs and 2) to establish a suitable reprogramming method for iPSC-EC generation. Using a previously established reprograming protocol [3], MEFs were plated on TCP or fibrin gels and transduced with lentiviruses. Transduced cells were then exposed to reprograming media to induce pluripotency and then differentiated using a VEGF based media,

EGM-2. We qualified differentiation of MEFs for each of the culture conditions through immunofluorescent staining for an endothelial cell marker.

## AC.2 Material and Methods

### AC.2.1 Lentiviral Production

293-T cells were cultured on TCP in two separate flasks at a density of 1 million cells per 15 $cm^2$ with DMEM + 10% FBS with Glutamax. Cells were cultured at 37°C and 5% $CO_2$ for 48 hours. Cells were then rinsed with PBS before being harvested via 0.25% trypsin incubation for 5 min at 37 °C and 5% $CO_2$. Trypsin was neutralized using DMEM supplemented with 10% FBS. The cellular suspension was centrifuged (200×G for 5 min) and supernatant was aspirated immediately. Cells were resuspended in fresh DMEM + 10% FBS with Glutamax and plated in a T-225 flask. 293-T cells were cultured at 37°C and 5% $CO_2$ until 70% confluency. Plasmid concentration was verified via a spectrophotometer to ensure the appropriate amount of each plasmid was added. Plasmids containing the following genes were added to 4.5 mL of Optimem in a 15 mL centrifuge tube: PLP1, PLP2, VSVG. M2rtTA and OSKM were then added to separate centrifuge tubes with the other 3 plasmids. Additionally, lipofectamine was added to 4.5 mL of Optimem in 15 mL tubes separate from the plasmid tubes. Plasmids and lipofectamine were incubated at room temperature for 5 minutes. Each plasmid tube, one for OSKM and another for M2rtTA, was then mixed with the lipofectamine Optimem tube. The two solutions were incubated at room temperature for 20 minutes. Media was aspirated from the 293-T cells and 21 mL of fresh media was added to each flask. The plasmid solutions were then added dropwise to separate 293-T flasks. After 24 hrs after transfection, media was aspirated and changed to fresh media. The next

day, 48 hrs after transfection, the media was collected and spun down at 3000 rpm for 15 mins at 4 °C. The supernatant was then aliquoted to vials and stored at -80 °C.

## AC.2.2 Fibrin Gel Assembly

Following lentiviral production, a fibrinogen (Sigma-Aldrich) solution of the desired concentration (2.5 mg/mL) was dissolved in an appropriate amount of serum-free DMEM and placed at 37 °C in a water bath. The solution was sterile filtered through a 0.22 μm syringe filter (Millipore, Billerica, MA). 5% FBS was then added to the fibrinogen solution. 500 μL of above mixture was added to a single well of a 24-well tissue culture plate and polymerized with 10 μL of thrombin (50 U/mL, Sigma-Aldrich). Fibrin constructs were left undisturbed for 5 min at room temperature before incubation for 30 min at 37 °C and 5% $CO^2$.

## AC.2.3 MEF Transduction

Mouse embryonic fibroblasts (MEFs) were plated on TCP or fibrin gels with DMEM + 10% FBS with Glutamax at a cell density of 3,500/$cm^2$ for 24 hrs prior to transduction. Cells were incubated at 37°C and 5% $CO_2$. The next day, viral supernatant and polybrene were thawed on ice. Media was aspirated from the cells and fresh media with 0.5 μL/ mL-of-media of polybrene was added the cell cultures. Cell equilibrated to the polybrene solution for 30 minutes. 107 μL of OSKM viral supernatant and 18 μL of M2rtTA viral supernatant per mL of media was added to the cells and then incubated for 6 hrs at 37°C and 5% $CO_2$. After 6 hrs, the solution was aspirated and changed to fresh with DMEM + 10% FBS with Glutamax.

## AC.2.4 MEF Reprograming

After transduction, cells were cultured for 24 hrs, and then the media was changed to reprograming media 1 with 0.5% of 2 mg/mL doxycycline. Reprograming media 1 consists of 15% FBS, 5% Knockout Serum (KOSR), 1% Glutamax, 1% Non-Essential Amino Acids (NEAA), and 0.1 mM beta-mercaptoethanol (BME) in Knockout DMEM. Cells were cultured in knockout media 1 for 7 days total. Media was then changed to knockout media 2 which consists of 1% FBS, 14% Knockout Serum (KOSR), 1% Glutamax, 1% Non-Essential Amino Acids (NEAA), and 0.1 mM beta-mercaptoethanol (BME) in Knockout DMEM. Cells were cultured in this media for 72 hrs.

## AC.2.5 Differentiation

Once MEFs were reprogramed to a pluripotent-like state, differentiation to an endothelial cell lineage was induced with EGM-2 (Lonza), an endothelial cell growth media. Cells were cultured for 7 days and fresh media was changed every 48 hours.

## AC.2.6 Reprogramed Cell Removal

While cells were reprogramed on either TCP or fibrin gels and then fixed, some cells were removed from their substrate and replated prior to enhance visualization. For cells removed with trypsin, cells were rinsed with PBS before being harvested via 0.25% trypsin incubation for 5 min at 37 °C and 5% $CO_2$. Trypsin was neutralized using DMEM supplemented with 10% FBS. The cellular suspension was centrifuged (200×G for 5 min) and supernatant was aspirated immediately. Cells were resuspended and plated onto new wells. For natto kinase removal, the fibrin gel was first digested using Natto Kinase (NSK-SD, Japan BioSceince Laboratoy Co. Ltd) dissolved in a 1mM EDTA PBS solution. 1 mL of the aforementioned solution was added to each well and

incubated for 45 minutes at 37 °C. The degraded fibrin cell solution was centrifuged (200×G for 5 min) and supernatant was aspirated immediately. The cells pellet was then suspended in 0.25% trypsin incubation for 5 min at 37 °C and 5% $CO_2$ to break apart the cell sheet. Trypsin was neutralized, and the cellular suspension was centrifuged (200×G for 5 min) and supernatant was aspirated immediately. Cells were resuspended and plated onto new wells. Cells were cultured for 24 hrs in fresh EGM-2 to allow cells to adhere to the plate.

## AC.2.7 Immunofluorescent staining

After the cells were cultured for with the EGM-2 for 7 days, cultures were rinsed 3x with PBS solution for 5 min at room temperature. Gels were then fixed with 500 µL of formalin (1 mL of 36.5% Formaldehyde solution (Sigma), 1 mL of PBS, and 8 mL of d.d.H2O) for 15 min at 4 °C. Cultures are rinsed again 3x with PBS for 5 min, then permeabilized with 0.5% Triton-X100 in TBS for 30 min at 4 °C. Following a rinse 3x for 5 min at room temperature with 0.1% Triton X-100 in TBS (TBS-T), samples were blocked overnight at 4 °C with a 2% Abdil solution (bovine serum albumin (Sigma) dissolved in TBS-T). The primary antibody/staining agent was dissolved in 2% Abdil at the appropriate concentration (Rabbit anti mouse-CD31, 1:200) and 1 mL of this solution was added to each gel for overnight incubation at 4 °C. The following day gels were rinsed 3x for 5 min with TBS-T. 1 mL of the appropriate secondary antibody (1:400, Alexa Fluor 488 Goat anti-rabbit IgG) dissolved in 2% Abdil was added to each gel for overnight incubation at 4 °C. Following a 3x rinse for 5 min at room temperature with TBS-T, gels were incubated with TBS-T overnight at 4 °C.

### AC.2.8 Fluorescent Imaging

Phase contrast and fluorescent images were captured utilizing an Olympus IX81 equipped with Disc Spinning Unit and a 100 W high-pressure mercury burner (Olympus America, Center Valley, PA), a Hamamatsu Orca II CCD camera (Hamamatsu Photonics, K.K., Hamamatsu City, Japan), and Metamorph Premier software (Molecular Devices, Sunnyvale, CA).

## AC.3 Results

Mouse embryonic fibroblasts (MEFs) were reprogramed and differentiated into an endothelial cell lineage on 2D fibrin or TCP cultures and compared to a control source of mouse endothelial cells. Phase contrast images revealed different morphologies between each of the culture conditions (Fig. AC-1). Typsinized cells, either seeded on fibrin or TCP, show areas with high density of cells. In contrast, the control mouse ECs and fixed reprogramed cells, either on fibrin or TCP, demonstrated a more uniform distribution of the cells. Immunofluorescent staining for mouse CD31 in these cultures demonstrated varying expression of the marker. The trypsinized conditions, both fibrin and TCP cultures, displayed the brightest signal for the reprogramed cells, while the natto kinase fibrin condition and fixed TCP demonstrated some signal intensity. However, the fibrin fixed cultured displayed weak to no signal. In comparison to the control EC, no condition expressed the same level of signal intensity or the expression of CD31 along the cell-to-cell junctions.

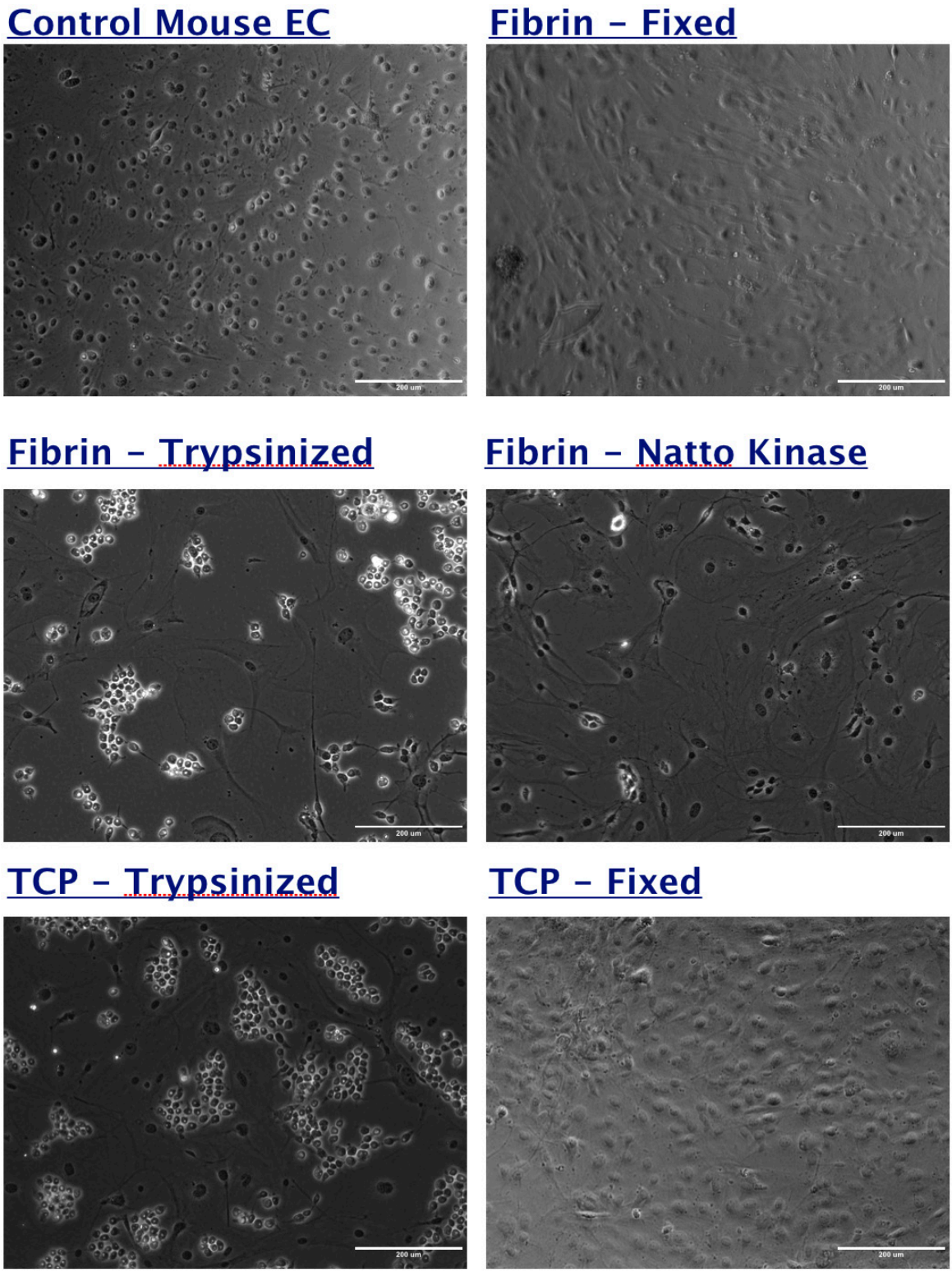


**Figure AC-1: Reprogramed MEF morphology is different from control Mouse ECs.**
MEF were reprogramed to a pluripotent like state and then differentiated into an EC lineage on 2.5 mg/mL fibrin or tissue culture plastic. Some cultures were removed with trypsin or natto kinase and replated to enhance visualization. Representative Images of phase contrast microscopy of the various cultures. Scale bar = 200 µm.

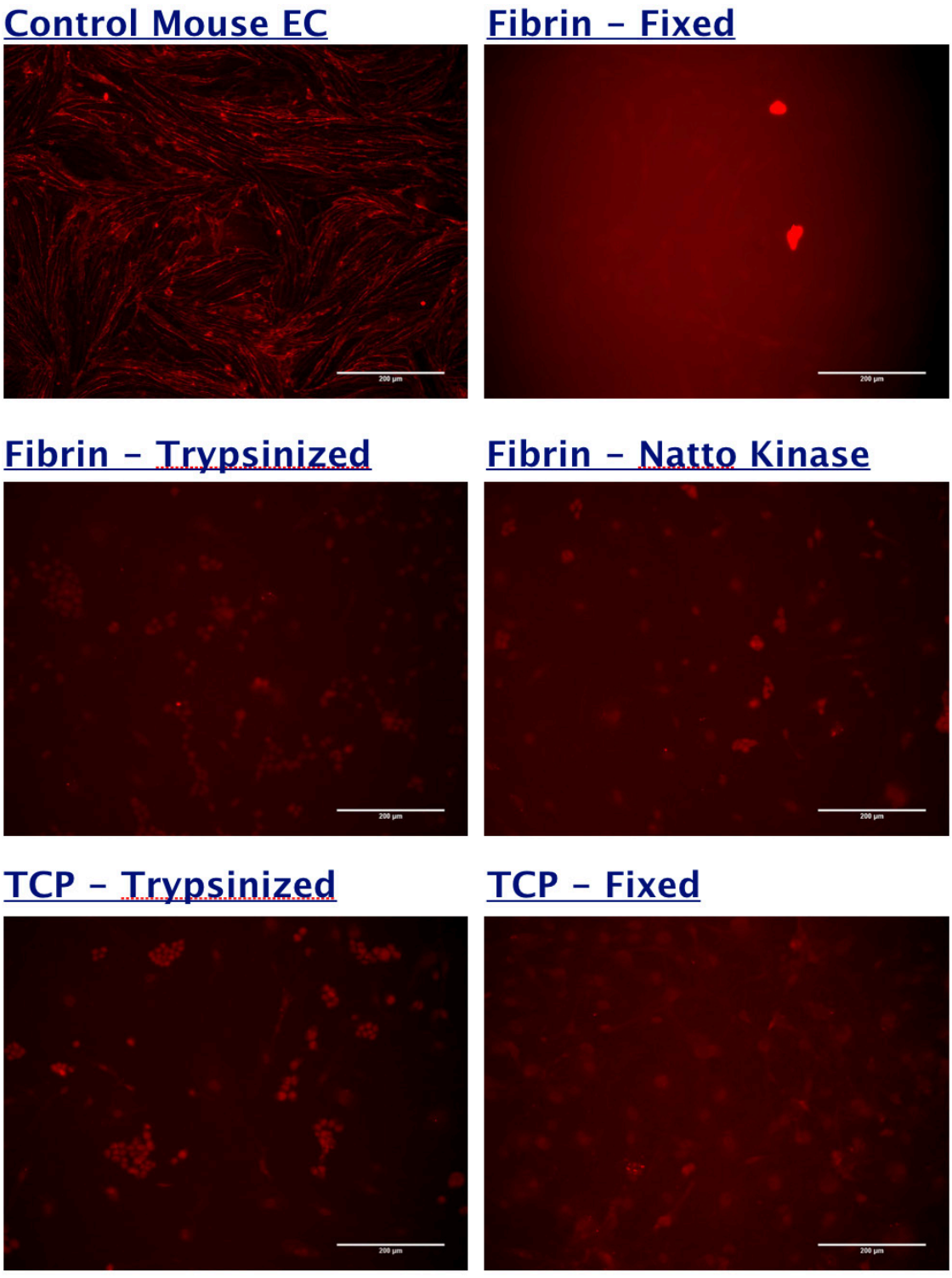


**Figure AC-2: CD31 expression of reprogramed MEFs is significantly lower than Mouse ECs.**
MEF were reprogramed to a pluripotent like state and then differentiated into an EC lineage on 2.5 mg/mL fibrin or tissue culture plastic. Some cultures were removed with trypsin or natto kinase and replated to enhance visualization. Cultures were IF stained for mCD31 and visualized via fluorescent microscopy. Scale bar = 200 µm.

## AC.4 Discussion and Conclusions

iPSC-ECs are a potentially alternative cell source for revascularization therapies. This dissertation explored two different external sources of iPSC-ECs. However, iPSC-EC creation requires a complex method of reprograming stromal cells and typically only a low percentage of cells are successful differentiated [4]. In order to assess vasculogenic differences between additional sources of iPSC-ECs, this study explored the ability to produce in-house iPSC-ECs through reprograming stromal cells into a pluripotent state and then differentiating into an endothelial lineage. This data shows that MEFs were unsuccessfully reprogramed and differentiated into an EC lineage across all culture conditions. While research has demonstrated varying reprograming efficiencies on different matrix stiffnesses, no differences were seen between the TCP and fibrin cultures [3]. While signal intensity of the trypsinized fibrin and TCP cultures was stronger than other cultures, the intensity is most likely an artifact of the confocal microscopy caused by the large grouping of cells. The signal intensity was also stronger for these conditions as cells were removed and placed on fresh plates, allowing little time for ECM matrix deposition [5]. The high density pockets of the culture conditions is most likely caused by the trypsinization process only partly breaking apart cell-cell junctions, leaving groups of cells clumped together once plated again [6]. The fixed fibrin condition had weak signaling due to high background from the fibrin gel. The most important distinction between all the cell conditions and the control ECs is the location of CD31 expression. Typically, CD31 is expressed on the surface and between the cell-cell junctions of ECs, as seen with the mouse EC [7]. Ultimately, this study demonstrated additional studies, such as FACS analysis of CD31, other EC marker expression, and reprograming of human cells, are necessary to successfully create in-house iPSC-ECs.

## AC.5 References


[1] K. Takahashi and S. Yamanaka, "Induction of pluripotent stem cells from mouse embryonic and adult fibroblast cultures by defined factors," *Cell*, vol. 126, no. 4, pp. 663–676, Aug. 2006.

[2] X. Liu *et al.*, "Yamanaka factors critically regulate the developmental signaling network in mouse embryonic stem cells," *Cell Res.*, vol. 18, no. 12, pp. 1177–1189, Dec. 2008.

[3] Y. P. Kong, B. Carrion, R. K. Singh, and A. J. Putnam, "Matrix identity and tractional forces influence indirect cardiac reprogramming," *Sci. Rep.*, vol. 3, p. 3474, Dec. 2013.

[4] A. Margariti *et al.*, "Direct reprogramming of fibroblasts into endothelial cells capable of angiogenesis and reendothelialization in tissue-engineered vessels," *Proc. Natl. Acad. Sci. U. S. A.*, vol. 109, no. 34, pp. 13793–13798, Aug. 2012.

[5] D. Aharoni, I. Meiri, R. Atzmon, I. Vlodavsky, and A. Amsterdam, "Differential effect of components of the extracellular matrix on differentiation and apoptosis," *Curr. Biol.*, vol. 7, no. 1, pp. 43–51, Jan. 1997.

[6] H.-L. Huang *et al.*, "Trypsin-induced proteome alteration during cell subculture in mammalian cells," *J. Biomed. Sci.*, vol. 17, no. 1, p. 36, May 2010.

[7] L. Liu and G.-P. Shi, "CD31: beyond a marker for endothelial cells," *Cardiovasc. Res.*, vol. 94, no. 1, pp. 3–5, Apr. 2012.

# Appendix D – Media Effect on HUVEC Capillary Morphogenesis

## AD.1 Introduction

ECs require a variety of growth factors and signals to regulate angiogenesis [1]. To simulate this complex physiological environment, ECs are cultured *in vitro* using media designed specifically to promote growth and proliferation of this lineage of cells. However, media formulations vary by vendor and there are no specific requirements for which growth factors and protein are added to the media. In Chapter 3, we investigated the effects of media formulation on various sources of ECs. While no differences were seen for iPSC-ECs, HUVECs demonstrated a reduced network formation in iPSC-EC media.

The present study explores whether HUVECs form the same robust, stable microvasculature in other growth media formulations. The overall goal of this study is to 1) assess the effects of media on HUVECs, and 2) to establish a suitable alternative media formulation for culturing HUVECs. Using the same well-established *in vitro* model, HUVECs were coated on dextran microcarrier beads and co-embedded in a 3D fibrin matrix with normal human lung fibroblasts (NHLF). We examined differences in capillary morphogenesis of HUVECs by quantifying total network lengths, the number of vessel-like segments, and vessel thickness.

## AD.2 Material and Methods

### AD.2.1 HUVEC Isolation and Cell Culture

Human umbilical vein endothelial cells were harvested from fresh umbilical cords from the University of Michigan Mott Children's Hospital via an IRB-exempt protocol and isolated from methods previously described. Briefly, the umbilical cord was rinsed in phosphate buffer saline (PBS) and then digested with 0.1% collagenase type I (195 U/ml, Worthington Biochemical, Lakewood, NJ) for 20 min at 37°C. The digested product was subsequently washed in PBS, collected, and centrifuged (200×G for 5 min). The pellet was resuspended in either endothelial growth media (EGM-2, Lonza), Vasculife VEGF endothelial media (Lifeline Cell Technology, Fredrick, MD), or Endothelial Cell Media (ECM, ScienCell, Carlsbad, CA) and the cells were plated in tissue culture flasks and cultured at 37°C and 5% $CO_2$. After 24 hours, HUVECs were rinsed with PBS to remove any non-adherent cells. Fresh media was changed every 48 hours. Cells from passage 3 were utilized for experiments. Normal human lung fibroblasts (NHLF, Lonza) were cultured at 37°C and 5% $CO_2$ in Dulbecco's modified eagle media (DMEM, Life Technologies, Grand Island, NY) with 10% fetal bovine serum (FBS). Culture media was replaced every 48 hours and cells from passage 6-10 were used in experiments.

### AD.2.2 Microcarrier Bead Assembly

Cytodex microcarrier beads (Sigma-Aldrich, St. Louis, MO) were hydrated and sterilized in phosphate buffer saline (PBS). Beads were prepared for coating by washing repeatedly with 1 mL of EGM-2, with time to settle between washes. Endothelial cells were cultured in T-75 flasks to 80% confluency and rinsed with PBS before being harvested via 0.25% trypsin incubation for 5 min at 37 °C and 5% $CO_2$. Trypsin was neutralized using DMEM supplemented with 10% FBS.

The cellular suspension was centrifuged (200×G for 5 min) and supernatant was aspirated immediately. The cell pellet was re-suspended in 4 mL of fresh EGM-2. 10,000 microcarrier beads were combined with four million HUVECs (5 mL total) in an inverted T-25 culture flask. Over a 4 hour incubation period, the culture flask was agitated every 30 minutes to ensure EC coating of beads. After 4 hours, the cell-bead mixture was added to a new T-25 culture flask. Fresh EGM-2 (5 mL) was added to the old flask to remove any remaining beads and transferred to the new culture flask. The total volume (10 mL) was incubated overnight in standard cell culture position.

### AD.2.3 Fibrin Tissue Assembly

The next day, following bead coating, a fibrinogen (Sigma-Aldrich) solution of the desired concentration (2.5 mg/mL) was dissolved in an appropriate amount of serum-free EGM-2 and placed at 37 °C in a water bath. The solution was sterile filtered through a 0.22 μm syringe filter (Millipore, Billerica, MA). The previous day's cell-bead solution was removed from the culture flask and placed in a 15 mL centrifuge tube. After the beads settled, the remaining supernatant was used to remove any remaining beads adhering to the culture flask and added to the centrifuge tube. Upon the beads settling, the supernatant was removed and 5 mL of fresh serum-free EGM-2 was added to the cell-coated beads. The appropriate amount of bead solution (~ 50 beads per well) was added to the fibrinogen solution with 5% FBS. Fibroblasts were prepared using a similar rinsing/trypsinization procedure as described above. 25,000 NHLFs per well were added to the bead-fibrinogen solution or plated on top of each gel after polymerization in distributed and monolayer conditions respectively. 500 μL of above mixture was added to a single well of a 24-well tissue culture plate and polymerized with 10 μL of thrombin (50 U/mL, Sigma-Aldrich). Tissue constructs were left undisturbed for 5 min at room temperature before incubation for 30

min at 37 °C and 5% CO2. 1 mL of media [EGM-2 (Lonza), Vasculife VEGF media (Lifeline), or ECM (ScienCell)] was added on top of the gels following incubation and changed the following day and every other day thereafter.

### AD.2.4 Immunofluorescent staining

After the constructs were cultured for a specified period of time (7 or 14 days), gels were rinsed 3x with PBS solution for 5 min at room temperature. Gels were then fixed with 500 µL of formalin (1 mL of 36.5% Formaldehyde solution (Sigma), 1 mL of PBS, and 8 mL of d.d.H2O) for 15 min at 4 °C. Gels are rinsed again 3x with PBS for 5 min. The primary antibody/staining agent was dissolved PBS (Ulex Europaeus Lectin 1 (UEA), 1:100 (Vector Labs, Burlingame, CA)) and 1 mL of this solution was added to each gel for 1 hr and 30 min incubation at room temperature. Gels were rinsed 3x for 5 min with PBS and incubated with PBS overnight at 4 °C as a final rinse.

### AD.2.5 Fluorescent Imaging and Vessel Quantification

Vessel formation was assessed at the aforementioned time points. Fluorescent images were captured utilizing an Olympus IX81 equipped with Disc Spinning Unit and a 100 W high-pressure mercury burner (Olympus America, Center Valley, PA), a Hamamatsu Orca II CCD camera (Hamamatsu Photonics, K.K., Hamamatsu City, Japan), and Metamorph Premier software (Molecular Devices, Sunnyvale, CA). Images from at least 30 beads per condition were captured over three separate trials at low magnification (4×) for each independent experiment and processed using the Angiogenesis Tube Formation module in Metamorph Premier (Molecular Devices). Each image was segmented and analyzed based on any tube-like pattern that falls within a specified

minimum and maximum width of each segment above a contrast threshold. The total network length, the number of branch points, and tube thickness were quantified.

### AD.2.6 Statistical Analysis

Statistical analyses were performed using StatPlus (AnalystSoft Inc.,Walnut, CA). Data are reported as mean ± standard error of mean (SEM). One- or two-way analysis of variance (ANOVA) with a Bonferroni post-test was used to assess statistical significance between data sets. Statistical significance was assumed when $p<0.05$.

## AD.3 Results

In-house isolated HUVECs were characterized for the ability to sprout from microcarrier beads when co-cultured with NHLFs in a 3D fibrin matrix with various media formulations. Immunofluorescent staining for UEA in these cultures demonstrated successful attachment, invasion into the ECM, and similar sprouting across media formulations at day 7. However, on days 14, the capillary sprouting of HUVECs in ScienCell Endothelial Cell Media (ScienCell) showed significant reductions in their networks compared to Lonza EGM-2 (Lonza) and Lifeline VEGF media (Lifeline) (Fig. AD-1.1). Quantification of these networks (Fig. AD-1.2) demonstrated a significant decrease in total network length between the ScienCell condition and the other two media formulations (30977 ± 2167 µm ScienCell versus 45368 ± 2126 µm for Lonza and 41949 ± 2762 µm for Lifeline on day 14). This reduced total network length was accompanied by a two-fold decrease in number of segments formed. The tube thickness of HUVECs cultured in the ScienCell media was also significantly smaller than the other two conditions at both timepoints (6.17± 0.23 µm ScienCell versus 7.16 ± 0.23 µm for Lonza and 8.00 ± 0.24 µm for Lifeline on

day 7 and 16.40 ± 0.26 µm ScienCell versus 18.36 ± 0.56 µm for Lonza and 20.27 ± 0.46 µm for Lifeline on day 14). There was no statistical difference between the Lonza and Lifeline media conditions, despite slightly reduced total network length and number of segments.

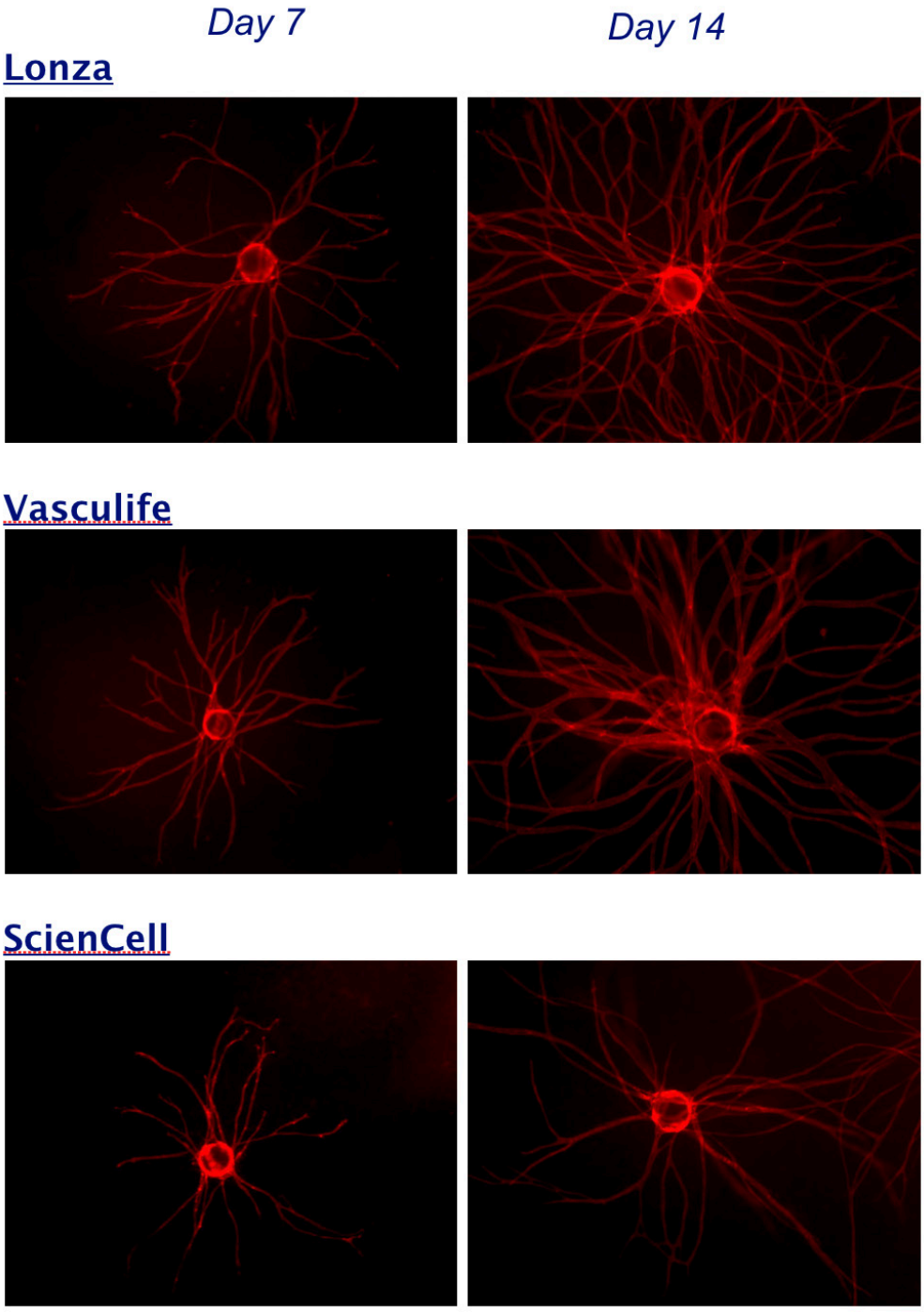


**Figure AD-1.1: Variations in media formulations affect HUVEC capillary morphogenesis.** ***[Rep. Images]***
**(A)** HUVEC-coated microbeads embedded in 2.5 mg/mL fibrin with NHLF at various time points were stained for UEA and visualized via fluorescent microscopy. Scale bar = 200 µm.

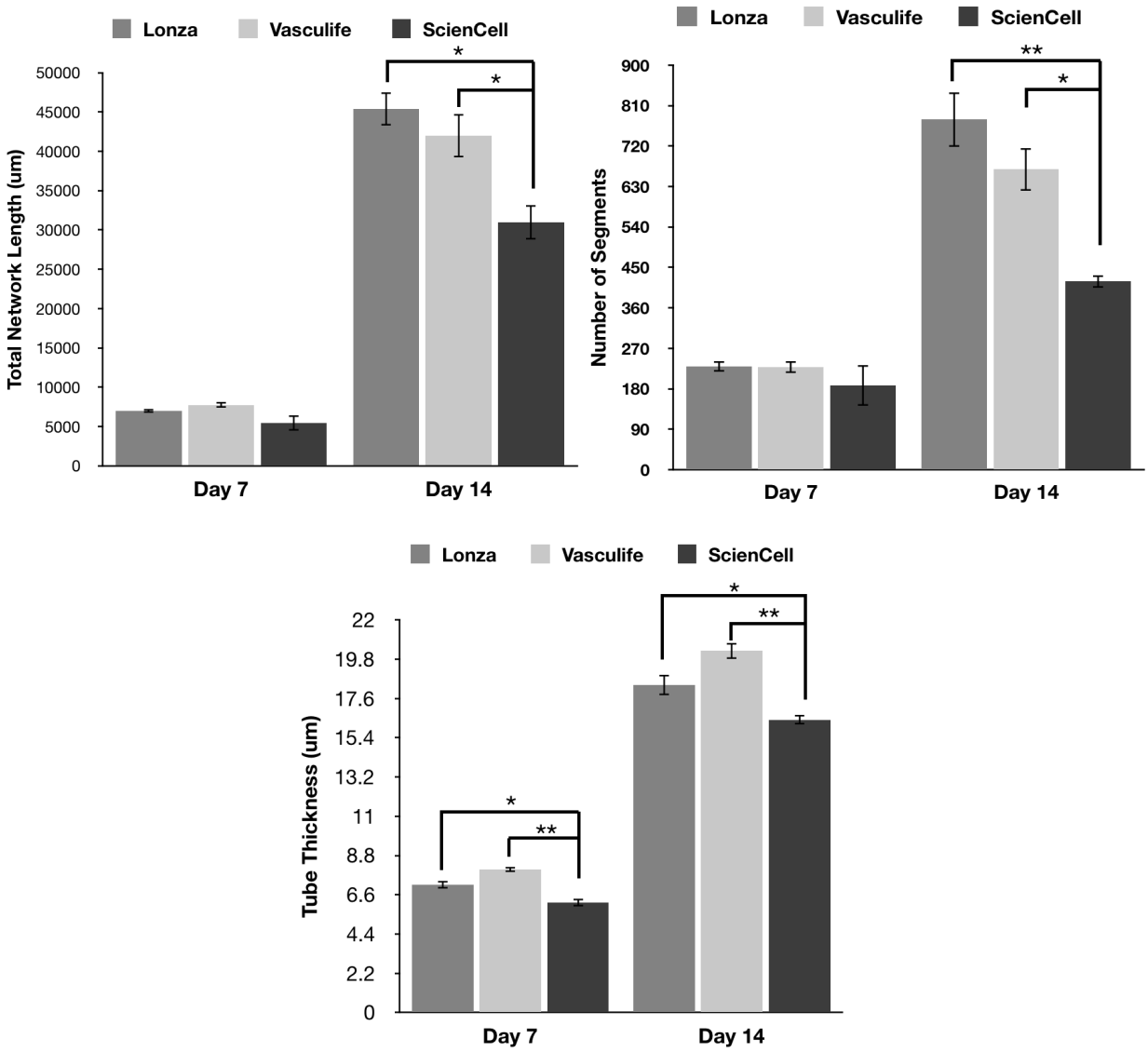


**Figure AD-1.2: Variations in media formulations affect HUVEC capillary morphogenesis.** ***[Quantification]***
Over 3 separate experiments, a total of 30 beads per EC were quantified and averaged for total capillary network length, number of segments, and tube thickness *p<0.05 and **p<0.01 when comparing the indicated condition at that time point. Error bars indicate ±SEM

## AD.4 Discussion and Conclusions

HUVECs are a robust source of ECs with proven capability of capillary morphogenesis, particularly in the assay used here. However, HUVEC cultures require media specifically designed to promote growth and proliferation. The study therefore explored the ability of various media

formulations from different vendors to promote functional vessel-like structures in a clinically relevant 3D *in vitro* model of angiogenesis. This data shows that HUVECs coated on microcarrier beads embedded in fibrin with NHLFs cultured in Endothelial Cell Media from ScienCell yield networks with significantly shorter total network lengths compared to both Lonza EGM-2 and Lifeline VEGF media. Furthermore, the thickness of vessels formed in ScienCell media are significantly smaller as well. Clearly, something in the ScienCell media is affecting the capillary morphogenesis of HUVECs. However, it is impossible to know specifically due to the proprietary nature of the ScienCell media. Unlike Lonza and Lifeline which include small aliquots of growth factors to add the base media, ScienCell media includes an unspecified vial of endothelial cell growth supplement. While one can assume similar growth factors are in this supplement, which exact growth factors and their concentrations are unknown. Similar to the iPSC-EC media in Chapter 3, one thing known about the supplement is a higher serum concentration. As previously mentioned, one of the prominent issues surrounding serum is batch-to-batch variations due to the unknown composition of each batch [2]. The additional serum in the ScienCell supplement could potentially explain the differences seen between the HUVEC conditions. Additionally, no statistical differences were seen between Lonza and Lifeline media. This similarity can be attributed to both media formulations adding the same growth factors at the same exact concentration. The only difference between the Lonza and Lifeline media are the base media formulation which could account for the slight differences observed. While the ScienCell media demonstrated small vessel thickness, the larger diameters for the other media formulations could indicate less mature vessel formation. As the neovasculature matures, ECs form tightly regulated junctions to each other [3]. The HUVECs in the Lonza and Lifeline media may not have formed these tight boundaries yet, leading to increased extracellular space between each cell. Future

studies can investigate vessel maturity differences between media formulation. Ultimately, this study demonstrated Lifeline Vasculife VEGF media could be used as an alternative media to Lonza EGM-2.

## AD.5 References


[1] T. H. Adair and J.-P. Montani, *Overview of Angiogenesis*. Morgan & Claypool Life Sciences, 2010.

[2] C.-Y. Fang, C.-C. Wu, C.-L. Fang, W.-Y. Chen, and C.-L. Chen, "Long-term growth comparison studies of FBS and FBS alternatives in six head and neck cell lines," *PLOS ONE*, vol. 12, no. 6, p. e0178960, Jun. 2017.

[3] Xu, K., & Cleaver, O. *Tubulogenesis during blood vessel formation.* Seminars in Cell & Developmental Biology, *22*(9), 993–1004, 2011.

# Appendix E – General Cell Culture Passaging and Freezing

**Unfreezing Cells**

1. Warm up media in water bath 37 °C.
2. Open hood sash. Open hood until set at appropriate level (alarm should stop sounding)
3. Turn on vacuum pump
4. Once airflow indicator light turns green on hood control panel, spray down and wipe down work surface with ethanol
5. Put necessary supplies into hood by first spraying with 70% ethanol and wiping down with paper towel
   ******* ANYTHING that enters hood needs to be sprayed with 70% ethanol
6. Once media has warmed up, transfer media bottle to hood. Spray with 70% ethanol first before placing in hood
7. Press indicator light/button on liquid nitrogen tank lid and then remove lid. Let it hang from the side handle of the tank
8. Remove respective rack where cells are stored from tank. Let all liquid nitrogen drain into tank before completely removing
9. Find cell vial in the respective box and remove from box
10. Place rack back in liquid nitrogen, close lid, and repress indicator light/button.
11. Place vial of cells in a foam float and thaw in water bath at 37 °C
12. Once cells are near completely thawed (some ice still left in vial), transfer vial to cell culture hood
13. Using micropipetter, transfer the content of the vial to a centrifuge tube.
14. Add 1 mL of respective media, using a micropipetter, to the empty vial to ensure all cells are removed from the vial and add to the centrifuge tube.
15. Add an additional 8 mL of media to the centrifuge tube bringing the total to 10 mLs
16. Spin cells down at 200 X G for 5 mins. Make sure appropriate counterweight is used in centrifuge to balance machine
17. After centrifugation is complete, aspirate off supernatant.
18. Flick apart cell pellet and add 10 mL of fresh media to the centrifuge tube
19. Add the cell solution to a respective flask or well plate at the appropriate seeding density
    1. 100K – 500K in T-25
    2. 500K-2M cells in T-75
    3. 2M – 6M in T-225
    4. 20K -40K 24 well plate
    5. 50-100K in 6 well plate
20. Label flask or plate with initials, cell type/lineage, cell passage number, # of cells plated, and date

21. Change media the day after and every day thereafter until cells are confluent
    1. 1 mL for 24 well
    2. 2 mL for 6 well
    3. 5 mL for T-25
    4. 10mL for T-75
    5. 30 mL for T-225

**Passaging Cells**

22. Warm up media and PBS and thaw trypsin and FBS in water bath
23. Follow steps 2-6 above to prep hood.
24. Aspirate off old media of ECs and fibroblasts
25. Rinse with equal volume of PBS to media
26. Aspirate off PBS
27. Add appropriate amount of trypsin to each flask
    a. T-25 – 2 mL
    b. T-75 – 5 mL
    c. T-225 – 10 mL
28. Incubate for 5 mins at 37 °C
29. Verify cells are detached from plate using microscope. If not, enough cells are detached, gently tap sides of plate to detach remaining cells. If cells still seem adherent, incubate for a few more minutes
30. Once cells are detached, add equivalent amount of media + 10% FBS to cells to neutralize trypsin
31. Collect cells with serological pipette and add to centrifuge tube
32. Spin down cells at 200 X G for 5 minutes
33. Once cells are pelleted, aspirate off supernatant
34. Flick pellet of cells to break pellet apart.
35. Resuspend cells in 5 mL of media. Ensure cells are properly suspend by pipetting
36. Take 10 µL of solution and count using hematocytometer
    *a.* Count cells in 4 – 4x4 corners
    *b.* Divide by 4
    *c.* Times number by 10000, this is your cells per mL
    *d.* Multiply by number of mLs used to resuspend cells (if following above, will be by 5. Resuspending vol. amount can vary depending on number of cells you expect to have)
37. Add additional media to the cell solution to bring cell suspension the desired cell concentration.
38. Split cells into multiple flasks/plates to achieve respective cell number listed in [step 19]
39. Label flask or plate with initials, cell type/lineage, cell passage number, # of cells plated, and date
40. Change media the day after and every day thereafter until cells are confluent (see step 21 for respective amounts)

**Freezing Cells**

41. Repeat steps 22-36 above

42. Once cells have been counted, spin down cells again at 200 X G for 5 minutes
43. While cells are spinning down, calculate amount of cryopreservation solution needed
    **a.** Cells can be frozen down at varying concentration
    **b.** Typically, each vial will have 1 mL of solution
    **c.** Cryopreservation solution needed is determined by desired cell concentration and number of cells counted
44. Prepare cryopreservation solution in a centrifuge tube
    **a.** 70% respective cell media
    **b.** 20% FBS
    **c.** 10% DMSO
45. Obtain the respective number of cryopreservation vials and label them with date, initials, cell type, passage, and cell count

**NOTE:** Passage to label vial is current passage if cells were to be plated instead of frozen down. i.e. If cells came from a plate labeled P2, label the vials P3

46. Once cells are spun down, aspirate off supernatant
47. Flick pellet and add cryopreservation solution to cells
48. Using a micropipetter, add cells to each vial.
    ** After adding cryopreservation solution to cells, cells need to be frozen ASAP as DMSO can affect cell viability
49. Once all vials are filled, place vials in a Mr. Frosty
50. Place Mr. Frosty in -80 °C freezer overnight
51. The next days, place vials in a box in liquid nitrogen tank
52. Record in lab cell log what vials were added to the liquid nitrogen tank

**Respective Media for Varying Cells**

- In-house isolated HUVEC – EGM-2 [LONZA], can use Vasculife VEGF media [Lifeline]
- Commercial LONZA HUVEC – EGM-2 [LONZA]
- NHLFs – DMEM + 5% FBS [Invitrogen]
- iPSC-ECs (Cellular Dynamics) – Vasculife VEGF media + iPSC-EC supplement [LIFELINE, Celluar Dynamic respectively].
- MVECs – EGM-2MV
- iPSC-ECs (Ngan Huang Lab) - EGM-2MV

**General Tips for Culturing iPSC-ECs**

****Flasks/plates must be coated with fibronectin prior to culture iPSC-ECs

53. Preparing fibronectin Plates/Flasks
    a. Reconstitute fibronectin in sterile water to make a stock solution at 1 mg/mL
    b. Prior to coating, make a working solution of 30 µg/mL
        i. For T-75, 225 µL of stock fibronectin solution (1 mg/mL) in 7.5 mL of sterile water
    c. Add working solution of fibronectin to plate/flask
    d. Incubate flask/plate for at least 1 hr at RT

***** iPSC-ECs use **TyrpLE** to detach cells not the typical trypsin used for other cells
***** Seeding density is MINIMUM 750K in T-75 flask, but ideally 1M in T-75 Flask
***** Cell morphology is larger than other ECs, specifically HUVECs, but still make cobblestone pattern

# Appendix F - Isolation of HUVECs from umbilical cords

**Materials:**

- 2 Haemostats
- 1 pair of scissors
- 2 L beaker
- Foil and autoclave tape
- 2, 5 mL syringe
- 1, 33 mm Millex filter
- 2, 20 mL syringes
- Butterfly needle
- 1, 18-gauge needle (or 16-gauge needle)
- 40 mL of sterile PBS
- 5 mL of 0.1% collagenase (sterile-filter)
- 5 mL of EGM-2
- Umbilical Cord

**Protocol:**

Sterilization of Surgical Tools

- Place 2 haemostats, and 1 pair of scissors in a 2 L beaker. *One pair of scissors doesn't work properly; therefore, it's better to add the 2 pairs of scissors to the beaker.*
- Cover the beaker with aluminum foil and then tape one side of the aluminum foil to the beaker using autoclave tape.
- Autoclave beaker using the textiles setting.
    a. Sterilization time: 45 minutes
    b. Drying time: 10 minutes
- Check to make sure water level of pipe in the autoclave is at the specific set level. Then start the process.

HUVEC isolation:

1. Place the umbilical cord and the sterile PBS in the water bath. *Make sure that the cord is in the biohazard delivery bag to avoid contaminating the water bath.*
2. Make 5 mL of 0.1% of collagenase in PBS. *Make sure to make this solution every time this protocol is repeated, DO NOT store solution after experiment is completed. [Concentration = 5 mg/mL]*
3. Sterile filter the 0.1% collagenase solution using a 5 mL syringe with a 33 mm Millex filter.

4. Connect an 18-gauge needle to a 5 mL syringe and suction 5 mL of the sterile-filter collagenase. Place the syringe back in its wrapper for storage.
5. Remove the needle from the syringe carefully and throw it in the sharps needle biohazard container. *Make sure you don't recap the needle.*
6. Suction 20 mL of PBS in each 20 mL syringe. Put the syringes back in their wrappers for storage
7. Sterilize the hood and all the materials needed in this protocol prior to putting them in the hood.
8. Place paper towels inside the hood *(use sufficient amount to cover your working area properly).*
9. Soak the towels with bleach *(make sure surface is completely wet with bleach).*
10. Put on a second pair of gloves prior to placing the umbilical cord in the container and especially prior to opening the umbilical cord container.
11. Take out the umbilical cord and PBS from the water bath and place them inside the hood after wiping them down with ethanol.
12. Take out the umbilical cord from its container and wipe off the clotted blood in the paper towels.
13. Locate the lines where they clamped the hemostats on both ends of the cord. Cut the cord below the clamp marks. *Use cord container as a waste container for the pieces cut from the cord. The cleaner the cut is the easier it is to locate the veins and arteries.*
14. Gently slide half of the butterfly needle into the vein and clamp the cord with the needle using the hemostat. *You must spiral the needle around because vein spirals around the outside. NOTE – Leave the plastic casing of the butterfly needle covering the needle when inserting it into the vein. The vein looks like a stretch mark. You shouldn't have to put a lot of force when inserting the needle to the vein, there should be no resistance.*
15. Remove the extra part of the butterfly needle so that you only have the tube connected to the butterfly needle. Attach the first 20mL syringe of PBS and inject all of it slowly into the vein making sure there are no clots. *Make sure the cord is on top of the waste container.*
16. Attach the collagenase syringe and begin injecting the solution until the liquid coming down changes its color to gold. (It takes approximately 1 mL of collagenase of color change to occur). *Make sure to put the cord on top of the white towel to make it easier to notice the liquid color change.*
17. Clamp the other end of the cord and very carefully re-inflate the vein with the 4 mL of collagenase remaining in the syringe.
18. Carefully place everything in the autoclaved beaker which initially contained the hemostats and scissors. Cover the top with the aluminum foil taped at one side of the beaker.
19. Remove your outer pair of gloves and take the 2 L beaker to the bottom shelf of the incubator.
    *If there is no space, then use the top incubator instead. Don't clean up workspace yet.*
20. Leave the cord in the incubator for **20 min**.
21. Put on a second pair of gloves and take out the cord from the incubator. Remove the hemostat that is *not* holding the needle and then attach the last 20 mL syringe of PBS.
22. Place the cord on top of a 50 mL centrifuge tube and begin injecting the PBS in the vein very slowly to wash off the cells but avoid bursting the vein. Collect the entire solution in the 50mL tube and then discard the cord in the waste container after removing the needle and the hemostat holding it in place.
23. Make sure all waste goes in the biohazard bag. Clean up the hood with bleach and ethanol (rinsing).

Cell Culturing:

24. Centrifuge the tube in Setting 1 (200g for 5 min).
25. Take out a 25 mL flask and place it in the clean hood. Label it: “HUVEC P.0, Date, Your initials”.
26. Remove the 50 mL tube from the centrifuge and aspirate off the supernatant. *Make sure to do it carefully to avoid aspirating off the HUVECs.*
27. Add 5 mL of EGM-2 into centrifuge tube and mix well. Put the cell-media solution into the 25 mL flask.
28. Place the flask in the incubator overnight.
29. Place flask in the hood and aspirate off the medium. Add 5 mL of PBS and rock the flask.
30. Aspirate off the PBS and add 5 mL of PBS (2X).
31. Remove PBS and add 5 mL of EGM-2.
32. Look at the HUVECs under microscope. Let them grow on the T-25 flask and make sure to check on them every day. Cells should be confluent in less than 1 week. If not, throw the cells away.
33. Once the cells are confluent, trypsinize and passage them into 2 T-75 flasks.
34. Grow to confluency and freeze them down. Label them P.2.

# Appendix G - Vasculogenesis Assay Protocol

**Preparing fibrinogen solution**

Note: Gels are *2.5 mg/mL* of fibrinogen

- You will add 5% FBS to the fibrinogen solution in the end. To adjust for this use *2.625% mg/mL*.

1. Take fibrinogen out of freezer and warm up to room temperature
2. To get amount of fibrinogen needed, calculate how many gels you are making
    a. Each gel is 500 µL
    b. Calculation is # of gels X 500 µL = # of mLs of fibrinogen solution needed
    c. Add 2 mL to # of mLs of fibrinogen solution needed to account for loss during filtering
    d. Divide *2.625 mg/mL* by the protein content and clottable content of the fibrinogen to get actual concentration (Typically listed on the bottle. Varies Lot-Lot)
    e. Multiply # of mLs of fibrinogen by actual concentration to get # of grams to measure
3. Measure out calculated fibrinogen and add to 50 mL centrifuge tube
4. In cell culture hood, add serum -free EGM-2 equal to the # of mLs of fibrinogen solution needed to centrifuge tube with fibrinogen**.**
5. Place fibrinogen solution in water bath to dissolve fibrinogen

**Prepare Cells**

While fibrinogen solution is dissolving, prepare cells.

6. Aspirate off old media of ECs and fibroblasts
7. Rinse with equal volume of PBS to media
8. Add appropriate amount of trypsin to each flask
    a. T-25 – 2 mL
    b. T-75 – 5 mL
    c. T-225 – 10 mL
9. Incubate for 5 mins at 37 °C
10. Verify cells are detached from plate using microscope
11. Once cells are detached, add equivalent amount of media + 10% FBS to cells to neutralize trypsin
12. Collect cells with serological pipette and add to centrifuge tube
13. Spin down cells at 200 X G for 5 minutes
14. Once cells are pelleted, aspirate off supernatant
15. Flick pellet of cells to break pellet apart

**Assembling Gel Tissue Constructs**

16. Once fibrinogen solution has dissolved, using a needle and syringe, pull solution into syringe
17. Using a 0.22 μL filter, filter fibrinogen solution into a clean centrifuge tube
    *Note:* May need to use multiple filters as filters can clog
18. Add 10 μL of thrombin to the bottom of each well that a gel will be cast in a 24 well plate
    a. Note: Need one-24 well plate per timepoint due to fixation
19. Determine cell concentration and cell ratio need for gels e.g. 250k/mL and 1:1 ratio of EC to stromal cells
20. Add appropriate amount of stromal cells to ECs based on # of gels, amount of cells, and ratio
    a. e.g 10 gels needed, at 250k/mL (125k/ gel [gels are 500 μL]) = 1.25 M cells
    b. 1.25 M cells at 1:1 ratio is 625K each of ECs and stromal cells
21. Add appropriate amount of fibrinogen solution to EC/stromal cells suspension
    a. e.g. 5 mLs of sterile-fibrinogen solution if using above example
22. Add 5% FBS to fibrinogen/cell solution
23. Pipette 500 μL of the FBS/fibrinogen/cell solution (using P1000) to each well
24. All gels to polymerize at room temperature for 5 mins
25. Incubate gels for 30 minutes at 37 °C to complete polymerization
26. Add 1 mL of media to the top of each gel after polymerization is complete
27. Change media on day 1 and every day thereafter.

# Appendix H – Dextran Bead Coating Protocol

**Preparing dextran beads**

1. Measure 75 mg of powdered Cytodex dextran beads (~ 0.1 g is 200K beads)
2. Suspend beads in 15 mL of 1x – PBS in small glass vial
3. Autoclave beads for 40 minutes with cap unscrewed
4. After autoclaving calculate concentration of beads
    a. Place 10 µL of solution on cover slip
    b. Count how many beads total are in droplet
    c. Concentration = count X 100
5. Wrap beads in parafilm and store at 4 °C

**Prepare Cells**

6. Aspirate off old media of ECs and fibroblasts
7. Rinse with equal volume of PBS to media
8. Aspirate off PBS
9. Add appropriate amount of trypsin to each flask
    *e.* T-25 – 2 mL
    *f.* T-75 – 5 mL
    *g.* T-225 – 10 mL
10. Incubate for 5 mins at 37 °C
11. Verify cells are detached from plate using microscope
12. Once cells are detached, add equivalent amount of media + 10% FBS to cells to neutralize trypsin
13. Collect cells with serological pipette and add to centrifuge tube
14. Spin down cells at 200 X G for 5 minutes
15. Once cells are pelleted, aspirate off supernatant
16. Flick pellet of cells to break pellet apart

**Bead Equilibration:**

17. Take 10000 beads (based on concertation calculated) and add to a microcentrifuge tube
18. Let beads settle by gravity
19. Quickly spin down beads (~10 s) in centrifuge at max speed
20. Aspirate off supernatant
21. Add 1 mL of EGM-2 to beads
22. Repeat 18-21 for a total of 3 times
23. After final wash, resuspend beads in 1 mL of fresh EGM-2

**Bead Coating:**

24. Resuspend cells in 5 mL of EGM-2
25. Count using hematocytometer (need ~4 M cells)
26. Add 4 M cells of cells to T-25 in **upright** position
27. Bring total volume in flask to 4 mL
28. Add all beads to T-25 flask with cells
29. Shake flask side to side while holding **upright** for 1 minute
30. Place in incubator at 37 °C in upright position
31. Shake flask for 1 minute at the following timepoints from initially placing in incubator 5 min, 25 min, 55 min, 1hr 25 min, 1 hr 55 min, 2 hr 25 min, 2 hr 55 min, 3 hr 25 min, 3 hr 55 min
32. After all timepoints have been shaken, take beads/cell solution and add to a a new T-25 flask
33. Add 5 mL of fresh EGM-2
34. Incubate overnight in standard culture position

# Appendix I – Angiogenic Bead Assay Protocol

**Preparing fibrinogen solution**

Note: Gels are *2.5 mg/mL* of fibrinogen

- You will add 5% FBS to the fibrinogen solution in the end. To adjust for this use *2.625% mg/mL*.

1. Take fibrinogen out of freezer and warm up to room temperature
2. To get amount of fibrinogen needed, calculate how many gels you are making
    a. Each gel is 500 µL
    b. Calculation is # of gels X 500 µL = # of mLs of fibrinogen solution needed
    c. Add 2 mL to # of mLs of fibrinogen solution needed to account for loss during filtering
    d. Divide *2.625 mg/mL* by the protein content and clottable content of the fibrinogen to get actual concentration (Typically listed on the bottle. Varies Lot-Lot)
    e. Multiply # of mLs of fibrinogen by actual concentration to get # of grams to measure
3. Measure out calculated fibrinogen and add to 50 mL centrifuge tube
4. In cell culture hood, add serum -free EGM-2 equal to the # of mLs of fibrinogen solution needed to centrifuge tube with fibrinogen**.**
5. Place fibrinogen solution in water bath to dissolve fibrinogen

**Prepare Stromal Cells**

While fibrinogen solution is dissolving, prepare cells.

6. Aspirate off old media of fibroblasts
7. Rinse with equal volume of PBS to media
8. Add appropriate amount of trypsin to each flask
    a. T-25 – 2 mL
    b. T-75 – 5 mL
    c. T-225 – 10 mL
9. Incubate for 5 mins at 37 °C
10. Verify cells are detached from plate using microscope
11. Once cells are detached, add equivalent amount of media + 10% FBS to cells to neutralize trypsin
12. Collect cells with serological pipette and add to centrifuge tube
13. Spin down cells at 200 X G for 5 minutes
14. Once cells are pelleted, aspirate off supernatant
15. Flick pellet of cells to break pellet apart

**Prepare EC Coated Beads**

16. Remove all media and beads from T-25 flask
17. Place in 15 mL centrifuge tubes
18. Let beads settle by gravity
19. Once bead have settled, take supernatant and rinse flask to remove remaining beads stuck to flask
20. Add supernatant to centrifuge tube
21. Once beads have resettled by gravity, aspirate off supernatant
22. Resuspend beads in 5 mL of fresh serum free EGM-2
    Note: Concentration should be ~ 2000 beads/ mL
23. Calculate # of beads needed:
    a. 50 -100 beads per gel for protein assay
    b. 25 beads per gel for imaging
24. Mix EC coated bead solution well
25. Transfer # of beads needed to new centrifuge tube
26. Let beads settle and aspirate off supernatant

**Assembling Gel Tissue Constructs**

27. Once fibrinogen solution has dissolved, using a needle and syringe, pull solution into syringe
28. Using a 0.22 µL filter, filter fibrinogen solution into a clean centrifuge tube
    *Note:* May need to use multiple filters as filters can clog
29. Add 10 µL of thrombin to the bottom of each well that a gel will be cast in a 24 well plate
    a. Note: Need one-24 well plate per timepoint due to fixation

If using distributed stromal cell model: (if not skip to step 32)

30. Add 1 mL of fibrinogen solution to stromal cells
31. Add appropriate amount of stromal cells to centrifuge tube with beads **(25 K stromal cells per 500 µL gel)**

32. Add FBS to tube with beads
    a. Volume to add is equal to 5% X of # of gels X 500 µL
33. Add remaining volume (# of gels X 500 µL X 0.95) of fibirnogen solution to beads in centrifuge tube
34. Mix well
35. Pipette 500 µL of gel/bead solution into each well using p1000
    a. Mix solution well before pipetting into each well as bead settle quickly
36. All gels to polymerize at room temperature for 5 mins
37. Incubate gels for 30 minutes at 37 °C to complete polymerization

If using monolayer stromal cell model: (if not skip to step 41).

38. Calculate number of cell needed **(25K per 500 µL gel)**
39. Aliquot appropriate amount of fibroblasts into a new tube
40. Add 1 mL per gel of EGM-2 to fibroblasts
41. Add 1 mL of EGM-2 or EGM-2 + fibroblasts to the top of each gel after polymerization is complete
42. Change with fresh EGM-2 on day 1 and every day thereafter.

# Appendix J - Immunofluorescent Staining of Fibrin Gels

**Solutions:**

10 X TBS: 44 g NaCl
15.75 g Tris (base)
500 mL of di H2O
pH balance to 7.4

TBS-T: 50 mL of 10 X TBS
0.5 mL of Trition X-100
Quench to 500 mL of dd H2O

Abdil: 2% (2g/100mL) of Bovine serum albumin in TBS-T

Formalin: 1 mL of saturated formaldehyde solution (36.5%)
1 mL of 1 X PBS
8 mL of dd H2O

**Fixation**:

1. Aspirate off old media in cell culture hood
2. Add 2x gel volume (1mL for 500 µL) of 1 X PBS to each well
3. Rinse for 5 minutes at RT
4. Aspirate off PBS using vacuum pump
5. Repeat 2-4 a total **3 times**
6. Add formalin equal to gel volume to each well in fume hood
7. Place in fridge (4 °C) for 15 minutes
8. Remove formalin using pipette in hood.
9. Dispose of formalin in appropriate waste container
10. Add PBS equal to 2X volume of gel to each well
11. Rinse for 5 minutes at RT
12. Aspirate off PBS using vacuum pump
13. Repeat 2-4 a total **3 times**

**Staining**:

Depending on the target, permeabilization may be required, if so:

14. Add 2X gel volume of TBS-T for 1 hr at RT
15. Aspirate off TBS-T

16. Block unspecific target with 2X gel volume of abdil solution for 1 hr RT or overnight at 4 °C
17. Aspirate off abdil block solution
18. Prepare Antibody solution:
    a. For CD31, use 1:200 dilution in abdil
    b. For UEA, use 1:100 dilution in abdil
19. Add 2X gel volume of primary antibody solution to well
20. Cover well plate with aluminum foil
21. Incubate for 1 hr at RT
22. Aspirate of antibody solution and rinse with 2X gel volume of PBS for 5 mins at RT.
23. Rinse a total of 3X

If secondary is needed:

24. Prepare secondary antibody solution:
    a. Varies on primary antibody
    b. For CD31, use 1:450 of alexa fluro 488 goat anti-mouse in abdil
25. Add secondary antibody solution to each well, 2X gel volume
26. Incubate for 45 min-1 hr at RT
27. Aspirate of antibody solution and rinse with 2X gel volume of PBS for 5 mins at RT.
28. Rinse a total of 3X
29. Add 1 mL of PBS to each well to keep gels moist

**Optional:**

30. Incubate gels overnight in fridge (4 °C) with PBS
31. Aspirate off old PBS and add 1 mL of PBS to each well
    a. Sometimes an extra overnight rinse is needed if there is too much background noise

**Optional DAPI Staining:**

32. After rinse with PBS, prepare DAPI solution
    a. Dilute DAPI in PBS (1:10000) [Only for concentrated DAPI
    b. Some stocks are 500X (1:500 dilution needed)
33. Add 2x gel volume of DAPI solution to each well
34. Incubate for 10 min at RT
35. Aspirate of DAPI solution
36. Rinse with 2X gel volume of PBS for 5 mins at RT.
37. Rinse a total of 3X
38. Add 1 mL of PBS to each well to keep gels moist

Note: UEA does not need permeabilization or blocking step can skip from step 13 to 18

# Appendix K - Immunofluorescent Staining in Suspension

**Cell Harvesting:**

1. Remove media from the cell flasks
2. Rinse cells with volume equal to media volume PBS
3. Aspirate off PBS
4. Add appropriate amount of trypsin to each flask
    1. T-25 – 2 mL
    2. T-75 – 5 mL
    3. T-225 – 10 mL
5. Incubate for 5 mins at 37 °C
6. Inhibit trypsin with media and 5% FBS
7. Collect cells and solution from flask in a centrifuge tube
8. Spin down cells in centrifuge at 200 X G for 5 mins
9. Aspirate off supernatant
10. Flick tube to break apart cell pellet
11. Add 5 mL of PBS to cells
12. Count cells using a hematocytometer
13. Filter cells and PBS through a 40 μm nylon into a new centrifuge tube
14. Spin down cells in centrifuge at 200 X G for 5 mins

**Primary Antibody Suspension Staining:**

15. Prepare solution of PBS + 0.1% BSA and cool on ice
16. Once cells are pelleted, add ice cold PBS + 0.1% BSA solution to pellet so final concentration is 2M-5M per mL
    1. Cell concentration can vary depending on how many cells you have and want to use
    2. Minimum cell concentration is 1M cells / mL per sample for FACS
17. Distribute 1 mL of cells solution to a microcentrifuge tube
18. Spin down cells at 200 X G for 4 mins
19. Aspirate of solution
20. Rinse cells with 1 mL of ice cold PBS + 0.1% BSA
21. Repeat 18 – 20 a total of 3X washes
22. Prepare primary antibody solution
    1. Antibody diluted in ice cold PBS + 0.1% BSA solution
    2. CD31 1:50 dilution (20 μL in 1 mL)
    3. CD144 1:50 dilution (20 μL in 1 mL)
23. Add 1 mL of antibody solution to their respective microcentrifuge tube

24. Place microcentrifuge tubes on mechanical rotator in fridge ( 4 °C)
    1. Cells need to be rotated to ensure proper binding
25. Incubate for 1 hr

**Secondary Antibody Suspension Staining:**

26. Spin down cells at 200 X G for 4 mins
27. Aspirate of solution
28. Rinse cells with 1 mL of ice cold PBS + 0.1% BSA
29. Repeat 16 – 28 a total of 3X washes
30. Prepare secondary antibody solution
    1. Antibody diluted in ice cold PBS + 0.1% BSA solution
    2. Alexa Fluro Goat Anti Mouse 488 1:400 dilution (12.5 µL in 1 mL)
31. Add 1 mL of antibody solution to their respective microcentrifuge tube
32. Place microcentrifuge tubes on mechanical rotator in fridge (4 °C)
33. Incubate for 40 mins - 1 hr
34. Spin down cells at 200 X G for 4 mins
35. Aspirate of solution
36. Rinse cells with 1 mL of ice cold PBS + 0.1% BSA
37. Repeat 34– 36 a total of 3X washes

If cells are for FACS and analysis or sorting occurs over 2 hrs after step 37 is completed, cells need to be fixed

38. Remove all solution from cells
39. Fix cells by incubating with 1 mL 0.1%-1% paraformaldehyde in PBS.
40. Place microcentrifuge tubes on mechanical rotator in fridge (4 °C)
41. Incubate for 10 – 20 mins
42. Spin down cells at 200 X G for 4 mins
43. Aspirate of solution
44. Rinse cells with 1 mL of ice cold PBS + 0.1% BSA
45. Repeat wash 2X total

# Appendix L - Immunofluorescent staining of 2D plate

- *Use protocol when staining for markers on cell surface and between cells*
- *Adapting protocol from fibrin gels will results in cell contraction and possible removal of cell adherence to plate*

**Fixation**

1. Warm up paraformaldehyde to RT
2. Aspirate media off of plated cells
3. Quickly rinse cells in PBS for second with equal volume of PBS to media
4. Rinse for a total of 2X
    1. DO NOT leave PBS on cells as it will cause them to contract
    2. This is due to Mg and Ca ions present in DPBS powder
    3. If no, Mg or Ca, PBS can be left on longer
    4. Add PBS and then remove almost immediately for rinse. If less than 10 wells, can add PBS to all wells first and then aspirate PBS off
5. Add 4% paraformaldehyde to cells. Volume to use is half of media volume used to culture cells
6. Fix cells for 10 minutes at RT.
    1. Do not fix for longer than 10 mins as it could affect cell integrity
    2. Paraformaldehyde is used to ensure integrins stay bound to TCP and keep cells adherent

**Permeabilization and blocking**

7. Permeabilize for 10 min at RT with 0.1% TBS-T (Trition-X100)
8. Can leave cells in TBS-T for extended periods of time and before blocking
9. Block cells in 2% BSA dissolved in 0.1% TBS-T (Tween 20 pH 7.4) for at least 1 hr RT or overnight at 4 C

**Antibody Staining:**

10. Dilute primary antibody in 2% BSA dissolved in 0.1% TBS-T. Volume to add is equal to culture media volume
    1. CD31 [DAKO, Clone JC70A] 1:200
    2. VE-Cadherin [Invitrogen, BV-9, MA1-198] 1:200
    3. VWF [Invitrogen, MA5-14029,  ] 1:200
11. Incubate for 1 hr at RT
12. Rinse 3X with PBS at RT for 5 min
13. Dilute secondary antibody in 2% BSA dissolved in 0.1% TBS-T. Volume to add is equal to culture media volume
    1. Goat anti-mouse alexa fluro 488 1:450

2. Can add DAPI at this step, (1:500)

14. Rinse 3X with PBS at RT for 5 min
15. Cells can be stored in 0.1% TBS-T until microscopy is performed.

# Appendix M – Fluorescent Microscopy and Quantification of In Vitro Vascular Networks in Fibrin Gels

**Microscope Set-Up**

1. Turn on the microscope computer
2. Login to PutnamOlympus. Password: rhoa
3. Take the cover off the microscope
4. Turn on microscope (Olympus 1x2), mercury lamp, camera controller (hamamatsu), and slide controller (prior)
5. Record mercury lamp "ON" hr on data sheet next to microscope
6. Open metamorph premier on computer
7. Once open, on top tool bar, go to "AQUIRE". On the drop down menu, click "AQUIRE"
    1. This opens a window which controls exposure, binning, gamma, and scaling
8. In the window, the buttons do the following:
    1. AQUIRE – takes a picture of current field of view
    2. SAVE IMAGE – takes a picture of the current field of view and saves to a specified location
    3. SET SAVE – specify location to which save image button will save
    4. SAVE W/ SEQUENCE – automatically increment next image save file after you take an image using the save image button
    5. AUTO EXPOSE- determines optimal exposure for sample you are imaging (DO NOT USE)
    6. IMAGE GAMMA- increase or decreases the gamma
    7. IMAGE SCALING – set which band of light the camera will pick up (LEAVE AT MAX)
    8. AUTO SCALING – automatically sets the best exposure limits (max and min) for image
9. Click the show live button. This will open up a new window showing you your sample live
10. The buttons on the left screen do the following:
    1. BINOCULARS – look through the microscope eye piece
    2. CAMERA – will look through the standard microscope camera
    3. CIRCLE/DOT – will use the disc spinning unit
    4. RED - for mCherry/Red filter (580 μm)
    5. GREEN – is for GFP/Green filter (480-560 μm)
    6. BLUE – is for DAPI/blue filter (405-420 μm)
    7. GREY – brightfield (standard lamp)
11. Set filter to desired filter and camera

12. On tool bar, click APPs
13. On scroll down list, click “multi-dimensional acquisition”
14. In the new window, click “main”. From here you can select multiple stage positions to take images of multiple locations or select multiple wavelengths (if you need to take multiple images at different wavelengths)
15. Click “SAVING”
16. Click “select directory”
17. Pick where you want images to save (this is different from SAVE IMAGE discussed prior)
18. After you pick a location, set base name
19. Check “increment base name” to automatically increment file name for multiple images
20. Click exposure and set exposure time
21. Click stage and click position location
22. Delete all previous locations by clicking the red “X” in the window
23. Set name of your location in the position label field
24. Click “load” to load a previous stage position file
25. Click “save” to save you current. Stage positions list to a file
26. On the top tool bar, click “devices”
27. On the scroll down menu, go to stage, and click “move stage to absolute position”
28. Using the Prior stage controller, move microscope stage to one corner. Pick a corner and remember which corner you picked

- By moving to one corner, microscopy stage will not be able to move any more in those directions. This is how you know you have reached the corner

29. In “move stage position to absolute corner” window, click “set origin”

- This will set the (X,Y) origin at the corner
- Do this so your stage positions will always be relative to this corner
- This will protect you and your stage positions if:
    - 1. You image on multiple days
    - 2. The camera stage messes-up/sticks

**Fluorescent Imaging:**

30. Move stage using stage controller to desired location of sample (Use the “live” window to view location)
31. Focus using the microscope dials to obtain best focal plane or get the image in focus
32. On “multi-dimensional acquisition” window, make sure you are on stage tab
33. Click the black “+” button to set current stage position
34. You have two options now:
    1. Continue moving stage to all locations you want to image and then take pictures (steps 34 – 38)
    2. Take a picture of current location and then move to next location (steps 41 – 44)
35. For the earlier option, using microscope stage controller move to next position
36. Adjust focus
37. Click the black “+” button on the “multidimensional” window to save current position
38. Repeat 34-36 until all sample images are taken
39. Once done, click “acquire” on “multidimensional acquisition”

1. This will take a picture at all locations you just specified at the desired exposure set in step 2- and save to the location in step 17

40. Once complete, click save on "multi dimensional window"
41. Choose a location on computer to save you position locations for future use.

42. For the latter option, on "Acquire" window, click save image
43. Using the microscope control, move to the next position
44. Adjust focus
45. Repeat 41-43 until all sample images are taken
46. Repeat if you have multiple slides, dishes, or plates you need to image
47. Once complete, turn off all microscope components
    NOTE: Mercury lamp needs to be on for 1 hr after turning it on before turning off again. IF it hasn't been 1 hr wait to turn lamp until 1 hr has passed from turning it off
    NOTE: Mercury lamp needs to cool down for 1 hr after turning off. If someone else is going to use the microscope within an hour, leave the lamp on
48. On record sheet, write down lamp off hours, time turned off and your name
49. Turn of computer
50. Put microscope cover back on

General Notes:

- Exposure times:
  10-20 for brightfield
  100-200 for DAPI/BLUE
  200-250 for GFP/GREEN
  200-300 for mCHERRY/RED
- On the show live screen window, on the left side there are 5 buttons. Look at the button that looks like a balance
  - The number next to the balance icon should say 12 to get best images
  - If it doesn't, increase exposure time
- On acquire window, look at black box with green bars, this is a histogram of the image exposure
  - Best images will have histogram bars peaking near the middle (Adjust exposure to do so)

**Quantification of vessels:**

1. Open metamorph
2. Open images you want to quantify. Either:
   1. File -> Open and find your images
   2. Drag and drop from your folder into metamorph
3. On the top tool bar, click "APPS"
4. Go to "Angiogenesis Tube Formation" and click. A new window should appear
5. Oon main computer desktop, go to start menu, and open up a new excel file
6. Once excel is open go back to metamorph
7. On the top tool bar, go to "Log" and click "Summary log" on the drop down menu
8. A new window should appear. Click OK
9. A second window should appear. On this window make sure Microsoft excel is selected

10. In the same window, name the sheet you will write to, and select the column and row you want to start writing to.
11. In the "Angiogenesis Tube" window, click the top button which says source
12. On the drop down menu, select image you want to quantify
13. Check min, and max tube width values and make sure they are set to "3" and "60" respectively
- These values set the minimum and maximum width the program will consider a tube
- You can adjust these if your vessels are smaller or wider

14. Next, you need to set the threshold value. The default is 100.
    1. To set the optimal threshold for your image, drag mouse cursor over the image
    2. On the bottom of metamorph, as you move the cursor, numbers will change. The first 2 are position (x.y) and the third is intensity
    3. Determine the intensity of the background (place mouse over background and record intensity value)
    4. Place mouse cursor over vessel and record intensity value
    5. The threshold you should use is Intensity of vessel – Intensity of background
    6. Threshold value should be adjusted by a bit (20 – 50 lower than calculated to account for fluctuations in sprout intensity)
15. After the threshold value are set, click "start"
16. The module will begin to quantify the sprouts. Once done it will write the values to the excel file you opened
17. Repeat will all the images you need to quantify.
18. Save the excel file when you are finished and turn everything off.

**Optional:**

If there is too much background noise use the following steps:

19. Open ImageJ
20. Open Image you are quantifying in ImageJ
21. Crop image to only have vessels in the frame
- You can use selection tool to crop around vessels

22. Save the image
23. Open the cropped image in metamorph
24. On the top tool bar, click measure
25. Then click, "calibrate distances"
26. A new window should appear. Click the cropped image
27. In the "calibrate" window, select the focal lens used (4x, 10x, etc.)
28. Click apply to the image
29. Follow steps 11-17

# Appendix N – Degradation of Fibrin Gels using Natto Kinase

**Preparation of Natto Kinase**

1. Prepare 1 mM of EDTA in PBS
2. Calculate amount of Natto kinase ((NSK-SD, Japan Bio Science Laboratory Co. Ltd.)
3. needed
    1. Need 50 FU/ mL (FU = fibrin degrading unit)
    2. FU/ g varies by lot
4. Measure out Natto kinase and add respective amount to EDTA-PBS solution
5. Natto kinase can be prepared and stored for up to a week

**Degradation of Fibrin gels**

6. Warm up Natto Kinase solution in water bath to 37 °C
    1. Only warm up amount on Natto Kinase needed
    2. Do not warm up solution multiple time as it will degrade or affect Natto Kinase activity
7. Remove media from fibrin gels
8. Rinse gels with PBS
9. Aspirate off PBS
10. Add Natto Kinase to gels. Volumes to add is equal to gel volume.
11. Using a pipette tip, metal measuring spoon, or other small tool, gently move/disassociate gel away from edges of gel
12. Gently separate gel from bottom of well. This will ensure uniform degradation of gel and speed up degradation
13. Incubate gel in Natto Kinase solution at 37 °C until gel degrades. Typically, 35-45 mins, but could vary. Should not take more than 1 hr (See note below)
14. Once gel is degraded, spin down solution and cells at 200 X G for 5 minutes
15. Aspirate off degrade fibrinogen from cells
16. Rinse cells in PBS and spin down at 200 X G for 5 minutes.
17. Aspirate off PBS and proceed with experiment

*Optional:*

NOTE: If large constructs still appear in solution after an hour or incubation with Natto Kinase, fibrin may all be degraded, but a cell sheet may be present.

18. Incubate cells/cell sheet in 1 mL trypsin for 5 mins at 37 °C.
19. Neutralize trypsin with 1 mL of culture media and Spin down solution and cells at 200 X G for 5 minutes
20. Aspirate off solution from cells and proceed with experiment

**** This procedure was used to harvest vasculature from fibrin gels for western blot, qPCR, and gel zymography experiment

****Can also be used to harvest cells that are cultured on-top of fibrin gels in a monolayer as trypsinization is not effective.

# Appendix O – Inhibition of Proteases in Fibrin Gels

** Follow protocol in Appendix I for synthesis of fibrin tissue constructs with embedded cell coated microcarrier bead

**Inhibition of Capillary Morphogenesis:**

1. Prepare inhibitor solutions
    1. BB2516 stock concentration of 100 mM
    2. Aprotinin stock concentration 10 mg/mL (1540 μM)
    3. Dilute 0.2 μL of BB25126 in 2 mL of DMSO (10 μM final concentration)
    4. Dilute 0.4 μL of BB25126 in 2 mL of DMSO (20 μM final concentration)
    5. Dilute 2.2 μL of aprotinin in 2 mL of DMSO (2.2 μM final concentration)
       NOTE: Aprotinin can be diluted in water, but to remain consistent with BB2516 DMSO was used as diluent
    6. Dilute 0.2 μL of BB25126 and 2.2 μL of aprotinin in 2 mL of DMSO [For DUAL condition]
2. As fibrin gels are polymerizing, prepare inhibitor-media solution
3. Calculate out amount of media needed for each inhibitor condition. (1 mL per gel per inhibitor condition)
4. Add respective amount of media to a centrifuge tube
5. Add 10 μL of inhibitor solution per 1 mL other respective media
    1. i.e. 180 μL of BB2516 inhbitor solution (10 μM concentration) to 18 mL of EGM-2
       Note: Final concentration will be 0.1 μM BB2516
6. For vehicle control, Add 10 μL of DMSO per 1 mL of media
7. Once gels are done polymerizing, add respective media-inhibitor solution to the respective gels
8. During each media change, make new media-inhibitor solution and add this solution over standard media. If inhibitors are not added at each media change, vasculogenesis may no longer be inhibited

**NOTES for inhibitor studies for present research**

- Inhibitor Concentration are much lower than previous documented or used within the lab
- Concentrations listed above (0.1 and 0.2 μM for BB2516 and 22 nM for aprotinin) are the FINAL concentration for iPSC-ECs experiments. These values are at least 2-10x the IC50 values for the respective proteases to be inhibited

- While 0.1 and 0.2 μM for BB2516 and 22 nM for aprotinin was used, it is POSSIBLE to increase stock concentration (Step 1.3-5) to 1 mM, 2 mM for BB2516 and 220 μM for aprotinin, so final concentrations are actually 10 μM, 20 μM, and 2.2 μM respectively
- 10 μL for vehicle control may be excess as well.
    - Consider using only 1 μL of vehicle control and adjust inhibitor concentrations accordingly

# Appendix P – Cell Lysis for Protein Harvest

**Solutions**:

*RIPA Lysis Buffer* *(store at 4* °C)

| | For 100 mL solution: |
|---|---|
| 150 mM of NaCl | 0.87735 g NaCl |
| 1.0% Trition-X 100 | 1 mL Trition-X 100 |
| 0.5% Sodium Deoxycholate | 0.5 g Sodium Deoxycholate |
| 0.1% Sodium dodecyl sulfate (SDS) | 0.1 g SDS |
| 50 mM Tris (base) | 0.607 g Tris |

*Protease Cocktail* *(store at* -20 °C)

Aprotinin, 10 mg/mL (1000x) in ddH2O
Leupeptin, 10 mg/mL (1000x) in ddH2O
Pepstatin A, 1 mg/mL (1000x) in methanol
PMSF, 100mM (100x) in anhydrous isopropanol
EDTA 500mM (100x) in ddH2O
Sodium Fluoride, 500 mM (100x) in ddH2O
Sodium Orthovanadate, 100 mM (100x) in ddH2O

For 1 mL aliquots,
Aprotinin - add 1 mL of H2O to 10 mg
Leupeptin – add 1 mL of H2O to 10 mg
Pepstatin A, 5 mL of methanol to 5 mg, place in water bath on hot plate until it dissolves (60 °C)
- Won't fit in brown bottle pepstatin arrives in

PMSF – 17.41 mg in 1mL of anhydrous isopropanol
Can be thawed multiple times
Warm up to RT before opening
After using anhydrous isopropanol, vent with extra dry N2 for 20 secs in hood
EDTA – 146.115 mg in 1 mL of H2O, adjust pH to 8.0 to dissolve
Sodium Fluoride – 41.0 mg in 1 mL of H2O
Sodium Orthovanadate – 18.38 mg in 1 mL of H2O

* Note: Alternative to house made protease cocktail is **Thermo Scientific™ Halt™ Protease and Phosphatase Inhibitor Cocktails with EDTA** [PI78442]
- Still need to add Pepstain A and PMSF

**Cell lysis:**

1. Thaw protease inhibitors on ice
2. Add protease inhibitors to RIPA lysis buffer
    1. For 1 mL of cell lysis solution
        1. 0.2 µL of 1000x aprotinin
        2. 1 µL of 1000x leupeptin
        3. 1 µL of 1000x Pepstatin A
        4. 10 µL of 1000x PMSF
        5. 10 µL of 1000x EDTA
        6. 10 µL of 1000x Sodium Fluoride
        7. 10 µL of 1000x Sodium Orthovanadate
    2. If using Halt Protease Cocktail, (skip 1-8), for 1 mL of RIPA lysis
        1. 10 µL of single use cocktail
        2. 10 µL of EDTA
        3. 1 µL of 1000x Pepstatin A
        4. 10 µL of 1000x PMSF
3. Cool PBS, cell lysis buffer, and microcentifuge tube on ice
4. Place cell scrapper in freezer to cool
5. Once cooled, remove cells from incubator and place on ice
6. Aspirate off old media
7. Wash cells with 10 mL of ice cold PBS
8. Aspirate off PBS
9. Add 0.5 mL per 5M cells of ice cold lysis buffer to flask using P1000
    1. Add in a line at top of flask
    2. Have flask angled downward on ice
10. Using a prechilled ice scraper, scrap down cells into lysis solution
11. Gently transfer solution to precooled microcentrifuge tube
12. Centrifuge at 4 °C for 30 mins at 12000 RPM
13. Remove tubes from centrifuge and place on ice
14. Pipette supernatant into a precooled microcentrifuge tube
    1. Supernatant is where protein is located
    2. Make sure you do not pipette any cell debris pelleted at bottom of tube
15. Preform a BCA assay to measure protein concentration (See appendix Q)
16. Store protein in -80 °C freezer

Note: Whenever using protein samples are harvesting, ALWAYS keep on ice and thaw on ice. Protein warming could denature or degrade proteins

# Appendix Q - BCA Protein Concentration Assay Protocol

** Protocol adapted from Thermo Fisher Pierce BCA Protein Assay Kit [23225]*

1. Thaw samples on ice if needed
2. Prepare BSA standard stock for standards
    a. Make 5 mLs at 2mg/mL in 15 mL centrifuge tube
    b. May need to make larger stock to accurately measure BSA
3. Prepare standards in microcentrifuge tube accordioning to following table

| Vial | Vol. of Diluents (µL) | Vol. of Stock (µL) | Protein Conc. (µg/mL) |
|---|---|---|---|
| A | 0 | 300 of stock BSA | 2000 |
| B | 125 | 375 of stock BSA | 1500 |
| C | 325 | 325 of stock BSA | 1000 |
| D | 175 | 175 of vial B | 750 |
| E | 325 | 325 of vial C | 500 |
| F | 325 | 325 of vial E | 250 |
| G | 325 | 325 of vial F | 125 |
| H | 400 | 100 of vial F | 25 |
| I | 400 | 0 | 0 |

**Table 1: Solution Prep for BCA Assay**

- Diluent is cell RIPA lysis buffer without protease inhibitors (see appendix P)

4. Prepare working reagent (WR) in centrifuge tube
    1. Need (9 + # of samples) x 2 mLs of WR
    2. Make at 50:1 ratio of BCA reagent A to BCA reagent B

**For centrifuge tube protocol:**

5. Pipette 0.1 mL of each sample into separate 15 mL centrifuge tube
6. Pipette 0.1 mL of each standard (A-I) into separate 15 mL centrifuge tube
7. Pipette 2.0 mL of WR into each centrifuge tube
8. Incubate in water bath for 30 mins (37 °C)
9. Cool all tubes to RT
10. Set spectrophotometer to photometric mode
11. Go to set up, change wavelength to 562

12. Place 1 mL of water in a cuvette
13. Calibrate/zero spectrophotometer to water
14. One at a time, measure each standard in a new cuvette and record absorbance
15. Measure each sample/unknown in a new cuvette and record absorbance

**For microplate protocol:**

16. Pipette 25 µL of each standard into a microplate well (96 well plates)
17. Pipette 25 µL of each sample/unknown into a microplate well (96 well plates)
18. Add 200 µL of the WR to each well and mix thoroughly on a plate shaker for 30 secs
19. Cover plate and incubate at 37 °C for 30 mins (Typically used bacteria incubator)
20. Cool plate to RT
21. Using a plate reader, measure absorbance at 562 nm

**Determine Protein Concertation**

22. Subtract standard I from all other samples and standards
23. Plot on graph standard vs absorbance (X - Y)
24. Fit a $2^{nd}$ order polynomial curve to graph
25. Using sample absorbance (Y), solve for sample protein concentration (X)
26. Throw away cuvettes, standards, and tubes in hazardous waste bin

# Appendix R - Western Blot Electrophoresis and Transfer Protocol

**Solutions**:

*6X reducing laemlli sample buffer (store at -20* °C) — For 10 mL solution:

| | |
|---|---|
| 12% SDS | 1.2 g SDS |
| 30% Mecaptoethanol | 3 mL of mecaptoethanol |
| 60% Glycerol | 6 mL of 100 % glycerol |
| 0.012% Bromophenol blue | 1.2 mg Bromophenol blue |
| 375 mM Tris-HCl pH 6.8 | 1 mL of 3.75 M |

Note: Dissolve SDS, mercaptoethanol and bromophenol blue in Tris-HCl first before adding glycerol

*Running Buffer PAGE 1X Tris-Glycine (store at 4* °C) — For 1L stock solution:

| | |
|---|---|
| 25mM Tris Base | 3.0375 g of Tris |
| 190 mM Glycine | 14.26 g of Glycine |
| 0.1% Sodium dodecyl sulfate (SDS) | 1 g SDS |
| dd H2O | 1000 mL of H2O |
| ** DO NOT pH adjust ** | |

*Transfer Buffer (store at 4* °C) — For 1L stock solution:

| | |
|---|---|
| 4% Tris-glycine buffer (25X) i.e 1:25 dilution | 40 mL of Tris-Glycine |
| 20% Methanol | 200 mL of methanol |
| DI H2O | 760 mL of H2O |

*Tris-Glycine Buffer (25X) (store at RT*) — For 500 mL stock solution:

| | |
|---|---|
| Tris base | 18.2 g of Tris |
| Glycine | 90 g of glycine |
| DI H2O | 500 mL of H2O |

Note: Add tris and glycine to 400 mL of ddH2O
Place on water bath to dissolve
Bring final volume to 500 mL
Shelf life 6 months at RT

**Electrophoresis:**

1. Place 300 mL of water in a larger beaker and place on hot plate to boil
2. Calculate amount of protein volume need for experiment (Typically loading 20 – 40 µg will suffice)
3. Calculate how much laemilli buffer (6X) to add to each sample (typically 6 µL if loading at max volume of 36 µL)
4. Calculate out amount of DI water to add to each sample
   (Water vol. = Total Vol. – protein vol. – laemilli vol)
   e.g. Water vol. = 40 µL – protein vol. – 7 µL
5. Thaw protein samples on ice
6. Add protein, water, and laemilli buffer to microcentrifuge tube
7. Boil samples at 97 °C for 8 mins in water on hot plate
8. Place samples on ice when done
9. While samples are boiling, assemble electrophoresis chamber
    1. Take out 10% Tris-glycine gel and cut open packet
    2. Remove tape from bottom of gel cassette
    3. Carefully remove well comb from top of cassette
    4. Check to make sure all wells are intact
    5. Rinse wells 2X with running buffer. Shake out between rinses
    6. Place gel in electrophoresis machine. If using one gel, place blocker/blank slide into another slot
    7. Pour 200 mL of running buffer into electrode side of electrophoresis machine or until wells are submerged in buffer
    8. Pour ~600 mL of running buffer into out chamber or until buffer is 80% near top of chamber
10. Using special loading tips, add 10 µL of kaleidoscope marker to first well
11. Add molecular weight marker to last well (Typically 3 - 5 µL)
12. Add samples/unknowns to wells as desired. Try to balance so samples are in the middle of the gel
13. If less samples than number of wells, and blanks (30 µL water + 6 µL laemilli loading buffer) to wells not being used to balance running lanes.
14. Place electrophoresis lid on chamber
15. Turn on machine
16. Select Tris-Glycine gel setting
17. Enter # of gels
18. Run for 1 hr 30 mins @ 125 V

- May run longer if protein bands need more separation

**Protein Transfer**

19. 10 minutes before electrophoresis is done, soak 5 sponge pads, 2 filters in transfer buffer in western blot tray
20. Cut out PVDF membrane to template size. Cut off one corner of membrane to remember orientation
21. Soak PVDF membrane in methanol for 1 – 2 mins
22. Quickly transfer membrane to deionized water to rinse
    *** DO NOT let membrane dry out

23. Soak membrane in transfer buffer
24. Once electrophoresis is done, remove gel cassette
25. Using gel knife, beak open cassette.
26. Using the gel knife, cut off top wells and discard
27. Cut off foot of gel and discard
28. Place a presoaked filter paper on top of gel
29. Flip gel and filter paper over
30. Using gel knife, remove gel carefully from cassette.
31. Transfer presoaked PVDF membrane on top of gel. Place notched corner near top of gel next to kaleidoscope marker lane
32. Place presoaked filter paper on top of membrane
33. Using glass pipette, gently roll out air bubbles
34. Assemble transfer cassette
    1. Place 2 soaked sponge pads on cathode (-, back) of cell blot apparatus
    2. Place filter paper, gel, membrane sandwich on top of pads
       **** NOTE: Gel should be closest to back of cell blot and PVDF membrane closest to front of apparatus. If reversed, transfer WILL NOT occur.
    3. Place 3 soaked sponge pads on anode side (+. Front)
    4. Place front lid on top and close cell lock
35. Hold blot module firmly and place into cell sure lock apparatus
36. Fill cell blot [where gel and membrane are] with transfer buffer (~200 mL)
37. Fill buffer chamber ice
38. Add deionized water to buffer chamber with ice
39. Place lid on top of chamber. Set to WB setting
40. Set to 25 V, 165 mA for 3 hrs
41. While waiting, clean up excess buffer and discard in appropriate waste containers
42. Throw away cassette a gel pieces in hazardous waste bin
43. Pour 50 mL of 5% BSA in TBS-T (Tween 20) solution into a block tray
    Note: DO this step before removing membrane so membrane doesn't dry out
44. Once transfer is complete, remove PVDF membrane and place in tray with BSA solution
45. Cover with parafilm
46. Block overnight at 4 °C

# Appendix S - Western Blot Staining and Development Protocol

**Solutions**:

*P-Coumaric solution* — For 2 mL solution:
- 90 mM p-Coumaric — 0.02894 g of p-coumaric
- DMSO — 2 mL of DMSO

*Luminol solution* — For 2 mL solution:
- 250 mM luminol — 0.0885 g of luminol
- DMSO — 2 mL of DMSO

*Activator Solution A* — For 5 mL solution:
- 100 mM of Tris-HCl pH 8.6 — 5 mL of Tris -HCl
- 0.06% Hydrogen Peroxide (30%) — 3 µL of Hydrogen Peroxide

Note: DO NOT prepare solution early. Prepare when mentioned in protocol

*Activator Solution B* — For 5 mL solution:
- 100 mM of Tris-HCl pH 8.6 — 5 mL of Tris -HCl
- 0.44% p-coumaric — 22 µL of p-coumaric solution
- 1% Luminol — 50 µL of luminol solution

Note: DO NOT prepare solution early. Prepare when mentioned in protocol

*Developer solution (store at RT)* — For 500 mL stock solution:
- Kodak Developer powder — 80 g of developer
- DI H2O — 500 mL of H2O

Note: May need to be stirred to dissolve

*Fixer solution (store at RT)* — For 500 mL stock solution:
- Kodax Fixer powder — 92 g of fixer
- DI H2O — 500 mL of H2O

**Primary Antibody Staining:**

1. After membrane was blocked, prepare 5 mL of antibody solution in 50 mL tube
    1. Dilution of primary antibody in 5% BSA dissolved in TBS-T (Tween 20)
    2. MT1-MMP [Abcam: EP12647 (ab51074)] - 1:2000 dilution

    3. MMP-2 [Abcam CA-4001 (ab3158)] - 1:400 dilution
    4. MMP-9 [Abcam 56-2A4 (ab58803)] - 1:400 dilution
2. Using clean gloves, remove PVDF membrane from blocking tray
3. Roll membrane and place inside tube. Top side of membrane should be oriented to face top of tube.
4. Cap centrifuge tube and place on rotary rack. Rack should rotate so solution flow is parallel to bands
5. Incubate at RT for 1 hr 30 mins
6. Pour TBS-T (Tween 20) into wash tray
7. Remove PVDF membrane from centrifuge tube and place in wash tray
8. Rinse 6X for 5 mins each at room temperature with gentle agitation

**Secondary Antibody Staining**

9. During last wash, prepare 5 mL of secondary antibody solution in 50 mL tube
    1. Dilution of secondary antibody in TBS-T (Tween 20)
    2. Pierce Goat Anti-Rabbit HRP [Thermo Fisher: (31466)] - 1:10000 dilution
    3. Pierce Goat Anti-Mouse HRP [Thermo Fisher (31431)] - 1:10000 dilution
    4. GAPDH HRP - 1:2000 dilution
10. Using clean gloves, remove PVDF membrane from blocking tray
11. Roll membrane and place inside tube. Top side of membrane should be oriented to face top of tube.
12. Cap centrifuge tube and place on rotary rack. Rack should rotate so solution flow is parallel to bands
13. Incubate at RT for 1 hr 30 mins
14. Pour TBS-T (Tween 20) into wash tray
15. Remove PVDF membrane from centrifuge tube and place in wash tray
16. Rinse 6X for 5 mins each at room temperature with gentle agitation

**Protein Band Visualization and Development:**

17. Prepare developer and fixer solutions
    1. Kodak Fixer
    2. Kodak Professional Developer D-19
18. During last rinse of secondary solution prepare developer trays
    1. Pour 500 mL of developer solution into developer tray
    2. Pour 500 mL of fixer solution into fixer tray
    3. Pout 500 mL of DI water into rinse tray
19. Prepare Activator Solution A and Activator Solution B
20. After final rinse, bring tray with membrane, developer trays, and activator solutions into dark room
21. Turn off lights, and block any excess sources of light (cracks)
22. Turn on red lamp in dark room.
23. Remove membrane and place in new tray
24. Mix Activator Solution A and Activator Solution B together
25. Add 2 mL of mixed solutions directly on top of membrane in tray. Make sure enough solution is added to completely cover on side of membrane
26. Allow activate solution to incubate for 1 min

27. Turn off red light to see if bands are illuminating
    1. If not, allow a few extra minutes of incubation with activator solution
    2. If bands still aren't seen, it possible bands are still present but just faint signal
28. Turn red lamp back on.
29. Place membrane in heat seal bag and seal off all but 1 side of bag.
30. Remove any bubbles from the bag. Use finger to push bubbles away from membrane. Bubbles can affect band visualization on film
31. Seal off final side of the bag.
32. Tape bag inside of x-ray cassette
33. Turn of red lamp
34. With the lights off, find x-ray film box
35. Remove 1 x-ray film from box and place inside x-ray cassette
36. Close x-ray cassette and exposure film for 30 seconds
37. While film is being exposed, close x-ray film box, to ensure no light ruin film
38. After set exposure time, remove film and place in developer tray
39. After 30 seconds, turn red lamp back on
40. After a few minutes of film being in developer solution, while rocking, bands should start to appear. Incubate films in developer for set period of time for each film (~4-5 mins)
41. Pick up film and shake off of excess developer
42. Place in fixer tray
43. Rock fixer tray for 3-5 mins
44. Place in DI tray
45. Repeat 33-43 for varying exposure times
    1. IF bands are too dark after first exposure, shorten exposure time
    2. If bands are faint after first exposure, increase exposure time
46. Turn on lights
47. Hang up each film to dry
48. Record exposure time for each film
49. Pour developer and fixer solutions into bottle. These can be reused multiple times (~20 films)
50. Throw away other solutions and materials into proper waste bins
51. Place PVDF membrane bag into freezer. Membrane can be restained in the future if needed
52. ****Rinse and dry developer trays****
    1. Developer and fixer trays that are not cleaned/maintained properly can lead to dirty films or increased background on films

# Appendix T - Gel Zymography Protocol

**Solutions**:

*5X non-reducing sample buffer (store at -20* °C)

| | For 25 mL solution: |
|---|---|
| 4% SDS | 1 g SDS |
| 20% Glycerol | 5 mL of 100 % glycerol |
| 0.01% Bromophenol blue | 2.5 mg Bromophenol blue |
| 125 mM Tris-HCl pH 6.8 | 0.491 g Tis base pH balanced |
| H2O | 19.58 ml of DI H2O |

Note: add 15 ml of H2O at first. Wait until all is dissolved/bubbles gone and add remaining H2O to bring volume to 25 mL

*Running Buffer PAGE 1X Tris-Glycine (store at 4* °C)

| | For 1L stock solution: |
|---|---|
| 25mM Tris Base | 3.0375 g of Tris |
| 190 mM Glycine | 14.26 g of Glycine |
| 0.1% Sodium dodecyl sulfate (SDS) | 1 g SDS |
| ** DO NOT pH adjust ** | |

*MMP2+MMP9 Wash buffer (store at RT*)

| | For 250 mL solution: |
|---|---|
| 2.5% Trition X-100 | 6.25mL of 100% |
| 50 mM Tris-HCl pH 7.5 | 12.5 mL of 1M stock |
| 10 mM CaCL2 | 2.5 mL of 1 M stock |
| DI H2O | 228.75 mL of H2O |

*MT1-MMP Wash buffer (store at RT*)

| | For 250 mL solution: |
|---|---|
| 2.5% Trition X-100 | 6.25mL of 100% |
| 50 mM Tris-HCl pH 7.5 | 12.5 mL of 1M stock |
| 10 mM CaCL2 | 2.5 mL of 1 M stock |
| 200 mM NaCl | 10 mL of 5M stock |
| DI H2O | 218.75 mL of H2O |

*MMP2+MMP9 Incubation Buffer (store at RT*)

| | For 500 mL solution: |
|---|---|
| 1% Trition X-100 | 5 mL of 100% |
| 50 mM Tris-HCl pH 7.5 | 25 mL of 1M stock |
| 10 mM CaCL2 | 5 mL of 1 M stock |
| DI H2O | 465 mL of H2O |

*MT1-MMP Incubation Buffer (store at RT*)

| | For 500 mL solution: |
|---|---|
| 1% Trition X-100 | 5 mL of 100% |

| | |
|---|---|
| 50 mM Tris-HCl pH 7.5 | 25 mL of 1M stock |
| 10 mM CaCL2 | 5 mL of 1 M stock |
| 200 mM NaCl | 20 mL of 5M stock |
| DI H2O | 445 mL of H2O |

| *Coomassie Staining Solution (store at RT*) | For 500 mL solution: |
|---|---|
| 40% Methanol | 200 mL |
| 10% Acetic Acid | 50 mL of glacial acetic acid |
| 0.5% Coomassie blue dye | 2.5 g |
| dd H2O | 250 mL of H2O |

| *Destaining Solution (store at RT*) | For 1 L solution: |
|---|---|
| 40% Methanol | 400 mL |
| 10% Acetic Acid | 100 mL of glacial acetic acid |
| dd H2O | 500 mL of H2O |

**Electrophoresis:**

1. Calculate amount of protein volume need for experiment (Typically loading 5 – 15 µg will suffice)
2. Calculate how much laemilli buffer (5X) to add to each sample (typically 7 µL if loading at max volume of 35 µL)
3. Calculate out amount of DI water to add to each sample
   (Water vol. = Total Vol. – protein vol. – laemilli vol)
   e.g. Water vol. = 40 µL – protein vol. – 7 µL
4. Thaw protein samples on ice
   **** Activity will degrade! Keep samples on ice at all times!
5. Add protein, water, and laemilli buffer to microcentrifuge tube
6. Sample will not be denatured. DO NOT BOIL
7. Take out 10% Tris-glycine, 1% gelatin zymogram gel and cut open packet
8. Remove tape from bottom of gel cassette
9. Carefully remove well comb from top of cassette
10. Check to make sure all wells are intact
11. Place gel in electrophoresis machine
12. Pour 200 mL of running buffer into electrode side of electrophoresis machine or until wells are submerged in buffer
13. Pour ~500 mL of running buffer into out chamber or until buffer is 80% near top of chamber
14. Using special loading tips, add 10 µL of kaleidoscope marker to first well
15. Add 3X molecular weight volume to last well
    (If molecular weight maker used 4 µL for westerns, use 3X or 12 µL)

- Need higher amount due to dark background of the gel once stained

16. Add samples/unknowns to wells as desired. Try to balance so samples are in the middle of the gel
17. Place electrophoresis lid on chamber
18. Turn on machine
19. Select Tris-Glycine gel setting
20. Enter # of gels
21. Run for 1 hr 30 mins @ 125 V

- May run longer if protein bands need more separation

**Gel Incubation:**

22. While gel is running, make MMP wash buffer, incubation buffers, Coomassie stain, and destaining buffer
23. Once electrophoresis is done, remove gel cassette
24. Using gel knife, beak open cassette.
25. Using the gel knife, cut off top wells and discard
26. Cut off foot of gel and discard
27. Carefully, remove gel from cassette using gel knife and place in washing tray
    ** Be careful not to rip or damage gel
    ** OK is edges are torn because sample is near center of gel
    **** Use whatever method you find best to remove gel without destroying it
28. Add wash buffer (~50 mL) to tray
29. Gently agitate gel for 30 mins at RT
30. Remove washing buffer and add fresh washing buffer (~50 mL) to tray
31. Gently agitate gel for 30 min at RT
32. Remove washing buffer and add 50 mL of incubation buffer
33. Rinse for 10 mins at 37 °C with gentle agitation
    ** typically use bacteria flask incubator
34. Remove buffer and add 50 mL of fresh incubation buffer
35. Incubate for 16-24 hrs at 37 °C

**Gel Staining:**

36. Remove gels from incubator
37. Discard/decant incubation buffer from each tray
38. Pout 50 mL of Coomassie Solution into each tray with gel
39. Stain gel for 30 mins – 1 hr with gentle agitation
40. Decant Coomassie solution from gel
41. Gently rinse gel with DI H2O
42. Add 50 mL of destaining solution to tray until gel is completely covered
43. Roll up a kimwipe and place in tray alongside to absorb Coomassie stain
44. Place tray on orbital shaker and gently agitate for 15 mins
45. After 15 mins, discard destaining solution and kimwipe
46. Repeat 42-45 until bands can clearly be seen

** Bands will be white/clear. Proteases degraded gel, so negative space is what the band is

47. To save gels, add DI H2O to tray and cover so gels do not dehydrate
48. Gel images can be taken using scanner in the lab

# Appendix U - RNA Isolation Protocol

** Protocol adapted from Qiagen RNeasy Mini Kit [74104]*

* Note: RNA is sensitive to RNases which are present on every surface. Take extreme caution when isolating RNA and handling RNA sample to avoid contamination with RNase.

** Make sure all disposable used with RNA are RNase free and have only been handle with gloves

**Prepare Working Area:**

1. Ready hood in main lab area
    1. Remove all contents from hood
    2. Spray with 70% ethanol and wipe down hood
    3. Spray with RNAase Away and wipe down hood
    4. Spray a few spots on surface with 70% ethanol
    5. Place aluminum foil sheet on top of ethanol
    6. Repeat 2-3 on sheet of aluminum foil
    7. Spray RNAase on towel
    8. Wipe down all micropipetters with towel+RNAase and place on aluminum sheet
    9. Repeat 7 – 8 for pipette tips, tubes rack, sharpie, microcentrifuge tubes, and RNeasy Kit
        - DO for ANYTHING entering hood

**RNA Isolation:**

2. Cool PBS on ice
3. Place cell scrapper in freezer to cool
4. Once cooled, remove cells from incubator and place on ice
5. Aspirate off old media
6. Wash cells with 10 mL of ice cold PBS
7. Aspirate off PBS
8. Add the following amount of buffer RLT to cells
    1. 350 µL for < 5M cells
    2. 600 µL for > 5M cells
        a) Add in a line at top of flask
        b) Have flask angled downward on ice
    3. If using flask, scrape cells down into lysis buffer using prechilled cell scraper

Optional:

9. Remove lysis and cell suspension and add to QIAshredder tube to homogenize

10. Spin down from 2 mins at max speed in small centrifuge tube (provided in QIA shredder kit)

11. Add 1 vol of 70% ethanol (RNase free) to lysis (homogenized or not). i.e. 350 µL of ethanol for 350 µL lysis buffer or 600 µL of ethanol for 600 µL lysis buffer
12. Transfer up to 700 µL of sample to spin column (provided in kit)
    Note: If using 600 µL of buffer RLT, you will need 2 spin columns
13. Spin down at 12000 RPM for 1 min
14. Discard flow through (RNA is attached to membrane in spin column)
15. Add 700 µL of buffer RW1 to top of spin column
16. Spin down at 12000 RPM for 1 min
17. Discard flow through
18. Add 500 µL of buffer RPE to top of spin column
19. Spin down at 12000 RPM for 1 min
20. Discard flow through
21. Add 500 µL of buffer RPE to top of spin column
22. Spin down at 12000 RPM for 2 min
23. Discard flow through
24. Replace bottom collection tube with new 2 mL collection centrifuge tube
25. Spin down at max speed (~14700 RPM for 2 min to dry membrane
26. Place spin column in new 1.5 microcentrifuge tube (provided)
27. Add 30 µL to 50 µL of RNase free water to top of spin column (best to start at 30 µL unless you know you will have a lot of RNA)
28. Spin down for 1 min at 12000 RPM
29. Place samples on ice

**Measure RNA Concentration:**

30. Go to nanodrop machine to measure concentration
31. Start up Nanodrop Program
32. Choose nucleic acid
33. Add 1 µL of ultra pure water to nanodrop sensor
34. Blank machine
35. Rinse off nanodrop sensor with DI water
36. Dry sensor completely with Kimwipe
37. Add 1 µL of sample to sensor
38. Measure absorbance and record
39. Repeat 35-38 for each sample

40. Store RNA samples at -80 °C

********** **NOTE: Possible to harvest RNA from protein lysis samples. Add Buffer RLT directly to protein lysis.**

- Vol of Buffer RLT to use = 350 or 600 µL (depending on cell count) – vol of protein lysis

# Appendix V – First-Strand cDNA Synthesis Protocol

** Protocol adapted from Promega ImProm-II Reverse Transcription System [A3800]*

* Note: Store all components of kit in -20 °C and thaw on ice

** Make sure all disposable used with RNA are RNase free and have only been handle with gloves

**Primer Solution Preparation**

54. Place small, thin PCR tubes on ice. These tubes are specific to PCR. These are NOT small (0.6 mL) Eppendorf tubes
55. Thaw RNA samples on ice.
56. Remove Reverse Transcription Kit and thaw Primers, nuclease free water, ImProm-II 5X reaction buffer, MgCl2, dNTPs mix, RNasin Ribonuclease Inhibitor and Reverse Transcriptase on ice
57. Calculate amount of RNA for each sample.
    - **a.** Each experimental condition has to be the same amount of RNA loaded or results will be skewed during PCR
    - **b.** Depending on all concentrations of RNA, one will be limiting reagent for other conditions
    - **c.** Maximizing amount of cDNA is ideal
    - **d.** Max amount of RNA to load is 4.0 µL
    - **e.** E.g. *Sample 1* is 50 ng/µL and *Sample 2* is 75 ng/µL.
      Load 4 µL of *Sample 1* for a total of 200 ng of RNA.
      Load 2.67 µL of *Sample 2* for a total of 200 ng of RNA.
      Extra volume will be water for *Sample 2*
58. Calculate amount of water to add for each sample
    - *a.* 4.0 µL - Sample vol = Amount of water needed
    - *b.* Limiting reagent (RNA sample) will have no extra water added
59. Add RNA to PCR tube on ice
60. Add respective amount of H2O to each PCR tube
61. Add 1.0 µL of primer to each PCR tube
    - *a.* Oligo(dT) Primer binds to poly A tail
    - *b.* Random Primer binds to random sequence in RNA
    - *c.* Random primers can create first strand cDNA from all RNA types
    - *d.* Oligo primer is primer of choice is most cases, but random primer may be needed depending on protein of interest
    - *e.* For MMPs, random primer was used, but Oligo could be used as well

62. Close each tube tightly

**Primer Annealing:**

63. Bring PCR tubes on ice to PCR amplifier machine
64. Turn machine on (switch is in back)
65. Choose run, and find ImProm II program
    a. Some machines will already have a program ready, while others will need to be set manually
    b. Program set up for this experiment is the following
        i. 70 °C for 5 mins
        ii. 4 °C for at least 20 mins (best to set time to hold/infinite)
        iii. 25 °C for 5 mins
        iv. 42 °C for 1 hr
        v. 70 °C for 15 mins
        vi. 4 °C hold
66. Place small PCR blocker into machine to prevent small tubes from breaking (looks like a rectangle with small pegs in corner
67. Place PCR tubes into small holes in block. Larger holes are used for bigger PCR tubes/reactions
68. Close lid
69. Lock lid by turning until strong resistance is felt
70. Give lid an extra ¼ turn to ensure lid is properly sealed

**Reverse Transcription:**

71. While primer anneal, prepare reverse transcription reaction mix in sterile RNAse free 1.5 mL microcentrifuge tube. Recipe below is per sample (15 µL)
    a. 4.0 µL of ImProm-II 5X reaction buffer
    b. 1.0 µL of Reverse Transcriptase (RT)
    c. 1.0 µL of dNTPs
    d. 0.5 µL of RNAsin
    e. 1.2-6.4 µL of MgCl2
        i. Dependent on RNA size
        ii. Larger RNA (# of bases) need less MGCl2, while smaller RNA need more
        iii. For MMPs 4.9 mM = <u>3.9 µL MgCL2 was used</u>
    f. X µL of water
        i. Determined to bring final volume to 15 µL
        ii. Water vol = 15 µL – MgCL2 – Rnasin – dNTPS – RT – buffer
            Water vol = 15 µL – 3.9 µL – 0.5 µL – 1.0 µL – 1.0 µL – 4.0 µL
72. Vortex solution gently to mix
73. Keep on ice prior to adding to RNA
74. Once, primers are done annealing to RNA, pause program and remove PCR tubes
75. Spin tubes down for 10 seconds to collect condensate.
    Note: Need to use small microcentrifuge tube inside of a 1.5 mL centrifuge tube to spin down PCR tubes
76. Add 15 µL of reverse transcription reaction buffer to each 5.0 µL of RNA
    Note: Change tips between each addition to avoid cross-contamination

77. Close each tube tightly and bring PCR tubes on ice to PCR amplifier machine
78. Follow steps 14-17 to place tubes back into machine
79. Continue program. If 4 °C step was set to hold, will need to press skip to continue program
80. Once complete, store cDNA at -20 °C

# Appendix W – Quantitative PCR (qPCR) Protocol

** Protocol adapted from TaqMan Gene Expression Assays Protocol [PN 43333458N]*

* Note: Store all components of kit in -20 °C and thaw on ice

**Primer Selection**

1. Before to qPCR, primers need to be selected for your gene of interest
2. TaqMan [Thermo Fisher] assay has primers specifically designed and fluorescently labeled for specific genes
    1. No need to design primers
    2. Purchase directly form Thermo Fisher Catalog
3. TaqMan is more specific than SYBR green PCR as fluorescent tags are associated with primers. SYBR green has fluorescent dye in reaction mix which integrates between all double strand nucleic acids
4. If Thermo Fisher does not have primers, you will need to design you own for use with SYBR green
    1. Protocol will work for both SYBR green and TaqMan

**Reaction Mix Preparation:**

5. Thaw cDNA, and primers on ice. Keep lid on ice bucket because primers are photosensitive
6. Cool microcentrifuge tubes on ice. One per sample condition.
7. Prepare reaction mixture. Each sample to be tested will considered 1 reaction.
    1. 20.0 µL per reaction.
    2. Will need 2 replicates per sample
8. Calculate amount of cDNA needed
    1. Can load 1 ng to 100 ng
    2. Max cDNA volume is 20% of PCR mixture i.e. 4.0 µL if total reaction mixture is 20.0 µL
    3. 20.0 ng used for MMPs
9. Calculate amount of RNase-free water needed
    a) Determined to bring final volume to 20 µL
    b) Water vol = 20 µL – cDNA – Primers – TaqMan master mix
    Water vol = 20 µL – X µL – 1.0 µL – 10.0 µL
10. Add water to each precooled microcentrifuge tube
11. Add TaqMan Gene Expression Master Mix to each precooled microcentrifuge tube
    1. If using SYBR green, add SBYR mix here
12. Add primers (TaqMan Gene Expression Assay) to each tube

1. If using SYBR green, add designed primers here
2. MMP9
3. MMP2
4. MMP14
5. 18s

13. Add cDNA to each tube
14. Ensure each solution is properly mixed by pipetting
15. Centrifuge each tube briefly

**Quantitative Polymerase Chain Reaction**

16. Obtain a 96 well PCR plate. These plates are specific to each PCR machine.
    1. Plates used for Applied Biosystem 7500 Fast Real-Time system are MicroAmp Fast Optical 96-Well Reaction Plate with Barcode
17. Add 20 µL of each PCR reaction mix to a well. Ensure sample row and column is recorded to set up machine properly
18. Cover PCR plate with an PCR plate cover
    1. For aforementioned plate, use Optical Adhesive Covers
19. Centrifuge plate briefly to ensure all reaction mix is at bottom of well. 2 mins at 2000 RPM
20. Turn on PCR machine
21. Use air or compressed duster can to remove any dirt/dust from bottom to PCR plate
    1. Dust and debris can build up in PCR machine, leading to skewed results
22. Place PCR plate into machine and close
23. Run PCR program
    1. This guide will follow 7500 Fast Real-Time machine
24. On screen, under set up wizard, select design experiment
25. Enter experiment name in respective field
26. Choose machine type (7500 Fast PCR)
27. Choose quantification method
    1. Use ΔΔCt method for comparing the expression in two different cell population
28. Choose reagent used (TaqMan or SBYR Green)
29. Choose ramp speed/reaction time

    ******* USE STANDARD FOR TaqMan Gene Expression Master Mix**********

    - Only fast master mix can be used on fast setting
    - Original protocol from Thermo Fisher did not mention what speed for TaqMan Gene Expression Master Mix
    - Protocol Online from Thermo Fisher has been updated since to make this clear

30. Choose type template (cDNA)
31. Click plate set up
32. Enter target name for each gene testing
33. Enter sample names for each sample type
34. On plate layout window assign respective sample types and gene target to each well (Colors will vary depending on what program assigns)
35. Set up run program. Program should already be correct in system but double check
    1. Hold 50 °C for 2 mins
    2. Hold 95 °C for 10 mins

3. Cycle 95 °C for 15 seconds, then 60 °C for 1 min
4. Number of cycles 40
5. Ensure extend cycle box is checked to allow for ability to added extra cycles while running

36. Ensure everything from step 25-35 is correct and press run
    1. You DO NOT need to worry about reaction setup or ordering supplies as program prompts you
37. Program should take about 2 hrs to run
38. Depending on gene, amplification will occur at various cycles
    1. 18s ~ cycle 9
    2. MMP9 ~ 32
    3. MMP2 ~ 26
    4. MMP14 ~ 22
    5. GAPDH ~ 24
39. Extend cycles if needed, but if gene has not amplified by cycle 40, most likely gene of interest is not amplifying
    1. Possible problems could be primer, cDNA integrity, machine calibration, blocked PCR well in machine, old reagents and primers, etc.
    2. Extend cycle can only be performed once. Once an extra amount of cycle is added, you cannot add more cycle beyond that
40. Once machine runs all of its cycle, a Ct value will be given for each sample
41. Program can output results to an excel file which can then be saved
42. Remove plate from machine. Plate can be reused. Only use wells that we not used in previous experiments

**Calculating ΔΔCt**

43. ΔΔCt is taking the difference between two different populations to determine relative expression of one gene to another
44. ΔΔCt = [ (Experimental Gene of interest Ct value – experimental house keeping gene Ct) – (Control Sample gene of interest Ct – control house keeping gene Ct) ]
45. i.e. ΔΔCt = [ (Cell 1 MMP9 Ct value – Cell 1 18s Ct value) – Cell 2 MMP9 Ct value - Cell 2 18s Ct value) ]
    1. There a numerous house keeping genes (present is all cells) such as 18 s and GAPDH
    2. House keeping genes are to account for each cell types general cell activity/production
46. Fold change is expression is 2^ ( - ΔΔCt)

# Appendix X – In Vivo Subcutaneous Injection Protocol

** Protocol adapted from Ana Y. Rioja protocol*

**Materials:**

- Puralube® Vet Ointment – Sterile ocular lubricant (Dechra, Overland Park, KS)
- Small cotton-tipped applicators Cat. No. 23-400-115 (Fisher Scientific)
- Sterile alcohol prep pads (Fisherbrand®)
- Sterling nitrile sterile powder-free exam gloves. KC300 (Kimberly-clark, Roswell, GA)
- Polylined sterile drape field. (18 in. x 26 in.) Ref No. 697 (Bosse, Hauppauge, NY)
- Isoflurane
- Carprofen
- Additional materials: Cap, gown, mask, shoe covers, warming pad/blanket, heating lamp, nair hair removal, hair clipper, betadine antiseptic solution, forceps, and scissors, formalin, 20 mL vials, 70% ethanol.

**Cell Preparation for Injection Protocol:**

1. Culture cells (ECs, and stromal cells) prior to beginning experiment with accordance to standard cell culture practices
2. Take fibrinogen out of freezer and warm up to room temperature
3. To get amount of fibrinogen needed, calculate how many implants you need
    a. Each implant is 500 µL.
    **** Plan for (600 µL) so there is excess for injection
    b. Calculation is # of implant X 500 µL = # of mLs of fibrinogen solution needed
    c. Add 2 mL to # of mLs of fibrinogen solution needed to account for loss during filtering
    d. Divide *2.625 mg/mL* by the protein content and clottable content of the fibrinogen to get actual concentration (Typically listed on the bottle. Varies Lot-Lot)
    e. Multiply # of mLs of fibrinogen by actual concentration to get # of grams to measure
2. Measure out calculated fibrinogen and add to 50 mL centrifuge tube
3. In cell culture hood, add serum -free EGM-2 equal to the # of mLs of fibrinogen solution needed to centrifuge tube with fibrinogen**.**
4. Place fibrinogen solution in water bath to dissolve fibrinogen
5. Once dissolved, filter fibrinogen solution using a 0.22 µL filter into a clean centrifuge tube
6. Aspirate off old media of ECs and fibroblasts

7. Rinse with equal volume of PBS to media
8. Add appropriate amount of trypsin to each flask
    a. T-25 – 2 mL
    b. T-75 – 5 mL
    c. T-225 – 10 mL
9. Incubate for 5 mins at 37 °C
10. Verify cells are detached from plate using microscope
11. Once cells are detached, add equivalent amount of media + 10% FBS to cells to neutralize trypsin
12. Collect cells with serological pipette and add to centrifuge tube
13. Spin down cells at 200 X G for 5 minutes
14. Once cells are pelleted, aspirate off supernatant
15. Flick pellet of cells to break pellet apart
16. Create a suspension of cells for each implant in 30 μL FBS in a 1:1 ratio of ECs : stromal cells
    a. A final concentration of 4 million cells/mL
    b. Totaling 2 million cells per injection (500 μL)
    ***** Plan for (600 μL) so there is excess for injection
    c. While some implants may be the same condition, just different replicates or time points, have 1 centrifuge tube for each suspension. This is due to the time it takes after injection in mouse to polymerize implant. If only one large solution is made for each condition, fibrinogen will polymerize in tube before the next implant of same condition could be injected
17. Place cells and fibrinogen solution on ice and bring to surgery room
18. Thaw thrombin on ice

**Subcutaneous Injection Protocol:**

19. Mice must be left in their housing facility for 3 days to acclimate prior to surgery
    NOTE: Appropriate gown, gloves, face mask, cap, and shoe covers must be worn prior to handling animals
20. Spray down surgery hood with Clidox spray
21. Spray down various tools and solutions entering hood with Clidox
22. Spray down ice bucket with prepared cell materials and place in hood
23. Set up isoflurane machine
    a. Plug in active scavenging unit and turn on
    b. Ensure isoflurane tank has enough isoflurane in it. (Isoflurane can be purchased from ULAM)
    c. Attach Oxygen tube to Oxygen tank.
    d. Turn valves to flow through inoculation chamber (plastic box next to scavenging unit.
    e. Close valves going to nose cone
    f. Ensure charcoal filter from scavenging machine is attached
    g. Place a few paper towels in the inosculation chamber (mice tend to release excrement when under anesthesia)
    h. Turn flow to 1 L/min
24. Set up small area with paper towels and a surgery area

25. Place a plastic waste container on mini scale in the hood
26. Retrieve mouse cage from housing facility
27. Remove one mouse from the cage and place on scale. Record weight
28. Return remaining mice to housing facility
29. Carefully, put mouse into the inosculation chamber by inverting weight container
30. Turn isoflurane to 5%.
31. Wait until mouse stops moving and breathing is slowed
32. Record time of surgery begin.
33. Once mouse is anesthetized, move mouse to hood, and place on paper towels
34. Put nose cone over the mouse's face.
    Note: Metal bar in nose coin should be parallel to the table and positioned closest to the table. Metal bar is to prop the mouse's head up and allow for proper breathing
35. Turn valves closed going to inosculation chamber
36. Turn valves open going to nose cone
37. Change isoflurane to 1.5%
38. If mouse start waking up while steps (34-38) occur wait a minute before proceeding until next step.
39. Using a cotton tip applicator, apply Paralube Vet ointment to each eye to ensure the eye doesn't dry out during surgery
    a. Mouse will need to be removed from nose cone during this step
40. Prepare a solution on carprofen based on mouse's weight
    a. Dosage of carprofen (5 mg /kg)
    b. Dilute carprofen in sterile PBS
    c. Typically inject 50 μL
41. Using a 28G ½ needle and syringe, inject the mouse with carprofen intraperitoneally
    a. Before injection, briefly pull plunger on syringe back and ensure no blood enters syringe
    b. Can remove mouse from nose cone during this step
42. Once analgesia has been applied to mouse, shave the back of the mouse. DO NOT over shave and only shave the area where implant will be injected
43. Apply Nair to the shaved area to remove an excess hair.
44. Using PBS and ethanol, remove any excess Nair. The mice are sensitive to Nair and excess will lead to irritation and cause them to bite and scratch area around implant
45. Alternatively, apply a few drops of Betadine antiseptic solution to the surgery area and wipe away with an ethanol wipe
46. Repeat step 46 a total of 3X
47. Make a sterile area by placing a polylined sterile drape in the hood.
48. Drop syringes and needles (two of each) onto the sterile area
49. Remove gloves and put on sterling nitrile sterile powder-free exam gloves
50. In the meantime, second person should prepare samples by adding fibrinogen and thrombin to cells prepared earlier
    a. 558 μL of fibrinogen to cells in FBS
    b. Note – Thrombin shouldn't be added until person injecting samples is prepared to do so
51. Mix samples thoroughly and draw into a syringe using a needle
52. Lift mouse skin with forceps to create a tent in order to facilitate injection

53. Inject each implant subcutaneously on the dorsal flank of the mouse, one sample per flank.
54. After injection is complete, leave needle in the mouse for 1 min to let fibrinogen polymerize and the rinse the injection site with ethanol alcohol pads.
55. Repeat steps 51-55 for the other injection on the opposite dorsal flank, unless only 1 implant is needed
56. Prepare a recovery cage on top of a heating pad
57. Place mouse in recovery cage
58. Record time of surgery end
59. Once mouse is ambulatory, record on surgery log and return cage to house facility
60. Clean up surgery area from first mouse.
61. Repeat steps 26-62 for additional mice until all samples have been injected
62. Monitor mice each day for signs of distress or pain for up to 1 week, and then everyday thereafter

**Implant Removal and Fixation Protocol:**

63. Depending on timepoints to harvest implants, place mice in cage and turn on $CO_2$ to small mammals
64. Monitor mice to ensure they are not in distress.
65. Once mice stop breathing, one at a time, move mice to hood and place on paper towel.
66. Using surgical scissors, cut open the thoracic cavity of the mice. Continue to cut major external organs to cause exsanguination and ensure mouse is euthanized.
67. Wipe injection area with 70% ethanol
68. Using scissors and forceps, cut skin of mouse along spine and then make a traverse cut to create a skin flap.
69. Break facia away from skin to find implant.
70. Surgical excise the implant with the scissors and place each implant into 20 mL vials containing Z-fix formalin.
    a. Implant compacts over time
    b. Acellular conditions may not be present as mice may have degraded all the matrix
71. Once implants are removed, place paper towel and mouse carcass in a glove.
72. Tie off glove and place in appropriate disposal area (typically fridge in surgery room)
73. Repeat 67-73 for each mouse
74. Store vials in fridge for 24 hours
75. Rinse implants with PBS (2 to 4 times)
76. Add 70% ethanol to 20 mL vials containing implant and place it in fridge until tissue processing

# Appendix Y – Tissue Implant Embedding and Sectioning

**Tissue Embedding**

1. Obtain pink embedding cassettes pink cassettes (UNISETTE cassette with lid, Simport, Canada) and label with sample information
   NOTE: use a pencil for labeling as embedding chemicals will remove ink and markers
2. Fill a beaker with 70% ethanol.
3. Remove implant from previously fixed vials.
4. Cut, using surgical scissors and with the aid of forceps, excess mouse tissue away from implant. Excess tissue will result in additional sectioning. To optimize time and sections, excess tissue should be excised
5. Place extra pieces of tissue back into 70% ethanol in case some potions contained the implant.
6. Place the trimmed implant into the cassette. If implant is small and looks like it could fall through the holes in the cassette, add a tissue embedding sponge to the cassette.
7. Place cassette into the beaker with ethanol
8. Repeat 3-7 for each implant. You can process up to 20 samples at a time.
9. Take beaker of 70% ethanol and tissue cassettes to embedding machine
10. Place all tissue cassettes into the metal tissue embedding basket (usually next to the machine)
11. Raise the hood of the tissue processing machine.
    NOTE: When using tissue processing machine and hood is raised, individuals should where a protective mask as xylene vapors are hazardous
12. Slide the metal tissue embedding basket onto the metal hooks in the tissue embedding machine. Hooks may be above solution bucket 1, 4 or 12 depending on where the last person who used the machine placed it.
13. Once basket is attached, using the rotate button, rotate the basket so it is above solution bucket 4
14. Lower the hood of the tissue processing machine. Samples and the metal basket should now be submerged in 70% ethanol
15. Start the machine, by pressing the run button, and set to program 1 (P1)
    1. Program takes about 10 hours to run
    2. Typically, machine will run over night when no one is around to avoid exposure to xylene
    3. P1 is already programed to appropriately dehydrate and embed samples in paraffin

**Paraffin Block Formation:**

16. Press the cool button on the tissue embedding center machine to start cooling of the cold plate
17. Get a bucket of ice. Put a layer of aluminum foil over the ice.
18. After tissue processing machine finishes, raise hood of tissue processing machine.
19. Place tissue cassettes into paraffin bath in the tissue embedding machine.
20. Take a metal paraffin block mold (to the side of the tissue embedding center) and place on the heating blocks under the paraffin lever.
21. One at a time, remove a tissue cassette from the paraffin bath and break of the lid of the cassette
22. Using forceps, remove the implant and place in the center of metal paraffin block mold
23. Place the tissue cassette on top of the metal paraffin block mold. This is to keep a label for each implant as well as a way for the microtome (sectioning machine) to hold the paraffin tissue block.
24. Slowly, press the paraffin lever to dispense paraffin into the metal paraffin block mold through the holes in the tissue cassette.
25. Ensure the implant stays in the center of the mold. If not remove, the tissue cassette and adjust the implant.
26. Repeat 24-25 until implant is in the center of the mold and paraffin completely fills the mold
27. Place the mold on the cooling pad.
28. Once paraffin has hardened, (turned white), move mold onto aluminum foil in ice bucket.
29. Repeat 20-28 until all samples are complete.
30. Let sample harden on ice overnight. While tissue may harden after 4 hrs, typically the paraffin is still too soft to section, so it is best to wait overnight.

**Sectioning:**

31. Remove the paraffin tissue block from the metal paraffin block mold
32. Using a utility knife or metal blade, cut away excess paraffin surrounding the implant creating a smaller square of paraffin around the implant.
33. Cut the 2 of corners (create notches) on the paraffin square to create an orientation for sectioning
34. Place cut tissue blocks on ice to stiffen the paraffin for sectioning
35. Repeat 31-34 for each tissue sample. Typically can process 4 samples a day due to limitation of slide drying.
36. Turn on the slide heating/drying machine next to microtome
37. Create a solution of 10% ethanol, and pour into empty pipette container near microtome
38. Turn on water bath
39. While water bath is heating, label glass slides with initials, implant information, and a sequential number to identify order of slides
40. Uncover microtome.
41. Place a new blade in the microtome.
42. Place tissue block into the microtome holder.
43. Adjust the blade so it is close to the tissue block, but enough to still have visible space between the blade and tissue block.
44. Adjust the tissue block positioning so it is parallel both latitudinally and longitudinal.

45. Make sure microtome width is set to 6 microns
46. Slowly rotate the microtome. You will hear an audible click each time the tissue block moves closer to the blade.
47. Eventually, the blade will start slicing the tissue block making a thin strip of wax. Use forceps to hold the thin strip away from the cutting block.
48. Elongate the paraffin strip until a length of a bout 1 ft, or whatever length the individual is comfortable handling.
49. Using the brush, remove the last paraffin section from the blade and set the whole paraffin strip aside, shiny side down
50. Repeat 47-49 until all of the tissue block has been processed or there is no implant left NOTE: Keep an order of each paraffin strip next the machine as to not lose the correct order of each section.
51. Using a blade, cut 6 sections from a paraffin strip.
52. Using forceps, place the paraffin strip in the ethanol bath, shiny side down.
53. Remove any air bubble trapped underneath the paraffin sections with the forceps
54. Slowly dip the glass slide into the bath and use the slide to remove the paraffin sections.
55. Carefully, place the slide with the paraffin sections in the warm water bath. When dipping in the water bath, dip slide on an angle.
    1. Paraffin sections should detach form the slide
    2. Water bath is to remove wrinkles from the paraffin sections
56. After a few seconds, remove the paraffin sections from the water bath with the glass slide
57. Place the glass slide on the slide warming plate to dry
58. Repeat 51-57 using the next sequential slide number until all paraffins sections are on glass slides
59. Allow glass slides to dry overnight

**TIPS:**

- Typically, 30-40 slides of 6 sections per slide is required for each implant
- Typically, 4 implants of 40 slides each is max to fit on slide warming plates
- Leave white slide label overhanging on the edge as this portion does not need to dry. This will allow for more slides to be processed at a time
- If paraffin starts tearing as you are sectioning, try the following
    - Tissue block can become too soft causing the paraffin to tear. Using a paper towel, spray the tissue block with 70% ethanol. Then Place and hold an ice cube on the tissue block for a few minutes
    - Blade can get dull causing the paraffin to tear. Adjust the blade so a fresh section of the blade is cutting the tissue block.
- Avoid excess moisture around paraffin strips. Moisture will cause paraffin stripe to stick resulting in loss of sections
- It is possible you will lose sections, despite how careful you are with sectioning, This is ok as long as it is not in implant region or you have enough sample to mitigate losing some sections.

# Appendix Z - H&E Histology Staining

** Protocol adapted from Ana Y. Rioja protocol*

**Protocol:**

**Rehydration:**

1. Determine slide for staining and place into slide cassette
2. Prepare area in hood for staining and set up various slide cassette baths
3. Wash slides with Xylene **2X** for 5 mins per wash
4. Wash slides with 100% ethanol **2X** for 3 mins per wash at RT
5. Wash slides with 95% ethanol **2X** for 3 mins per wash at RT
6. Wash slides with 70% ethanol **1X** for 3 mins per wash at RT
7. Wash slides with DI water **1X** for 3 mins per wash at RT

**Hematoxylin and Eosin Staining:**

8. Incubate slide in hematoxylin solution for 15 mins at RT
9. Place slide cassette in tap water container
10. Pour rinse down drain
11. Add new tap water to container
12. Mover slide cassette up and down to rinse slides
13. Repeat 10 – 12 until waste solution is clear
14. Add new tap water to container and rinse for 15 mins at RT
15. Wash slides with 95% Ethanol **1X** for 30 seconds at RT
16. Stain slides with Eosin **1X** for 1 min at RT

**Dehydration of Slides**

17. Wash slides with 95% Ethanol **1X** for 1 min at RT
18. Wash slides with 100% Ethanol **2X** for 1 min at RT
19. Wash slides with Xylene **2X** for 3 mins at RT

**Mounting coverslips on slides**

20. Remove cover slips from container and set upright leaning on wash containers for easy access

    a. Xylene make gloves slicky and will be hard to remove from container between slides
21. One at a time, remove sample slides from cassette.
22. Add 3 to 4 small drops of Permount solution onto coverslip and place it on top of the slides
23. Lay slides flat and let slides dry overnight

# Appendix AA - CD31 Immunohistochemistry Staining

** Protocol adapted from Ana Y. Rioja protocol*

**Solution**:

TBS-T: 100 mL of 10 X TBS (pH balance 7.4)
1 mL of Tween 20
Quench to 1000 mL of dd H2O

**Rehydration:**

1. Pour tap water in the food steamer and turn on
2. Pour enough target retrieval solution (DAKO) in a 200 mL beaker to cover the slide cassette
3. Place slides in the cassette
4. Prepare area in hood for staining and set up various slide cassette baths
5. Wash slides with Xylene **2X** for 5 mins per wash
6. Wash slides with 100% ethanol **2X** for 3 mins per wash at RT
7. Wash slides with 95% ethanol **2X** for 3 mins per wash at RT
8. Wash slides with 70% ethanol **1X** for 3 mins per wash at RT
9. Wash slides with DI water **1X** for 30 second per wash at RT

**Antigen Retrieval Protocol:**

10. Place cassette in beaker containing the target retrieval solution.
11. Incubate slides in the steamer for 35 minutes
12. Take out beaker and let it cool for 30 minutes.
13. While your slides are cooling, prepare the slide chamber for the staining protocol.
    1. Cover the bottom of the slide chamber with a paper towel.
    2. Completely wet paper tower with DI H2O
14. Wash slides with TBS-T for **3X** for 2 minute per wash at RT.
15. Change baths for every TBS-T wash.
16. Remove excess TBS-T from slides with Kimwipe tissues carefully.
    1. Make sure to avoid touch tissues sections
17. Use PAP pen to circle area around the tissue section.
    1. Make sure not to touch the tissue with the pen.
    2. Minimize circles area to ensure solution will cover entire section

**Staining Protocol:**

15. Add peroxidase block solution to cover section completely.
16. Place slides in slide chamber to avoid slides from drying.
17. Incubate for 5 minutes.
18. Prepare primary antibody solution
    1. For CD31 1:50 dilution in TBS-T (5 µL CD31:245 µL of TBS-T)
19. Wash slides with TBS-T for **3X** for 2 minute per wash at RT.
20. Change baths for every TBS-T wash.
21. Remove excess TBS-T from slides with Kimwipe tissues carefully.
    1. Make sure to avoid touch tissues sections
22. Add peroxidase block solution to cover section completely.
23. Place each slide in slide chamber
24. Incubate for 16 hours at 4 °C.
25. Dip each slide gently into TBS-T solution
26. Wash slides with TBS-T for **3X** for 2 minute per wash at RT.
27. Change baths for every TBS-T wash.
28. Remove excess TBS-T from slides with Kimwipe tissues carefully.
    1. Make sure to avoid touch tissues section
29. Place slides in slide chamber and add peroxidase labelled polymer (enough to cover whole section)**.**
30. Incubate for 30 minutes at RT.
31. Prepare chromogen solution:
    1. Add 1 mL of buffer substrate into provided calibrated test tube (~40 drops)
    2. Add 1 drop of liquid DAB+ Chromogen per mL of buffer substrate
32. Dip each slide gently into TBS-T solution
33. Wash slides with TBS-T for **3X** for 2 minute per wash at RT. Change baths for every TBS-T wash.
34. Remove excess TBS-T from slides with Kimwipe tissues carefully.
35. Place slides in slide chamber and add prepared Liquid DAB+ substrate-chromogen solution to slides.
36. Incubate for 5 minutes**.** If done correctly, brown stain should appear on tissues sections within a few minutes

**Hematoxylin Staining:**

37. Dip each slide gently into DI H2O.
38. Place slide in slide cassette
39. Wash slides with DI water **1X** for 1 min per wash at RT
40. Incubate slide in hematoxylin solution for 15 mins at RT
41. Place slide cassette in tap water container
42. Pour rinse down drain
43. Add new tap water to container
44. Mover slide cassette up and down to rinse slides
45. Repeat 10 – 12 until waste solution is clear

**Dehydration of Slides**

77. Wash slides with 95% Ethanol **2X** for 1 min at RT
78. Wash slides with 100% Ethanol **2X** for 1 min at RT
79. Wash slides with Xylene **2X** for 3 mins at RT

**Mounting coverslips on slides**

1. Remove cover slips from container and set upright leaning on wash containers for easy access
    a. Xylene make gloves slicky and will be hard to remove from container between slides
2. One at a time, remove sample slides from cassette.
3. Add 3 to 4 small drops of Permount solution onto coverslip and place it on top of the slides
4. Lay slides flat and let slides dry overnight

# Appendix AB - αSMA Immunohistochemistry Staining

***Same protocol as Appendix F, except:***

- Primary antibody used: Smooth muscle actin monoclonal antibody (1A4 (asm-1)) [Invitrogen: Thermo Fisher Scientific]
- Concentration of antibody: 1:800 in TBS-T
- Incubation time: 2 hours at RT

# Appendix AC - Col-IV Immunohistochemistry Staining

***Same protocol as Appendix F, except:***

- Primary antibody used: Collagen IV Monoclonal Antibody (COL-94) [MA1-22148] [Thermo Fisher Scientfic]
- Concentration of antibody: 1:400 in TBS-T
- Incubation time: Overnight at 4 °C.

# Appendix AD – Histology Vessel Quantification

**Prep:**

Go to the shared google drive folder for CD31 quantification

1. Open up the indicated sample folder (e.g. M10R)
2. Download all of the indicated 20x images (these are noted in the original e-mail I sent for which images to quantify)
3. Open up the excel template (this was also sent in the original email)
4. Rename each sheet/tab to the appropriate image name. (Each separate 20x image should have its own sheet)

**Quantification**

5. Open up the 20x image in imageJ
6. Go to Analyze -> Set measurements
    1. Click area, shape descriptors, Feret's diameter, add to overlay, limit to threshold, and display label
    2. Decimal places: 2
    3. Click OK
7. Using the straight-line tool, draw a line across the inner diameter of a vessel lumen without erythrocytes (VL).
    1. In the case of an elongated/elliptical lumen, choose a diameter that is roughly halfway between the max and min diameter.
8. Click Cntrl M to measure the lumen (If control M doesn't work look under analyze -> measure to see what the short cut command is)
    1. A new window should appear with the measurements
9. Repeat 7-8 for all lumens without erythrocytes (VL)
10. Record the final label number, so you know where you stopped counting vessels lumens without erythrocytes (VL)
11. Repeat 7-8 for all lumens with erythrocytes (VE)
12. In data/measure window, (the window that appeared once clicked measure the first time) copy all the data.
13. Paste the data into the excel sheet (make sure the columns match the correct number)
14. Enter the label number into the box where you switched from vessels w/o erythrocytes (VL) to vessels w/ erythrocytes (VE).
15. Save a .jpeg image of the measured lumens with the data labels. Save as data set, image number, your last name (ex. M10R - 5 Putnam)
16. Repeat steps 5-15 for each image in the indicated image set using a new sheet/spreadsheet tab.

17. Once completing all images in a set, save the excel file with your last name, the image set name, and my last name. (ex. Putnam M10R Bezenah Quantification)
18. Repeat steps 16-17 for all images sets.

**Tips/Notes:**

- Excel Template is attached to the email
- Vessel = Redish Brown CD31 rim with or w/o erythrocytes
- The number of vessels with hollow lumens (VL)
- The number of vessels with hollow lumens and erythrocytes inside the lumen (VE)
- Erythrocytes have a brown/orange color to them and are completely circular.
- If data labels do not appear, go to image -> overlay -> labels and click show labels.
- Make sure you save images after you finish analysis
- Rule of Thumb:
    - Count the vessel if you can clearly see some white/greyish background completely surrounded by brown stain. DO NOT count vessels that have purple or brown lumens.
    - Smaller lumens may be hard to determine. If you can clearly see a white/greyish center to the lumen, DO NOT count it.
    - If you are not sure if there are erythrocytes or not (especially with smaller lumens), count it as w/o erythrocytes (VL)

# Appendix AE – List of Materials

## ***Antibodies:***

**Name:** Monoclonal Mouse Anti-Human CD31, Endothelial Clone, JC70A
**Vendor**: Dako
**Catalog Number:** M0823
**Experimental Use:** Endothelial Cell staining (in vitro and in vivo)
**Dilution:** 1:50 for histology, 1:200 for IF staining, 1:50 for FACS
**Dilution Buffer:** 0.1% TBS-T (Tween 20) for histology, 2% BSA in 0.1% TBS-T (Tween 20) for IF staining, 0.1% BSA in Ice Cold PBS for FACS

**Name:** Rhodamine Ulex Europaeus Agglutinin I (UEA)
**Vendor**: Vector Labs
**Catalog Number:** RL-1062
**Experimental Use:** Endothelial Cell staining (in vitro)
**Dilution:** 1:100 for IF staining
**Dilution Buffer:** 1 X PBS

**Name:** Alexa Fluor 488 goat anti-mouse IgG
**Vendor**: Life Technologies
**Catalog Number:** A11001
**Experimental Use:** Secondary for GFP (Green Fluorescent tag)
**Dilution:** 1:400
**Dilution Buffer:** 2% BSA in 0.1% TBS-T (Tween 20)

**Name:** Alexa Fluor 488 goat anti-rabbit IgG
**Vendor**: Life Technologies
**Catalog Number:** A11008
**Experimental Use:** Secondary for GFP (Green Fluorescent tag)
**Dilution:** 1:400
**Dilution Buffer:** 2% BSA in 0.1% TBS-T (Tween 20)

**Name:** Alexa Fluor 405 goat anti-mouse IgG
**Vendor**: Life Technologies
**Catalog Number:** A31553
**Experimental Use:** Secondary for DAPI (Blue Fluorescent tag)
**Dilution:** 1:300

**Dilution Buffer:** 2% BSA in 0.1% TBS-T (Tween 20)

**Name:** Actin Smooth Muscle Antibody (1A4 (asm-1)) [a-SMA]
**Vendor**: Invitrogen
**Catalog Number:** MA5-11547
**Experimental Use:** Stromal Cell/ Pericyte Staining
**Dilution:** 1:800 for histology, 1:200 for IF staining
**Dilution Buffer:** 0.1% TBS-T (Tween 20) for histology, 2% BSA in0.1% TBS-T (Tween 20) for IF staining

**Name:** Ms mAb to MMP-9 [56-2A4]
**Vendor**: Abcam
**Catalog Number:** ab58803
**Experimental Use:** Western Blot
**Dilution:** 1:400
**Dilution Buffer:** 5% BSA dissolved in TBS-T (Tween 20)

**Name:** Ms mAb to MMP-2 [CA4001/CA719E3C]
**Vendor**: Abcam
**Catalog Number:** ab3158
**Experimental Use:** Western Blot
**Dilution:** 1:400
**Dilution Buffer:** 5% BSA dissolved in TBS-T (Tween 20)

**Name:** Rb mAb to MMP-14 [EP1264Y] (MT1-MMP)
**Vendor**: Abcam
**Catalog Number:** ab51074
**Experimental Use:** Western Blot
**Dilution:** 1:2000
**Dilution Buffer:** 5% BSA dissolved in TBS-T (Tween 20)

**Name:** Pierce Goat anti-Rabbit IgG (H+L) Peroxidase Conjugated
**Vendor**: Thermo Scientific
**Catalog Number:** 31466
**Experimental Use:** Western Blot
**Dilution:** 1:10000
**Dilution Buffer:** 0.1% in TBS-T (Tween 20)

**Name:** Pierce Goat anti-Mouse IgG (H+L) Peroxidase Conjugated
**Vendor**: Thermo Scientific
**Catalog Number:** 31431
**Experimental Use:** Western Blot
**Dilution:** 1:10000
**Dilution Buffer:** 0.1% in TBS-T (Tween 20)

**Name:** GAPDH (V-18) HRP

**Vendor**: Santa Cruz Biotechnology
**Catalog Number:** sc-20357
**Experimental Use:** Western Blot
**Dilution:** 1:2000
**Dilution Buffer:** 0.1% in TBS-T (Tween 20)

**Name:** eBioScience Anti-Human CD144 [16B1] (VE-Cadherin)
**Vendor**: Invitrogen
**Catalog Number:** 14-1449-82
**Experimental Use:** IF staining and FACS
**Dilution:** 1:200 for IF staining, 1:50 for FACS
**Dilution Buffer**: 2% BSA in 0.1% TBS-T (Tween 20) for IF staining, 0.1% BSA in Ice Cold PBS for FACS

**Name:** vWF Antibody (F8/86)
**Vendor**: Invitrogen
**Catalog Number:** MA5-14029
**Experimental Use:** IF staining
**Dilution:** 1:200 for IF staining,
**Dilution Buffer**: 2% BSA in 0.1% TBS-T (Tween 20) for IF staining,

**Name:** Laminin beta-1 Antibody
**Vendor**: Invitrogen
**Catalog Number:** PA5-27271
**Experimental Use:** IF staining
**Dilution:** 1:200 for IF staining,
**Dilution Buffer**: 2% BSA in 0.1% TBS-T (Tween 20) for IF staining,

**Name:** Collagen IV Antibody
**Vendor**: Invitrogen
**Catalog Number:** MA1-22148
**Experimental Use:** IF staining, and histology
**Dilution:** 1:200 for IF staining, 1:400 for histology
**Dilution Buffer**: 2% BSA in 0.1% TBS-T (Tween 20) for IF staining, in 0.1% TBS-T (Tween 20) for histology

## ***Inhibitors:***

**Name:** Dimethyl Sulfoxide
**Vendor**: Sigma Aldrich
**Catalog Number:** D650-100mL
**Experimental Use:** Cryopreservation and Vehicle in Inhibitor Studies
**Dilution:** 1:100 (10 µL of DMSO in 1 mL of Media)

**Name:** Marimastat (BB-2516)
**Vendor**: TOCRIS Bioscience

**Catalog Number:** 2631
**Experimental Use:** Inhibitor Studies
**Dilution:** 10 µL of 20 µM in 1 mL of Media

**Name:** Aprotinin (BB-2516)
**Vendor**: Sigma Aldrich
**Catalog Number:** A1153-1 MG
**Experimental Use:** Inhibitor Studies
**Dilution:** 10 µL of 2.2 µM in 1 mL of Media

## ***Media and Cell Culture:***

**Name:** Human Plasma Fibronectin
**Vendor**: Life Technologies
**Catalog Number:** 33016-015
**Experimental Use:** Coating Culture Plates for iPSC-ECs
**Dilution:** 225 µL (of 1 mg/mL stock) in 7.5mL sterile water for T-75 flask

**Name:** Fibrinogen from bovine plasma
**Vendor**: Sigma Aldrich
**Catalog Number:** F8630-10G
**Experimental Use:** Making Fibrin Gels

**Name:** TrypLE Select
**Vendor**: Life Technologies
**Catalog Number:** 12563-011
**Experimental Use:** Trypsinizing iPSC-ECs

**Name:** Cytodex Microcarrier Beads
**Vendor**: Sigma Aldrich
**Catalog Number:** C3275-10G
**Experimental Use:** For Angiogenesis Assay

**Name:** Thrombin
**Vendor**: Sigma Aldrich
**Catalog Number:** T6634-500UN
**Experimental Use:** For polymerizing Fibrinogen

**Name:** EGM-2
**Vendor**: Lonza
**Catalog Number:** CC-3162
**Experimental Use:** Culturing ECs

**Name:** EGM-2MV
**Vendor**: Lonza

**Catalog Number:** CC-3202
**Experimental Use:** Culturing ECs

**Name:** Vasculife VEGF Endothelia Cell Medium
**Vendor**: Lifeline Cell Technologies
**Catalog Number:** LL-0003
**Experimental Use:** Culturing ECs, specifically iPSC-ECs

**Name:** iCell Endothelial Cells Medium Supplement
**Vendor**: Cellular Dynamics International
**Catalog Number:** M1019
**Experimental Use:** Culturing iPSC-ECs

**Name:** DMEM
**Vendor**: Life Technologies
**Catalog Number:** 11995065
**Experimental Use:** Culturing NHLFs

**Name:** FBS
**Vendor**: Life Technologies
**Catalog Number:** 10437-028
**Experimental Use:** Culturing cells

## ***Cell Lines:***

**Name:** HUVECs
**Vendor**: Lonza
**Catalog Number:** C2519A
**Lot:** 0000394986

**Name:** iPSC-ECs
**Vendor**: Cellular Dynamics
**Catalog Number:** R102
**Lot:** 0000394986

## ***Western Blot and Gel Zymography:***

**Name:** Precision Plus Protein Kaleidoscope
**Vendor**: BioRad
**Catalog Number:** 161-0375
**Loading Volume:** 10 μL

**Name:** Magic Mark XP Western Standard
**Vendor**: Invitrogen
**Catalog Number:** LC5602

**Loading Volume:** 4 μL

**Name:** Novex WedgeWell 10% Tris-Glycine Gel
**Vendor**: Invitrogen
**Catalog Number:** XP00100BOX
**Use:** Western Blot Electrophoresis

**Name:** Novex 10% Zymogram (Gelatin) Gel
**Vendor**: Invitrogen
**Catalog Number:** EC6175BOX
**Use:** Gel Zymography Electrophoresis

**Name:** Filter Paper Extra Thick Blot Paper
**Vendor**: BioRad
**Catalog Number:** 1703966
**Use:** Western Blot Transfer

**Name:** Immun-Blot PVDF Membrane For Protein Blotting
**Vendor**: BioRad
**Catalog Number:** 162-0176
**Use:** Western Blot Transfer

**Name:** Hyblot CL Autoradiography Film
**Vendor**: Denville Scientifc Inc
**Catalog Number:** E3012
**Use:** Western Blot Development

**Name:** Kodak Professional Fixer
**Vendor**: Electron Microscopy Sciences
**Catalog Number:** 74300
**Use:** Western Blot Development

**Name:** Kodak D-19 Developer Replacement Kit
**Vendor**: Electron Microscopy Sciences
**Catalog Number:** 74200
**Use:** Western Blot Development

**Name:** Halt Protease & Phosphatase Single Use Inhibitor Cocktail
**Vendor**: Thermo Scientific
**Catalog Number:** 78442
**Use:** Protein Lysis

**Name:** Pierce BCA Protein Assay Kit
**Vendor**: Thermo Scientific
**Catalog Number:** 23225
**Use:** Protein Concentration Analysis

## ***RNA Prep and qPCR:***

**Name:** RNeasy Mini Kit
**Vendor**: Qiagen
**Catalog Number:** 74104
**Use:** RNA Lysis

**Name:** QIAshredder
**Vendor**: Qiagen
**Catalog Number:** 79654
**Use:** RNA Lysis

**Name:** ImProm-II Reverse Transcription System
**Vendor**: Promega
**Catalog Number:** A3800
**Use:** cDNA Synthesis

**Name:** TaqMan Gene Expression Master Mix
**Vendor**: Applied Biosystems
**Catalog Number:** 4369016
**Use:** qPCR

**Name:** TaqMan Gene Expression Assay Primer (18s)
**Vendor**: Applied Biosystems
**Catalog Number:** Hs03003631_g1
**Use:** qPCR

**Name:** TaqMan Gene Expression Assay Primer (MMP2)
**Vendor**: Applied Biosystems
**Catalog Number:** Hs01548724_m1
**Use:** qPCR

**Name:** TaqMan Gene Expression Assay Primer (MMP9)
**Vendor**: Applied Biosystems
**Catalog Number:** Hs00957562_m1
**Use:** qPCR

**Name:** TaqMan Gene Expression Assay Primer (MMP14)
**Vendor**: Applied Biosystems
**Catalog Number:** Hs01037009_g1
**Use:** qPCR

**Name:** Optical Adhesive Covers
**Vendor**: Applied Biosystems

**Catalog Number:** 4360954
**Use:** qPCR

**Name:** MicroAmp Fast Optical 96-Well Reaction Plate with Barcode
**Vendor**: Applied Biosystems
**Catalog Number:** 4346906
**Use:** qPCR

## ***Histology:***

**Name:** Mayer's Hematoxylin
**Vendor**: Electron Microscope Services
**Catalog Number:** 26043-06
**Use:** H&E Staining

**Name:** Eosin Y Solution
**Vendor**: Sigma Aldrich
**Catalog Number:** HT110132-1L
**Use:** H&E Staining

**Name:** Target Retrieval Solution 10X Concentrate
**Vendor**: Dako
**Catalog Number:** S1699
**Use:** IHC Staining

**Name:** EnVision System- HRP (DAB) For Use with Mouse Primary Antibodies
**Vendor**: Dako
**Catalog Number:** K4006
**Use:** IHC Staining

**Name:** Unisette Tissue Processing/Embedding Cassette
**Vendor**: Simport
**Catalog Number:** M505-3
**Use:** Tissue Embedding

**Name:** Fisherbrand Superfrost Plus Microscope Slides
**Vendor**: Fisher Scientific
**Catalog Number:** 12-550-15